Bonn zoological Bulletin

Supplementum Vol. 65 (2020)

formerly: Bonner zoologische Monographien

Microscopic anatomy of *Eukoenenia spelaea* (Peyerimhoff, 1902) (Arachnida: Palpigradi: Eukoeneniidae)

Sandra Franz-Guess & J. Matthias Starck

An open access journal of organismal zoology, published by
Zoologisches Forschungsmuseum Alexander Koenig – Leibniz-Institut für Biodiversität der Tiere, Bonn

BONN ZOOLOGICAL BULLETIN – SUPPLEMENTUM (BZB-S),
formerly "Bonner zoologische Monographien",

Bonn zoological Bulletin, Editor-in-Chief
Ralph S. Peters, Zoologisches Forschungsmuseum Alexander Koenig – Leibniz-Institut für Biodiversität der Tiere (ZFMK), Hymenoptera Section, Adenauerallee 160, 53113 Bonn, Germany, tel. +49 228-9122-290, fax: +49 228-9122-212; r.peters@leibniz-zfmk.de

Managing Editor Supplementum Series
Thomas Wesener, ZFMK, Myriapoda Section, same address as above, tel. +49 228-9122-425, fax: +49 228-9122-212; t.wesener@leibniz-zfmk.de

The peer-reviewed series Bonn zoological Bulletin – Supplementum, formerly "Bonner zoologische Monographien", has existed since 1971. It is published by the Zoological Research Museum Alexander Koenig – Leibniz Institute for Animal Biodiversity (ZFMK), Bonn. Supplements on focus topics are produced in irregular succession. The BzB-S consists of original zoology papers too long for inclusion in our institute's regular journal, Bonn zoological Bulletin. Preferred manuscript topics are: systematics, taxonomy, biogeography, anatomy, and evolutionary biology. Manuscripts should be in American English. Authors are requested to contact the managing editor prior to manuscript submittal.

For subscription, back issues and institutional exchange, please contact the ZFMK library (ZFMK, Bibliothek, Mareike Kruppa, Adenauerallee 160, 53113 Bonn, Germany, tel. +49 228–9122–216, fax: +49 228–9122–212; m.kruppa@leibniz-zfmk.de). The online version of BzB -S is available free of charge at the BzB homepage: http://www.zoologicalbulletin.de.

Authors of this issue:
Sandra Franz-Guess & J. Matthias Starck
Published: Bonn zoological Bulletin – Supplementum Vol. 65, 125 pp.

© 2020 Zoologisches Forschungsmuseum Alexander Koenig – Leibniz-Institut für Biodiversität der Tiere, Bonn, Germany.

ISSN: 0302-671X

Produced by Eva-Maria Levermann, Bonn, Germany; E.Levermann@leibniz-zfmk.de; emlevermann@netcologne.de.
Printed and bound by Verlag Natur & Wissenschaft, Postfach 170209, 42624 Solingen, Germany.

Cover illustration:
Eukoenenia spelaea (Peyerimhoff, 1902). Light microscopic micrograph of a histological cross-section through the prosoma of a female at the level of the rostrosoma, including cheliceral and pedipalpal articulation. Please see caption of Figure 37 in this publication for details.

Microscopic anatomy of *Eukoenenia spelaea* (Peyerimhoff, 1902) (Arachnida: Palpigradi: Eukoeneniidae)

Sandra Franz-Guess & J. Matthias Starck

Bonn zoological Bulletin Supplementum 65: 1–125 ©ZFMK

Contents Volume 65

Abstract	3
Key words	3
Introduction	4
Material & Methods	6
Results	9
Discussion	68
Acknowledgements	94
References	94
Appendix I	103
Appendix II	117

Bonn zoological Bulletin – Supplementum 65: 1–125
2020 · Franz-Guess S. & Starck J.M.
https://doi.org/10.20363/BZB-S-2020.65

August 2020
ISSN 0302–671X
http://www.zoologicalbulletin.de

Research article

urn:lsid:zoobank.org:pub:09780AFE-1686-46DC-A629-5784EF0E59E7

Microscopic anatomy of *Eukoenenia spelaea* (Peyerimhoff, 1902) (Arachnida: Palpigradi: Eukoeneniidae)

Sandra Franz-Guess[1] & J. Matthias Starck[2,*]

[1,2] *Ludwig-Maximilians-University (LMU) Munich, Department of Biology II, Biocenter Martinsried, Großhadernerstr. 2, D-82152 Planegg-Martinsried, Germany*
**Corresponding author: Email: starck@lmu.de*

[1] urn:lsid:zoobank.org:author:98DFBB07-6DD5-41C0-B21D-05298086A710
[2] urn:lsid:zoobank.org:author:529CA71E-01B6-407A-AAB0-4B0E4014057E
[1] https://orcid.org/0000-0003-2826-1248
[2] http://orcid.org/0000-0001-7882-9482

Abstract. *Eukoenenia spelaea* (Peyerimhoff, 1902) is a troglobiont palpigrade found in caves of the European Alps. Individuals are small, reaching a maximum body length of 1.5 mm (if measured without the terminal flagellum). They lack eyes and breathing organs, but have unique sensory organs. Morphological studies of Palpigradi date back the late 19th and early 20th century, but data on microscopic anatomy and comparative morphology is incomplete. Their small body size causes reduction, simplification and loss of organ systems, and their paedomorphic evolution results in some hyperplesiomorphic features (i.e., more plesiomorphic than the euchelicerate body plan) making their phylogenetic placement among arachnids difficult.

In this study, we use serial sectioning for light microscopy, transmission and scanning electron microscopy, and 3D-reconstructions to provide a complete account on the microscopic anatomy of *Eukoenenia spelaea*. We describe several new morphological features. For some already known structures we provide detailed morphological evidence allowing for new interpretations in the light of evolutionary morphology: (1) two prosomal shields, the pro- and metapeltidium, divide the prosoma dorsally. The traditionally described "mesopeltidium" is a sclerotization of the pleural membrane, but not a tergite. (2) The ventral plate is probably an osmoregulatory organ. (3) The prosternum consists of the fused sternites of segments 2–4. (4) The frontal organ and trichobothria have a unique morphology among euchelicerates. (5) We provide evidence for a tripartite syncerebrum. (6) The adult heart lacks innervation, lacks ostia, a pericardium, and shows an early developmental state of muscle differentiation. (7) The rostrosoma is not associated with chelicerae or pedipalps. (8) The midgut is simple and sac-like; a hindgut is missing. (9) The coxal organ (tubule and glandular section) has no lumen. (10) Females have an unpaired ovary with only few large eggs. (11) Aflagellate sperm have a prominent vacuole.

The small body size of *Eukoenenia spelaea* (and probably of all palpigrades) resulted in modification, reduction or even loss of structures like: (1) a distinct differentiation into endo- and exocuticle is lacking over large regions of the body; (2) absence of respiratory organs; (3) several muscles groups are reduced; (4) the prosomal ganglia are proportionally large and display a high level of fusion; (5) neuron size ranges at the minimum size for arthropods; (6) the coxal organ has a reduced number of cells; (7) absence of Malpighian tubules; (8) ovaries are unpaired; (9) small number of eggs. Some organs showed a typical paedomorphic morphology: (1) the heart lacks ostia, a pericardium, and the ultrastructure of the musculature resembles that of the hearts of early developmental stages of other arthropods; (2) the midgut is a simple sac with no epithelial differentiation; (3) the reappearance of ancient plesiomorphies like (i) the anterior oblique muscle, (ii) an almost complete set of posterior oblique muscles in the prosoma, (iii) the deutocerebral connectives embracing the esophagus, and (iv) the segmental chord of ganglia in the opisthosoma are interpreted hyperplesiomorphic, i.e., features that were rather present in the body plan of euarthropods and already reduced in euchelicerates. Hyperplesiomorphic features may be interpreted as resulting from "reverse recapitulation" indicating paedomorphosis by developmental truncation. – The morphological characters revealed in the present analyses were used to perform a phylogenetic analysis. Several autapomorphic characters were recognized to characterize Palpigradi (e.g., the prosoma is dorsally divided in only two peltidia; the anterior ventral sclerite of the prosoma is assigned to segments 2–4; the frontal organ; the lateral organ; the preoral cavity, mouth, and pharynx are inside a simple cuticular cone shaped rostrosoma; lack of a hindgut; the ventral plate; the ultrastructure of the trichobothria; anterior oblique suspensor muscle). A phylogenetic sister group relationship was found with Acaromorpha with which they share: the opening of the excretory pore on or near the coxa of appendage III (= leg 1); the lack of a postcerebral suction pump; aflagellate sperm that lack an acrosomal filament; the muscle topography of leg 4; the tubule of the coxal organ is differentiated in a proximal and a distal segment; the presence of a myogenic heart; the lack of the arcuate body in the syncerebrum. – Based on that sister group relationship, it becomes probable that evolutionary miniaturization did not occur in the stem lineage of Palpigradi, but in the lineage leading to the common ancestor of a clade Palpigradi + Acaromorpha. We suggest that Palpigradi with their simple and hyperplesiomorphic morphology represent an offshoot of this early lineage with little morphological variation, while the lineage leading to the Acaromorpha resulted in a species rich diversification based on a paedomorphic morphology.

Key words. Chelicerata, evolution, miniaturization, morphology, paedomorphosis.

INTRODUCTION

Palpigradi

Palpigradi is an enigmatic group of arachnids containing an estimated number of 107 extant species and two fossil species assigned to two taxa, Eukoeneniidae Petrunkevitch, 1955, and Prokoeneniidae Condé, 1996. Eukoeneniidae includes 4 extant genera, i.e., *Allokoenenia* Silvestri, 1913, with one species; *Eukoenenia* Börner, 1901, with 86 species; *Koeneniodes* Silvestri, 1913, with eight species, and *Leptokoenenia* Condé, 1965, with five species (Harvey 2003; Giribet et al. 2014; Bu et al. 2019; Souza & Ferreira 2013; Barranco & Mayoral 2007, 2014). Prokoeneniidae includes two extant genera, i.e., *Prokoenenia* Börner, 1901, with six species and *Triadokoenenia* Condé, 1991, with one species. Fossil genera are *Electrokoenenia* Engel & Huang, 2016 (Eukoeneniidae) and *Paleokoenenia* Rowland & Sissom, 1980 (Eukoeneniidae or incertae sedis) with one species each (Harvey 2002). Palpigrades are distributed in the pantropical region between 48° N and 40° S with most species in Africa and Europe (Condé 1996; Harvey 2003), and several new species recently described for South America (Souza & Ferreira 2010, 2011a, b; 2012; 2013). Species live in the upper soil layer or are troglobiont, especially those in Central Europe.

Palpigradi are small, the largest species reaching a body length of 3 mm (Kästner 1931a; Millot 1949a; Giribet et al. 2014; Dunlop 2019), including a prominent long terminal flagellum (it is relatively short in species of the genera *Allokoenenia* and *Leptokoenenia*) which they hold parallel to the ground while walking and hold erect during short stops (Kováč et al. 2002) sometimes moving it laterally (Souza and Ferreira 2010; Ferreira and Souza, 2012). They have no eyes, book lungs, or tracheae. Palpigrades are characterized by a unique set of sensory organs (frontal organ, lateral organs). They also carry numerous sensory setae and trichobothria as known from other arachnids. The prosomal dorsal shield is divided into three sclerites, a feature that is only known from Solifugae and Schizomida.

Morphological studies of Palpigradi date back to the late 19th and early 20th century [*Eukoenenia angusta* (Hansen, 1901), *Eukoenenia florenciae* (Rucker, 1903), *Eukoenenia grassii* (Hansen, 1901), *Eukoenenia mirabilis* (Grassi and Calandruccio, 1885) (Hansen & Sørensen 1897; Wheeler 1900, Hansen 1901; Börner 1904, Buxton 1917; Kästner 1931a; Millot 1942; 1943), *Eukoenenia siamensis* (Hansen, 1901), *Prokoenenia chilensis* (Hansen, 1901), and *Prokoenenia wheeleri* (Rucker, 1901) (Hansen 1901, Kästner 1931a)]. The main focus of these studies was on the external morphology. Some aspects of the internal morphology were described by Rucker (1901), Börner (1904), Buxton (1917), Kästner (1931a), Millot (1942, 1943, 1949a), and van der Hammen (1977a, b, 1982) using either dissections, or cleared specimens, or paraffin histology. Alberti (1979a) analyzed the ultrastructure and development of spermatozoa in *P. wheeleri*, Ludwig & Alberti (1992) documented the ultrastructure of the midgut in *P. wheeleri*, and Smrž et al. (2013) studied the gut content of *Eukoenenia spelaea* using light microscopy.

It has been frequently noted that Palpigradi are rich in plesiomorphic features [reviewed in Dunlop & Alberti (2008)] thus obscuring a phylogenetic analysis. Morphological character analyses and gene sequencing render diverging and often incompatible phylogenetic hypotheses of euchelicerate relationships (Fig. 1). Among the published phylogenetic hypotheses, Arachnida and Tetrapulmonata, as well as Pedipalpi (=Amblypygi + Uropygi) and Uropygi (=Thelyphonida+Schizomida) at the interordinal level, are those clades that have repeatedly been confirmed. All other higher order group relationships are debated including the phylogenetic position of Palpigradi. Van der Hammen (1977a) classified Palpigradi together with Actinotrichida (Acariformes) as "Epimerata" (also suggesting a diphyletic origin of the Acari; van der Hammen 1977a, b, 1982). Weygoldt & Paulus (1979a; Fig. 1A) considered Palpigradi to be the sister group to Holotracheata. Shultz (1990) considered Palpigradi as sister group to Tetrapulmonata (Fig. 1B). However, Shultz (2007a) presented a more complete analysis of morphological characters (including fossils) resulting in either a largely unresolved consensus tree (Fig. 1D; fig. 1 in Shultz 2007a) or, alternatively, a monophyletic taxon Arachnida with the topology ((Palpigradi (Acaromorpha (Tetrapulmonata (Haplocnemata, Stomothecata)); fig. 5 in Shultz (2007a). Giribet et al. (2002) considered morphological data, fossil record and gene sequences, and placed palpigrades on an unresolved polytomy together with Acari, Ricinulei, and Tetrapulmonata (Fig. 1C). Results from gene sequence analyses by Regier et al. (2010) showed Palpigradi and Acariformes together as sister group to all other arachnids (Fig. 1E). Pepato et al. (2019) combined molecular data and morphological data and recovered Palpigradi as sister group to a clade containing Solifugae and Acariformes (Cephalosomate = (Palpigradi (Solifugae+Acariformes)), however, as they state, with relatively low support. Garwood & Dunlop (2014) included fossil material in their morphological data set and placed palpigrades as sister group to an unresolved taxon containing Solifugae, Acariformes, Parasitiformes, Ricinulei, and Tetrapulmonata (Fig. 1F). Giribet et al. (2014) conducted a comprehensive phylogenetic analysis of Palpigradi (29 species) based on gene sequences and suggested a sister group relationship to Scorpiones and Thelyphonida. Finally, Sharma et al. (2014) and Sharma (2018) placed Palpigradi as sister to Parasitiformes, but pointed out that there was little support. – In summary, Palpigradi appear to take a rather basal position among

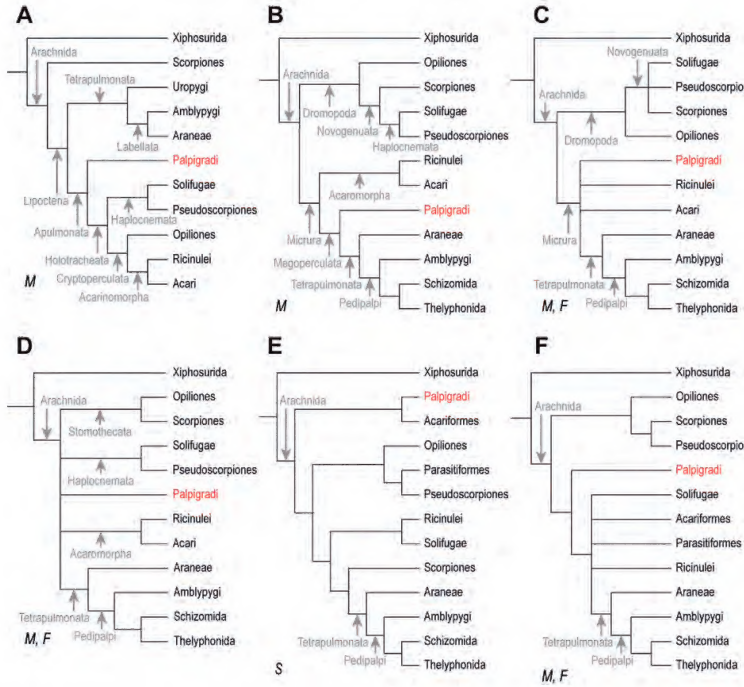

Fig. 1. Published phylogenetic hypotheses about euchelicerate relationships. **A**. Phylogeny by Weygoldt & Paulus (1979a) based on morphological characters. Scorpiones are the sister group to all other arachnids, with two major clades, i.e., Tetrapulmonata and Apulmonata. **B**. Phylogeny by Shultz (1990) based on morphological characters. Arachnida are divided into two clades, i.e., Dromopoda and Micrura. **C**. Phylogeny by Giribet et al. (2002) based on morphological characters, fossil records, and gene sequencing. The phylogeny of Micrura is largely unresolved. **D**. Phylogeny by Shultz (2007a) based on morphological characters of extant and fossil records. Except for Tetrapulmonata, the relationships of euchelicerate clades are not resolved. **E**. Phylogeny by Regier et al. (2010) based on gene sequencing. Palpigradi are positioned at the base and sister group to Acariformes. Scorpiones is sister group of Tetrapulmonata. **F**. Phylogeny by Garwood & Dunlop (2014) based on morphological characters and fossil records. While the base of the tree is resolved, the relationships between Solifugae, Acariformes, Parasitiformes, and Ricinulei is unresolved. Abbreviations: F = fossil record analysis; M = morphological character analysis; S = gene sequence analysis.

arachnids, but an explicit hypothesis about the phylogenetic position of Palpigradi remains concealed.

Miniaturization

Palpigradi are small (1–3 mm) when compared to most other arachnids. Only Acari [Parasitiformes (0.2–30 mm) and Acariformes (0.08–14 mm)] have smaller median body length (Dunlop 2019). Species of Micryphantinae, i.e., a taxon of Linyphiidae (Araneae) reach a similar body length of 1–4 mm. All other arachnids reach larger body sizes, e.g., Scorpiones (up to 210 mm body length), Solifugae (up to 70 mm body length), Amblypygi (up to 45 mm body length), or Thelyphonida (up to 75 mm body length). Extending the comparison to Euchelicerates and including fossil forms one encounters even larger body sizes. The observed trend in some euchelicerate groups towards a smaller body size might be considered evolu-

tionary miniaturization. Evolutionary miniaturization has been described for a number of invertebrate and vertebrate taxa (e.g., Hanken & Wake 1993; Polilov 2015a, 2016; Polilov & Makarova 2017; Dunlop 2019). As an evolutionary process, miniaturization results from directional selection on a large ancestor towards small body size; but the biological significance of scaling depends on the context in which size variation is studied. Reduction of body size may come along with a characteristic morphological pattern, e.g., (allometric) reduction of organ size, structural simplification (e.g., midgut differentiation simplified in insects; Polilov 2015a, 2016), complete loss of a structure or organ (e.g., lack of respiratory organs, lack of a heart in insects; Polilov 2015a, 2016), and proportionally large brains with small neurons.

A possible evolutionary mechanisms leading to reduced body size is heterochrony, specifically paedomorphosis (neoteny, progenesis/developmental truncation) resulting in the retention of larval structures within the adult (Gould 1977; Alberch et al. 1979). Progenesis / truncation is the accelerated maturation of an organism with respect to the overall somatic development. This is in contrast to neoteny that also produces paedomorphic adults, but results from retardation of organ development with respect to the overall development. Postdisplacement is the delayed start of development of an organ system at unchanged developmental rate and may result in paedomorphic appearance of adults (Gould 1977; Alberch 1980; McNamara 1986). According to Gould (1977) and McNamara (1986) all three processes produce paedomorphic adults, but only progenesis may lead to reduced body size. Alberch et al. (1979) introduced a more dynamic model of heterochrony also considering growth rate functions. In this model, all three processes potentially resulted in the same paedomorphic morphologies and reduced body size, and it was impossible deducing the ontogenetic mechanism from the study of adult organisms. The model by Alberch et al. (1979) also suggested that progenesis would result in reappearance of plesiomorphic features, what they called "*reverse recapitulation*". While this model is based on the assumptions of a strict anagenetic concept of evolution, it allows explicit predictions about the cumulative appearance of plesiomorphic features in a derived phylogenetic context.

Aims of the study

This study aims at providing a treatise of the complete microscopic anatomy of *Eukoenenia spelaea* (Peyerimhoff, 1902). By providing a detailed microscopic anatomical documentation of the species, we aim at re-evaluating the morphology of organ systems and body tagmatization of palpigrades based on explicit morphological evidence. We then proceed by providing a morphology based hypothesis about the phylogenetic position of Palpigradi among Euchelicerata and contribute to the ground pattern of euchelicerates/arachnids. This may be complicated by the fact that Palpigradi are rather characterized by plesiomorphic features than shared derived traits that would allow for a straightforward phylogenetic analysis. Therefore, we will test if paedomorphosis and evolutionary miniaturization may be associated with morphological simplification and/or enrichment of plesiomorphic features, thus creating the difficulty of analyzing their phylogenetic position among the arachnids. Supposing we find proof of evolutionary miniaturization of Palpigradi and paedomorphosis, the re-appearance of an array of plesiomorphic characters can become helpful in a phylogenetic analysis.

MATERIALS AND METHODS

Specimens

Eukoenenia spelaea is a troglobiont species found in caves of the Karst region in the European Alps and Carpathians (Christian et al. 2014), where they inhabit the sediments on the cave floor. Twenty-two specimens of *Eukoenenia spelaea* (Peyerimhoff, 1902) were collected in the Ardovská Cave (Slovak Aggtelek Karst, 48°31′18.613″ N, 20°25′13.798″ E) in April, July, and October 2016 and in August 2018. *Eukoenenia spelaea* occurs in four subspecies in Europe (Blick & Christian 2004). For Slovakia, *E. spelaea vagvoelgyii* (Szalay, 1956) has been determined as subspecies.

Access to the cave is restricted except for occasional visits by scientists, thus, it is largely undisturbed and has no artificial lighting. The temperature within Ardovská Cave ranges from +7.9 to +10.8 °C, and the humidity is approx. 97% (Kováč et al. 2002, 2014). The cave consists of numerous narrow passages as well as few larger caverns. It is characterized by the presence of stalactites and stalagmites of various sizes (Fig. 2A). The habitat of *Eukoenenia spelaea* are small patches of sediment consisting of mineral sediment, pieces of charcoal (brought in by scientists for an experimental setup on cave fauna), marten excrements, and bat guano (Fig. 2B).

The body length of the collected specimens without the flagellum was 1.23 mm ± 0.13 mm for adult females and 1.03 mm ± 0.13 mm for adult males. Nine animals (six females and three males) were fixed in buffered paraformaldehyde (PFA 5% in 0.1 mol l^{-1} phosphate buffered saline, pH 7.4). These animals were used for light microscopic (LM) histology and scanning electron microscopy (SEM). Ten animals (all females) were fixed using buffered glutardialdehyde (GDA 2.5% in 0.2 mol l^{-1} phosphate buffered saline, pH 7.4). These samples were used for transmission electron microscopy (TEM). Three specimens were fixed using a modified Karnovsky's fixative (GDA 2.5% and PFA 1.5% in 0.1 mol l^{-1} phosphate buffered saline, pH 7.4). All animal material (includ-

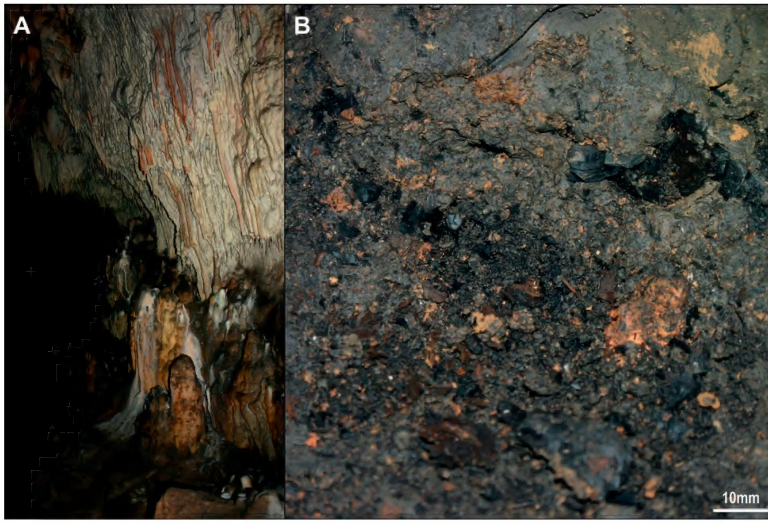

Fig. 2. Ardovská Cave, Slovakia. **A**. The cave is characterized by narrow passageways and large halls, where stalactites and stalagmites form the typical internal surface sculpturing of a karst cave. **B**. Close-up photograph of the habitat of *Eukoenenia spelaea*. The sediment consists of mineral sediments, pieces of charcoal, marten excrements, and bat guano.

ing unsectioned specimens) is stored at the Zoological State Collection in Munich, Germany (project numbers ZSMS20190030–ZSMS20190051).

Scanning electron microscopy

Scanning electron microscopy (SEM) was used to document the external anatomy of the animals. Fixed specimens were dehydrated through a graded series of acetone. The samples were then dried using the CO_2-critical point drying method. Samples were mounted on aluminum stubs and sputter coated for 200 s with gold. Images were captured using a LEO 1430VP SEM (LEO Elektronenmikroskopie GmbH, Oberkochen, Germany) and the software SmartSEM (version 5.07, Carl Zeiss AG, Oberkochen, Germany).

Histology

Specimens were washed four times in phosphate buffered saline (0.1 mol l^{-1}) over a period of 20 minutes, post fixed in 1% osmium tetroxide for two hours and washed again (four times, 20 minutes each) in phosphate buffered saline to remove excess osmium tetroxide. Samples were dehydrated through graded series of acetone (30–100%) and then embedded in Glycidether 100 (Carl Roth GmbH + Co. KG, Karlsruhe, Germany). Histological semithin sections were cut at 1.5 µm, 1 µm and 500 nm thickness using an RMC MTXL ultra-microtome (Boeckeler Instruments, Inc., Tucson, Arizona, USA) equipped with a histo Jumbo diamond knife (DiATOME Ltd, Biel, Switzerland). In order to obtain serial sections, the ventral side of the trimmed specimen block was covered with a thin layer of ethyl acetate/methyl cyclohexane glue (Pattex Kraftkleber Classic, Henkel AG & Co. KGaA, Düsseldorf, Germany) mixed with xylene in a 1:1 mixing ratio. The section bands were then collected in water, attached to a glass slide and dried. Sections were stained using Rüdeberg staining solution (Rüdeberg 1967). Light microscopic images were taken with an automated Olympus BX61VS microscope and DotSlide software (Olympus, Hamburg, Germany) or an Olympus BX51TF microscope (Olympus, Hamburg, Germany) equipped with a microscope camera (UCMOS camera, ToupTek Photonics, Hangzhou, P.R. China). Image capturing was processed via ToupView (ToupTek Photonics, Hangzhou, P.R. China). Image analysis was done using

OlyVIA (version 2.9, Build 13735, Olympus Soft Imaging Solutions GmbH, Münster, Germany).

Transmission electron microscopy

For transmission electron microscopy (TEM), ultrathin sections were cut at 50 nm thickness using an RMC MTXL ultra-microtome (Boeckeler Instruments, Inc., Tucson, Arizona, USA). Sections were collected on copper triple slot grids and contrasted using uranyl acetate and lead citrate following standard protocols (Reynolds 1963). For transmission electron microscopy, a Morgagni 268 electron microscope (FEI Company, Hillsboro, OR, USA) and MegaView III CCD – iTEM-SIS software (Olympus, Soft Imaging System GmbH, Münster, Germany) for image capture was used.

Image processing

All light microscopic (LM) and transmission electron microscopic (TEM) images were processed using ImageJ (version 1.50d, NIH, USA) and Adobe Photoshop CC 2014 (Adobe Systems Incorporated, San Jose, CA, USA). Image processing included background subtraction (LM), removal of non-relevant embedding material (TEM), and contrast enhancement. Assembly of images was done using Image Composite Editor (version 2.0.3.0, Microsoft Corporation, Redmond, WA, USA). Addition of labels and scale bars were done using Adobe Illustrator CC 2014 (Adobe Systems Incorporated, San Jose, CA, USA). To aid recognition of organs in some LM and TEM images, a color overlay was applied. The color code of the LM images corresponds with the color coding used in the schematic drawings.

Schematic drawings were created with Adobe Illustrator CC 2014 (Adobe Systems Incorporated, San Jose, CA, USA). They are strictly based on histological serial sections and 3D-reconstructions of the organ systems using Amira 6.0.0 (Mercury Computer Systems Inc., Chelmsford, MA, USA). Thus, the topography, the size and the shape of structures and organs are documented as precisely as possible based on the combination of two methods. The degree of interpretative illustration is minimal.

Phylogenetic analysis

The phylogenetic analysis is based on Shultz (2007a). He analyzed 59 euchelicerate taxa (41 extant, 18 fossil) coded for 202 binary and unordered multistate morphological characters. The matrix published by Shultz (2007a) was supplemented with additional data collected in this study, and several character states were added and updated according to new interpretations presented here (Appendix I: Tab. 6, Appendix II). Schultz (2007a) used a certain logic of construction of characters, i.e., some characters we consider as one character would be described as two, e.g.: carapace with distinct peltidial sclerites: 0 = absence; 1 = present, number of peltidial sclerites: 0 = two peltidia; 1 = three peltidia; inapplicable due to absence of sclerites. We consider such character as dependent of each other with restricted degrees of freedom and therefore consider them different states of one character (applies to characters 6, 32, 116, 131, 194, 198 in our table 6 (Appendix I)).

The newly described fossil *Chimerarachne yingi* was also included in the analysis based on the description of Wang et al. (2018). *Eukoenenia spelaea* was regarded as a separate taxon to allow independent analysis of its characters. Otherwise, the analysis was set up identical to Shultz (2007a), i.e., using Tree Analysis using New Technologies (TNT), but, the newer version 1.5 was used (Goloboff et al. 2008; Goloboff & Catalano 2016). The non-arachnid euchelicerate taxa, i.e., Xiphosurida, were chosen as outgroup. "Traditional" tree searches with 1000 replicates using TBR branch swapping were performed. Bootstrap percentages (Felsenstein 1985) and Bremer support (Bremer 1994) were calculated in TNT. Absolute bootstrap percentages were determined by 1000 pseudo-replicates, which were analyzed by ten random-addition replicates using TBR branch swapping, each. Absolut Bremer support was determined by measurement of the difference between the unconstrained and constrained minimal-length trees. Implied weights analysis (Goloboff 1993) was performed to examine homoplasy effects. Implied weights analyses with constant of concavity (k) values of 1–6 were conducted using "traditional" search based on 1000 replicates using TBR branch swapping. Lower k-values are weighted more strongly against homoplastic characters while higher k-values are weighted less.

Terminology

We wish to keep terminology neutral and simple without implications of unproven "homologies". Therefore, numbering of the body segments starts with 1 for the first segment (the "ocular" segment) and not with zero as used by several authors (Millot 1949b; van der Hammen 1989; Shultz 2007b; Dunlop & Lamsdell 2017).

The terminology of the articles of the pedipalps and legs is confusing and loaded with homology implications and inductive evolutionary reasoning (e.g., van der Hammen 1977b; Boxshall 2004; Waloszek et al. 2005; Dunlop & Alberti 2008; see also Tab. 8). Therefore, articles of appendages are numbered starting with 1 for the most proximal article (Tab. 8). Possible homologies are discussed.

RESULTS

Individuals of *Eukoenenia spelaea* are small and delicate with an elongate body shape, a long terminal flagellum, and a light, almost translucent body (Figs 3–4). The body length of the analyzed specimens varied between 0.90 mm and 1.35 mm (without the flagellum). The entire body is covered by a dense pubescence (Pub; Fig. 9), i.e., filiform cuticular microstructures ranging in length between 2 µm and 3 µm. Numerous large, spiked sensory setae (SS; Figs 3–4, 9; Tabs 1–4) are arranged on the body surface. The number and position of the setae was the same in all individuals. However, the number of setae associated with the genitalia differed between males and females (Tab. 3). We also observed a slight sexual dimorphism in the shape of the genitalia, the body length (females 1.23 ± 0.13 mm, males 1.03 ± 0.13 mm), the extent of imbrication of the opisthosomal tergites, and the musculature of prosoma and opisthosoma (see below).

External morphology

The tagmatization of *Eukoenenia spelaea* (Figs 3–5) follows the typical eucheliceratе body plan with a prosoma and an opisthosoma. The prosoma (seven segments) carries the extremities, i.e., the chelicerae, the pedipalps and four pairs of legs (Ch, PP, L1–4; Figs 3–5). The opisthosoma (11 segments) is subdivided into an anterior mesosoma (seven segments) and a posterior metasoma (four segments). The metasoma carries a terminal flagellum with 15 articles (Figs 3B, 4B). The flagellum has approximately the length of the entire body.

Prosoma dorsum

The seven segments of the prosoma are partially merged forming topographically distinct sclerites; however, the borders between sclerites differ on the dorsal and the ventral sides of the prosoma (Figs 3–5). Dorsally, the prosoma is covered by three sclerites that have traditionally been considered tergites and termed pro-, meso- and metapeltidium. As will be shown below, the propeltidium is the common dorsal sclerite (tergite) of segments 1–6 (not 1–5 as considered traditionally) with a posterior imbrication. The posterior end of the propeltidium tapers off and partially covers the mesopeltidium as well as the most anterior part of the metapeltidium (PrPlt, PaPlt, MtPlt; Figs 3A, C, 5A–B). The mesopeltidium is represented by a pair of small, poorly sclerotized, dorsolateral sclerites in the region of leg 3, and partially covers the anterior part of the metapeltidium. We will show below that the mesopeltidium is not a tergite, but a sclerotization of the dorsolateral pleural membrane. We therefore suggest the term *"lateral dorsal plate"* which will be used from here on. The metapeltidium is the tergite of segment 7, roughly triangular shaped with the pointed end towards anterior, and a broad margin towards posterior. It extends from the region between leg 2 and 3, i.e., at the beginning of the overhang of the propeltidium, to the end of the prosoma (Figs 3A, C, 5A–B). Each prosomal sclerite carries a fixed number of setae in the same topographic positions (Tab. 1).

Prosoma ventrum

The ventral side of the prosoma has four sclerites (Fig. 3D). A large anterior sclerite covers segments 2–4 (Figs 3D, 5C). This element has been termed deutotritosternum and was considered to contain 'epimera' of segments 2 and 3 (van der Hammen 1982). However, we provide evidence that it contains 3 prosomal sclerites related to segments 2–4. At its anterior margin, it has a medial concavity, which embraces the ventral plate (VP; Fig. 3D). Segments 5–7 carry individual segmental sclerites (Figs 3D, 5C). They cover the entire region between the first articles of the legs. All ventral prosomal sclerites are free of setae, with the exception of the larger anterior sclerite, which carries six setae (Tab. 1).

Table 1. *Eukoenenia spelaea*, number of setae located on the prosoma. The mesopeltidium is termed here "lateral dorsal plate" (see discussion). The fused sternite of segments 2–4 is termed here "prosternum" (see discussion).

	Number
Propeltidium	14(29)*
Lateral dorsal plate	–
Metapeltidium	6
Prosternum	6(5)*

* It is widely reported in the literature that individuals of *E. spelaea* have 20 setae on propeltidium (e.g., Christian et al. 2014, Condé 1956, Condé 1972). We give those literature values in brackets.

Ventral plate

In ventral view, the large lower lip covers the mouth opening and the bases of the chelicerae (Fig. 3D). Directly behind the posterior end of the lower lip, located in a notch of the anterior margin of the prosternum is a large ventral plate with a unique morphology (VP; Figs 3D, 6). The plate is externally covered with uniform cuticular teeth pointing to the posterior. They are approx. 2 µm long, 0.4 µm thick at the base and pointed (cT; Fig. 6B).

Rostrosoma

We use the term "rostrosoma" as a topographic description of the body region carrying the moth opening and associated structures; the term as used here does not imply a-priori homologies to the rostrosoma of other chelicerates (e.g., van der Hammen 1989). The rostrosoma is a prominent tubular structure hosting the preoral cavity, the mouth opening, and anterior parts of the pharynx. It originates ventromedial between the bases of the chelicerae and protrudes towards anterior, where it is nestled between the basal articles of the chelicerae (ROS; Fig. 3D). Anterior, the rostrosoma extends into an upper and a lower lip (Fig. 7). The upper lip forms lateral walls overarching the lower lip. These lateral walls emerge right from the point where upper and lower lip separate from the cuticular tube and extend to the anterior end of the lower lip (LL, UL; Fig. 7F). There, the left and the right lateral walls merge forming an anterior overhang in front of the lower lip. This anterior overhang of the upper lip is covered with a coarse pubescence on the outside and fine-toothed transversal ridges on the inside (tR; Fig. 7B, D–F). Five small setae insert on each side at the ventral margin of the upper lip (Fig. 7E). The lower lip extends into the anterior overhang of the upper lip where its cuticle also forms fine-toothed, transversal ridges. These transversal ridges probably function as counterparts to the transversal ridges on the inner side of the upper lip (tR; Fig. 7D). Fine-toothed, transversal ridges cover the ventral side of the lower lip. Each of these ridges intercalates laterally with two sections of elongated, hook-like teeth (fT, hT; Fig. 7E).

The mouth opening is small and located where upper and lower lip merge into a cuticular tube. Here, two sclerotized knobs reach from the inner surface of the upper lip to the lower lip (*, Fig. 7C–D, F). The cavity anterior to these knobs is the preoral cavity. The pharynx with its associated musculature is housed in the tubular part of the rostrosoma.

Sensory organs on the prosoma

The prosoma carries several sensory organs, i.e., the frontal organ, the paired lateral organs, numerous sensory setae, and trichobothria. The frontal organ is located dorsally on the apex of the prosoma and is partially covered by the propeltidium (FO; Fig. 3A, C). The frontal organ is unpaired and has a base that carries two modified setae. Each of these setae is approx. 25 µm long and has a diameter of approx. 5 µm. The cuticular surface of the frontal organ carries a honeycomb pattern (Fig. 8A) formed by cuticular ridges and pits.

The lateral organs are left and right dorsolateral under the propeltidium, above the base of the pedipalps (LO; Figs 3A, C). However, an explicit association with a prosomal segment is not possible because prosomal segments 1–6 are fused dorsally. Each lateral organ consists of four modified setae. These setae are similar in shape and size to the setae of the frontal organ (approx. 25 µm long and 4.5 µm in diameter; Fig. 8B). Their cuticular surface also carries a honeycomb pattern like the frontal organ. The surface of the pits, which are surrounded by the cuticular ridges, has cuticular grooves.

The entire animal carries numerous sensory setae. The topographic arrangement of sensory setae on the surface of the body was the same in all individuals studied (Fig. 3; Tabs 1–4). The spiked setae can reach up to 120 µm in length. Each sensory seta inserts on a circular socket (diameter approx. 2 µm) in the cuticle and is flexible (Fig. 9). The diameter of the sensory setae decreases gradually from base (approx. 1.2 µm) to tip (approx. 0.8 µm).

In *Eukoenenia spelaea*, trichobothria are exclusively located on the first pair of legs. The topographic distribution of trichobothria on the leg is as follows: article 4 carries one, article 6 carries four, and articles 8 and 10 carry one trichobothrium each (Fig. 3A). The trichobothria on articles 4, 8, and 10 are oriented toward dorsolateral and distal, i.e., away from the body median line. The four trichobothria on article 6 are arranged along a cuticular groove on the surface of the article. Of those four trichobothria, two insert distal to the cuticular groove, and the other two proximal (cGR, Fig. 3A). All trichobothria root in a cuticular, cup-shaped socket (bothrium, diameter approx. 6 µm) with a toothed rim (tBR, Tr; Fig. 9). The cuticular teeth surrounding the socket are approx. 1 µm long and 0.2 µm thick at the base (Fig. 9B). The maximum deflection of the seta before touching the cuticular teeth of the socket is 25–30°. The seta is longer (approx. 250 µm) and thinner (diameter consistently approx. 0.8 µm) than other sensory setae.

Chelicerae

The chelicerae are proportionally large, and are oriented straight towards anterior. They have three articles, i.e., the basal article, the fixed digit, and the movable digit, which together, form a chela (FD, MD; Figs 3A, 4C, 10A). The basal article has approximately the same length as the chela. The propeltidium overlaps parts of the basal article. The basal article is covered in pubes-

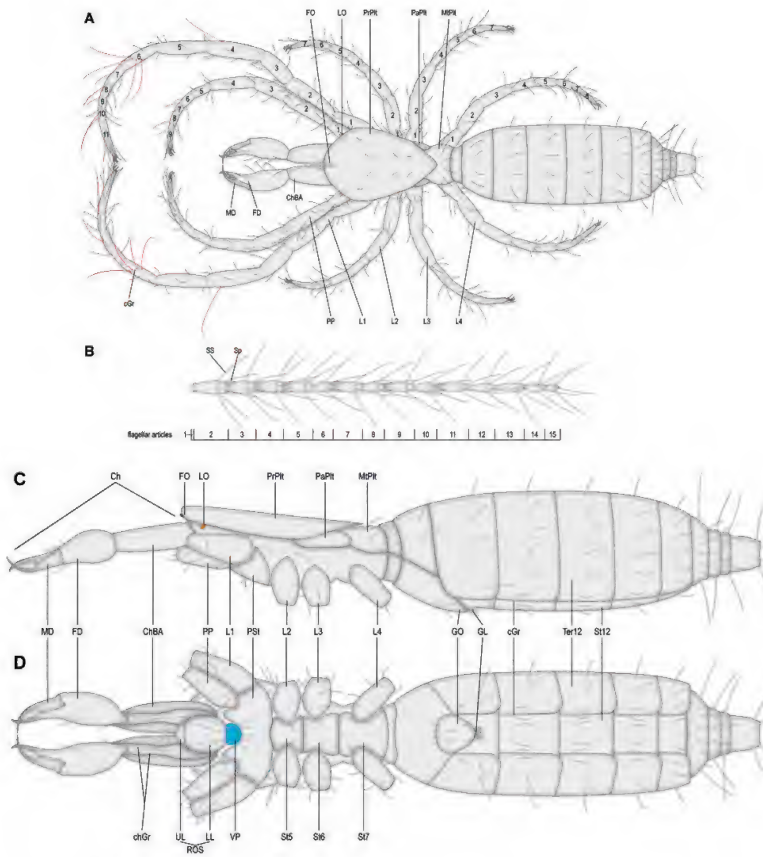

Fig. 3. *Eukoenenia spelaea* (Peyerimhoff, 1902), schematic drawing based on light microscopic and scanning electron microscopic images. **A**. Dorsally, the prosoma is divided into a pro-, para- (see discussion), and metapeltidium. The opisthosoma tapers off in segment 15. The chelicerae consist of three articles. Arabic numbers indicate leg articles, starting with 1 for the most proximal article. The frontal organ (green) and the lateral organ (orange) are largely covered by the propeltidium. Trichobothria are highlighted in red. **B**. The flagellum. Long setae are less numerous than spikes and located more proximal on the articles. **C**. Lateral view of a female. The frontal organ is nested underneath the anterior end of the propeltidium. **D**. Ventral view of a female. The prosternum (see discussion) is a fusion of ventral sclerites associated with the chelicerae, pedipalps and the 1st leg. The previously undescribed ventral plate (blue), is located between the rostrosoma and prosternum. Only large spiked setae are depicted. Abbreviations: Ch = Chelicerae; ChBA = cheliceral basal article; cGr = cuticular groove; chGr = cheliceral groove; FD = fixed digit; FO = frontal organ; GL = genital lobe; GO = genital operculum; L1–4 = leg 1–4; LL = lower lip; LO = lateral organ; MD = movable digit; MtPlt = metapeltidium; PaPlt = lateral dorsal plate; PP = pedipalp; PrPlt = propeltidium; PSt = prosternum; ROS = Rostrosoma; St = sternum; Ter = tergite; UL = upper lip; VP = ventral plate.

Table 2. *Eukoenenia spelaea*, number of setae located on each article of the extremities, excluding trichobothria on leg 1.

	Coxa/ basal article	Art. 2/ fixed digit	Art. 3/ movable digit	Art. 4	Art. 5	Art. 6	Art. 7	Art. 8	Art. 9	Art. 10	Art. 11
Chelicera	6(10)[1]	6(7)[1]	–	n.a.	n.a.	n.a.	n.a.	n.a.	n.a.	n.a.	n.a.
Pedipalp	19	9	7(8)[2]	10	3	6	1	6	20(24)[2]	n.a.	n.a.
Leg 1	15	13	9	9	9	9(8)[2]	4(3)[1,2]	5	4(5)[2]	6	22(25)[2]
Leg 2	13(14)[1,2]	3	5	5	5	4	11	n.a.	n.a.	n.a.	n.a.
Leg 3	13	3	5	5	5	4	11	n.a.	n.a.	n.a.	n.a.
Leg 4	10(9)[1,2]	3	3	5	4(5)[2]	4	4(5)[2]	7	n.a.	n.a.	n.a.

[1] Christian et al. (2010), [2] reviewer comment, unpublished material

Table 3. *Eukoenenia spelaea*, number of setae located on opisthosomal segments (S) 8–19. The number of setae on the genital plates are listed separately.

	S8	S9	S10	S11	S12	S13	S14	S15	S16	S17	S18
Tergite	–	8	12	12[1]	12[1]	12[1]	14	12	10	8	8
Sternite	–	4	–	4	4	4	2	4	4	n.a.	n.a.
Genitalia ♀	n.a.	22	n.a.	n.a.	n.a.	n.a.	n.a.	n.a.	n.a.	n.a.	n.a.
Genitalia ♂	n.a.	32	n.a.	n.a.	n.a.	n.a.	n.a.	n.a.	n.a.	n.a.	n.a.

[1] The taxonomic literature represents distinctly different numbers, probably because tergite and sternite are differently deliminated. The border between both sclerites is extremely difficult to see. Based on our histological samples, we recognize that the tergites reach far to the ventral site (Fig 3); taxonomic standard is tergite with 8 setae, sternite with 10 setae (with variability possible; Christian pers. comment)

Table 4. *Eukoenenia spelaea*, number of setae and spikes located on each article of the flagellum.

	Art. 1	Art. 2	Art. 3	Art. 4	Art. 5	Art. 6	Art. 7	Art. 8	Art. 9	Art. 10	Art. 11	Art. 12	Art. 13	Art. 14	Art. 15
Setae	4	11	10	10	10	8	8	8	8	8	7	7	7	7	6
Spikes		14	14	14	–	13	–	13	–	12	–	–	–	–	–

cence. Two cuticular grooves span along the entire length of the ventral side of the basal article. The lateral walls of these grooves are knobbed (arrows; Fig. 10B), whereas their inner ridge is smooth like the rest of the ventral side of the basal article. The medial face of the basal articles is concave providing space for the rostrosoma (Figs 3D, 7A).

The main body of the fixed digit is covered in pubescence, however, the medial faces of the chelicerae are smooth (*; Fig. 10A). We counted twelve setae on each chelicera: six on the basal article and six on the fixed digit (the taxonomic literature reports 10 and 7 setae on basis and hand, respectively; Christian et al. 2010). The movable digit has no setae (Figs 3, 10; Tab. 2). The teethed sections of the movable and fixed digits carry eight serrated teeth each (sT; Fig. 10A, C–D). The distance between the teeth is approx. 1–1.5 µm, and approx. 0.05–0.1 µm between the serrations on the teeth. The tips of the digits are elongated and almost as long as the toothed section of the digits. The tips cross each other (Figs 3, 10A, C).

Pedipalps and legs

All extremities carry numerous setae and a terminal claw (Tab. 2). The pedipalps and the first leg are both distinctly longer than the other legs, have more articles, and are directed to the anterior. The pedipalps and leg 1 are palp shaped. In this species, only leg 1 carries trichobothria (Fig. 3A). – The pedipalps are divided into nine articles. Leg 1 is the longest pair of extremities, it has 11 articles.

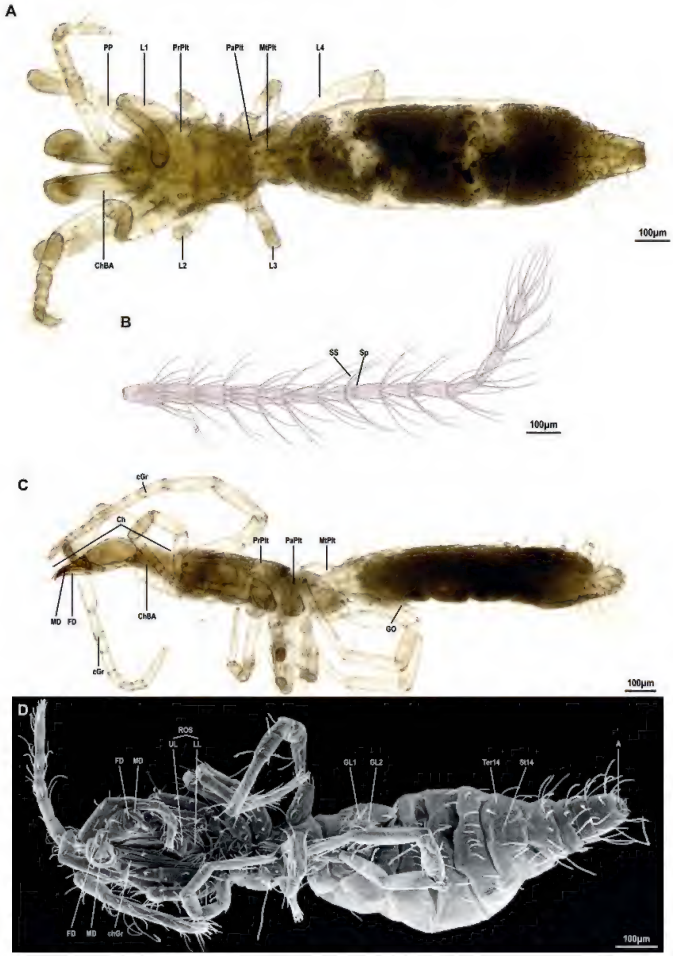

Fig. 4. *Eukoenenia spelaea* Peyerimhoff, 1902), overview images. **A**. Dorsal view of a female, light microscopy. **B**. Lateral view of a flagellum, light microscopy. **C.** Lateral view of a female, light microscopy. Sternites cannot be clearly seen due to the drying process. **D**. Ventral view of a male, scanning electron micrograph. Abbreviations: A = anus; cGr = cuticular groove; Ch = Chelicerae; ChBA = cheliceral basal article; chGr = cheliceral groove; FD = fixed digit; GL = genital lobe; GO = genital operculum; L1–4 = leg 1–4; LL = lower lip; MD = movable digit; MtPlt = metapeltidium; PaPlt = lateral dorsal plate; PP = pedipalp; PrPlt = propeltidium; ROS = Rostrosoma; SS = sensory seta; Sp = spike; St = sternite; Ter = tergite; UL = upper lip.

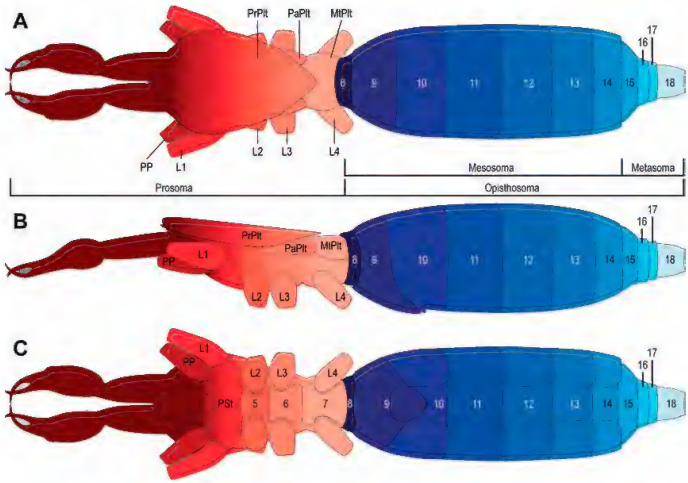

Fig. 5. *Eukoenenia spelaea* (Peyerimhoff, 1902), segmentation. Prosomal structures are marked in shades of red, opisthosomal structures are marked in shades of blue. Every hue marks a segment. **A**. Dorsal view. The propeltidium (horizontal hatching lines) extends to the level between the 3rd and 4th leg. The lateral dorsal plate (vertical hatching lines) is located at the level of the 3rd leg. The metapeltidium (diagonal hatching lines) covers the dorsum of the 7th prosomal segment, but extends anteriorly to the level between leg 2 and 3. The mesosomal segments 8–14 carry segmental tergites and sternites; the metasomal segments 15–18 have sclerotized rings instead of tergites and sternites. **B**. Lateral view. In lateral view, the prosomal segments are difficult to discern as there are no visible cuticular structures indicating segment borders. Opisthosomal segments are clearly delimited by their sclerites. **C**. Ventral view. Fused sclerites of the cheliceral segment, the pedipalpal segment and the segment of the 1st leg form a prosternum. Segments 5–7 carry individual ventral sclerites. Numbers indicate segments. Abbreviations: L1–4 = leg 1–4; MtPlt = metapeltidium; PaPlt = lateral dorsal plate; PP = pedipalp; PrPlt = propeltidium; PSt = prosternum.

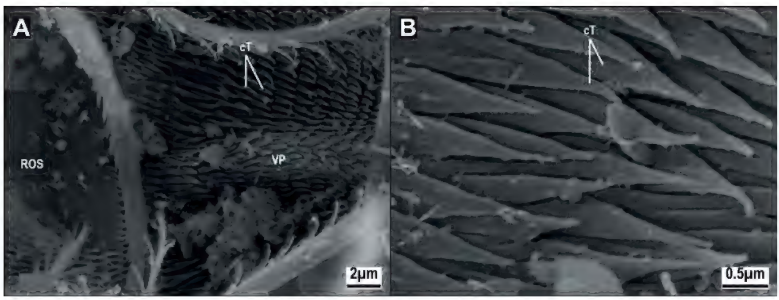

Fig. 6. *Eukoenenia spelaea* (Peyerimhoff, 1902), scanning electron micrographs of the ventral plate. **A**. Ventral view of the ventral plate. The cuticular teeth are arranged in even rows pointing posteriorly. **B**. Close-up image of the cuticular teeth. The teeth are elongated and taper off at the tip. Abbreviations: cT = cuticular teeth; ROS = rostrosoma; VP = ventral plate.

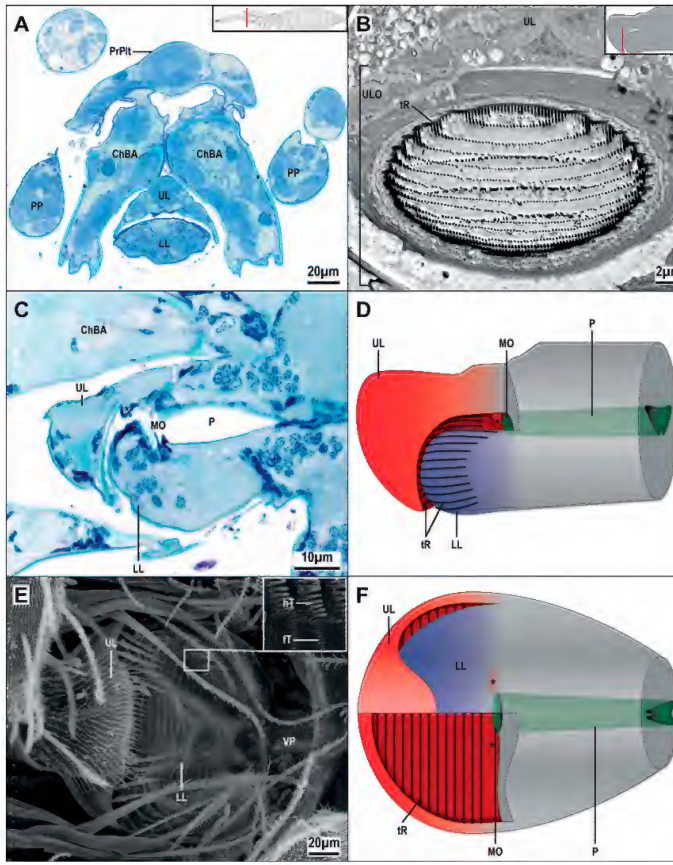

Fig. 7. *Eukoenenia spelaea* (Peyerimhoff, 1902), rostrosoma. **A**. Light micrograph of a cross-section through the rostrosoma anterior to the mouth opening (inset). The rostrosoma is nestled between the cheliceral basal articles. **B**. Transmission electron micrograph of cross-section of the anterior overhang of the upper lip (inset). The toothed ridges are spaced regularly. **C**. Light micrograph of a slightly oblique longitudinal section of the rostrosoma. The mouth opening lies posteriorly of the lateral protrusions (asterisk) of the upper lip. **D**. Lateral view of the rostrosoma, schematic drawing based on longitudinal and cross-section light micrographs. Parts of the upper lip (red) have been removed to display the mouth opening. The grey area indicates that upper and lower lip are fused. **E**. Ventral view of the rostrosoma, scanning electron micrograph. The lower lip is covered in finely toothed ridges and hook-like teeth (inset). **F**. Ventral view of the rostrosoma, schematic drawing based on cross-section light micrographs as well as scanning electron micrographs. Parts of the upper and lower lip have been removed to display the close association of the lateral protrusions with the mouth opening. Abbreviations: ChBA = cheliceral basal article; fT = fine tooth; hT = hook-like tooth; LL = lower lip; MO = mouth opening; P = pharynx; PP = pedipalp; PrPlt = propeltidium; tR = toothed ridge; asterisk = lateral protrusions of functional upper lip; UL =upper lip; ULO = lip overhang; VP = ventral plate.

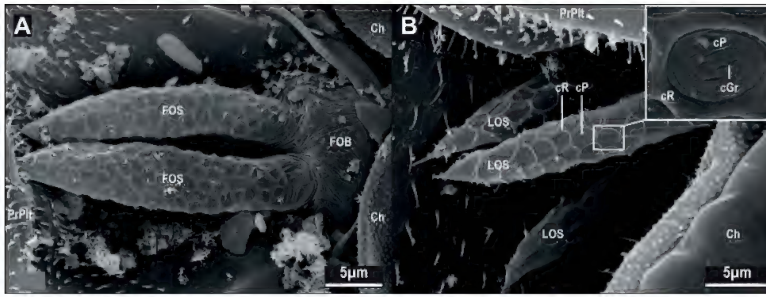

Fig. 8. *Eukoenenia spelaea* (Peyerimhoff, 1902), scanning electron micrographs of the frontal organ and lateral organ. **A**. Ventral view of the frontal organ. It consists of a base and two modified setae. The cuticular structure of the base is irregular. The setae carry a cuticular honeycomb pattern. **B**. Ventral view of the lateral organ. It consists of four modified setae. The setae carry the same honeycomb surface pattern like the frontal organ. The cuticular ridges form pits with grooved openings in the cuticle (inset). Abbreviations: Ch = chelicera; cGr = cuticular groove; cP = cuticular pit; cR = cuticular ridge; FOB = frontal organ base; FOS = frontal organ seta; LOS = lateral organ seta; PrPlt = propeltidium.

The most proximal articles of the pedipalps and leg 1 are elongate as compared to those of the following legs. Article 6 of leg 1 shows a cuticular groove which spans the entire article diagonally (Figs 3A, 4C). Legs 2 and 3 are located on segments 5 and 6, respectively. They are both oriented towards lateral and consist of seven articles. In both legs, the proximal article is short and appears wider than those of the other legs. Leg 4, is located in segment 7. It is oriented posteriorly and consists of eight articles. Its proximal article is elongated and borders the posterior ventral sclerite.

The articulations between articles of the legs are located dorsally in all appendages and all articles (Fig. 11A–C). In figure 11, we used the formalized schematic of van der Hammen (1977a) to document the position of joints and muscle/tendon attachments for a later comparative discussion. Despite this, the articulations between articles are rather like a broad ridge in the proximal articles (1/2–4/5, Fig. 11D–E) and rather like a point articulation in the distal articles (5/6–x/y). The membrane connecting the articles displays a knobbed surface (Fig. 11F). The articulations between the first article and the body could not be clearly determined.

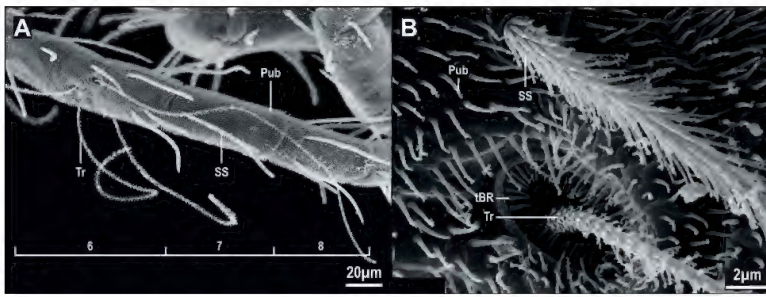

Fig. 9. *Eukoenenia spelaea* (Peyerimhoff, 1902), scanning electron micrographs of the different types of sensory hairs. **A**. Trichobothria and sensory hairs on articles 6–8 of leg 1. There are noticeable differences in length and thickness between sensory setae and trichobothria. **B**. Close-up of the bases of a sensory seta and a trichobothrium. The sensory seta is thicker and its spikes are longer than in the trichobothrium. However, the cuticular socket of the sensory seta is an approx. 3-fold smaller than that of the trichobothrium. The protuberances of the pubescence have no sockets. Abbreviations: Pub = pubescence; SS = sensory seta; tBR = toothed bothrial rim; Tr = trichobothrium.

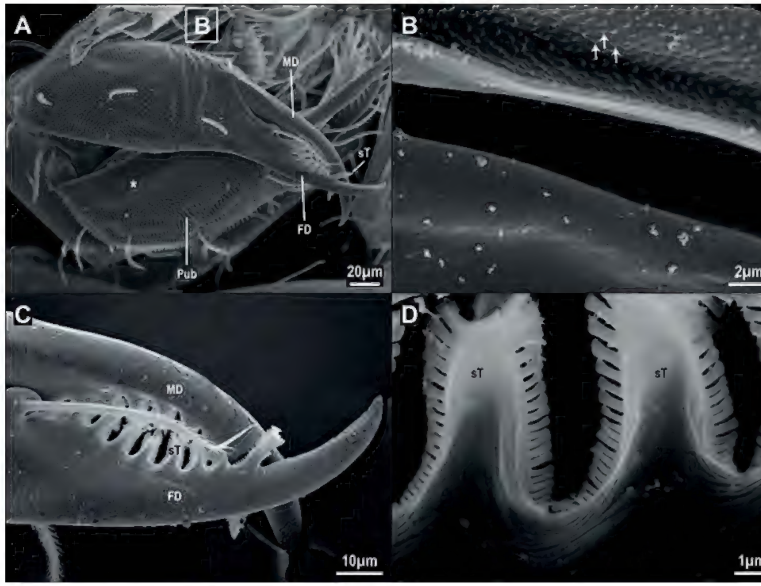

Fig. 10. *Eukoenenia spelaea* (Peyerimhoff, 1902), scanning electron micrographs of the chelicerae. **A**. Dorsal view of the fixed and the movable digits. The inward oriented part of the main body of the fixed digit is free of pubescence (asterisk). The basal article displays cuticular grooves (see B). **B**. The ridges of the lateral basal article grooves are knobbed (arrows), the central ridge is smooth. **C**) The tips of the cheliceral digits are crossed. **D**. Close-up image of the teethed section of the cheliceral digits. The teeth are serrated. Abbreviations: FD = fixed digit; MD = movable digit; Pub = pubescence; sT = serrated tooth.

Opisthosoma

The opisthosoma has 11 segments and is subdivided into a mesosoma (segments 8–14) and a metasoma (segments 15–18; Figs 3–5). Segment borders are recognized by the anterior and the posterior margins of the tergites and sternites, respectively (Figs 3–4). Mesosoma and metasoma are distinguished by their sclerites, i.e., segments of the mesosoma carry dorsal and ventral sclerites, and segments of the metasoma carry cuticular rings surrounding the entire segments. In the mesosoma, segment 8 is short and has a smaller diameter than the following six segments. In segments 9–17, the dorsal sclerites are imbricated forming posterior overhangs that reach over the anterior part of the following segment. In females, these overhangs are thicker than in males (SD; Fig. 12A–B), i.e., the base of the overhang is up to 20 µm wide while the distal part tapers off gradually (Fig. 12A). In males, the base of the overhang is 5 µm wide and the distal part is evenly thin (diameter max. 1 µm; Fig. 12B).

The segments of the metasoma, 15–18, decrease in diameter (Fig. 5). Attached to the last segment is a sclerotized ring, which is the base of the flagellum (Fig. 13). The anus is located between segment 18 and the annular basal article of the flagellum, i.e., ventral to the base of the flagellum. The number of setae on each segment were consistent in all individuals, except for the sex-specific number of setae on the genital plate (Tab. 3).

Opisthosomal sclerites

The tergites of the mesosomal segments expand far laterally (Figs 3C–D). The tergites of segments 8 and 9 reach to the lateral midline where they meet their respective sternites. In segments 10–14, the tergites reach further down to the ventral side (Fig. 12C), and the sternites of these segments are reduced to small medial sclerites.

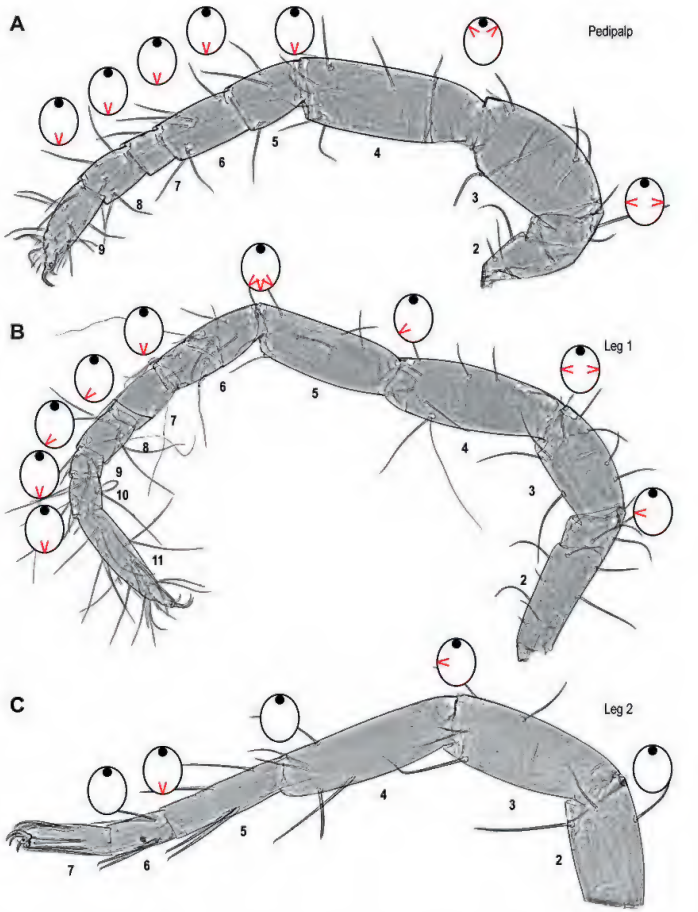

Fig. 11. *Eukoenenia spelaea* (Peyerimhoff, 1902), frontal views of pedipalp, leg 1 and leg 2 from the right side of the prosoma. Contrast enhanced light micrographs. The icons follow the formalized scheme of van der Hammen 1977a) documenting the position of the joints and muscle attachment sites for each article. Articles of the appendage are numbered, the black dot in the icon shows the position of the hinge, red arrow heads indicate the muscle/tendon attachment. **A**. Pedipalp. Muscle attachment in the joint between articles 2 and 3 are lateral. The muscle attachment at the following joint (3/4), has shifted to latero-dorsal. All distal muscle attachments are ventral. **B**. Leg 1. Two or three muscle attachment sites can only be found in the joints connecting articles 3/4 and 5/6, respectively. Single muscle attachment in all other joints is predominately located ventral and ventrolateral. **C**. Leg 2. Only two joints with muscle attachment sites are found in this leg. In the joint between articles 3 and 4, the attachment is located laterally, in the joint between articles 5 and 6, the attachment is ventral. All other joints lack any muscle attachments. – *continued.*

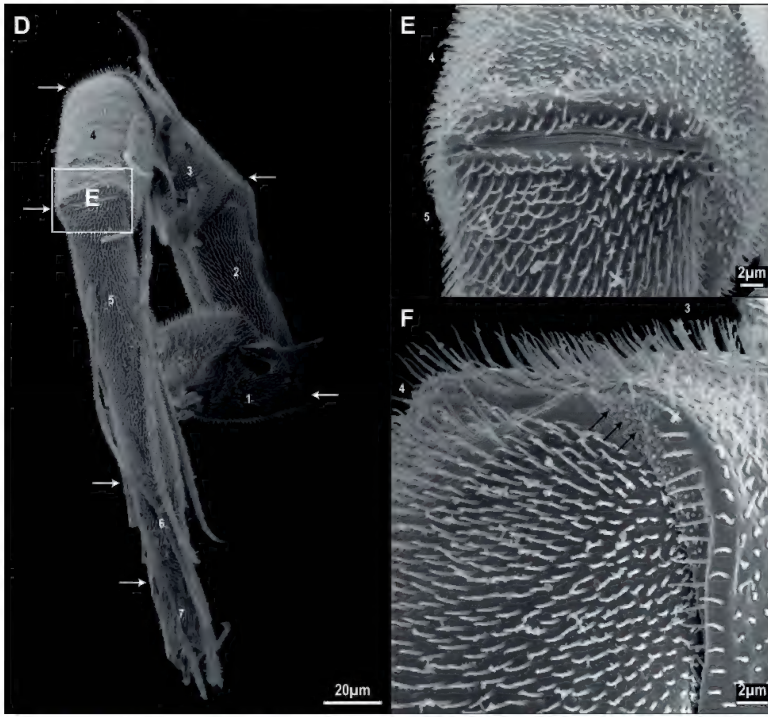

Fig. 11 *continued*. *Eukoenenia spelaea* (Peyerimhoff, 1902), joints on leg 2. Scanning electron micrographs. Numbers indicate the leg's articles. **D**. Overview of leg 2. Arrows indicate the location of the joints. Between the proximal articles (1/2, 2/3, 3/4, 4/5) the joint is broader than between the distal articles (5/6, 6/7). The same configuration can be found in the legs and the pedipalp. **E**. Articulation between articles 4 and 5. The articulation is a broad ridge. **F**. Close-up oblique view of the joint between articles 3 and 4. The membrane connecting both articles has a knobbed surface (arrows).

Each segment of the metasoma, 15–18, carries a cuticular ring surrounding the entire segment (Figs 3, 5).

On the ventral side of the mesosoma, the sternites differ between segments. The sternites are more distinct in males than in females. In both sexes, the cuticle of the sternites of segments 8–14 is weakly sclerotized and forms folds, which are particularly well developed on the lateral side of the sternite (Fig. 12C–E). The sternites of segments 8 and 9 cover the entire ventral side of the animal's body (Fig. 3C–D). The ventrum of segment 9 also carries the genital plate, which gives it a unique morphology (see below; Fig. 14). In segment 10, the sternite is restricted to the middle part of the ventral side (Fig. 3D). The anterior part of this sternite is also involved in building the genital plate, the rest of the sternite is shaped evenly. The sternites of segments 10–14 overlap posteriorly. A groove is vaguely perceptible between the tergite and the sternite (Fig. 3D).

Genital segment

In females, the external genital apparatus is formed by the genital operculum and the paired genital lobes (GL, GO; Figs 3C–D, 14A–C) which, however, are almost

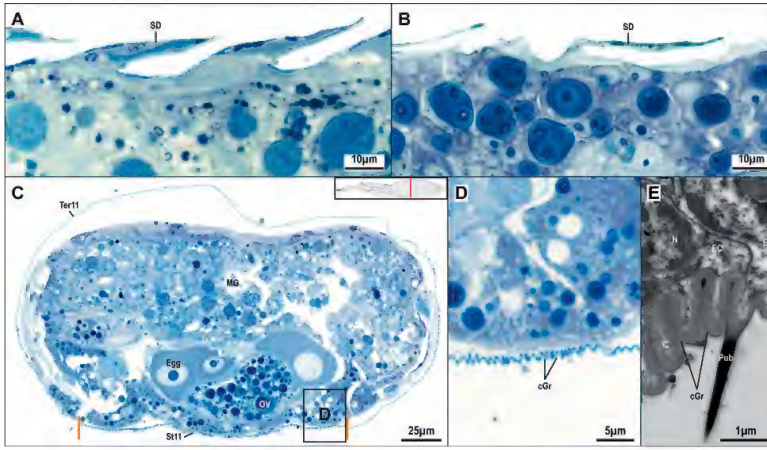

Fig. 12. *Eukoenenia spelaea* (Peyerimhoff, 1902), structure of the cuticle. **A**. Female, light micrograph of a sagittal section of the opisthosoma. Two segments are shown with their dorsal sclerites. The sclerites overlap broadly. The base of the sclerite duplicature is between 10 µm and 20 µm wide. The distal part of the duplicature is thicker in females than in males (see B). **B**. Light micrograph of longitudinal section of the opisthosoma cuticle of a male. The base of the duplicature is approx. 5 µm wide. The distal part of the duplicature is max. 1 µm in thickness. **C**. Light micrograph of a cross-section through segment 11 (inset). The ventral sclerite carries cuticular folds laterally. Orange lines indicate the border of tergite and sternite. **D**. High power light micrograph of the lateral region of the sternite from C. The cuticular folds are clearly visible. **E**. Transmission electron micrograph of cross-section of the same region as D. The cuticle in this area is thin compared to the neighboring areas. Abbreviations: C = cuticle; cF = cuticular folds; EC = epidermal cell; MG = midgut; N = nucleus; OV = ovary; Pub = pubescence; SD = sclerite duplicature; St11 = sternite of segment 11; Ter11 = tergite of segment 11.

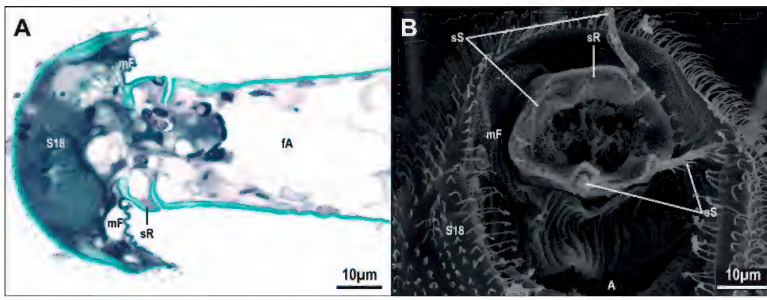

Fig. 13. *Eukoenenia spelaea* (Peyerimhoff, 1902), structure of the terminal ring. **A**. Light micrograph of longitudinal section through the terminal structures. The sclerotized ring is articulated with segment 18 and the following flagellar article. **B**. Scanning electron micrograph of the sclerotized ring, viewed from posterior. The membranous fold between segment 18 and flagellar base lacks pubescence but shows a knobbed structure. Four short setae insert on the sclerotized ring. Abbreviations: A = anus; fA = flagellar article; mF = membranous fold; S18 = segment 18; sR = sclerotized ring; sS = short seta.

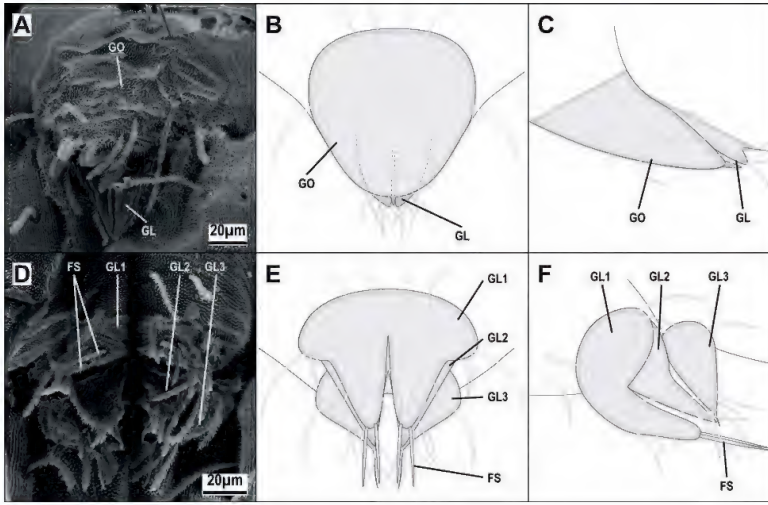

Fig. 14. *Eukoenenia spelaea* (Peyerimhoff, 1902), genital structures. **A**. Scanning electron micrograph of female genitalia in slightly oblique dorsal view. The genital operculum covers the genital lobes. **B**. Schematic drawing of female genitalia in dorsal view. The extension of the genital operculum is elongated. **C**. Schematic drawing of female genitalia in lateral view. The finger-like genital lobes originate at the junction of segments 9 and 10. **D**. Scanning electron micrograph of male genitalia in dorsal view. The number of setae is larger in comparison to the female genitalia. **E**. Schematic drawing of male genitalia in dorsal view. The base of the first pair of genital lobes is broadest compared to genital lobes 2 and 3. At the base, all genital lobes are closely together, at their tips, the lobes are spread farther apart. **F**. Schematic drawing of male genitalia in lateral view. The first pair of genital lobes has a rounded tip, whereas lobes 2 and 3 are pointed. The paired fusules originate on genital lobe 1. These fusules extend posterior past genital lobe 3. Abbreviations: FS = fusules; GL = genital lobe; GO = genital operculum.

entirely covered by the genital operculum. The genital operculum is formed by the sternite of segment 9; the genital lobes originate at the junction of segments 9 and 10. At its posterior end, the genital operculum shows a short extension, whose sides arch upward to create a tube-like structure. The genital operculum carries 16 setae, the genital lobes carry three setae each (Fig. 14A–C; Tab. 3).

In males, the external genital apparatus consists of three pairs of genital lobes. Two pairs of genital lobes emerge from the central and posterior part of segment 9, probably representing the genital operculum, followed by a third pair of genital lobes originating at the border to segment 10. The first pair of genital lobes has a broad base and two finger-like processes. At the tip of each process are two adjoining fusules (FS, GL1; Fig. 14D–F). The second pair of genital lobes, originating from the posterior part of segment 9, is located just posterior to the first pair and has triangular-shaped lobes (GL2; Fig. 14D–F). The third pair of genital lobes is similar in shape to the second pair, but ends in two needle-like processes (GL3; Fig. 14D–F). The tips of the lobes are in contact with the tips of the preceding lobes. A total of 32 setae are located on the genital lobes: 18 on the first pair, six on the second pair, and eight on the third pair (Fig. 14D–F; Tab. 3).

Flagellum

The flagellum is a long terminal attachment to the metasoma and carries numerous flexible setae and inflexible spikes. It is extremely delicate and fragile. Only one intact flagellum was obtained from all analyzed specimens. It consists of 15 articles and has a total length of 1.40 mm (Fig. 3B). The flagellar base article is a sclerotized ring and is connected with segment 18 with a membranous fold, which displays a knobbed surface (mF; Fig. 13). This base article carries four short setae (approx. 20 µm each) in a square arrangement. The other articles are sim-

ilar to each other in shape, but vary in size, number of setae, and number of spikes. The general number of setae and spikes decreases from proximal to distal (Tab. 4).

The setae are located posteriorly on each article. The spikes are located towards the apical end. The surface of the spikes is, in contrast to that of the setae, smooth. The length of a spike (approx. 30 µm) is about one-sixth the length of a seta (approx. 200 µm; Figs 3B, 4B).

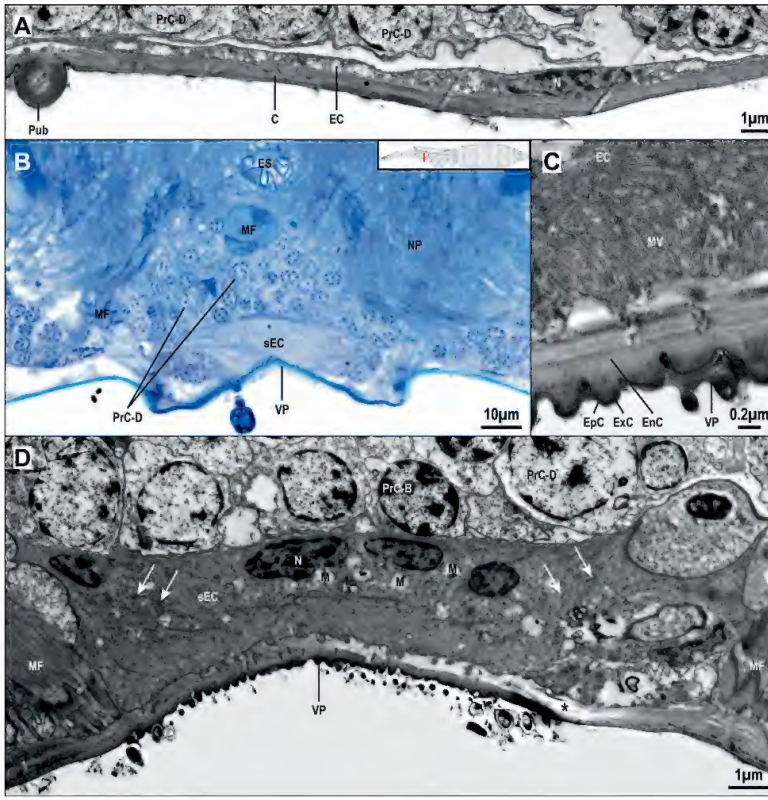

Fig. 15. *Eukoenenia spelaea* (Peyerimhoff, 1902), epidermis. **A**. Transmission electron micrograph of the cuticle and epidermis on the ventral side of the prosoma. The epidermal cells are arranged as squamous epithelium with flattened nuclei. **B**. Light micrograph of the ventral part of a cross-section through the prosoma at the level of the pedipalp (inset). The epidermal cells under the ventral plate are modified. **C**. Transmission electron micrograph of the epidermis cells under the ventral plate showing microvilli which extend into the cuticle. **D**. Transmission electron micrograph of the epidermis under the ventral plate. The nuclei and mitochondria are located basal in the cells, whereas the apical part carries microvilli. The basal part of the cells contains glycogen granules (arrows). The light layer within the cuticle (asterisk) is a fixation artefact. Abbreviations: C = cuticle; EC = epidermal cell; EnC = endocuticle; EpC = epicuticle; ES = esophagus; ExC = exocuticle; M = mitochondria; MF = muscle fiber; MV = microvilli; N = nucleus; NP = neuropil; Pub = pubescence; PrC-B = type B pericarya; PrC-D = type D pericarya; sEC = specialized epidermal cell; VP = ventral plate.

Internal morphology

Epidermis

The epidermis of *Eukoenenia spelaea* is a typical single-layered, squamous epithelium with elongated, heterochromatin-rich nuclei. The thickness of the epidermis varies over the body. In the tightly packed prosoma, the squamous cells can be thin with a height of less than 1 µm. In these regions, the heterochromatin-rich nuclei of the epidermal cells are also flattened (Fig. 15A).

The epidermis cells of the ventral plate differ from those of the rest of the body. In light microscopy, they appear as a homogenously stained cytoplasmic region between the subesophageal ganglion and the cuticle (sEC; Fig. 15B). These modified epidermal cells occupy the entire region of the ventral plate (Figs 3D, 15B, D). Transmission electron microscopy reveals cellular polarity with the nuclei and mitochondria located basally (M, N; Fig. 15D). The basal part of the cells contains glycogen granules and has membranous invaginations, i.e., a basal labyrinth. The apical borders of the cells form numerous microvilli (MV; Fig. 15C) that extend into the cuticle, tightly connecting the epidermal cells with the overlaying cuticle. Cuticular pores associated with the microvilli were not found. The apical part of the specialized epidermal cells is almost completely void of glycogen granules. The cuticle covering the specialized epidermal cells carries smooth cuticular teeth. These cuticular teeth are part of the exocuticle and are covered by electron-dense epicuticle (EpC, ExC, VP; Fig. 15C).

Cuticle

The cuticle of *Eukoenenia spelaea*, like that of other arthropods, consists of two layers: the procuticle and the epicuticle (EpC, ProC; Fig. 16). The thickness of the procuticle is about 0.2 µm in the region of the epidermal folds of the opisthosoma (Fig. 12E) and 1.5 µm in the region of the prosomal sclerites (Fig. 16E). In contrast to the rest of the body, the procuticle of the prosomal sclerites and the ventral plate is stratified into an endo- and an exocuticle (EnC, ExC; Figs 15C–D, 16E). The exocuticle is approx. 0.3 µm thick. Pore canals of different shape and size are found within the procuticle (PC; Fig. 16). The epicuticle is uniform in thickness (0.01 µm), but differs in electron density. While overall the epicuticle is electron-dense, it is electron-translucent in the esophagus (Fig. 37D), on the frontal (Fig. 27B), and the lateral organ, as well as some regions of the opisthosoma (Fig. 16F). The pubescence, which occurs over almost the entire body, represents cuticular surface sculpturing and is formed by procuticle, but it appears to lack an epicuticle (Figs 12E, 16C).

Endosternite

The endosternite lies in the center of the prosoma. It extends from the region of the 1st leg to the region of the 4th leg. The two lateral arms of the endosternite form a horizontal V in an anterior-posterior axis, with the opening towards anterior (EBr; Fig. 21A). The anterior transverse bridge connects both lateral arms (EaB; Fig. 21). The lateral arms continue towards posterior to the posterior transverse bridge at the level of the 3rd leg (EpB; Fig. 21). A medial central bridge (EcB; Fig. 21A) connects the anterior and the posterior bridges. Posterior to the level of the 3rd leg, the endosternite narrows and makes a concave bend towards ventral (EU; Fig. 21B). It then broadens into a stylized W in an anterior-posterior axis, with the opening towards posterior, before terminating in the last prosoma segment (EpS; Fig. 21A).

The endosternite is cellular (ESt; Fig. 17A). The endosternal cells are surrounded by an approx. 1.5 µm thick extra-cellular matrix (Fig. 17B, D). This matrix is the point of attachment for a large number of muscles. These muscles attach to the ECM with hemidesmosomes (arrows; Fig. 17B, D). The endosternite cells have a central heterochromatin-rich nucleus, which is surrounded by the cytoplasmic compartment containing all other cellular organelles. The cytoplasm stains light in light microscopy and is electron-translucent in transmission electron microscopy (Fig. 17A–B). The rough endoplasmic reticulum does not form flattened cisternae, but large compartments filled with fine granules (Fig. 17B–C). Few glycogen granules and free ribosomes are also found in the cytoplasm.

Muscle ultrastructure

The somatic musculature of *Eukoenenia spelaea* is transversely striated, and each fiber consists of several myofibrils (MF, MyF; Fig. 18A–B). The visceral musculature is also striated, but muscle fibers are small, usually containing only one, single myofibril (Fig. 18D). In the somatic muscles, the Z-line, A-band and I-band are clearly visible in longitudinal section (A, J, Z; Fig. 18B). On their surface, the muscle fibers have membrane invaginations at positions corresponding with the Z-lines of the sarcomeres (arrowheads; Fig. 18B). These invaginations probably lead into the T-tubular system. The sarcoplasmic reticulum is well developed (SR; Fig. 18C). Both components, the T-tubular system and the sarcoplasmic reticulum, form diads (arrows, Fig. 18C inset) throughout the muscle fiber. The nuclei are positioned centrally and are surrounded by a perinuclear cytoplasmic compartment that contains all cellular organelles. Mitochondria are scattered throughout the muscle fibers (M; Fig. 18C). — The prosoma contains prominent musculature associated with the endosternite and the body wall as well as musculature in the legs (Figs 19–21; Appendix I: Tab. 5).

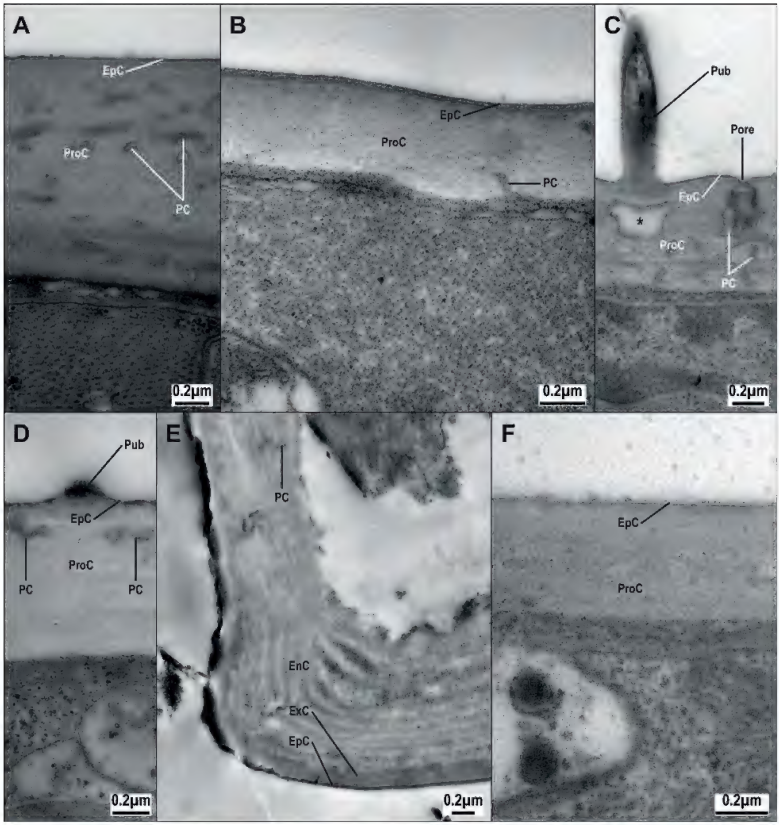

Fig. 16. *Eukoenenia spelaea* (Peyerimhoff, 1902), transmission electron micrographs of the cuticle. **A**. Cross-section of the basal article of the chelicera. The procuticle is contains numerous thin pore canals. **B**. Cross-section of the rostrosoma. The electron-translucent procuticle appears single layered and has only few pore canals. The epicuticle appears electron-dense. **C**. Cross-section of the propeltidium. The pore canals in the procuticle widen towards the surface of the cuticle and show electron-dense content. The area below a process of the pubescence is electron-translucent (asterisk). The pubescence consists of electron-dense procuticle. **D**. Cuticle of a leg. The procuticle shows few pore canals. The electron-dense epicuticle appears frayed. **E**. Cuticle of prosomal sternum associated with leg 2. The layering of the procuticle in endo- and exocuticle is clearly visible. The endocuticle is multi-layered as well. The exocuticle is electron-denser than the endocuticle **F**. Cuticle of the opisthosoma. The procuticle is approx. 0.4 µm thin. The epicuticle is electron-translucent. Abbreviations: EnC = endocuticle; EpC = epicuticle; ExC = exocuticle; PC = pore canal; ProC = procuticle; Pub = pubescence.

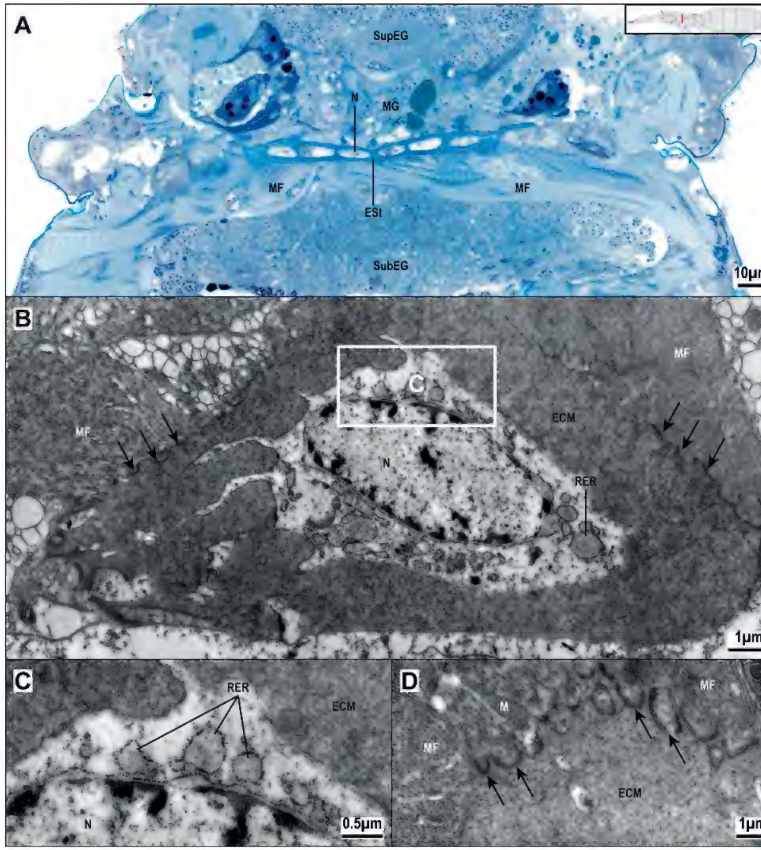

Fig. 17. *Eukoenenia spelaea* (Peyerimhoff, 1902), endosternite. **A**. Light micrograph of a cross-section of the middle position at the level of the 2nd leg. The cells of the endosternite have a central nucleus, peripheral cytoplasm and substantial extracellular matrix around the cells. **B**. Transmission electron micrograph of the endosternite. Cytoplasmic extensions of the endosternite cells extend into the ECM. Musculature attaches to the ECM by hemidesmosomes (arrows). **C**. High power transmission electron micrograph of the rough endoplasmic reticulum surrounding the nucleus from B. The RER forms large compartments instead of the typical flattened cisternae. **D**. Transmission electron micrograph of the extracellular matrix of the endosternite. Muscles attach with hemidesmosomes (arrows). The ECM has a granular character. Abbreviations: ECM = extra cellular matrix; ESt = endosternite; M = mitochondrion; MF = muscle fiber; MG = midgut; N = nucleus; RER = rough endoplasmic reticulum; SubEG = subesophageal ganglion; SupEG = supraesophageal ganglion.

The musculature of the opisthosoma is less prominently developed than in the prosoma (Figs 19–20).

Musculature of the prosoma

The description of the musculature of the prosoma follows major topographic relationships, i.e., muscles of the extremities, muscles of the body wall, and muscles associated with the endosternite. This formal distinction is for descriptive purposes and does not intend to be a functional interpretation. Detailed descriptions with points of origin and insertion for each muscle are given in table 5. Possible antagonists are described according to the topography of their origin and insertion points.

Musculature of the extremities

The musculatures of the chelicerae, the pedipalps and legs 1–4 are described for the right side. Thirteen muscles insert on the chelicera. Three extrinsic muscle strands (C1, C3, and C4; Tabs 5, 10) originate dorsal from the propeltidium and insert at the basal article of the chelicerae. These muscles might move the chelicerae up and down, with muscles C1 and C3 probably being antagonists to C4 (Figs 19B, 20A). The basal article of the chelicera contains three strands of prominent intrinsic musculature (C5–7) and two minor intrinsic muscle strands (C2 and C8). Muscles C5 and C7 are possible antagonists to C6 (Figs 19A, 20A). The movable digit of the chelicera as well as the tip of the fixed digit are free of musculature. Cheliceral muscles C9–13 insert with tendons on the movable digit immediately distal to the joint between movable and fixed digit. They probably close the chela. No musculature with antagonistic topography was found, thus hemolymph pressure and/or elasticity presumably provide the necessary antagonism for opening the chela (Figs 19A, 20A).

The pedipalp has a total of five muscles (PP1–PP5) in its proximal articles and five tendons (PP6t–PP10t) in its distal articles (Figs 11A, 19A–B, 20A, C; Tabs 5, 12). One extrinsic muscle (PP1) originates dorsal from the propeltidium. Like the pedipalp, leg 1 has muscles (LI1–LI8) in the proximal articles but tendons (LI9t–LI14t) in the distal articles. In both extremities, the tendons are attached to the cuticle by pulleys in each article. The two extrinsic muscles of legs 1–3 (LI1, LI2, LII1, LII2, LIII1, and LIII2), originate from the propeltidium and the endosternite, respectively (Figs 19A–B, 20A, C; Tabs 5, 12). In addition, legs 2 and 3 have seven (LII3–LII9) and eight (LIII3–LIII10) intrinsic muscles, respectively. Leg 4 has 11 intrinsic (LIV4–LIV14) and three extrinsic (LIV1–LIV3) muscles. Most extrinsic muscles originate from the endosternite (except PP1, LI1, LII1, and LIII1; Figs 19A–B, 20A, C; Appendix I: Tab. 5). The determination of origin and insertion of intrinsic leg muscles from the analysis of serial sections of pedipalps and legs suggests that some pairs of intrinsic muscles might function as antagonists, while other muscles have no antagonist and hemolymph pressure might provide the antagonistic function. In the pedipalp, articles 7–9 have no intrinsic antagonistic pair of muscles. The same is true for articles 6–11 of leg 1. The muscle and tendon of article 6 span the entire article. Articles 6 and 7 in legs 2 and 3, and articles 6–8 in leg 4 also have no intrinsic antagonistic pair of muscles (Figs 19A, 20C). For comparative purpose, it is important to note that no leg musculature originates from the ventral sclerites of the prosoma.

Musculature of the body wall

Thirteen muscles (P1–13) originate from the body wall, but are not directly associated with the extremities or the endosternite. Prosomal muscles 1 and 2 are associated with the upper lip of the rostrosoma. The paired P2 muscles might act as antagonists to each other to enable lateral movement of the upper lip. An antagonistic muscle for P1 was not recognized. The muscles associated with the pharynx (unpaired P3 and paired P4) function as dilatators of the pharynx. The circular muscle of the pharynx wall might serve as their antagonist (Figs 19B, 20A, 37A).

The majority of the other prosomal muscles (P5–12) originates dorsal, and inserts posterolateral on the body wall (Figs 19B, 20A; Appendix I: Tab. 5). Sexdimorphism in the musculature of the body wall can be found in P11 and P12. Muscles P11 and P12 are actually extensions of the dorsal longitudinal muscle system of the opisthosoma into the prosoma. In females, the longitudinal prosomal muscle P11 is paired and elongated; it connects the propeltidium with the metapeltidium. It has a thin lateral branch that insert on the pleural membrane posterior to leg 3. In males, muscle P11 is paired, but shorter as compared to females. Thickness and branching of the muscle, however, show no differences between females and males (Figs 19B–C, 20A–B). In females, muscle P12 is largely reduced, unpaired, short, and does not extend into the following segment. In males, this muscle is paired and connects the metapeltidium with the first opisthosomal segment (Figs 19B, 20B; Appendix I: Tab. 5).

Musculature of the endosternite

Dorsal suspensor muscles: Dorsal suspensor muscles are diagnosed as the segmental muscles originating from the endosternite and inserting on the dorsal shield of their prosomal segments. Because segmental borders are not recognizable on the endosternite or the dorsal shields of Palpigradi the assignment of muscles to segments remains to some degree arbitrary. However, the relationship to the prosomal extremities is always clear, thus our description uses the topographic relationship to the prosoma appendages as landmark for segment assignment.

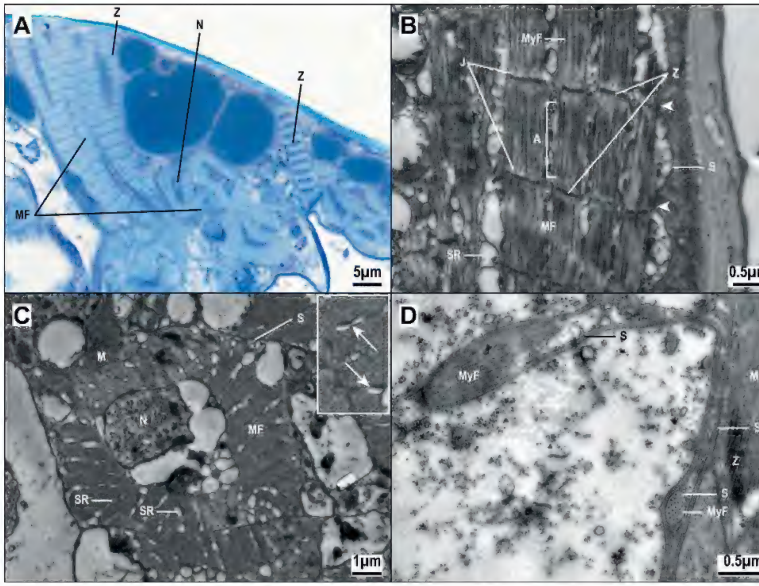

Fig. 18. *Eukoenenia spelaea* (Peyerimhoff, 1902), musculature. **A**. Cross-section through the prosoma, light microscopy. Striated muscles fibers are arranged in a bundle, the nuclei are located centrally. The Z-lines are clearly visible. **B**. Prosomal muscle fiber, transmission electron micrograph. The Z-lines as well as the A-band and I-band are clearly visible. The lateral invaginations of the sarcolemma (arrowheads) represent the T-tubular system. **C**. Prosomal muscle fiber, transmission electron micrograph. The sarcoplasmic reticulum (SR) displays narrow as well as widened areas. The nucleus is located in the center. The T-tubular system together with the SR form dyads throughout the muscle (inset, arrows). **D**. Visceral muscle of the midgut, transmission electron micrograph. The muscles are delicate in comparison with the somatic muscles. Abbreviations: A = A-band, J = I-band; M = mitochondrion; MF = muscle fiber; MyF = myofibril; N = nucleus; S = sarcolemma; SR = sarcoplasmic reticulum; Z = Z-line.

Five muscles (E3, E5, E11, E14, E17) originate from the dorsal side of the endosternite and insert dorsally on the body wall (Fig. 21; Tabs 5, 7). Muscle E3 originates from the anterior end of the endosternite (pedipalpal segment) and extends straight dorsally where it inserts on the propeltidium; it is recognized as the dorsal suspensor muscle of the third segment (pedipalpal segment). Muscle E5 originates posterior to E3 in the region of leg 1 and extends dorsally but with a slight posterior orientation; it also inserts on the propeltidium. Muscles E11 and E14 originate posterior of leg 2 and posterior of leg 3, respectively. Both muscles converge to the same posterior insertion point on the posterior part of the propeltidium. Muscle E17 originates from the endosternite in the region of leg 4, extends straight dorsal and inserts on the metapeltidium.

Anterior oblique suspensor muscle: Muscle E6 originates dorsal from the endosternite close to the origin of muscle E5 (dorsal suspensor of the 4th segment) and extends to the pleural membrane where the chelicera articulates with the prosoma. Based on the topography of its origin and insertion, it is diagnosed as the only anterior oblique suspensor muscle found in the prosoma (Fig. 21; Tabs 5, 7).

Posterior oblique suspensors muscles: The posterior oblique suspensor muscles originate dorsal from the endosternite and insert posterolateral on the body wall. We found four segmental muscles (E4, E12, E15, E20) in such a topographic position (Fig. 21; Tabs 5, 7). Muscle E4 originates from the endosternite in the topographic neighborhood to leg 1, and inserts posterior on the propeltidium in the region of leg 2. Muscles E12 and E15 originate in topographic relationship to legs two and

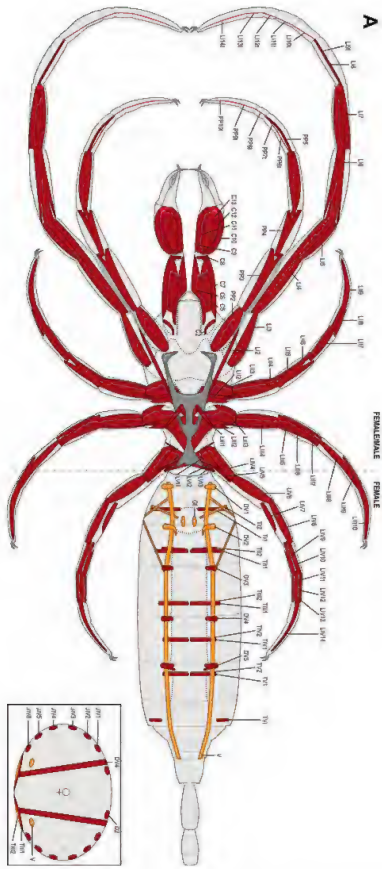

Fig. 19. *Eukoenenia spelaea* (Peyerimhoff, 1902), schematic drawing of a dorsal view of the musculature. The drawing is based on serial cross-section light micrographs and 3D-reconstructions of the musculature. Female/Male indicates that the musculature is identical in both sexes. Female or male indicates sex dimorphism of musculature. **A**. In the prosoma, only extrinsic muscles of the extremities originating from the endosternite, and the intrinsic muscles of the walking legs, the pedipalps and the chelicerae are shown; all other prosomal musculature is shown in B (males) and C (females). Tendons in the chelicerae, pedipalps, and leg1 are highlighted in red. Tendons are labeled by a terminal 't' in their name. In the opisthosoma, only the ventral longitudinal muscles, the dorsoventral muscles, and transverse muscles are show. The dorsal longitudinal, the intersegmental and the flagellar musculature are not shown (see Fig. 19C, 20 A, B for those muscles). Inset: cross-section of the mid-section of segment 11 of a female. Female-specific opisthosomal muscles are marked orange. Abbreviations: C2–13 = cheliceral muscle; DV1–5 = dorsoventral muscle; Gf = genital muscle female; LI2–14t = leg 1 muscle/tendon; LII2–9 = leg 2 muscle; LIII1–10t = leg 3 muscle; LIV1–14 = leg 4 muscle; PP2–10t = pedipalps muscle/tendon; TI1–2 = transversal muscle 1; TII1–2 = transversal muscle 2; TIII1–2 = transversal muscle 3; TIV1–2 = transversal muscle 4; TV1–2 = transversal muscle 5; TVI1 = transversal muscle 6; V = ventral muscle. – *continued.*

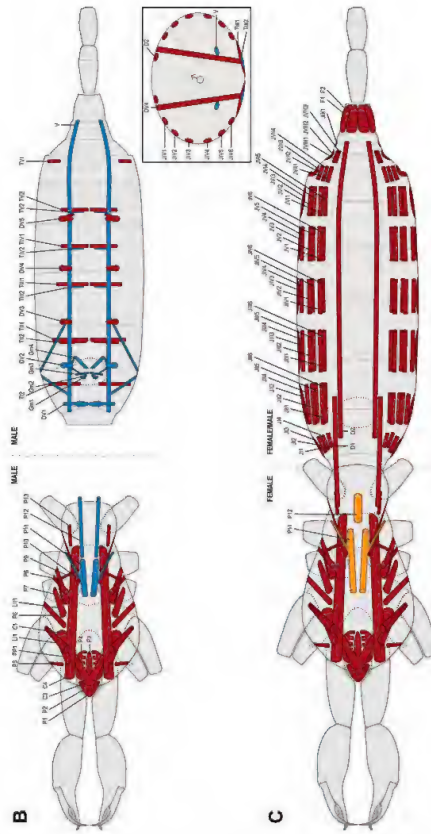

Fig. 19 *continued*. **B**. Male. Serial segmental muscles, longitudinal muscles and intrinsic prosoma muscles are shown, for other musculature see figure 19A. Sex-dimorph male prosomal and opisthosomal musculature is marked blue. In the opisthosoma, only the ventral longitudinal muscles, the dorsoventral muscles and transverse muscles are show. The dorsal longitudinal, the intersegmental and the flagellar musculature are not shown (see Figs. 19C, 20A,B for those muscles). Inset: cross-section of the mid-section of segment 11. **C**. The female specific pattern of muscle anatomy is shown for the prosoma. In the opisthosoma, only the dorsal longitudinal, the intersegmental and the flagellar musculature are shown. Ventral longitudinal muscles, the dorsoventral muscles and transverse muscles are not show (see Figs. 19A, 20 A, B for those muscles). Sex-dimorph musculature is marked orange (female). Abbreviations: C1–4 = cheliceral muscle; D1–2 = dorsal muscle; DV1–5 = dorsoventral muscle; F1–2 = flagellar muscle; Gm1–4 = genital muscle male; JI1–4 = intersegmental muscle 1; JII1–6 = intersegmental muscle 2; JIII1–6 = intersegmental muscle 3; JIV1–6 = intersegmental muscle 4; JV1–6 = intersegmental muscle 5; JVI1–5 = intersegmental muscle 6; JVII1–4 = intersegmental muscle 7; JVIII1–3 = intersegmental muscle 8; JIX1 = intersegmental muscle 9; LI1 = leg 1 muscle; LII1 = leg 2 muscle; P1–13 = prosomal muscle; PP1 = pedipalpal muscle; TI1–2 = transversal muscle 1;TII1–2 = transversal muscle 2; TIII1–2 = transversal muscle 3; TIV1–2 = transversal muscle 4; TV1–2 = transversal muscle 5; TVI1 = transversal muscle 6; V = ventral muscle.

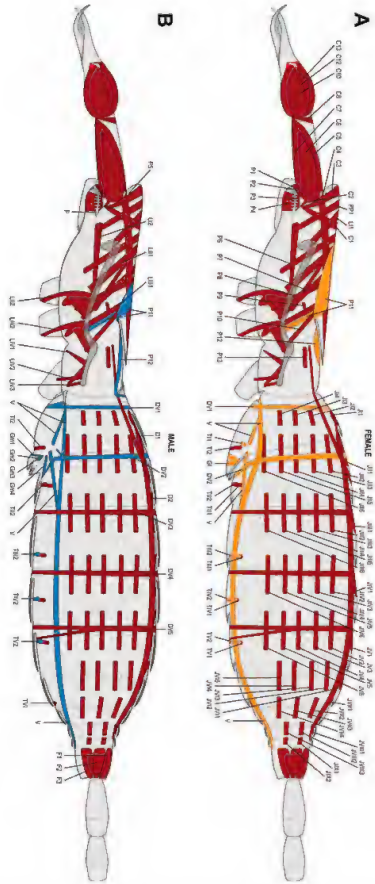

Fig. 20 *Eukoenenia spelaea* (Peyerimhoff, 1902), schematic drawing of a lateral view of the musculature based on serial cross-section light micrographs and 3D-reconstruction. **A**. Female; the right body side is shown. Tendons within the chelicerae are highlighted in red. Sexually dimorphic opisthosomal muscles for females are marked orange. **B**. Male; only the right body side is shown. Sexually dimorphic prosomal and opisthosomal musculature is marked blue. Abbreviations: C1–13 = cheliceral muscle; D1–2 = dorsal muscle; DV1–5 = dorsoventral muscle; F1–3 = flagellar muscle; Gf = genital muscle female; Gm1–4 = genital muscle male; JI1–4 = intersegmental muscle 1; JII1–6 = intersegmental muscle 2; JIII1–6 = intersegmental muscle 3; JIV1–6 = intersegmental muscle 4; JV1–6 = intersegmental muscle 5; JVI1–5 = intersegmental muscle 6; JVII1–4 = intersegmental muscle 7; JVIII1–3 = intersegmental muscle 8; JIX1–2 = intersegmental muscle 9; LII2 = leg 2 muscle; LIII2 = leg 3 muscle; LIV1–3 = leg 4 muscle; P = pharynx; P1–13 = prosomal muscle; TI1–2 = transversal muscle 1; TII1–2 = transversal muscle 2; TIII1–2 = transversal muscle 3; TIV1–2 = transversal muscle 4; TV1–2 = transversal muscle 5; TVI1 = transversal muscle 6; V = ventral muscle. – *continued.*

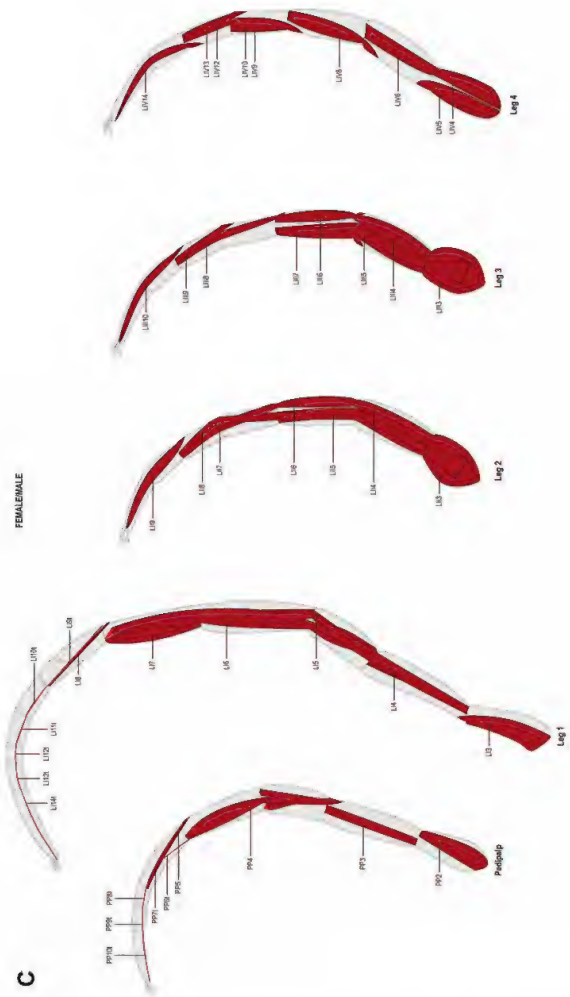

Fig. 20 *continued*. **C.** Schematic drawings of the intrinsic musculature of pedipalp and legs based on serial cross-section light micrographs and 3D-reconstruction. Frontal view of the pedipalps and legs. Tendons are labeled by a terminal 't' in their name. Abbreviations: LI3–14t = leg 1 muscle/tendon; LII3–9 = leg 2 muscle; LIII3–10t = leg 3 muscle; LIV4–14 = leg 4 muscle; PP2–10t = pedipalps muscle/tendon.

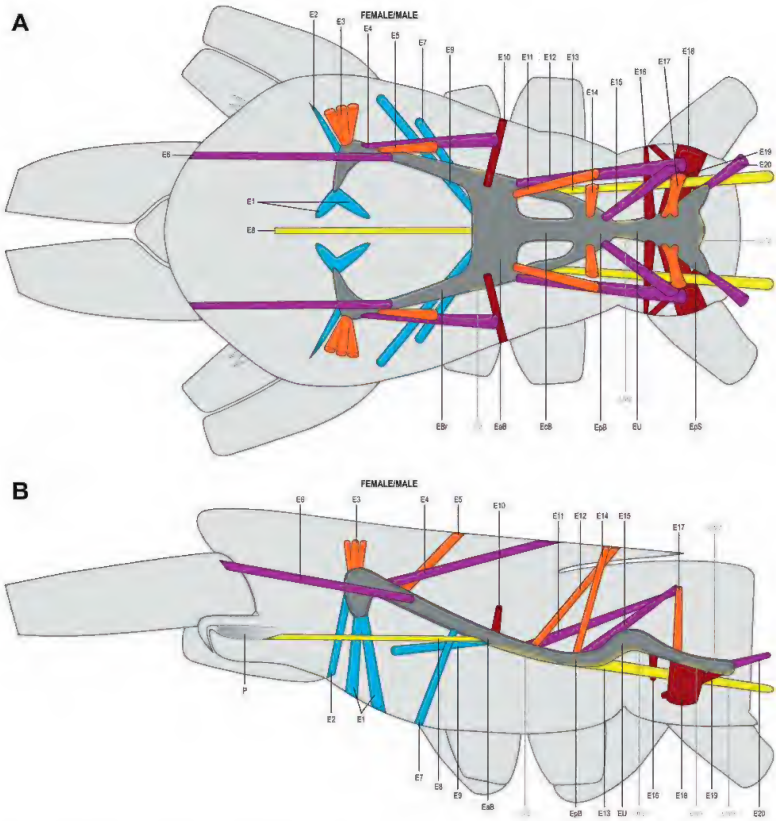

Fig. 21. *Eukoenenia spelaea* (Peyerimhoff, 1902), schematic drawings of the endosternite musculature based on serial cross-section light micrographs and 3D-reconstruction. No sex-dimorphism was found. Only axial segmental muscles originating from the endosternite are shown. Color coding is as follows: orange = dorsal suspensor muscles, purple = anterior and posterior oblique suspensor muscles, dark red = lateral suspensor muscles, blue = ventral suspensor muscles, yellow = muscles extending anterior or into the opisthosoma. Endosternite musculature associated with the legs (LI2, LII2, LIV1–3) is only shown with its point of origin (yellow shaded). **A**. Dorsal view. **B**. Lateral view. Abbreviations: E1–20 = endosternite muscle; EaB = endosternite anterior bridge; EBr, endosternite branch; EcB = endosternite central bridge; EpB = endosternite posterior bridge; EpS = endosternite posterior section; EU = endosternite upturned U section; P = pharynx.

three, respectively. Both muscles insert on the metapeltidium (next to the insertion of dorsal suspensor E17). Muscle E20, which is possibly also part of the posterior oblique suspensors, originates at the posterior end of the endosternite and inserts laterally at the pleural membrane between the prosoma and segment 8 (Fig. 21; Tabs 5, 7).

Lateral suspensor muscles: The lateral suspensors originate lateral from the endosternite and insert lateral at the pleural membrane. We diagnosed four muscles in two clusters (E10, E16, E18, E19) as lateral suspensor muscles (Fig. 21; Tabs 5, 7). Muscles E16, E18, and E19 are clustered and originate in the same region of leg 4. Muscle E10 is located in the region of leg 2.

Ventral suspensor muscles: The ventral suspensors (E1, E2, E7, E9) originate ventral from the endosternite and insert ventral at the pleural membrane (Fig. 21; Tabs 5, 7). Muscles E1 and E2 originate both at the anterior end of the endosternite (Fig. 21). Muscle E2 is associated with the palpal segment; muscle E1 that has an anterior and a posterior branch and is the only muscle which inserts straight ventral, is associated with leg 1. The anterior branch of this muscle inserts at the intersegmental membrane between the ventral plate and the prosternum; the posterior branch inserts on the prosternum (Fig. 21; Tabs 5, 7). Muscles E7 and E9 both originate from the endosternite in the region of leg 2 (anterior to lateral suspensor muscle E10), and insert anterolateral on the pleural membrane between the basis of leg 1 and leg 2.

Two muscles were observed that do not fit into the pattern of BTAMS. Muscle E8 originates medial from the anterior endosternal bridge and extends to the posteroventral end of the pharynx (Fig. 21; Appendix I: Tab. 5). Endosternal muscle E13 originates from the lateral branch of the endosternite and extends into the opisthosoma where it inserts at the border of segment 8 and 9 (Fig. 21).

Musculature of the opisthosoma

In *Eukoenenia spelaea*, the opisthosomal musculature consists of the dorsal longitudinal, dorso-ventral, intersegmental, transversal, genital, ventral longitudinal and flagellar musculature. The dorsal longitudinal, dorso-ventral, and ventral longitudinal musculature are elements of the box truss muscle system (Shultz 2001, 2007b). Sexdimorphism can be found in the dorso-ventral, transversal, genital, and ventral longitudinal musculature. The following description is an account on the general topography of the musculature. Detailed descriptions of origin and insertion for each muscle are given in table 5. Possible antagonistic functions are hypothesized according to the topography of muscle origin and insertion.

Dorsal longitudinal musculature: The dorsal longitudinal musculature is divided into a paired anterior strand (D1) and a paired posterior strand (D2; Figs 19C, 20A–B; Appendix I: Tab. 5). The anterior strand, D1, originates dorsolateral from the metapeltidium. From there, it passes into the opisthosoma and inserts dorsal in segment 10, lateral to the body median line. Muscle D2 originates dorsal in segment 9, medial to D1, and inserts on the anterior margin of the tergite of segment 17. Consequently, both muscles, D1 and D2, overlap in segments 9 and 10 (Figs 19C, 20A–B). The topography of these two muscles suggest that their contraction moves the opisthosoma upward against the prosoma in segments 8–10. – The dorsal longitudinal muscle system extends into the prosoma (muscles P11, P12).

Ventral longitudinal musculature: The ventral longitudinal musculature consists of a pair of strands (V) extending from the posterior margin of the sternite of segment 8 to the border between segments 17 and 18. It branches in segments 9 and 11 with both branches converging to a ventro-lateral insertion in the posterior region of segment 9 (Figs 19A–B, 20A–B; Appendix I: Tab. 5). In females, the ventral longitudinal muscle has a more ventrolateral position except in the genital region (Figs 18A, 19A, 20A). In males, the muscle is more medial than in females but more ventrolateral in the metasoma, i.e., segments 15–18 (Figs 19A, 20A, 19B, 20B).

Segmental dorso-ventral musculature: The first opisthosomal segment (segment 8) is void of dorso-ventral muscles. Segmental dorso-ventral musculature (DV1–DV5) is found in segments 9–13. These muscles are paired and located in the anterior part of each segment; they span the opisthosoma from dorsal to ventral. Dorsal, they originate just lateral to the strands of the dorsal longitudinal musculature. Ventral, they insert just medial of the ventral longitudinal musculature. The dorso-ventral muscles of segments 9 and 10 (DV1 and DV2) are sexually dimorphic. In females, DV1 and DV2 are simple strands with no branching (Figs 19A, 20A; Appendix I: Tab. 5). Muscle DV2, however, bends slightly toward posterior before inserting just posterior to the base of the genital lobes. In males, both muscles branch ventrally. The anterior branch of DV1 inserts on the dorsal side of the ventral overlap of segment 9. Muscle DV2 splits just dorsal of the genital atrium. Its anterior branch then inserts lateral on the center of the genital atrium's anterior-posterior axis (Figs 19B, 20B; Appendix I: Tab. 5). The posterior branch inserts just posterior to the base of the third pair of genital lobes. In both sexes, DV5 branches, with the posterior branch inserting close to the transversal muscle TV (Figs 19A–B, 20A–B).

Intersegmental musculature: The intersegmental musculature forms several parallel strands that span the pleural membranes in anterior-posterior direction (Figs 19C, 20A–B; Appendix I: Tab. 5). These parallel muscle strands are evenly spaced from dorsal to ventrolateral along the body wall. There is a total of nine sets of intersegmental muscle strands (JI–JIX). Six strands,

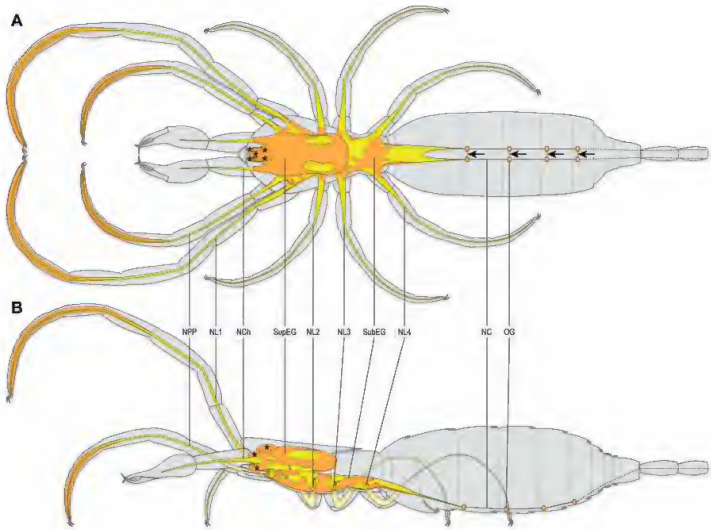

Fig. 22. *Eukoenenia spelaea* (Peyerimhoff, 1902), schematic drawing of the nervous system based on serial cross-section light micrographs and 3D-reconstruction. **A**. Dorsal view. The supraesophageal ganglion is the prominent feature of the dorsal prosoma in the area of the propeltidium. It gives rise to the cheliceral nerves as well as several lobes (asterisk) into the anterior part of the propeltidium and into the rostrosoma. The subesophageal ganglion is larger than the supraesophageal ganglion and is the prominent feature of the ventral prosoma. It extends into the opisthosoma into segment 9. The perikarya layer (orange) is patchy all over the prosomal ganglial mass, leaving areas of neuropil (yellow) exposed. The distal articles of pedipalps and leg 1 are filled with sensory cells of the sensory setae and trichobothria (orange). Paired opisthosomal ganglia are found in segments 11–14. The opisthosomal commissures (arrows) and the nerve leaving the last opisthosomal ganglion are drawn as dashed lines because their topography could not be resolved by histology. **B**. Lateral view. The prosomal ganglia extend through most of the prosoma, especially in the area of the propeltidium. The thickness of the leg nerves decreases in the extremities from proximal to distal. Abbreviations: asterisk = ganglial lobes; NC = nerve cord; NCh = cheliceral nerve; NL1–4 = leg nerve 1–4; NPP = pedipalpal nerve; OG = opisthosomal ganglion; SubEG = subesophageal ganglion; SupEG = supraesophageal ganglion.

on each side of the opisthosoma, are present in segments 9/10–12/13 (JII1–6, JIII1-6, JIV1-6, and JV1–6). Set JVI consists of five strands, JVII of four strands, and JVIII of three strands. JIX, between segments 16 and 17 consists of only one strand of muscles on each side. Segment 8 does not have any intrinsic musculature. Interestingly, we found four small muscle strands in the anterior half of segment 9, JI1–4, in a position similar to other intersegmental muscles, but not bridging over to segment 8. All other sets, JII–JIX, originate from the posterior part of one segment, span the segmental border, and insert in the anterior half of the following segment (Figs 19C, 20A–B; Appendix I: Tab. 5). There is no intersegmental musculature spanning between segments 17 and 18 (Figs 19C, 20A–B).

Genital musculature: The most distinct sexual difference of the opisthosomal musculature can be found in the genital musculature. Whereas females have only one, paired genital muscle (Gf), males possess four pairs of genital muscles (Gm1–Gm4). In females, the genital muscle is located inside the genital operculum, lateral to the body median line. It inserts on the dorsal opercular wall, which is oriented toward the genital opening. Muscle Gf then splits into two branches and inserts anterior and posterior on the ventral opercular wall (Figs 19A, 20A; Appendix I: Tab. 5).

The male genital musculature consists of four thin, paired muscle strands associated with the genital lobes and the genital atrium. Muscles Gm1–Gm3 are grouped together and originate from the ventral wall of the atrium. The most anterior muscle (Gm1) extends ventrally

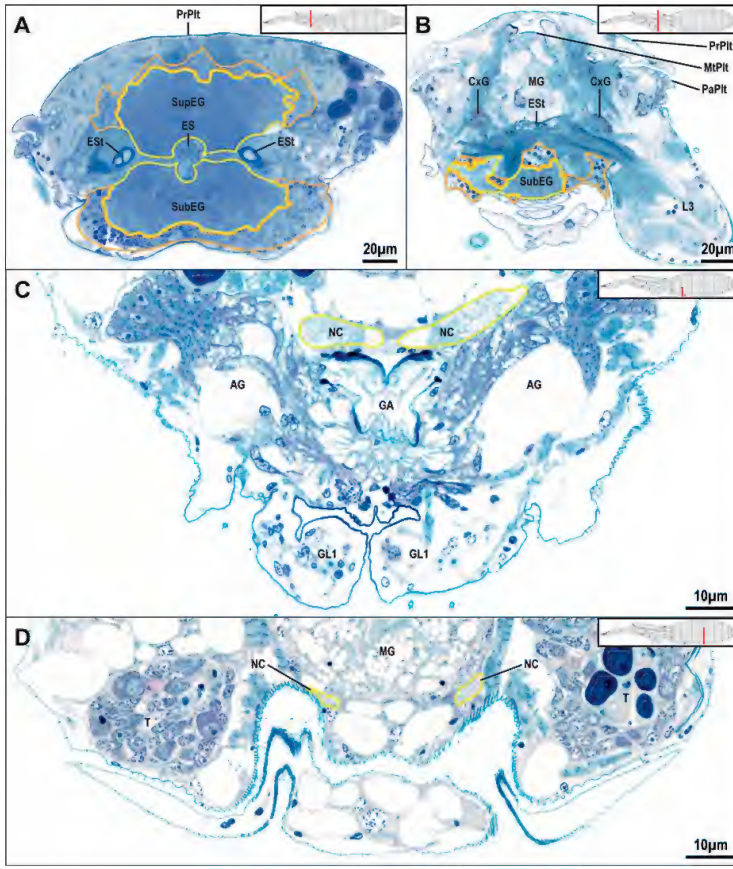

Fig. 23. *Eukoenenia spelaea* (Peyerimhoff, 1902), light microscopic cross-sections of the nervous system. **A**. Area of the border of segments 4 and 5. The prosomal ganglia fill a large portion of the prosoma. The perikarya layer (orange line) forms an incomplete cortex to the more central neuropil (yellow line). Large type-D perikarya are present. **B**. Cross-section of the area of leg 3. In the posterior section of the subesophageal ganglion the central neuropil is reduced. The surrounding perikarya layer consists of predominantly small type-B neurons, but is incomplete. In some areas, the neuropil is in direct contact with musculature and epidermis. **C**. Light micrograph of a cross-section through segment 9 with the genital atrium. At their origin, the paired nerves supplying the posterior section of the body are enlarged. They are located dorsal to the genital atrium and accessory gland. **D**. Area of the border of segments 11 and 12, just anterior to the opisthosomal ganglia of segment 12. The nerve cords of the rope ladder system of the opisthosomal nervous system are located ventral, and medial of the dorsoventral musculature. Abbreviations: AG = accessory gland; CxG = coxal organ glandular section; ES = esophagus; ESt = endosternite; GA = genital atrium; GL1 = genital lobe 1; L3 = leg 3; MG = midgut; MtPlt = metapeltidium; NC = nerve cord; PaPlt = lateral dorsal plate; PrPlt = propeltidium; SubEG = subesophageal ganglion; SupEG = supraesophageal ganglion; T = testes.

and inserts on the anterior wall of the first genital lobe. The muscle pairs Gm2 and Gm3 insert on the second pair of genital lobes and possibly move them up and medial. Muscle Gm4 originates from the lower third of the genital atrium. It inserts on the ventral body wall (Figs 19B, 20B).

Transversal musculature: The transversal musculature (TI–TVI) consists of paired strands of two parallel muscles in segments 9–14. The transversal muscles are located ventral, below the nerve cord; they are missing in the metasoma. The transversal musculature spans the short pleural membrane between the lateral extensions of the tergite and inserts on the sternite. There are paired transversal muscle strands per body half with the exception of TI in males and TVI in both females and males, which consist of only one strand per body half (Figs 19A–B,

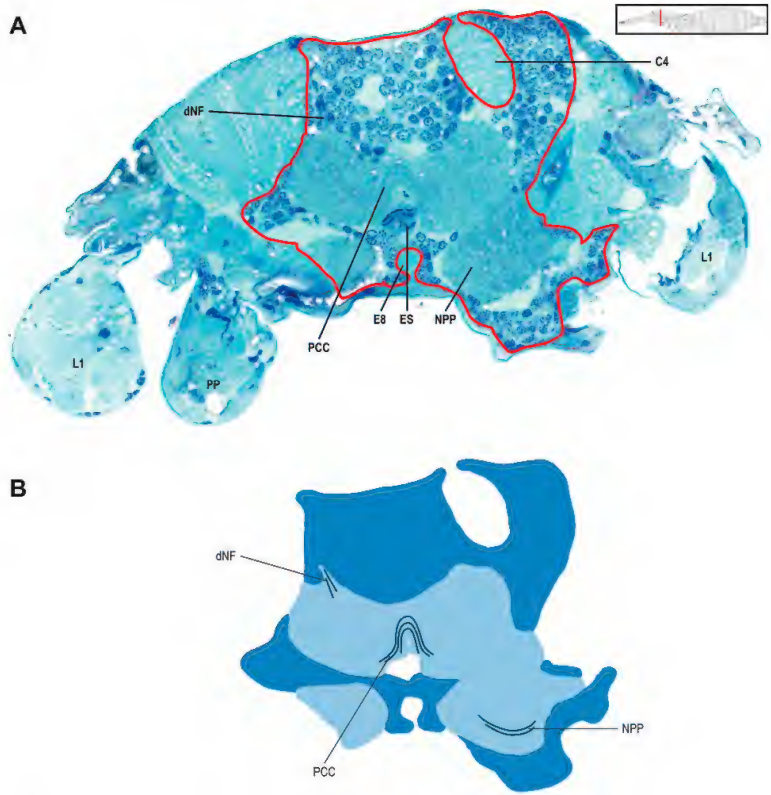

Fig. 24. *Eukoenenia spelaea* (Peyerimhoff, 1902), commissures in the syncerebrum. **A**. Light micrograph of a slightly oblique cross-section in the region of the pedipalp and leg 1.The perikarya partially surrounds cheliceral muscle C4 and endosternal muscle E8. **B**. Simplified and schematic drawing of the section in (A) to highlight the protocerebral commissure (perikarya layer, dark blue; neuropil, light blue). The protocerebral commissure is dorsal to the esophagus. Abbreviations: C4 = cheliceral muscle; ChC = cheliceral commissure; dNF = descending fiber; E8–9 = endosternal muscle; ES = esophagus; L1–2 = leg 1–2; NL1 = nerve of leg 1; NPP = nerve of pedipalp; PCC = protocerebral commissure; PP = pedipalp; PPC = pedipalpal commissure. – *continued.*

20A, B; Appendix I: Tab. 5). Muscle TI1 of females inserts ventrolateral and is possibly involved in widening of the genital opening. The ventral strands TIII2, TIV2, and TV2 are longer in females than in males. Muscle TVI is located more posterolateral in segment 14. It is as short as the ventral transversal muscle strands of the male, and it is shorter than the dorsal strands of the transversal muscles in the other segments of both females and males (TIII1, TIV1, and TV1; Figs 19A–B, 20A–B).

The last opisthosomal segment carries the flagellar musculature. It consists of three paired thick parallel muscle strands (F1–F3). The muscles are arranged parallel to the body axis and encircle almost the entire segment. The most ventral part of segment 18 is free of musculature.

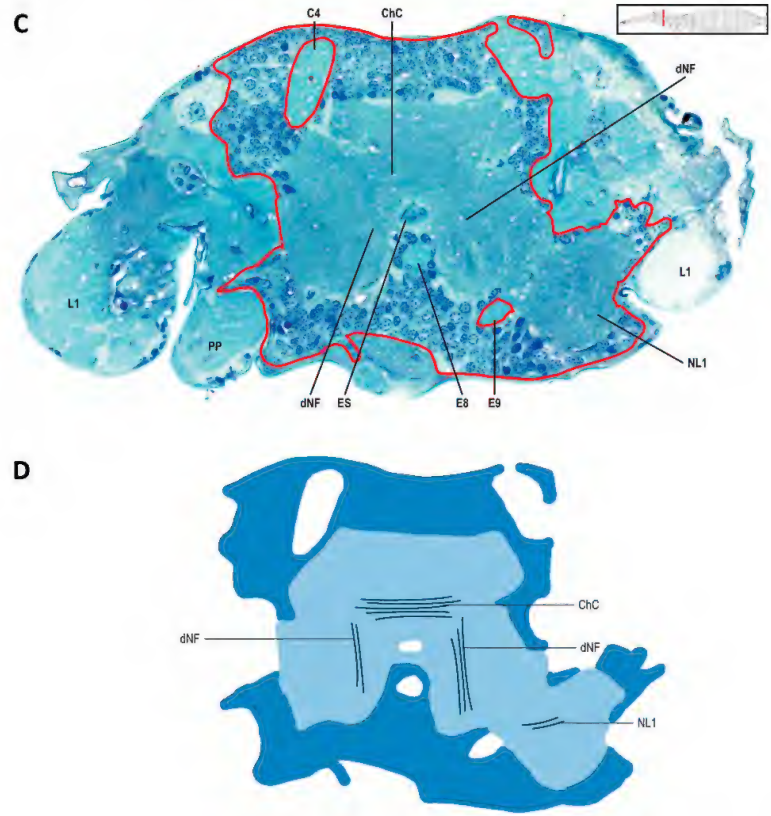

Fig. 24 *continued*. **C**. Light micrograph of a slightly oblique cross-section through the region between pedipalp and leg 1. The perikarya layer of the synganglion partially envelops the cheliceral muscle C4 and muscle E8. **D**. Schematic drawing of the perikarya layer and neuropil in the region between pedipalp and leg 1 based on C. The cheliceral commissure is more pronounced than all other commissures within the synganglion. The lateral nerve fibers are potentially part of the circumesophageal commissure. Abbreviations: C4 = cheliceral muscle; ChC = cheliceral commissure; dNF = descending fiber; E8–9 = endosternal muscle; ES = esophagus; L1 = leg 1; NL1 = nerve of leg 1; PP = pedipalp. – *continued*.

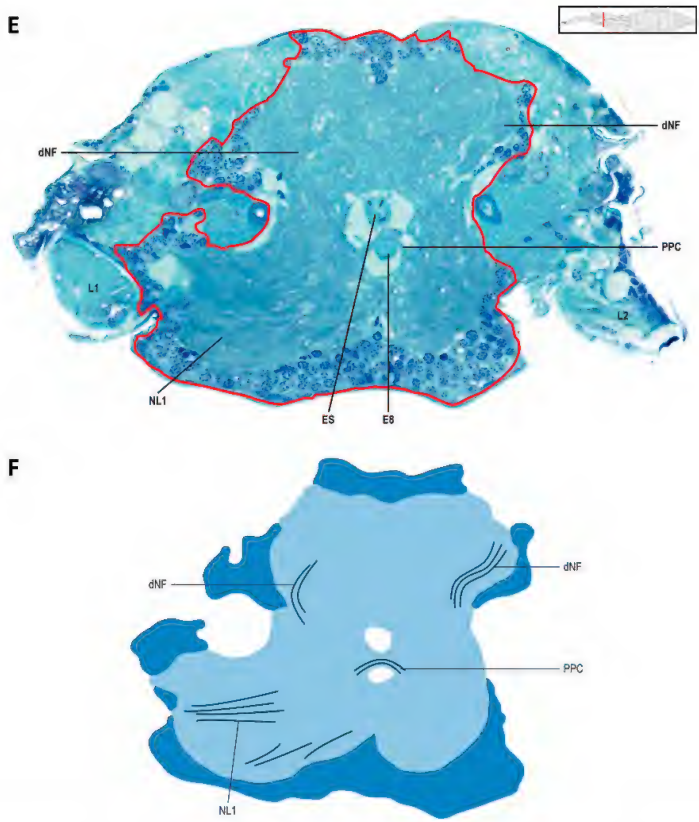

Fig. 24 *continued*. **E**. Light micrograph of a slightly oblique cross-section in the region between leg 1 and 2. The pedipalpal commissure is located between esophagus and muscle E8. The broad base of the nerve of leg 1 is clearly visible. **F**. Schematic drawing of the perikarya layer and neuropil based on E. The delicate pedipalpal commissure is nestled between the esophagus and endosternal muscle E8. Abbreviations: dNF = descending fiber; E8 = endosternal muscle 8; ES = esophagus; L1–2 = leg 1–2; NL1 = nerve of leg 1; PPC = pedipalpal commissure.

Muscles F1–F3 insert anterior on the basal article of the flagellum. Muscle F1 might be associated with the up movement of the flagellum; F2 and F3 are possibly associated with down and lateral movement (Figs 19A, 20B). The flagellum has no intrinsic musculature.

Nervous system

The nervous system of *Eukoenenia spelaea* consists of a prominent prosomal synganglion, which occupies large

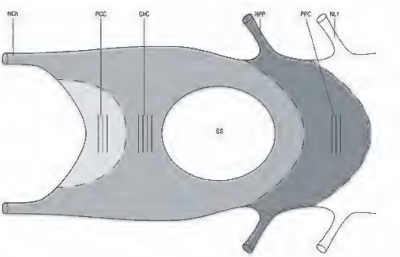

Fig. 25. *Eukoenenia spelaea* (Peyerimhoff, 1902), schematic drawing of the anterior region of the synganglion. The small protocerebrum with its commissure has a position between the roots of the cheliceral nerves leaving the supposed deutocerebrum. The cheliceral commissure is located dorsally of the esophagus. The pedipalpal commissure is located ventral of the esophagus. Abbreviations: ChC = cheliceral commissure; ES = esophagus; NL1 = nerve of leg 1; NPP = nerve of pedipalp; PCC = protocerebral commissure; PPC = pedipalpal commissure.

parts of the prosoma. It is the origin for the prosomal nerves and for a pair of parallel opisthosomal nerve cords (Figs 22–23). The synganglion consists of the supraesophageal ganglion (syncerebrum) and the subesophageal ganglion. The supraesophageal ganglion reaches from the base of the chelicerae to the posterior end of the propeltidium (SupEG; Fig. 22). Using standard light microscopic histology, we identified three commissures: (1) the most anterior commissure is located dorsal to the esophagus in the anterior region of the syncerebrum. This commissure is possibly the protocerebral commissure (PCC; Figs 24A–B, 25). (2) The second commissure is more prominent and also located dorsal to the esophagus. It is possibly the cheliceral commissure (ChC; Figs 24C–D, 25). (3) The posterior commissure is located just ventral to the esophagus between esophagus and endosternal muscle E8. It probably represents the pedipalpal commissure, because nerve fibers from the commissure lead to the base of the pedipalpal coxae (PPC; Figs 24E–F, 25). – The presumed protocerebral part of the syncerebrum is small. An arcuate body, a constitutive element of the ground pattern of the euchelicerate brain, was not found.

The subesophageal ganglion is larger than the supraesophageal ganglion. It extends from the base of the pedipalps into the opisthosoma to the genital plate (SubEG; Fig. 22). The ganglial lobes of the respective legs can be distinguished. Neuropil around the esophagus (circumesophageal connective) connects the supra- and subesophageal ganglia (Fig. 37C) just anterior to the anterior endosternal bridge. The supraesophageal ganglion is never in direct contact with the endosternal bridge because the midgut separates both structures (Fig. 17A).

We did not find a hemolymph space surrounding the ganglia, which is typical for (larger) euchelicerates (Figs 23A, 26A–B). The ganglia are surrounded by a glial cell sheath, the perineurium, and a thin extracellular matrix, i.e., the neurilemma. The neurilemma has a uniform thickness of approx. 50–100 nm around all structures adjacent to the ganglia, e.g., esophagus and muscles (Figs 26A–B, 37C).

A patchy and incomplete cortex of the perikarya (Figs 22, 23A) surrounds the neuropil of the synganglion. In the supraesophageal ganglion, the perikarya layer extends far anterior, sending out several lobes into the rostrosoma (*; Fig. 22). The supra- and subesophageal ganglion are penetrated by muscle strands which originate from the endosternite and attach dorsal, ventral, and lateral to the body (Figs 17A, 23B, 24A, C, E).

Following the neuron categorization by Babu (1985), two types of neurons can be recognized: (1) type B neurons. The nucleus of type B neurons is approx. 1–2 µm in diameter. They are predominantly found in the cortex of the posterior part of the subesophageal ganglion, and in the opisthosomal ganglia (Fig. 26C–D). In light microscopy, their nucleus stains darker and their cytoplasm lighter. The nucleus is the prominent structure of the neuron in transmission electron microscopy, the cytoplasm is largely reduced. (2) Type D neurons. These neurons are larger with a nucleus of approx. 3–4 µm in diameter (Figs 15A–B, D, 26C). A thin layer of cytoplasm, like in type B neurons, surrounds the nucleus of type D neurons. They can be found in the cortex of the supraesophageal ganglion and the anterior part of the subesophageal ganglion. Their nucleus stains lighter in and the cytoplasm darker in light microscopy (Figs 15B, 26C). Cell organelles, glycogen granules and free ribosomes are present in the cytoplasm of both types of neurons. Neurons of type A (typically associated with the mushroom bodies of the visual center) and type C (neurosecretory) were not identified. The neuropil consists of axons and dendrites from the cortical neurons, and nerve fibers with microtubules, free ribosomes and glycogen granules (Fig. 26B).

Several nerves originate from the syncerebrum. The cheliceral nerve (NCh; Figs 22, 25), originates lateral on each side of the supraesophageal ganglion just above the pharynx (Fig. 22B). The nerves of the pedipalps and legs 1–4 originate laterally from the circumesophageal connectives and decrease in diameter in article 2 (NL1–4, NPP, PrC-B, PrC-D; Figs 22, 26C). In the pedipalp and leg 1, the number of type B and D neurons increases towards the more distal articles. Therefore, their distal articles are almost entirely filled with nerve cells. In contrast, legs 2–4 have only a few neurons distributed along the leg, with musculature being the prominent feature within the leg (Fig. 22). Several lobes originating from the supraesophageal ganglion reaching anterior in the

 ©ZFMK

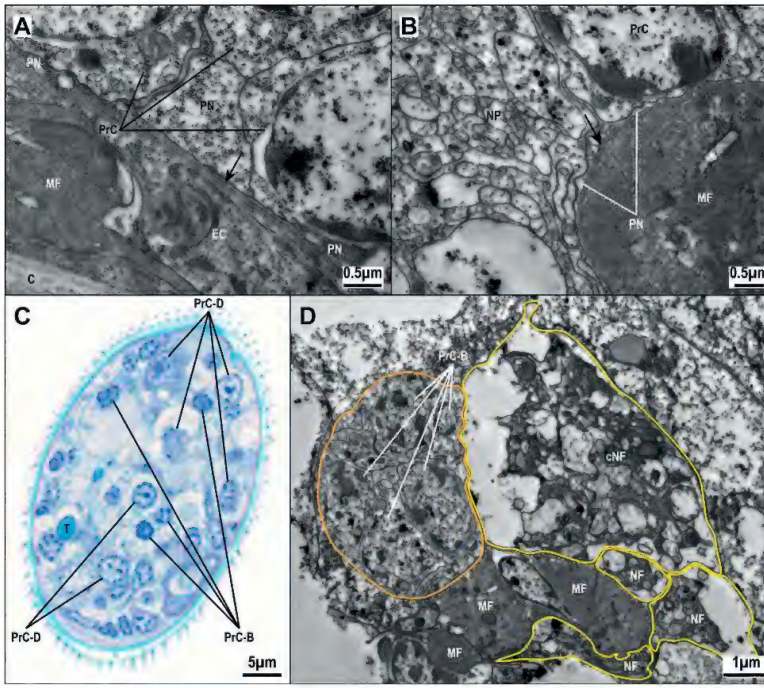

Fig. 26. *Eukoenenia spelaea* (Peyerimhoff, 1902), nervous system. **A**. Transmission electron micrograph of the supraesophageal ganglion just below the body wall. A thin neurilemma (arrow) separates the perikarya from the epidermis. **B**. Transmission electron micrograph of the subesophageal ganglion in close neighborhood to a muscle. The thin neurilemma separates the muscle and the ganglion (arrow). **C**. Light micrograph of a cross-section through a distal article of leg 1. Neurons are dispersed throughout the leg. The enlarged nuclei are surrounded by darker staining cytoplasm. **D**. Transmission electron micrograph of an opisthosomal ganglion. The connective nerve (yellow line) lies dorsal to the ganglion (orange line) and is thicker in diameter than the ganglion itself. One of the adjacent nerve fibers is possibly the commissure. Abbreviations: C = cuticle; cNF = connective nerve fibers; EC = epidermal cell; MF = muscle fiber; NF = nerve fiber; PN = perineurium; PrC-B = type B perikarya; PrC-D = type D perikarya; T = tendon.

prosoma (*; Fig. 22). These lobes cannot be associated with sensory structures like the frontal organ or lateral organs.

From the posterior end of the subesophageal ganglion in segment 9, two parallel nerve cords extend into the opisthosoma (Fig. 22). These nerve cords contain four pairs of opisthosomal ganglia in segments 11–14 and their respective connectives (OG; Fig. 22). More anterior in the opisthosoma, the nerve cords have a larger diameter than further distal (Figs 23C–D). Each opisthosomal ganglion consists of approx. 25 type B neurons (Fig. 26D). The connectives are thicker in diameter than the ganglia and connect to the ganglia on their dorsal side (cNF; Fig. 26D). Additional nerve fibers are located mediolateral of the connective (NF; Fig. 26D). These nerves might represent commissures connecting the left and right opisthosomal ganglia. However, distinct commissures were not identified using light microscopy. The origin of the nerves supplying the sensory setae of segments 15–18 and the flagellum could also not be identified.

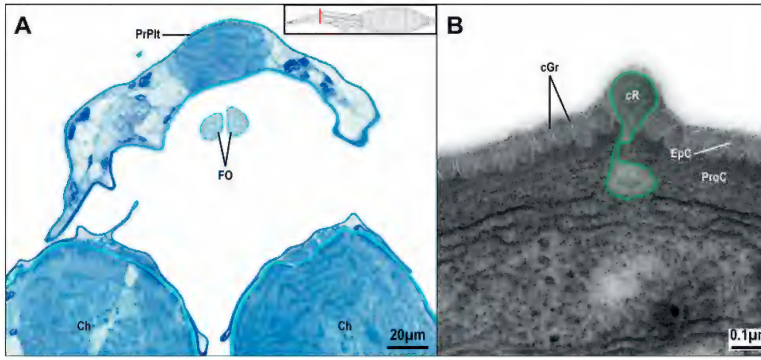

Fig. 27. *Eukoenenia spelaea* (Peyerimhoff, 1902), frontal organ. **A**. Light microscopic cross-section through the modified setae of the frontal organ. The frontal organ is located in a medial position at the anterior end of the prosoma, but partially covered by the propeltidium. **B**. Transmission electron micrograph of a cross-section of the cuticular wall of a modified seta of the frontal organ. The procuticle is generally electron-dense, but electron-translucent in the root of the cuticular ridges (green line). The procuticle of the cuticular ridges and of the wall pores/grooves is less electron-dense and covered by epicuticle. The epicuticle extends between the pores/grooves. Abbreviations: cGr = cuticular groove; Ch = chelicera; cR = cuticular ridge; EpC = epicuticle; FO = frontal organ; PrPlt = propeltidium; ProC = procuticle.

Sensory organs

Sensory organs of *Eukoenenia spelaea* are the frontal organ, the lateral organs, the sensory setae, and the trichobothria. They all have the same basic structure: (1) an outer cuticular structure, i.e., hair or modified hair, (2) two or more sensory cells, and (3) several enveloping cells. The nervous elements are the same in all sensory organs: (1) the inner dendritic segment containing the mitochondria, (2) the ciliary segment with the typical 9 x 2 + 0 arrangement of microtubules, and (3) the outer dendritic segment with more or less loosely arranged microtubules in varying numbers.

Frontal organ

The frontal organ is located medial at the most anterior part of the prosoma, just below the propeltidium, and dorsal to the chelicerae (FO; Figs 3A–B, 8A, 27A). It has a broad base with two finger-like sensory setae that extend to the anterior (Figs 3A, 8A, 27A). The setae are approx. 25 µm long and have a diameter of approx. 5–10 µm. Cuticular ridges on the surface of the frontal organ form a hexagonal honeycomb pattern. Transmission electron micrographs show that these ridges reach deep into the procuticle, with their base being electron-translucent (cR; Fig. 27B). The cuticle of the area surrounded by the ridges is rich in cuticular grooves and covered with an electron-translucent epicuticle (cGr, EpC; Fig. 26B). The procuticle is electron-dense at the base, but is less electron-dense in the more apical parts that form the grooves (ProC; Fig. 27B). The cuticle of the ridges is 0.35–0.5 µm thick, in the area between the ridges it is only 0.2 µm thick. The cuticular grooves are 0.1 µm deep. The diffusion distance through the cuticle is therefore approx. 0.1 µm. The base of the frontal organ (Fig. 28A, J) is filled with electron-dense material and displays fewer pores than the setae.

In the base, there are wide spaces between the cells of both dendrite pairs, which might be part of the receptor lymph cavity. The dendrites reaching into the left and right setae differ from one another. In the right seta, we find two mitochondria-rich dendrites (diameter 0.2 µm) enclosed by nine enveloping cells (IDS 1/2, EnvC; Fig. 28A, J). The electron density of the cytoplasm of both dendrites and the enveloping cells is equally high and similar to the electron density of the surrounding dense material. Distally, the dendrites branch cylindrically multiple times (dBr; Fig. 28B, K). The diameter of the branches varies between 0.1 and 2.5 µm. The dendritic branches show an irregular arrangement of microtubules and are enveloped in dense material (DM; Fig. 28B, K). Some dendritic branches have small, electron-dense regions, or droplets as well as deteriorated vacuoles and lamellar bodies (*; Fig. 28B–E). The dense material is mostly found just underneath the setal wall.

In the left seta, we find also two mitochondria-rich dendrites. However, the mitochondria are larger than in the

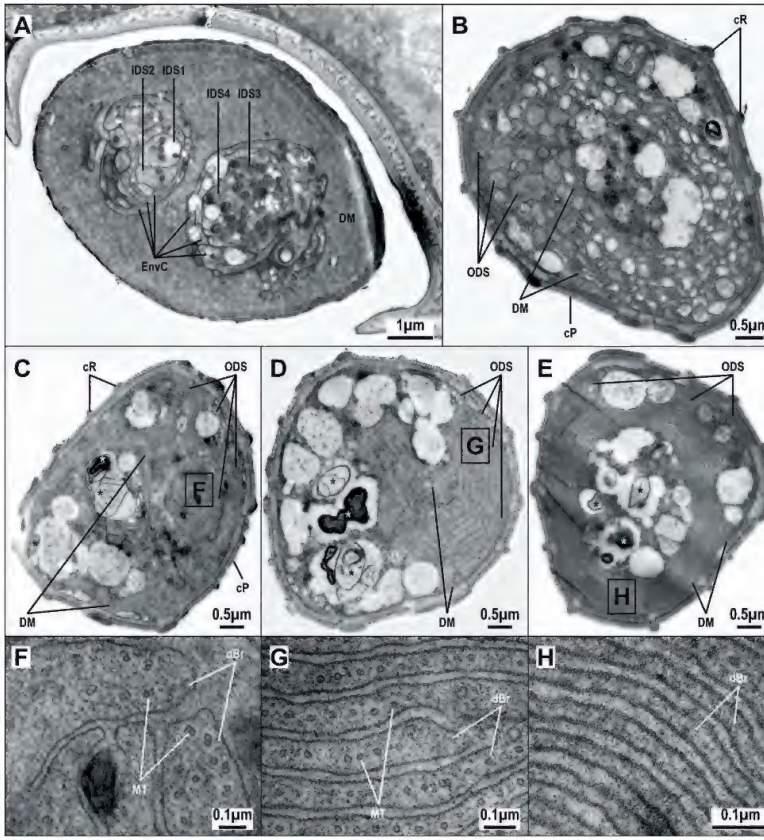

Fig. 28. *Eukoenenia spelaea* (Peyerimhoff, 1902), transmission electron micrographs of cross-sections through the frontal organ. **A**. Section through the basis of the frontal organ containing two distinct units of two dendrites, each surrounded by enveloping cells. The dendritic units are surrounded by a thick layer of dense material. **B**. Right seta. The dendrites have branched cylindrically. In cross-section, cuticular ridges and pits are distinguishable. A lamellar body is closely associated with a dendritic branch (asterisk). **C**. Proximal part of the left seta. In addition to the cylindrically branched dendrite, a dendrite with flattened branches is present. In the left seta, lamellar bodies are found in close association with dendrites as well (asterisk). **D**. Medial part of the left seta. The dendritic branches have become more flattened. **E**. Proximal part of the left seta. The flattened dendritic branches have become lamellate. **F**. Close-up of the flattened dendritic branches in C. The microtubule doublets are clearly visible. **G**. Close-up of the flattened dendritic branches in D. The microtubules are now all single microtubuli. **H**. Close-up of the flattened dendritic branches in E. No microtubules are present. Abbreviations: cP = cuticular pit, cR = cuticular ridge; dBr = dendritic branch; DM = dense material; EnvC = enveloping cell; IDS1–4 = inner dendritic segment 1–4; MT = microtubule; ODS = outer dendritic segment. - *continued.*

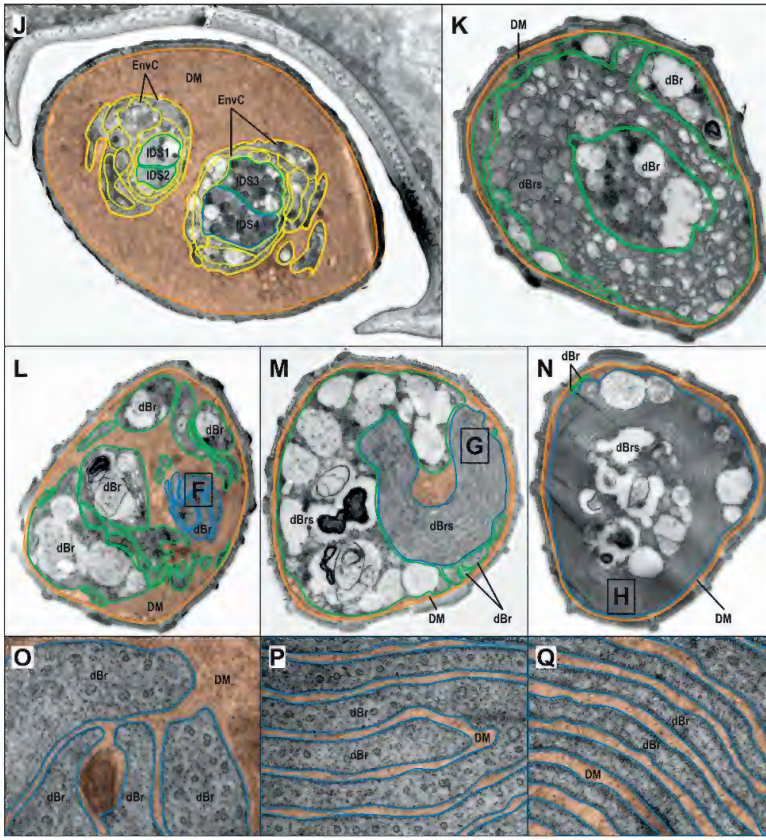

Fig. 28 *continued*. Same images as figures A–H but with colored overlay. **J**. Basis of frontal organ. The inner dendritic segments 1 and 2 of the right seta (green line) are enveloped in nine enveloping cells (yellow line). The inner dendritic segments 3 and 4 that reach into the left seta (blue line) have 12 enveloping cells (yellow line). The dendrites and their enveloping cells are packed in a thick layer of dense material (orange overlay). **K**. The right seta is filled with a large number of dendritic branches (green line). The dense material (orange line) is a thin layer in the periphery. **L**. The cylindrically branched dendrite 3 (green line) of the left seta has differently sized branches. Dendrite 4 has a lamellar type of branching. **M**. As the dendrites increase their branching, the amount of dense material is reduced. **N**. Distally, dendrite 3 is reduced to two small branches, whereas the lamellate branches of dendrite 4 (blue line) take up most of the space within the seta. Dense material (orange overlay) is reduced to a thin layer at the setal wall. **O**. The flattened dendritic branches of dendrite 4 at the basal part of the left seta are still similar in thickness to cylindrically branched dendrites. **P**. The arrangement of the flattened branches of dendrite 4 becomes more regular, the branches themselves become more flattened. **Q**. Distally, the dendritic branches of dendrite 4 are now so flat, that they appear as lamella. Abbreviations: dBr = dendritic branch; dBrs = dendritic branches; DM = dense material; EnvC = enveloping cell; IDS1–4 = inner dendritic segment 1–4.

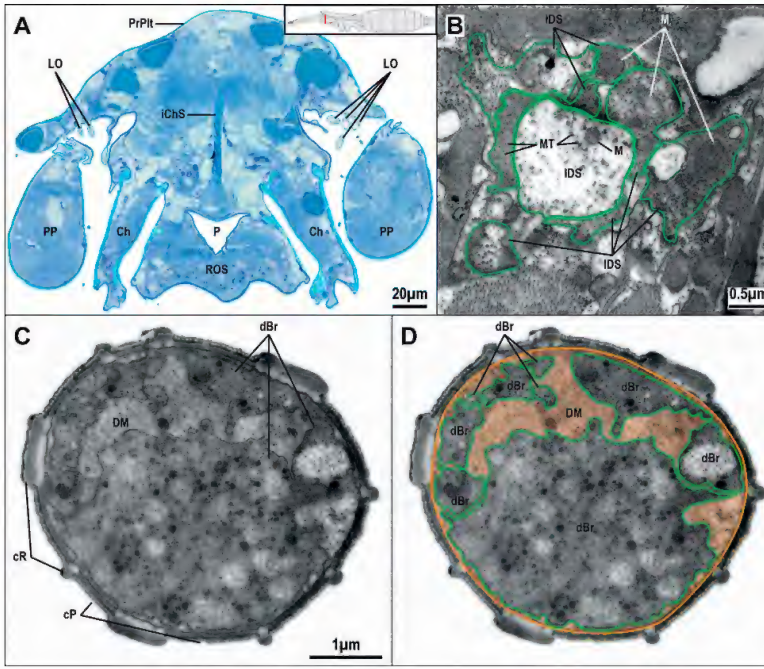

Fig. 29. *Eukoenenia spelaea* (Peyerimhoff, 1902), lateral organ. **A**. Light micrograph of a cross-section at the level of the chelicerae and pedipalps of a male. The lateral organs are located laterally beneath the propeltidium. Each modified seta is attached separately to the body. **B**. Transmission electron micrograph of the eight inner dendritic segments (green line) associated with the four lateral organs of one body half. The microtubules are arranged irregularly. **C**. Transmission electron micrograph of a cross-section of a modified seta. The dendrites are branched cylindrically. Like in the frontal organ, the cuticular wall consists of cuticular ridges, which build the honeycomb pattern, and cuticular pits, which carry the wall pores. **D**. Same as C with colored overlay. The dendritic branches vary in size. The dense material (orange overlay) is largely located towards the inside, while the dendritic branches are oriented towards the setal wall. Abbreviations: Ch = chelicera; cP = cuticular pit; cR = cuticular ridge; dBr = dendritic branch; DM = dense material; iChS = intercheliceral septum; IDS = inner dendritic segment; LO = lateral organ; M = mitochondrion; MT = microtubule; P = pharynx; P3–4 = prosomal muscle; PP = pedipalp = PrPlt = propeltidium; ROS = rostrosoma.

right seta (diameter 0.5 µm). The dendrites are surrounded by twelve enveloping cells (IDS 3/4, EnvC; Fig. 28A, J). Dendrites and enveloping cells have the same cytoplasm electron density. The widenings between the enveloping cells are larger than in the right receptor and could be part of the receptor lymph cavity. In the seta, one dendrite branches and folds, and displays an irregular arrangement of microtubule doublets (IDS 4, ODS, MT; Fig. 28C, F, L, O). Along the seta, the ranching, flattening and folding of this dendrite increases from proximal to apical. Within the branches, the microtubuli doublets become single microtubuli and the arrangement becomes regular (Fig. 28D, G, M, P). Towards the distal end of the seta, the dendrite forms concentrically wrapped laminae. Within this lamellate section, microtubules are no longer recognizable (Fig. 28E, H, N, Q). Many vacuoles in the center of the dendrite show deterioration and indicate incomplete fixation. The second dendrite branches cylindrically and is pushed towards the periphery of the seta by the first dendrite (Fig. 28C–E, L–N). The second dendrite contains numerous deteriorated vacuoles and lamellar bodies. However, there are more of these in the left

seta than in the right seta (*; Fig. 28C–E). Regions where vacuoles are present show also small electron-dense droplets. Similar to the right seta, the dense material is mostly found just below the setal wall. However, in the left seta the amount of dense material decreases from basal to apical (Fig. 28C–E, L–N).

Lateral organ

Lateral organs are located at the left and right side on the prosoma, just below the propeltidium and anterior to the base of the pedipalps (LO; Figs 3A, C, 29A). Each lateral organ consists of four single, finger-like modified setae extending anteroventral (Figs 8B, 29A). The setae are arranged slightly diagonally from anterior to posterior

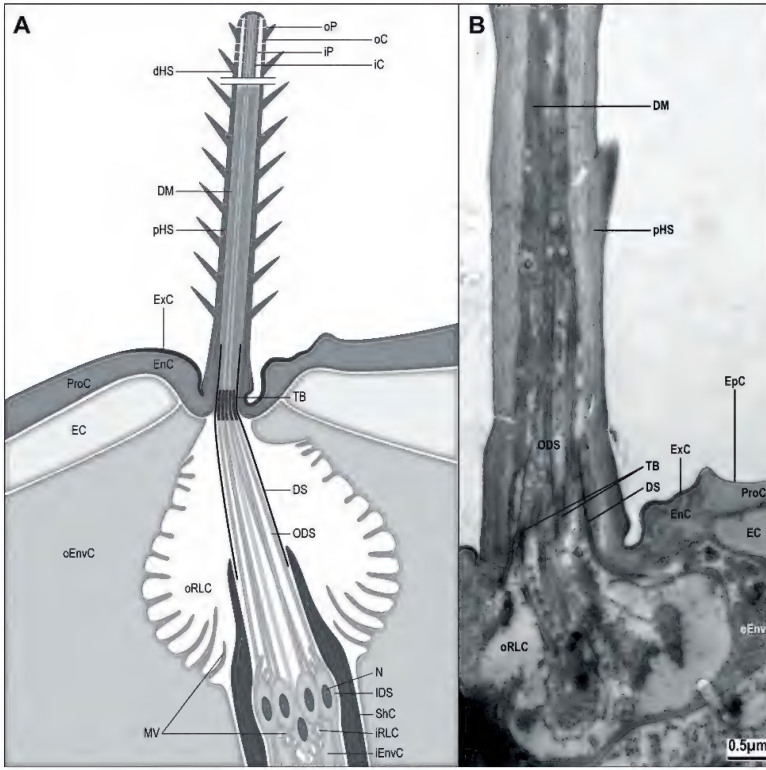

Fig. 30. *Eukoenenia spelaea* (Peyerimhoff, 1902), sensory seta. **A**. Schematic drawing of the microscopic anatomy of the sensory seta based on transmission electron micrographs. Seven dendrites are associated with the seta, two dendrites extend into the hair shaft. The distal part of the hair shaft has double walls and wall pores. **B**. Transmission electron micrograph of a longitudinal section of the basal part of a sensory seta. The outer dendritic segments extend into the hair shaft. Abbreviations: C = cuticle; dHS = distal hair shaft; DM = dense material; DS = dendritic sheath; EC = epidermal cell; ExC = exocuticle; iC = inner cuticle; IDS = inner dendritic segment; iEnvC = enveloping cell of the inner receptor lymph cavity; iP = inner pore; iRLC = inner receptor lymph cavity; oC = outer cuticle; ODS = outer dendritic segment; oEnvC = enveloping cell of the outer receptor lymph cavity; oP = outer pore; oRLC = outer receptor lymph cavity; pHS = proximal hair shaft; ShC = sheath cell; TB = tubular body.

 ©ZFMK

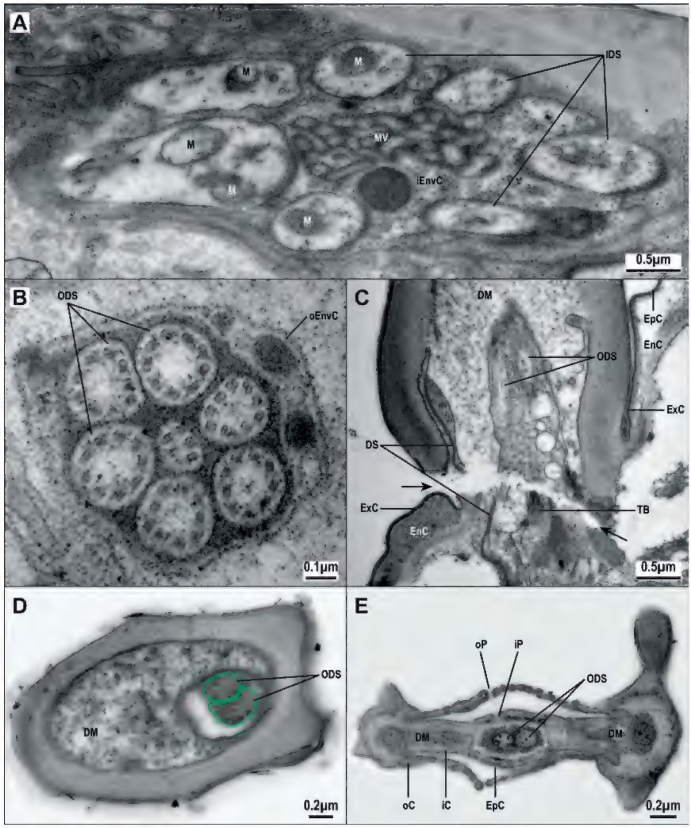

Fig. 31. *Eukoenenia spelaea* (Peyerimhoff, 1902), transmission electron micrographs of sections through a sensory seta. **A**. Cross-section through the base of the seta, through the inner receptor lymph cavity. Seven dendrites are arranged around the microvilli of the central enveloping cell. **B**. Cross-section through the base of a sensory seta at the level of the outer dendritic segments. Six outer dendritic segments are arranged in a circle with the seventh dendrite located centrally. The central dendrite has a reduced number of microtubule doublets. **C**. Longitudinal section through the base of a sensory seta. The dendritic sheath extends into the hair shaft. Two of the original seven dendrites continue into the hair. Arrows indicate an artefact. **D**. Cross-section through the proximal hair shaft containing two dendrites (circled by green line). **E**. Cross-section through the apical hair shaft. The two dendrites are located centrally within the hair. The hair itself has an inner and outer cuticle with wall pores. The outer pore is open, the inner pore is clogged with electron-translucent material. The inner wall is covered with epicuticle. Abbreviations: DM = dense material; DS = dendritic sheath; EnC = endocuticle; EpC = epicuticle; ExC = exocuticle; iC = inner cuticle; IDS = inner dendritic segment; iEnvC = enveloping cell of the inner receptor lymph cavity; iP = inner pore; M = mitochondrion; MV = microvilli; oC = outer cuticle; ODS = outer dendritic segment; oEnvC = enveloping cell of the outer receptor lymph cavity; oP = outer pore; TB = tubular body.

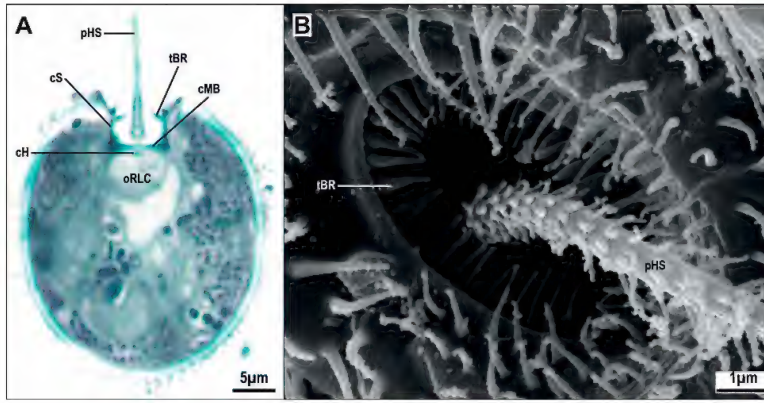

Fig. 32. *Eukoenenia spelaea* (Peyerimhoff, 1902), trichobothrium. **A**. Light micrograph of a cross-section through leg 1, with a longitudinal section of a trichobothrium. The hair shaft is located within a cuticular socket. The outer receptor lymph cavity is separated from the socket by a cuticular membrane. **B**. Scanning electron micrograph of the basal part of the trichobothrium. The hair shaft is covered with small cuticular spikes which are arranged regularly along the shaft. A row of cuticular teeth forms the margin of the bothrium. Abbreviations: cH = cuticular helmet; cMB = cuticular membrane; cS = cuticular socket; oRLC = outer receptor lymph cavity; pHS = proximal hair shaft; tBR = toothed bothrial margin.

along the ventral side of the propeltidium. The size of the setae is similar to the setae of the frontal organ with an approximate length of 25 µm and an approximate thickness of 4.5 µm. Like in the frontal organ, the cuticle is rich in cuticular grooves and reinforced with honeycomb patterned cuticular ridges (cP, cR; Fig. 29C). The ultrastructure of the cuticle is the same as in the frontal organ.

The nerve supplying the lateral organ consists of eight dendritic units (IDS; Fig. 29B). This suggests that two dendrites extend into each seta. The enveloping cells could not be identified, because the transmission electron microscopic section of the nerve is too far proximal. The dendrites branch cylindrically within the setae (dBr; Fig. 29C–D). The branches display an uneven thickness, which ranges between 0.1 and 4.2 µm and show only few microtubules. Like in the frontal organ, the dendritic branches have accumulations of dense material between them (DM; Fig. 29C–D). The dense material is largely located towards the inside of the setae. In contrast to the frontal organ, all dendritic branches of the lateral organ contain numerous small electron-dense droplets as well as few electron-translucent droplets. Deteriorated vacuoles were not found.

Sensory setae

Sensory setae are found all over the body and flagellum (Tabs 1–4). At their insertion, the procuticle is differentiated into an endocuticle and an electron-dense exocuticle (EnC, ExC, ProC; Figs 30B, 31C) probably providing some flexibility. The epicuticle is electron-translucent. At the base of each seta, we found seven sensory cells in a circular arrangement around a central enveloping cell. The enveloping cell has apical microvilli, which extend into the inner receptor lymph cavity (iEnvC, iRLC, MV; Figs 30A, 31A). The inner dendritic segment of the sensory cells is characterized by the presence of mitochondria (IDS, M; Fig. 31A).

The outer dendritic segments of the sensory cells are characterized by a specific arrangement of their microtubules (ODS; Figs 30A, 31B). In cross section, six dendrites are in circular arrangement around a smaller central dendrite. The six peripheral dendrites have a 9 x 2 + 0 arrangement of microtubule, but the small central dendrite displays a 6 x 2 + 0 arrangement (Fig. 31B). The outer dendritic segments extend through the outer receptor lymph cavity. They are wrapped by the enveloping cell(s) and embedded in an electron-dense dendritic sheath. This sheath is present only in the region of the cuticular socket and the basal part of the seta (DS, oRLC; Figs 30, 31C).

Two of the seven dendrites of a sensory seta extend to the tip of the seta; the other dendrites form a number of tubular bodies at the seta's point of insertion (TB; Figs 30A, 31C). The two dendrites extending to the tip of the seta are unbranched and surrounded by dense ma-

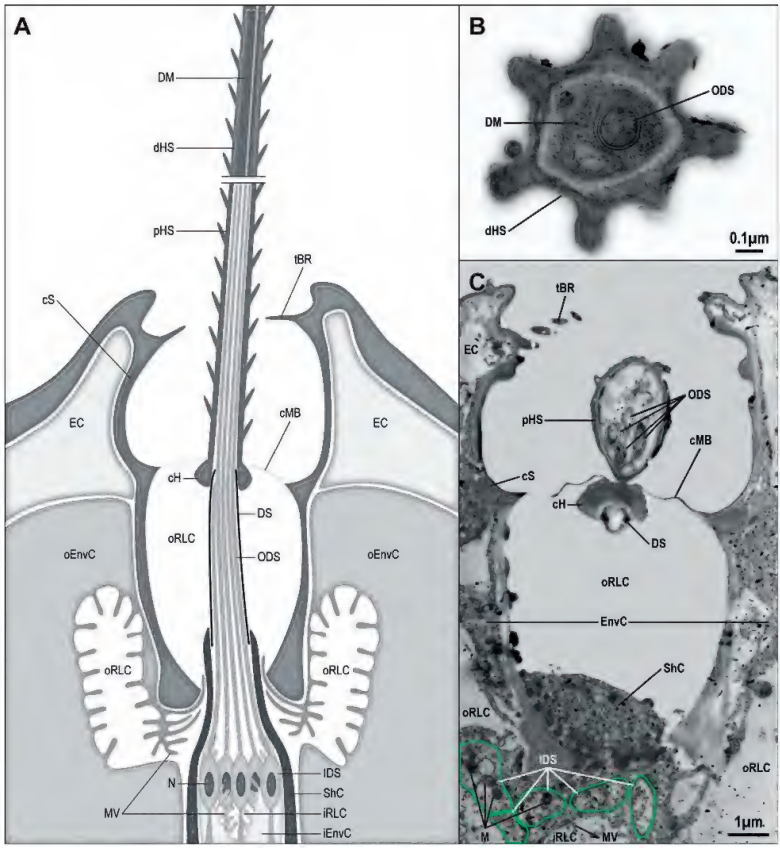

Fig. 33. *Eukoenenia spelaea* (Peyerimhoff, 1902), trichobothrium. **A**. Schematic drawing of the microscopic anatomy of a trichobothrium, reconstruction based on TEM-sections. The cuticular socket of the bothrial wall extends down to the sheath cells. The cuticular helmet is open allowing the outer dendritic segments to extend into the hair shaft. **B**. Transmission electron micrograph of a cross-section of the distal hair shaft. Of the four dendrites entering the hair shaft proximally, only one dendrite extends to the distal part of the hair. The outer dendritic segment is enveloped by dense material. **C**. Transmission electron micrograph of a longitudinal section of the socket area. The sheath cells extend into the basal part of the cuticular socket. Four of the five inner dendritic segments (green line) extend into the hair shaft. The dendritic sheath terminates at the cuticular helmet. Abbreviations: cH = cuticular helmet; cMB = cuticular membrane; cS = cuticular socket; dHS = distal hair shaft; DM = dense material; DS = dendritic sheath; EC = epidermal cell; EnvC = enveloping cell; IDS = inner dendritic segment; iRLC = inner receptor lymph cavity; ODS = outer dendritic segment; M = mitochondrion; MV = microvilli; oRLC = outer receptor lymph cavity; pHS = proximal hair shaft; ShC = sheath cell; tBR = toothed bothrial rim.

terial (Figs 30, 31C–E). The number of microtubules in the dendrites decreases towards the tip of the seta. At the distal part of the seta, the cuticle wall is doubled and has wall pores (iC, oC, iP, oP; Figs 30A, 31E). The exact number of wall pores could not be established. The outer cuticular wall is approx. 0.05 µm thick, while the inner cuticular wall is only approx. 0.1 µm. The pores of the outer wall are completely open, whereas the pores of the inner wall are plugged and covered with epicuticle (Figs 30A, 31E).

Trichobothria

In *Eukoenenia spelaea*, trichobothria are found exclusively on leg 1. The hair of each trichobothrium is nested in a cup-shaped cuticular socket, i.e., the bothrium, which is divided by a thin cuticular membrane into an inner and an outer compartment (cMB, cS; Figs 32A, 33A, C). The apical opening of the bothrium is ornamented by a ring of cuticular teeth (tBR; Figs 32, 33A, C). The diameter of the outer compartment is approx. 6 µm, and is surrounded by epidermal cells. The diameter of the inner compartment below the membrane is approx. 4.5 µm.
The receptor lymph cavity is divided into two parts, the inner and the outer receptor lymph cavity (iRLC, oRLC; Fig. 33A, C). The outer receptor lymph cavity has a basal and an apical part. The apical part of the outer receptor lymph cavity is formed by a cup-shaped cuticula extending the bothrium basal to the cuticular membrane that spans across the bothrium. The basal part is located at the base of the inner compartment (Fig. 33A, C) and is surrounded by enveloping cells with microvilli (oEnvC; Fig. 33A, C).

The inner receptor lymph cavity is located centrally between the inner dendritic segments. The cuticular wall of the inner compartment tapers off at the base, leaving a narrow opening where the dendrites enter the inner compartment (Fig. 33). Like in the outer receptor lymph cavity, the enveloping cells of the inner receptor lymph cavity have microvilli (iEnvC, MV; Fig. 33C). A total of five dendrites is associated with a trichobothrium (IDS, ODS; Fig. 33A, C). The dendrites enter the outer receptor lymph cavity and are enveloped by a dendritic sheath, which is built by sheath cells (DS, ShC; Fig. 33A, C). The dendrites connect to the helmet (cH). The helmet is a cuticular structure connected to the base of the hair shaft, which is located centrally in the outer compartment of the socket (pHS; Fig. 33, C). In contrast to described

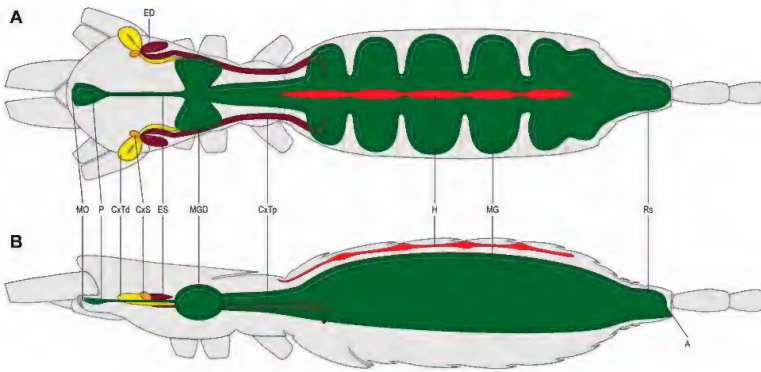

Fig. 34. *Eukoenenia spelaea* (Peyerimhoff, 1902), schematic drawing of the heart, the alimentary system, and the coxal organ based on serial cross-section light micrographs and 3D-reconstruction. **A**. Dorsal view. The heart (red) extends from the posterior end of the prosoma to segment 14. The prosomal midgut (green) has two lateral diverticula in the area of leg 2 and 3, just posterior to where the esophagus terminates. The opisthosomal midgut is a sac with lateral indentations where the dorsoventral musculature extends between tergites and sternites. The saccule (orange) of the coxal organ is located in the region of leg 1; the proximal (brown) and distal tubule (yellow) of the coxal organ extend into segments anterior and posterior; the proximal tubule extends as far posterior as into segment 9, the distal tubule extends into the coxa of leg 1. The excretory duct opens posterior to the basal article of leg 1. **B**. Lateral view. The heart has a flattened appearance within a segment and has a roundish diameter at the junction of two segments. The anal opening lies in the membranous fold between segment 18 and the flagellum's basal article. Abbreviations: A = anus; CxS = coxal organ saccule; CxTd = coxal organ distal tubule; CxTp = coxal organ proximal tubule; ED = excretory duct; ES = esophagus; H = heart; MG = midgut; MGD = midgut diverticula; MO = mouth opening; P = pharynx; Rs = rectal sac.

trichobothria of other arachnids, the helmet is open and ciliary sections of four dendrites continue through the opening into the proximal part of the shaft (Fig. 33). The arrangement of microtubules is 9 x 2 + 0. Distally, only one outer dendritic segment is present inside the shaft. It is surrounded by dense material (DM; Fig. 33B). Cuticular pores could not be observed on the hair shaft.

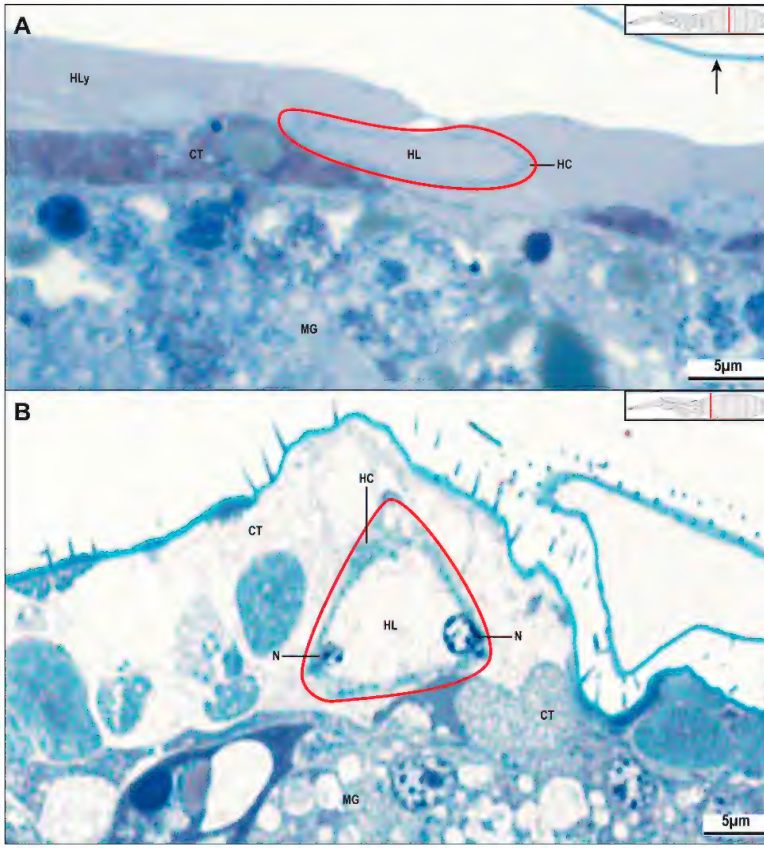

Fig. 35. *Eukoenenia spelaea* (Peyerimhoff, 1902), cross-sections through the heart. **A**. Light micrograph of the heart in segment 11 of the opisthosoma. The overall shape of the heart is flattened. The heart is surrounded by hemolymph and connective tissue. The arrow indicates an artefactual separation of the cuticle from the body. **B**. Light microscopic image of the heart between segment 9 and 10. The lumen of the heart is open and extended as compared to the flattened appearance in a more central position of a segment (see A). Abbreviations: CT = connective tissue; HC = heart cells; HL = heart lumen; HLy = hemolymph; MG = midgut; N = nucleus.

Heart

The heart is a vestigial muscular tube located in the dorsal midline of segments 7–14 (H; Fig. 34). Its cross-sectional diameter changes along the anterior-posterior axis within each segment. In the middle of a segment, the cross-section of the heart is dorso-ventrally flattened, but it is more roundish with a wide lumen in the region between neighboring segments (Fig. 35). Ostia, which are part of the ground pattern of the heart in arthropods, were not found. Using transmission electron microscopy, we did not detect any hemolymph cells in the heart lumen. The heart tube consists of one thin layer of circular musculature. Over its entire length, the heart consists of approximately 80 cells (Fig. 35). The tissue surrounding the heart is difficult to diagnose using light microscopy, and probably represents hemolymph and connective tissue. We did neither find a pericardial space nor a dilator musculature.

In transmission electron microscopic cross-sections, the heart tube appears as a syncytium with loosely scattered, irregular bundles of contractile filaments (Fig. 36A). However, a sarcoplasmic reticulum could not be clearly identified. The myofibrils seem to be interrupted and the filaments are irregularly scattered throughout the fibril (arrowheads; Fig. 36B–C). A sarcomere structure is barely recognizable, with the membrane of the muscle cells forming lateral infoldings wherever a Z-line is located (arrows; Fig. 36B–C). These membrane infoldings might represent structures equivalent to the T-tubular system. The muscle cell is enlarged in the region of the heterochromatin rich oblong nucleus. Few mitochondria of various sizes are dispersed throughout the muscle cell. A nerve for stimulation of the heart muscle was not found.

Digestive tract

The digestive tract consists of the foregut (mouth opening and pharynx within the rostrosoma, and esophagus), the midgut, the prosomal midgut diverticula, and the rectal sac. A postcerebral stomach, as reported for other arachnid groups, is not present. The pharynx and esophagus are lined with a cuticle intima. The midgut, the prosomal midgut diverticula and the rectal sac have no cuticle lining. A cuticle-lined hindgut, typical for arthropods, is not present. The midgut was free of identifiable food particles. The anal opening is located ventral in the membrane between segment 18 and the flagellar base ring (A; Fig. 34).

Pharynx

The pharynx begins at the mouth opening. It is X-shaped with the two upper arms of the X wide open, while the lower arms have no open lumen (P; Fig. 37A). Four strands of musculature attach to the pharynx forming a precerebral suction pump: two strands of lateral musculature (P4), one strand of dorsal musculature (P3),

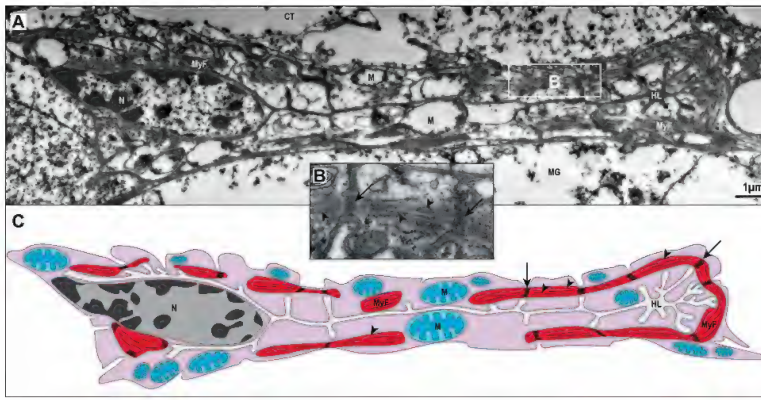

Fig. 36. *Eukoenenia spelaea* (Peyerimhoff, 1902), cross-sections through the heart. **A**. Transmission electron micrograph of a cross section through the heart. The lumen is reduced. No distinct pericardium was found. The heart is located adjacent to the midgut. **B**. Transmission electron micrographic close-up of a myofibril. Dark areas, similar to Z-lines (arrows), are associated with the infoldings of the cell membrane. Between these areas are muscle filaments visible (arrowheads). **C**. Schematic drawing of A. The cell is enlarged in the area of the nucleus. The thick filaments (arrowheads) are distributed irregularly within the myofibril. Abbreviations: CT = connective tissue; HL = heart lumen; M = mitochondrion; MG = midgut; MyF = myofibril; N = nucleus.

 ©ZFMK

and one strand of endosternal musculature (E8; Fig. 21). A layer of circular musculature is located around the pharynx. The circular muscle fibers are located alternating between the muscle fibers of pharyngeal muscles P3 and P4 (Figs 19B, 20A). The lumen of the pharynx is covered by a thick cuticle (EnC, EpC, ExC; Fig. 37A, B). The cuticle consists of an electron-translucent endocuticle and an electron-dense exocuticle. The exocuticle

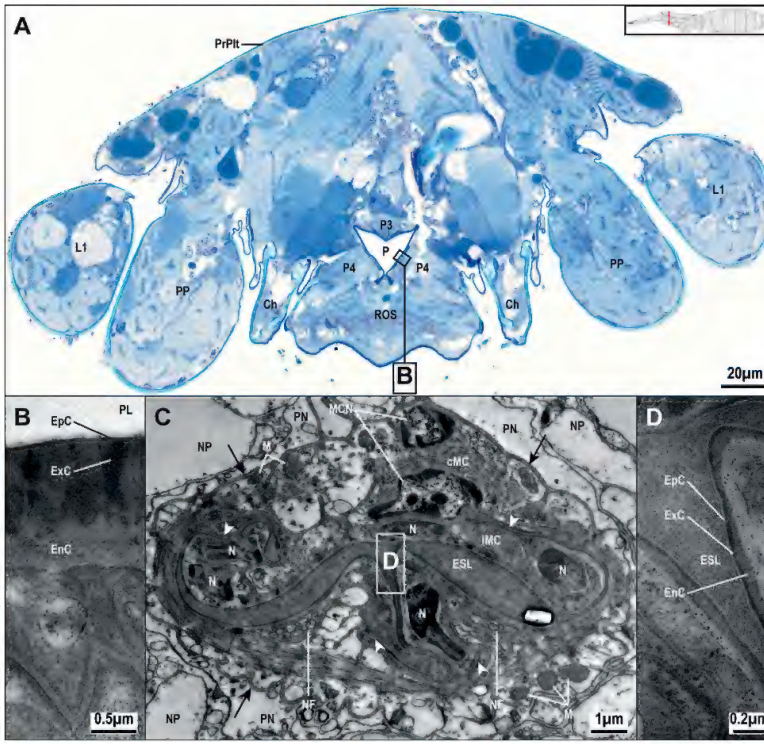

Fig. 37. *Eukoenenia spelaea* (Peyerimhoff, 1902), pharynx and esophagus. **A**. Light micrograph of a cross-section through a female at the level of the pedipalpal articulation. The pharynx is X-shaped; however, the lower shanks of the pharynx have no open lumen, thus, in cross-section, the actual open lumen of the pharynx resembles a "V". **B**. Transmission electron micrograph of the cuticular intima of the pharynx. The exocuticle is heterogeneous electron-dense and thicker than the electron-translucent endocuticle. **C**. Transmission electron micrograph of a cross-section through the esophagus. The lumen in the lateral branches of the esophagus is largely reduced/collapsed (white arrowheads). Two nuclei but no sarcolemma can be found indicating the syncytial character of the circular muscle cell. Two nerve fibers are located ventrolateral. The esophagus is surrounded by the neurilemma (black arrows), which is produced by the perineurium. **D**. Close-up transmission electron micrograph of the cuticular intima of the esophagus in C. The endocuticle is the thickest of the three cuticle layers. The epicuticle is electron-translucent. Abbreviations: Ch = chelicera; cMC = circular muscle cell; EnC = endocuticle; EpC = epicuticle; ESL = esophagus lumen; ExC = exocuticle; L1 = leg 1; lMC = longitudinal muscle cell; M = mitochondrion; MCN = muscle cell nucleus; N = nucleus; NF = nerve fiber; NP = neuropil; P = pharynx; P3/P4 = prosomal muscle 3/4; PL = pharynx lumen; PN = perineurium; PP = pedipalp; PrPlt = propeltidium; ROS = rostrosoma.

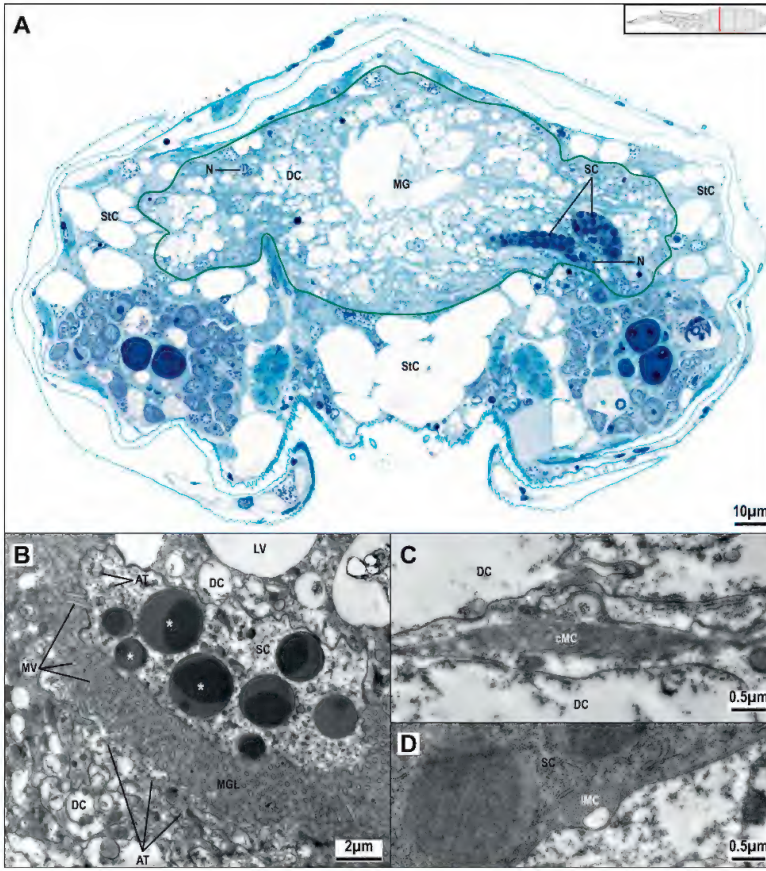

Fig. 38. *Eukoenenia spelaea* (Peyerimhoff, 1902), midgut in the opisthosoma. **A**. Light micrograph of a cross-section through segment 10 of a male. The midgut (green line) is a simple sac. Secretory cells can be easily distinguished from digestive cells. **B**. Transmission electron micrograph of the midgut epithelium. Secretory cells are recognized by the electron-dense secretion granules (asterisk). The microvilli of the secretory and digestive cells extend into the midgut lumen. Apical microtubuli are more numerous in digestive cells than in secretory cells. The digestive cells have large electron-translucent excretory vesicles. **C**. Transmission electron micrograph of the semicircular midgut musculature. The muscle cells are located within indentations between digestive cells. **D**. Transmission electron micrograph of the longitudinal midgut musculature. The thin muscle cells can be found spread sparsely along the midgut. Abbreviations: AT = apical microtubule; cMC = circular muscle cell; DC = digestive cell; ExV = excretory vesicle; lMC = longitudinal muscle cell; LV = lipid vesicles; MG = midgut; MGD = midgut diverticula; MV = microvilli; N = nucleus; SC = secretory cell; StC = storage cell.

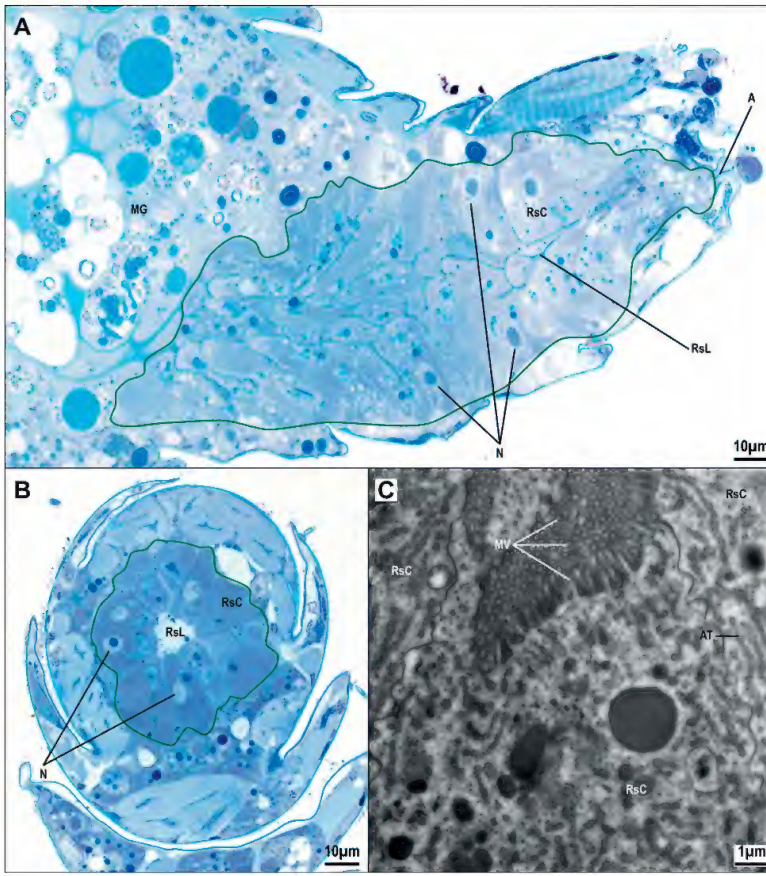

Fig. 39. *Eukoenenia spelaea* (Peyerimhoff, 1902), rectal sac. **A**. Light micrograph of a sagittal section through the metasoma of a female. The rectal sac (encircled by a green line) fills almost the entire metasoma. The nuclei of the high prismatic cells are located mostly basally. The lumen of the rectal sac is narrow. A distinct ectodermal, cuticula cover is missing. **B**. Light microscopic, slightly oblique cross-section of the rectal sac (green line) of segments 16–18. Small droplets are located mostly apically in the cells of the rectal sac. **C**. Transmission electron micrograph of the rectal sac epithelium. The dense microvilli of the rectal sac epithelial cells extend into the lumen. Abbreviations: A = anus; AT = apical tubule; MG = midgut; MV = microvilli; N = nucleus; RsC = rectal sac cells; RsL = rectal sac lumen.

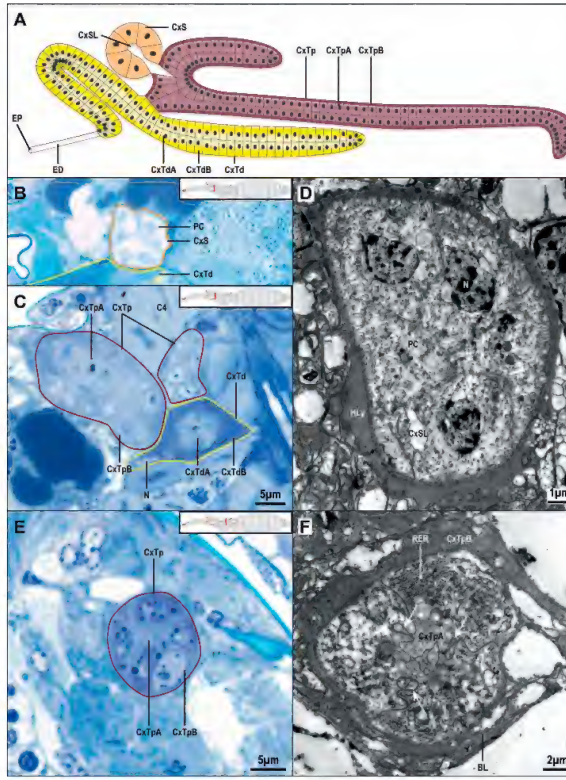

Fig. 40. *Eukoenenia spelaea* (Peyerimhoff, 1902), coxal organ. **A**. Schematic drawing of the coxal organ based on serial cross-section light micrographs and 3D-reconstruction. It consists of the saccule (orange), proximal tubule (brown) and distal tubule (yellow). The proximal and distal segments of the tubule have a basal labyrinth (dark) and an apical cytoplasmic part (light). The excretory duct is connected with the cytoplasmic part of the tubule cells. **B**. Light micrograph of a cross-section through the coxal organ region at the level of the 1st leg of a female. The saccule is not attached to musculature. The podocytes stain light and no lumen is visible. **C**. Light micrograph of a cross-section posterior to the saccule. The proximal segment of the tubule stains lighter than the distal segment tubule allowing for a straightforward distinction in light microscopy. Within the distal tubule, the nucleus is sometimes located in the basal region of the cells. **D**. Transmission electron micrograph of the saccule. It is completely surrounded by hemolymph. The saccule has a small lumen. **E**. Light micrograph of a cross-section of the proximal tubule at the level of the 3rd leg of a male. The basal part of the glandular cells contain dark staining secretion granules. **F**. Transmission electron micrograph of the proximal tubule. The basal labyrinth is filled with electron-dense material. Lateral membrane folds of the tubule cells interdigitae thus connecting the apical parts of the tubule cells (arrows). Abbreviations: BL = basal labyrinth; C4 = cheliceral muscle 4; CxS = coxal organ saccule; CxSL = coxal organ saccule lumen; CxTd = coxal organ distal tubule; CxTdA = distal tubular cell apical region; CxTdB = distal tubular cell basal region; CxTp = coxal organ proximal tubule; CxTpA = proximal tubular cell apical region; CxTpB = proximal tubular cell basal region; ED = excretory duct; EP = excretory pore; HLy = hemolymph; N = nucleus; PC = podocyte; RER = rough endoplasmic reticulum.

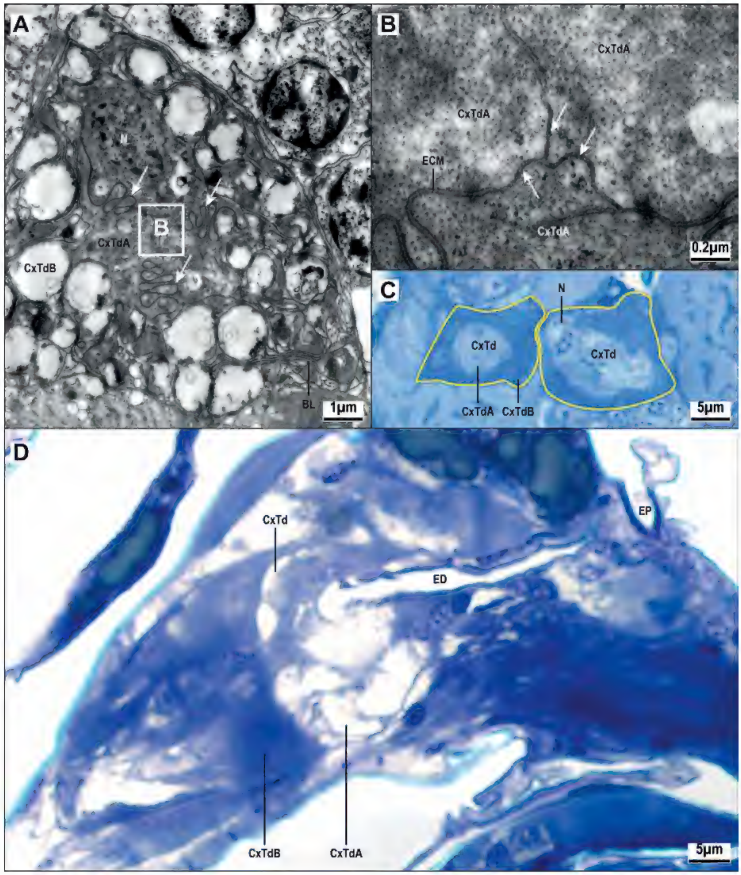

Fig. 41. *Eukoenenia spelaea* (Peyerimhoff, 1902), coxal organ. **A**. Transmission electron micrograph of the distal segment of the tubule. A large number of electron-translucent (almost empty) vesicles occurs within the basal labyrinth. The cells are tightly connected by membrane interdigitations (arrows). **B**. Close-up transmission electron micrograph of the apical cell region in A, where septate junctions connect the cells apically (arrows). There is no visible lumen due to the tight connection of the cells, only a thin layer of extra-cellular matrix. **C**. Light micrograph of a cross-section of the anterior loop of the distal segment of the tubule. Both arms of the tubule are closely neighboring each other. **D**. Light micrograph of a slightly oblique longitudinal section of the excretory duct. The duct originates between the apical parts of the tubule cells. It is lined with a thin cuticle intima. The excretory pore has a thicker cuticle. Abbreviations: BL = basal labyrinth; CxTd = coxal organ distal tubule; CxTdA = distal tubular cell apical region; CxTdB = distal tubular cell basal region; ECM = extra-cellular matrix; ED = excretory duct; EP = excretory pore; N = nucleus.

is approximately twice as thick as the endocuticle and shows regions of increased electron density (Fig. 37B). The epicuticle is a thin layer covering the exocuticle and appears to be electron-dense.

Esophagus

The esophagus extends from the posterior end of the pharynx to the region of the 2nd leg (Fig. 34). Its lumen has the shape of a stylized X. It is (partially) surrounded by the connectives between the supra- and subesophageal ganglia, and is separated from the neuropil by the neurilemma. The esophagus is surrounded by a few, irregular placed thin fibers of longitudinal musculature followed by an outer ring of thin circular musculature (cMC, lMC; Fig. 37C). The circular musculature is a syncytium (Fig. 37C). The outer cell membrane of the circular muscle layer is invaginated at the Z-lines, similar to what we described for the ultrastructure of the heart muscle. The paired nerve supplying the esophagus is located ventrolateral between the circular musculature and the epithelial cells (NF; Fig. 37C). The epithelium of the esophagus consists of about five cells in cross-section (Fig. 37C). These cells have irregularly shaped nuclei, perinuclear cytoplasm, and few mitochondria. The lumen of the esophagus is covered by cuticle with a thick electron-translucent layer of endocuticle, a thin electron-dense layer of exocuticle, and a thin electron-translucent layer of epicuticle (EnC, EpC, ExC; Fig. 37D).

Midgut

The prosomal midgut is tube-shaped and forms two lateral diverticula in the region of the 3rd leg (MGD; Fig. 34). The diverticula are simple evaginations of the midgut tube. The midgut and its diverticula are surrounded by few strands of longitudinal and incomplete circular musculature, which consists of one myofibril per muscle cell (lMC, cMC; Fig. 38C–D). The lumen of the midgut and diverticula is narrow. The epithelium is pseudo-stratified and is identical in both the midgut tube and the diverticula. It consists of two distinct types of cells, digestive cells and secretory cells (DC, SC; Figs 38A–B). Digestive cells are more numerous than secretory cells, they are high prismatic and have a basal nucleus. Numerous lipid vesicles can be seen in the lightly stained cytoplasm of the digestive cells (LV; Fig. 38B). Secretory cells are fewer in number, but are easily recognized in LM due to the dark staining cytoplasm and the high number of intensively staining secretory vesicles (*, SC; Fig. 38A–B). Like in the digestive cells, their nuclei are located at the base of the cells. Transmission electron micrographs show a microvilli border in both cell types. The microvilli are numerous and extend into the small midgut lumen (MV; Fig. 38B). Apical tubuli are more abundant in digestive cells than in secretory cells (AT; Fig. 38B).

The opisthosomal midgut (Fig. 38A) is a large sac with constrictions caused by the segmental dorso-ventral musculature (Fig. 34A). The epithelium of the opisthosomal midgut is the same like that of the prosomal midgut and a cytological distinction between midgut and midgut diverticula is not possible.

Rectal sac

The rectal sac is located in the metasoma, segments 15–18 (Rs; Fig. 34). It is differentiated from the midgut by a single-layered epithelium consisting of large, high-prismatic cells (RsC; Fig. 39A–B) with more or less basal nuclei of the rectal sac cells. The cytoplasm stains intensively in light microscopy. Small (secretory?) granules and larger lipid vesicles are located mostly in the apical cell region (Fig. 39A–B). Transmission electron micrographs show an apical microvilli border with a higher microvilli density than in the midgut epithelium. The epithelial cells of the rectal sac are rich in apical tubuli (AT; Fig. 39C). – It should be noted that no cuticle lining was found and the rectal sac continues directly into the anus, which is located ventral to the flagellum within the membrane of segment 18 (A; Figs 34, 39A). The membrane surrounding the anal opening is arranged in folds (Fig. 13B).

Excretory organ

Eukoenenia spelaea has one pair of coxal organs as the only excretory organs, Malpighian tubes are not present. The coxal organ consists of a saccule, a proximal and a distal tubule, an excretory duct, and an excretory pore (CxS, CxTd, CxTp, ED, EP; Figs 34, 40–41). The proximal and the distal segment of the tubule both have long, blind ending appendices, that reach from the forth segment in a posterior direction. The appendix of the proximal tubule reaches into the 9th segment.

The saccule is located in the region of the 1st leg, just posterior to the insertion of the basal article of the first leg on the prosoma. In total, it consists of seven to eight podocytes (PC; Fig. 40B, D). The pedicels of the podocytes are oriented towards the surrounding hemolymph. The center of the saccule has a narrow lumen (CxSL; Fig. 40D). The nuclei of the podocytes are oblong and central in the cytoplasm. The cytoplasm is rich in rough endoplasmic reticulum, free ribosomes and glycogen granules, but has few electron-dense droplets. The saccule connects to the most anterior end of the glandular section (Fig. 40A). A distinct collecting tubule was not identified.

The proximal segment of the tubule has a long, blind ending extension, reaching straight along the lateral body wall into segment 9 (Fig. 34). At the anterior, where the proximal tubule connects with the saccule and the distal tubule, it makes a sharp U-turn (Fig. 40A). At the pos-

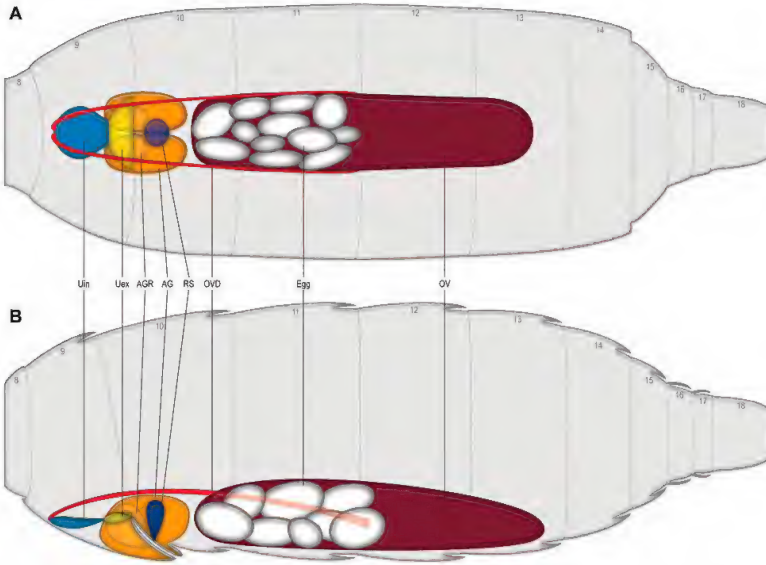

Fig. 42. *Eukoenenia spelaea* (Peyerimhoff, 1902), schematic drawing of the female reproductive organs based on serial cross-section light micrographs and 3D-reconstruction. **A**. Dorsal view. The unpaired ovary (brown) extends from segment 10 to segment 13. The eggs are positioned in an anterior position within the ovary. The accessory gland (orange) is located anterior to the ovary. The reservoirs of the accessory gland are located anterior to the club-shaped receptaculum seminis (dark blue). The accessory gland and the ovarian ducts (red) are the only paired internal structure of the female reproductive system. The ovarian ducts connect to the uterus interna (light blue) in segment 9. The uterus externa (yellow) opens toward the outside. **B.** Sagittal view. The ovarian ducts originate from a middle position along the ovary in segment 12. The accessory gland is located within the genital operculum and the genital lobes. The receptaculum seminis opens halfway between the genital opening and the posterior end of the genital operculum. Arabic numbers indicate the segments. Abbreviations: AG = accessory gland; AGR = accessory gland reservoir; OV = ovary; OVD = ovarian duct; RS = receptaculum seminis; Uex = uterus externa; Uin = uterus interna.

terior, it bends ventral and slightly towards the median line before ending blind. The proximal segment of the tubule has a prismatic epithelium with an apical cytoplasmic part and a basal labyrinth (CxTpA, CxTpB, BL; Fig. 40C, E–F). Cross sections show only three cells (Fig. 40F). Their heterochromatin-rich nuclei are located in the cytoplasmic part of the cells. The lateral walls of the cytoplasmic part of neighboring tubule cells interdigitate by lateral folds of the cell membrane; a thin layer of extra cellular matrix (arrows, Fig. 40F) is found between their cell membranes. Secretion granules are also present. The basal labyrinth contains vesicles of different electron density. The proximal segment has no open lumen. This appearance is uniform throughout, from the anterior to the posterior end.

The distal segment of the tubule is located within the basal article of leg 1 (Fig. 34). It originates from the proximal segment in close neighborhood to the connection with the saccule. The distal tubule forms a hairpin turn before it connects to the excretory duct (Figs 40A, 41C). The distal segment of the tubule also has a long extension that parallels closely the proximal tubule to the region of the 2nd leg where it ends blind. The epithelium of the distal tubule consists of prismatic cells with an extensive basal labyrinth (Fig. 41A). A minimum of three cells is found to build the tubule in cross-section (Fig. 41A). The nuclei are located mostly apical, however, they can also be found within the basal labyrinth (N; Fig. 41C). The cells of the basal labyrinth contain various electron-dense and electron-translucent vesicles.

Like in the proximal segment of the tubule, the apical cytoplasmic parts of the cells are connected by membrane interdigitations and septate junctions. The tubule has no lumen (arrows; Fig. 41B). The tubule connects to the cuticle-lined excretory duct (ED; Fig. 41D). The excretory pore is internally covered by thick cuticle and opens posteroventral to the basal article of leg 1, at the transition region between basal article and prosoma.

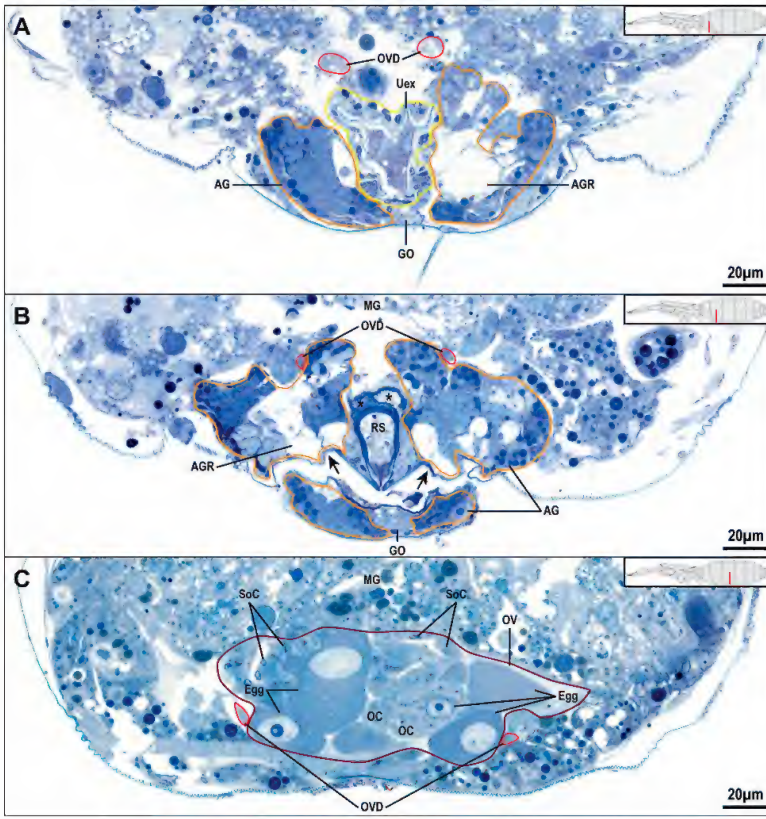

Fig. 43. *Eukoenenia spelaea* (Peyerimhoff, 1902), light micrographs of cross-sections through the female reproductive organs. **A**. Area of the genital operculum in segment 9. The cells of the paired accessory glands (orange line) contain numerous secretion vesicles. The uterus externa (yellow line) has numerous infoldings and a thin cuticle intima. **B**. Area of the receptaculum seminis in segment 10. The accessory gland extends into the genital operculum. The cuticle next to the reservoirs (arrows) differs from the neighboring cuticle. The receptaculum seminis has a thick cuticle lining. **C**. Area of the ovary (brown) in segment 11. The lumen of the ovarian duct (red line) is narrow and barely visible. The eggs next to the oocytes vary in size. Abbreviations: AG = accessory gland; AGR = accessory gland reservoir; GO = genital operculum; MG = midgut; OC = oocyte; OV = ovary; OVD = ovarian duct; RS = receptaculum seminis; SoC = somatic cell; Uex = uterus externa.

 ©ZFMK

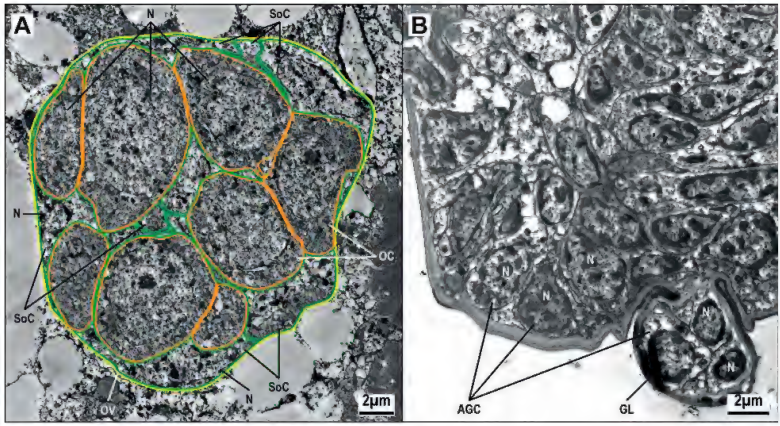

Fig. 44. *Eukoenenia spelaea* (Peyerimhoff, 1902), transmission electron micrographs of female reproductive organs. **A**. Cross-section through the ovary (yellow line) in segment 11. The large roundish oocytes (orange line) are nested between the irregularly shaped somatic cells (green line). The somatic cells are located at the wall of the ovary. **B**. Cross-section of the right genital lobe in segment 10. The epithelial cells of the accessory gland are high-prismatic with a basal nucleus. The gland extends into the genital lobe. Abbreviations: AGC = accessory gland cells; GL = genital lobe; N = nucleus; OC = oocyte; OV = ovary; SoC = somatic cell.

Reproductive organs

Details of the reproductive organs of *Eukoenenia spelaea* are based on light microscopic (LM) observations and transmission electron microscopy (TEM) of the female ovary and accessory gland. Due to material limitations, male structures were described using LM serial sections only.

Female

The female reproductive organs consist of the ovary, the ovarian ducts, the uterus interna, the uterus externa, the accessory gland, and the receptaculum seminis. The genital opening is located between the posterior genital operculum on segment 9 and the anterior pair of genital lobes on segment 10.

The ovary is a median, sac-shaped, unpaired organ and located in segments 10–13 (OV; Fig. 42). It consists of somatic cells, eggs of different sizes, oocytes as well as a lipid-rich secretion in larger specimens (Figs 12C, 43C). No musculature was found associated with the ovary wall. The somatic cells are flattened, irregularly shaped cells which attach directly to the ovarian wall (Figs 43C, 44A). The nuclei are also irregularly shaped. The oocytes are nested between the somatic cells. They have a characteristic large, heterochromatin-poor nucleus (Fig. 44A). Oocytes are found at the apex of the ovary while developed eggs were found close to the opening to the oviduct. Two of the studied females carried 6 and 12 eggs, respectively. In the larger specimen, the eggs were between 15 µm and 60 µm in diameter. The eggs were located anterior in the ovary while the posterior region of the ovary was filled with of lipid-rich secretions (Fig. 12C). In the smallest specimen, the eggs were between 15 µm and 25 µm diameter, probably representing an earlier develoopmental stage. In this specimen, the eggs were located posteriorly within the ovary and no secretion was found in the lumen of the ovary.

One pair of ovarian ducts originates lateral from the ovary at the border of segments 11 and 12 (OVD; Fig. 42). The ducts extend anterior into segment 9, where they connect to the unpaired uterus interna. The lumen of the ovarian ducts is narrow (Fig. 43). The uterus interna is located in the anterior part of segment 9 (Uin; Fig. 42). It is flat, sac-shaped, and has a thin squamous epithelium. It continues into the uterus externa, which is also located in segment 9 but posterior to the uterus interna (Uex; Fig. 42). Like the uterus interna, the uterus externa has a squamous epithelium, however, it displays many infoldings and it is lined with a thin cuticle intima (Fig. 43A). The nuclei are located basally (Fig. 43A).

The receptaculum seminis is an unpaired structure located in segment 10, mediposterior to the genital opening (RS; Fig. 42). The overall shape of the receptaculum is club-shaped in a dorsal-ventral axis, with the opening

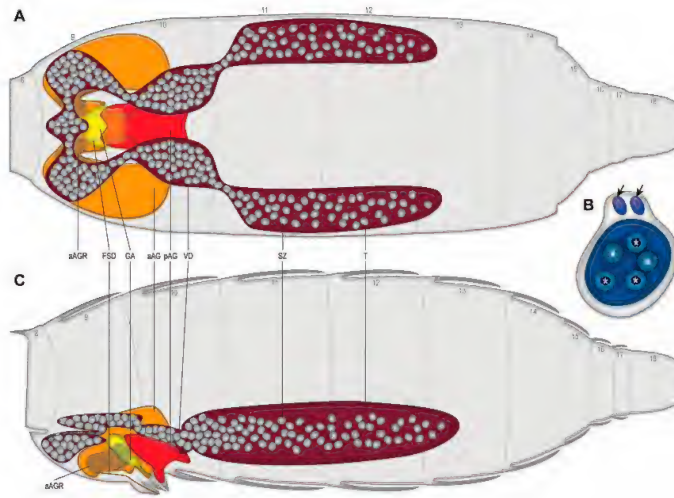

Fig. 45. *Eukoenenia spelaea* (Peyerimhoff, 1902), schematic drawing of the male reproductive organs based on serial cross-section light micrographs and 3D-reconstruction. **A**. Dorsal view. The paired testes (brown) continue into the winding deferent ducts which fuse anteriorly before terminating at the genital atrium (yellow). The paired anterior accessory gland (orange) is located ventral and lateral to the genital atrium and deferent ducts. The unpaired posterior accessory gland (red) is dorsal to the genital atrium and extends far into segment 10. **B**. Reconstruction of a spermatozoon. The large vacuole includes five dark staining spherical vesicles surrounded by several smaller light staining vesicles (asterisk). Two oblong structures are located at the apex of the spermatozoon (arrows). **C**. Sagittal view with a large number of spermatozoa contained in the vas deferens. Two fusule ducts originate from an anterior accessory gland reservoir and extend into the genital lobe 1. The posterior accessory gland has extensions into genital lobe 3. Arabic numbers indicate the segments. Abbreviations: aAG = anterior accessory gland; aAGR = anterior accessory gland reservoir; pAG = posterior accessory gland; FSD = fusule duct; GA = genital atrium; SZ = spermatozoon; T = testes; VD = vas deferens.

ventral in the gap between the genital operculum and the base of the genital lobes (Figs 42B; 43B). The epithelium is flattened and barely distinguishable in light microscopy. The lumen of the receptaculum is covered by a thick cuticle intima (Fig. 43B). Dorsal, the cuticle is arranged in two wrinkled lobes, originating medial and extending towards lateral (*; Fig. 43B). These lobes build a closed tube anterior, but are open posterior. No spermatozoa were found in the receptaculum.

The paired accessory glands extend from the junction of uterus interna and uterus externa to just anterior to the ovary in segments 9 and 10 (AG; Fig. 42). The gland is lobed, and extends into the genital operculum as well as the genital lobes (Figs 42B, 43B, 44B). The epithelium consists of high prismatic cells, which are filled with numerous secretory vesicles (Fig. 43B). Two lateral reservoirs are located within the accessory glands. They extend anterior from the genital operculum to both sides of the receptaculum seminis posterior. Both reservoirs are oriented towards the uterus externa and the genital opening (AGR; Figs 42, 43B). A glandular opening could not be identified, however, in regions where the reservoir touches the body wall, i.e., just past the genital opening, the epidermis and the cuticle are thin (arrows; Fig. 43B).

Male

The male reproductive organs consist of the testes, the vas deferens, a paired anterior accessory gland, an unpaired posterior accessory gland, and the genital atrium. The genital opening is located between the second and third pair of genital lobes between segments 9 and 10.

The testes are paired and located lateroventrally in segments 10–13 (T; Fig. 45). They extend lateral and parallel to the ventral musculature. No musculature was found associated with the testes wall. The epithelium consists

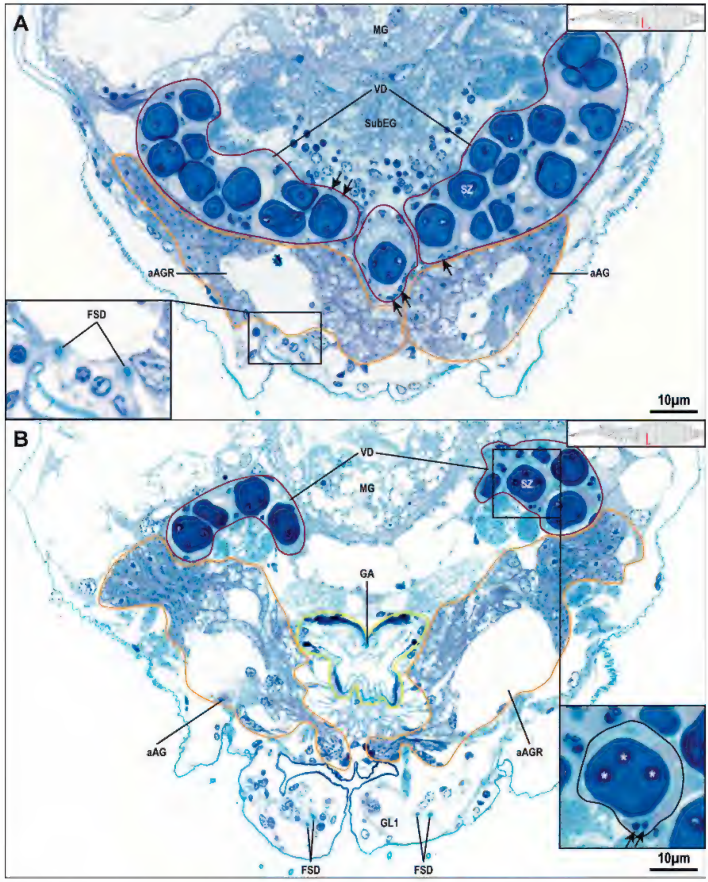

Fig. 46. *Eukoenenia spelaea* (Peyerimhoff, 1902), light micrograph of a cross-sections of the male reproductive organs. **A**. Anterior region of left and right vas deferens (brown line) and the paired anterior accessory gland (orange line) in segment 9. In the middle is the fused part of the vas deferens. The vas deferens has a flat squamous epithelium (arrows) and is filled with fully developed spermatozoa. The posterior end of the subesophageal ganglion is located dorsal to the vas deferens. The secretory vesicles of the anterior accessory gland epithelial cells stain differently. The fusule ducts originate at the anterior accessory gland's reservoir (inset). **B**. Genital atrium (yellow line) in segment 9. The spherical enclosures of the spermatozoan vacuole have lighter outer and darker inner vesicles (asterisk, inset). The spermatozoa have paired structures located in their apex (arrows, inset). The genital atrium is lined with a thick layer of cuticle. The fusule ducts are located inside the genital lobe 1. Abbreviations: aAG = anterior accessory gland; aAGR = anterior accessory gland reservoir; FSD = fusule duct; GA = genital atrium; GL1 = genital lobe 1; MG = midgut; SubEG = subesophageal ganglion; SZ = spermatozoon; VD = vas deferens.

of squamous cells and is barely discernible in light microscopy (Fig. 47B). Two cell types are present, somatic cells and germ cells. The somatic cells are small, of equal shape and size, and the cytoplasm stains bluish (SoC; Fig. 47B). They are irregularly dispersed between the germ cells. Germ cells vary in size and the cytoplasm stains purple in light microscopy (GC; Fig. 47B). Spermatozoa of different developmental stages, i.e., spermatogonia, spermatocytes, and spermatids, are found throughout the entire length of the testes (SpC, SZ; Figs 46–47). The largest spermatozoa are 12–15 µm in diameter and have a large vacuole (diameter 10–14 µm) with five spherical enclosures (diameter 4.5–5 µm) each (*in inset; Figs 45B, 46B). These enclosures contain several small droplets. The droplets in the periphery of an enclosure stain light in LM, the droplets in the cen-

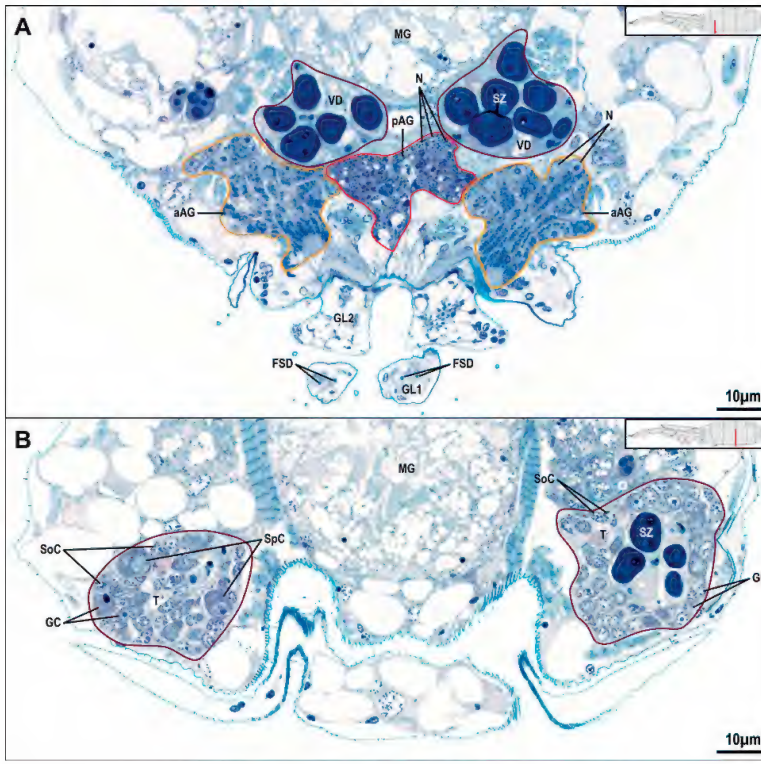

Fig. 47. *Eukoenenia spelaea* (Peyerimhoff, 1902), light micrographs of cross-sections through the male reproductive organs. **A**. Section through the anterior part of the second genital lobe in segment 9. The epithelial cells of the posterior section of the anterior accessory gland (orange line) have only smaller and darker staining secretory vesicles. The unpaired posterior accessory gland (red line) has prismatic cells with nuclei located basally. **B**. Section through the testes (brown line) at the border of segments 11 and 12. The number of fully developed spermatozoa is reduced. The posterior section of the testes is filled with different developmental stages of spermatozoa. Abbreviations**:** aAG = anterior accessory gland; pAG = posterior accessory gland; FSD = fusule duct; GC = germ cell; GL1/2 = genital lobe 1/2; MG = midgut; SoC = somatic cell; SpC = spermatocyte; SZ = spermatozoon; T = testes; VD = vas deferens.

 ©ZFMK

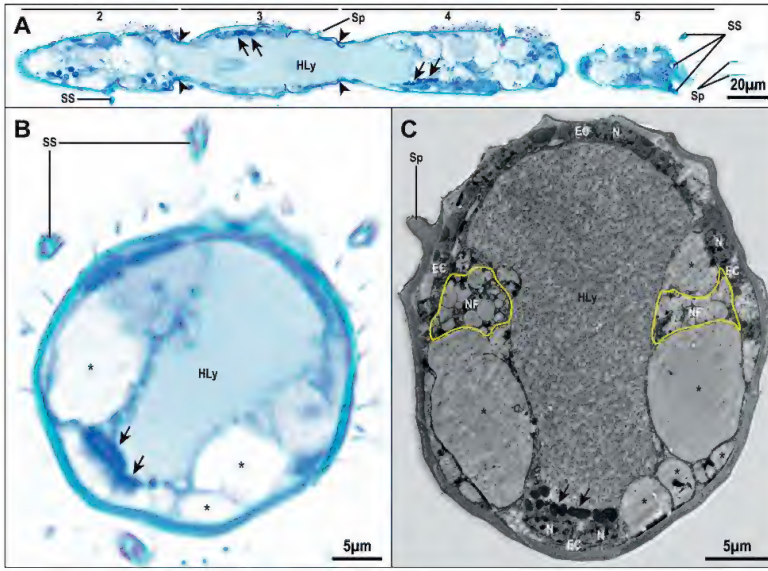

Fig. 48. *Eukoenenia spelaea* (Peyerimhoff, 1902), flagellum. **A**. Light micrograph of a longitudinal section of flagellar articles 2–5. The flagellum has no intrinsic musculature and is mostly filled with hemolymph. The cuticle is thinner where the flagellar articles connect (arrowheads). Secretory vesicles are located lateral in the hemolymph space (arrows). Numbers indicate flagellar articles. **B**. Light microscopic cross-section of a flagellar article. The hemolymph space is surrounded by large vesicles (asterisk). Secretory vesicles are only found towards one side of the flagellar article (arrows). **C**. Transmission electron micrographic cross-section of a flagellar article with a pair of lateral nerve fibers (yellow). Vesicles of varying sizes are found adjacent to the nerves. The secrete vesicles appear to be located within the hemolymph (arrows). Abbreviations: EC = epidermal cell; HLy = hemolymph; N = nucleus; NF = nerve fibers; SS = sensory seta; Sp = spike.

ter of the enclosure stain intensively (Figs 45B, 46). The nucleus of the large spermatozoa is located basal and is difficult to diagnose in LM because it is comparatively small and oblong. Two small, dark staining, oblong structures are located at the apex of the spermatozoa (arrows; Figs 45B, 46B). The nature of these structures is unclear. During development of the spermatozoa, the vacuole with the spherical enclosures increases in size, the nucleus changes shape from round to oblong, and the paired apical structure is still missing.

The vasa deferentes extend from the anterior end of the testes in segment 10 into segment 8, where they merge into a short single tube before opening into the genital atrium in segment 9 (VD; Fig. 45). The course of the vas deferens is not straight but winding (Fig. 45). It is located laterally of the dorso-ventral musculature of segments 9 and 10 (DV2, DV3; Fig. 19B). In segment 9, the vas deferens is oriented towards the median line, in segment 10, it is oriented towards the body wall. The tubes are filled with spermatozoa. The epithelium consists of flat squamous epithelial cells (Figs 46, 47A).

The paired anterior accessory gland is located ventral to the vas deferens in segments 9 and 10 (aAG; Fig. 45). The two glandular sacs have anterior extensions, which form an anterior loop. The extensions are oriented toward posterior, just anterior to the genital atrium. The sacs extend posterior, and are located close to the body wall and lateral to the dorso-ventral muscle DV2. The epithelium of the anterior accessory gland consists of high prismatic cells with the nuclei located basally (Figs 46, 47A). The cytoplasm is filled with secretory vesicles of different composition, large and lightly stained, and small and darker stained in light microscopy (LM). The larger vesicles are found within cells oriented towards the median line and closely associated with the reservoirs (Fig. 46). The smaller vesicles, however, are found in cells oriented

towards the body wall and towards posterior in the glandular sac (Figs 46, 47A). Anterior within the loop, the anterior accessory gland has large reservoirs, which stain lightly in LM (aAGR; Figs 45–46). Connected to these reservoirs are the fusule ducts. There are two fusule ducts per gland. These cuticle lined tubules extend through the first genital lobes to the fusules, two per genital lobe (FSD, GL1; Figs 14D–F, 45–46).

The posterior accessory gland is unpaired, sac-like in appearance, and is located in segments 9 and 10. It lies posteriorly to the genital atrium and has extensions into the third pair of genital lobes. Posteriorly it extends mid-section in segment 10 (pAG; Fig. 45). The posterior accessory gland consists of prismatic cells filled with two types of secretory vesicles, one small type staining dark and one larger type staining light (Fig. 47A). The nuclei are located basally within the cells. No secretory duct was found, but a region with thin epidermis and cuticle just posterior to the genital opening.

The genital atrium is located in the posterior half of segment 9 (GA; Fig. 45). It is a flattened sac with anterodorsal/posteroventral orientation and terminates at the genital opening between genital lobes 2 and 3. In cross-section, the lumen of the atrium has the shape of a stylized W in the anterior region (Fig. 46B). Towards the genital opening, the lumen is flattened. The genital atrium is internally covered by a squamous epithelium which secretes a thick layer of cuticle into the lumen. The cuticle stains heterogeneous and is darker in the dorsal and ventrolateral parts of the genital atrium (Fig. 46B).

Flagellum

The terminal flagellum is a prominent feature of *Eukoenenia spelaea*. It has a sclerotized basal ring-shaped socket that connects it to the last opisthosomal segment. The cuticle between flagellar articles is thinner than on the articles (arrowheads; Fig. 48A). The flagellum has no intrinsic musculature (Fig. 48). On each article, a superficial cuticular groove surrounds the article separating a proximal part with a group of sensory setae from a distal part which carries cuticular spikes on articles 1–3, 5, 7 and 9 (Sp; Figs 3B, 4B, 48A). The epidermis of the flagellum is a squamous epithelium with oblong nuclei. The epidermal cells contain light staining vesicles of different sizes (Fig. 48). A pair of nerves is located lateral in the flagellum (Fig. 48C). The central lumen of the flagellum is filled with hemolymph, which makes up approx. 50% of the total flagellar volume. Within the hemolymph, small dark staining vesicles can be found. These vesicles are clustered and located adjacent to the epidermis. The nature of the vesicles is unclear.

Phylogenetic analysis

Phylogenetic position of Eukoenenia spelaea

Not surprisingly, when adding *Eukoenenia spelaea* to Shultz's (2007a) original character matrices either for extant or for both, extant and fossil taxa (Appendix II), the two unweighted analyses result in consensus trees similar to Shultz's (2007a) original analysis.

Changes in character states and new characters in the data matrix

Based on our results, we had to modify some of the existing character states in the matrix and also created new character codes, thus augmenting the data matrix of Shultz (2007a; Appendix I: Tab. 6).

The first modified character state (6) is the division of the carapace with distinct pro-, meso- or metapeltidial sclerites. Our analysis of the musculature of *Eukoenenia spelaea* showed that the middle sclerites ("mesopeltidia") are not tergites of a segment, as previously assumed. Palpigrades have only two peltidia in a strict sense. Therefore, the character coding was changed to "absent", "two peltidia" and "three" peltidia). The coding was adjusted for *E. spelaea*, Palpigradi, Schizomida, and Solifugae (Appendix I: Tab. 6).

The first new character is the prosternum (12a). Our analysis showed that contrary to previous interpretations, the anterior-most sternum of *Eukoenenia spelaea* incorporates the sterna of segments 2–4. It was previously assumed that the sternum includes the sterna of segments 3 and 4 only. The coding was adjusted in *E. spelaea* to character state 1 = present, and in the other palpigrade groups to ? = unknown. All other taxa were coded 0 = absent (Appendix I: Tab. 6).

The original character state involving the rostrosoma (32) took only structures into account that included the pedipalp coxae and anterior elements of the prosoma. However, the rostrosoma of *Eukoenenia spelaea* is an independent structure that does not involve the pedipalp coxae or prosomal structures and would, therefore, be coded as absent. To accommodate the specific morphology of the palpigrade rostrosoma without pedipalpal contributions, the character state was rephrased in a more neutral way and the coding was adjusted for *E. spelaea* and Palpigradi (Appendix I: Tab. 6).

Character (61) coding for a trochanter-femur joint with a dorsal hinge or pivot operated by flexor muscles only, was deleted. It was an assumed autapomorphy for Palpigradi, however, our analysis revealed that an antagonistic pair of muscles is present in legs 2 and 3 (Figs 19A, 20C).

The number of metasomal sclerites (116) lacked an appropriate number for *Eukoenenia spelaea*. The original coding included only zero, two, three, five and nine sclerites. However, palpigrades have four metasomal sclerites.

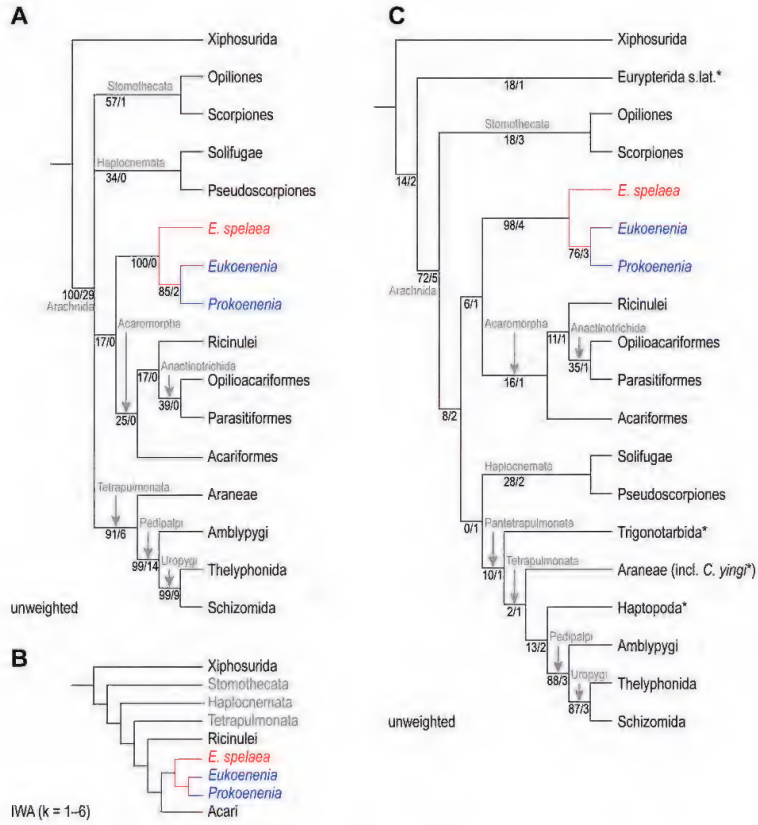

Fig. 49. Hypotheses about the phylogenetic relationship of Palpigradi. **A**. Minimal-length topology of the unweighted analysis of extant taxa. Numbers below internodes indicate bootstrap percentages/Bremer support values. Deepest relationships within Arachnida are unresolved. Palpigradi are placed as sister group to Acaromorpha. **B**. Implied weights topology of extant taxa. The implied weights analysis (IWA) of the matrix of extant taxa with k = 1 (1 tree, best score = 56.72381), k = 2 (1 tree, best score = 42.10714), k = 3 (1 tree, best score = 33.75952), k = 4 (1 tree, best score = 28.27460), k = 5 (1 tree, best score = 24.36688), and k = 6 (1 tree, best score = 21.43009) all resulted in the same major group topology. Palpigradi are sister group of the monophyletic Acari. Ricinulei are placed as sister group to this clade. **C**. Minimal-length topology of the unweighted analysis of extant and fossil taxa. Numbers below internodes indicate bootstrap percentages/Bremer support values. Major group relationships are resolved. Palpigradi are placed as sister group to Acaromorpha, the same result as in the analysis of extant taxa only. Implied weights analysis resulted in topologies identical to the unweighted analysis. Conflicts were limited to relationships between terminal taxa. Extinct taxa are marked by an asterisk.

Thus, the character coding was adjusted to include four sclerites (Appendix I: Tab. 6).

Our analysis of the segmental musculature in the prosoma of *Eukoenenia spelaea* revealed the presence of anterior oblique muscles. In the original data matrix of Shultz (2007a), such a character was not available. To accommodate the presence of this muscle type in *E. spelaea*, we created the new character (128a) "anterior oblique muscles of BTAMS anterior to postoral somite VI (state 1 only in *E. spelaea*)" (Appendix I: Tab. 6). The character coding was adjusted for all taxa.

The suboral suspensor was originally included in the matrix (Shultz 2007a) with the character state "a tendon that arises from the BTAMS and inserts on the ventral surface of the oral cavity via muscle" (131). We showed that in *Eukoenenia spelaea* muscle E8 (Fig. 21; Tab 5) does not insert on the oral cavity but posteriorly on the pharynx. In order to include this result, the term "oral cavity" was replaced with "foregut" and the character coding was adjusted to include the options "ventral on oral cavity" and "ventral and posterior on pharynx" (Appendix I: Tab. 6).

Character (135a) coding for the presence of the arcuate body in the protocerebrum was added to the analysis. This was done to accommodate the lack of this particular brain structure in *Eukoenenia spelaea* as well as Acari. The coding was changed accordingly (Appendix I: Tab. 6).

A new character (143a) was introduced to account for the (so far) unique morphology of the trichobothria in *Eukoenenia spelaea*. We showed that in contrast to the known morphology of trichobothrial dendrites of other euchelicerates, the dendrites of *E. spelaea* reach into the shaft of the trichobothrium, possibly adding a second sense modality to the trichobothrium, which has never been described in Eucheliceratа. The character coding was adjusted to reflect this (Appendix I: Tab. 6).

The frontal organ of *Eukoenenia spelaea* is located dorsal to the chelicerae. Therefore, character (148) was rephrased from "intercheliceral" to "supracheliceral" to accommodate that fact (Appendix I: Tab. 6).

The lateral organ (148a) of *Eukoenenia spelaea* as well as Palpigradi was added to the analysis (Appendix I: Tab. 6). The coding for all taxa was adjusted accordingly (present in *E. spelaea* and Palpigradi, absent in all other taxa).

The coxal organ of *Eukoenenia spelaea* includes a morphologically different proximal and distal section of the tubule. Such morphology of the tubule can also be found in some Acari. To allow for a more complete phylogenetic analysis, we added the character state "coxal organ with tubule differentiated into proximal and distal section" (178a). The coding was adjusted for Acari, *E. spelaea*, and Palpigradi (Appendix I: Tab. 6).

The ventral plate with its unique morphology has previously never been described for euchelicerates or any palpigrade. It has been added as character 179a for *Eukoenenia spelaea*. The coding was adjusted in *E. spelaea* to character state 1 = present. All other taxa were coded 0 = absent (Appendix I: Tab. 6).

The character state involving the dilator muscle of the precerebral pharynx and/or preoral cavity (194) was described in the original data matrix (Shultz 2007a) as "attaching to ventral surface of prosoma". However, in *Eukoenenia spelaea*, these dilator muscles attach ventrolateral on the rostrosoma. The character state was expanded to "attaching to ventral surface of prosoma or rostrosoma" and the coding was adjusted accordingly for *E. spelaea* and Palpigradi (Appendix I: Tab. 6).

The hindgut with a cuticular lining (203) is part of the ground pattern of euchelicerates. It is, however, missing in *Eukoenenia spelaea*. Thus, the matrix was adjusted to accommodate this result (Appendix I: Tab. 6).

Results of the analysis of the updated character matrix including data for Eukoenenia spelaea

The unweighted analysis of the adjusted matrix (Appendix I: Tab. 6, A1) for the extant taxa produced eight minimal-length trees (length 426, CI 0.560). The deepest interordinal relationships within Arachnida are unresolved (Fig. 49A). Five monophyletic groups with a bootstrap percentage above 80 were recovered, i.e., Arachnida (BP 100), Uropygi (Schizomida + Thelyphonida, BP 99), Pedipalpi (Uropygi + Amblypygi, BP 99), Tetrapulmonata (Pedipalpi + Araneae, BP 91), and Palpigradi (*Eukoenenia* + *Prokoenenia*, BP 85). Acaromorpha (Acariformes, Anactinotrichida, and Ricinulei) were reconstructed as with a bootstrap percentage of 25 and placed as sister group to Palpigradi. The placement of *Eukoenenia spelaea* with Palpigradi showed a nodal support of BP 100, all other groups had nodal support below BP 60. The weighted analysis of extant taxa placed Palpigradi as sister group to Acari (Fig. 49B). Ricinulei are the sister group to this relationship.

The unweighted analysis of the matrix containing extant and fossil taxa resulted in 12 minimal-length trees (length 475, CI 0.536; Fig. 49C). Only two monophyletic groups with bootstrap percentage above 80 were recovered, i.e., Uropygi (Schizomida + Thelyphonida, BP 87), and Pedipalpi (Uropygi + Amblypygi, BP 91). Arachnida showed a nodal support of BP 72. Acari were reconstructed as diphyletic with Anactinotrichida (Opilioacariformes + Parasitiformes) as sister group to Ricinulei. Palpigradi were recovered as sister group to Acaromorpha, however, with relatively weak support (BP 6). The placement of *Eukoenenia spelaea* with Palpigradi showed a nodal support of BP 98. Palpigradi (*Eukoenenia* + *Prokoenenia*) showed a nodal support of BP 76. All other groups showed nodal support below BP 40 (Fig. 49C).

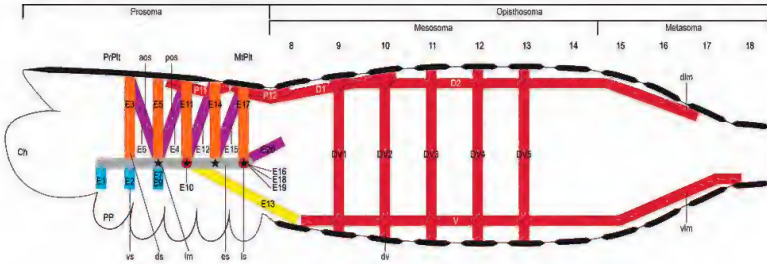

Fig. 50. *Eukoenenia spelaea* (Peyerimhoff, 1902), schematized representation of the segmental axial musculature. In the prosoma, dorsal suspensors are found in association with the pedipalp, 1st, 2nd, 3rd, and 4th leg. Three posterior oblique suspensors are associated with segments five, six and seven. From the second dorsal suspensor an anterior oblique suspensor arises. The posterior oblique suspensor at the posterior end of the endosternite inserts at the pleural membrane of segment 8. Ventral suspensor muscles are present in the first three segments. Muscle E13 originates in the region of leg 2 and inserts in the opisthosoma just anterior of where the ventral longitudinal musculature inserts. Lateral suspensor muscles are present in the region associated with leg 2 (E10) and leg 4 (E16, E18, E19). Two dorsal longitudinal muscles in the prosoma might be extensions of the dorsal longitudinal musculature of the opisthosoma. The first opisthosomal segment is free of dorsoventral and posterior oblique musculature. The following five opisthosomal segments follow the BTAMS but lack posterior oblique muscles. The last mesosomal segment lacks the dorsoventral musculature. Stars indicate the attachment sites of extrinsic leg musculature originating at the endosternite associated with legs 1–4. Abbreviations: aos = anterior oblique suspensor; Ch = chelicera; dlm = dorsal longitudinal muscle; ds = dorsal suspensor; dv = dorsoventral muscle; es = endosternite; lm = leg musculature; ls = lateral suspensor; MtPlt = metapeltidium; PP = pedipalp; PrPlt = propeltidium; Po = posterior oblique muscle; pos = posterior oblique suspensor; vlm = ventral longitudinal muscle; vs = ventral suspensor.

DISCUSSION

Body tagmatization

The arthropod body is organized as an array of segments. Blocks of segments may be integrated morphologically and/or functionally, forming tagmata. As reviewed by Fusco & Minelli (2013), the terms "segment" and "tagma" are descriptive, and the application of the terms is conceptually variable and differs between authors. Clearly, *[…] "their value as developmental units or units of evolutionary change should not be uncritically assumed" […]* (Fusco & Minelli 2013, p. 218). The term "somite" is occasionally used instead of "segment". Recently, Dunlop & Lamsdell (2017) suggested differentiating between "somite" and "segment", with the "somite" representing a developmental blueprint and the "segment" being the externally expressed, morphologically recognizable expression of the "somite". However, this suggested distinction is potentially confusing for three reasons: (1) "somite" denominates the serial mesodermal rudiments of the dorsal musculature in chordate embryos. (2) As suggested, it has an inherent component of idealistic morphology, i.e., assumes an archetypic blueprint of segmental organization from which "real" animals deviate. (3) The genetic layout of segmentation is conceptualized by "parasegments", which have been documented for all arthropods, including chelicerates (Damen 2002, 2007; Deutsch 2004; Peel 2004; Peel et al. 2005).

Fusion may affect the whole segment or only the dorsal or ventral part of it. Lamsdell (2013) reviews concepts of "tagmosis", suggesting that true tagmata should be defined by functional differences related to appendages. While this approach conjures a functional perspective, it remains fundamentally descriptive and typological, because most frequently, function is induced from topographic morphology. We follow Fusco & Minelli (2013) in their pragmatic approach, using "segment" and "tagma" as descriptive terms of modular organization of arthropods, and do not imply a priori homology when referring to segment numbers or tagmata. Because segment borders and tagmata can vary according to methods used, life stages, and phylogenetic relationship, they need to be determined explicitly for each taxon and each life stage. However, by using internal landmarks like serial axial musculature, we provide a powerful interpretative framework for segment homology.

The body of euchelicerates is divided into prosoma and opisthosoma. The border between prosoma and opisthosoma varies along the longitudinal axis and may even differ between the dorsal and the ventral side of the body (e.g., Xiphosurida, Scorpiones, Schizomida, Thelyphonida, Ricinulei; Dunlop & Lamsdell 2017). In some taxa, the opisthosoma is subdivided into meso- and metasoma (e.g., Amblypygi, Thelyphonida, Schizomida, Ricinulei,

Table 7. Comparison of the endosternal musculature associated with the box-truss axial muscle system (BTAMS) by Shultz (2001, 2007b). The complete set of segmental, axial prosoma muscles occurring in the supposed euarthropod ground pattern is given in the top row and mirrored as the grid system underlying the empirically observed/described muscles in various groups of euchelicerates. We included the original muscle terminology in each cell of the table so that reference to the original literature is straightforward. The identification of the muscles of a specific suspensor and segment is based on origin and insertion points. Due to the unclear segment borders in the prosoma, assignment of suspensor muscles is additionally based on directionality of the muscles. The original terminology of the previous authors was used to aid recognition. Question marks indicate that the association with a segment is unclear. Color codes are as follows: orange = dorsal suspensors, purple = anterior and posterior oblique suspensors, red = lateral suspensors, blue = ventral suspensors. Abbreviations: aos = anterior oblique suspensor, ds = dorsal suspensor, ls = lateral suspensor, pos = posterior oblique suspensor, vs = ventral suspensor.

		Segment 1	Segment 2	Segment 3	Segment 4	Segment 5	Segment 6	Segment 7	References
Euarthropod BTAMS	ds								Firstman (1973), Shultz (2001, 2007b)
	vs								
	ls								
	aos								
	pos								
Limulus sp.	ds		13_{i}	13_{ii}	13_{iii}	13_{iv}	13_{v}	13_{vi}	Shultz (2001)
	vs		15		16_{iii}	16_{iv}	16_{v}	16_{vi}	
	ls								
	aos								
	pos							14	
Arachnid BTAMS	ds								Shultz (2001, 2007b)
	vs								
	ls								
	aos								
	pos								
Eukoenenia spelaea	ds			E3	E5	E11	E14	E17	this study
	vs		E1	E2	E7/9	E13?			
	ls					E10		E16/19/20	
	aos				E6				
	pos				E4	E12	E15	E20	
Eukoenenia mirabilis	ds		d1	?	d3	d4		d5	Millot (1943)
	vs		v1	v2	v3	v4	v5	v6	
	ls			l	l	l	l	l	
	aos								
	pos					Sp		Sp	
Prokoenenia wheeleri	ds		ds		ds	Ds	ds		Firstman (1973)
	vs		vs	vs	vs	Vs	vs	vs	
	ls			ls	ls	ls	ls	ls	
	aos								
	pos								
Opiliones	ds				8			9	Shultz (2000)
	vs					12	12	12	
	ls								
	aos								
	pos								
Scorpiones	ds		EP1	EP3				ES4	Shultz (2007b)
	vs			EP6	$ES10_{iii}$	$ES10_{iv}$	$ES10_{v}$		
	ls								
	aos								
	pos		EP2	EP4					
Amblypygi	ds				17_{iii}	17_{iv}	17_{v}	17_{vi}	Shultz (1999)
	vs				20_{iii}		20_{v}	20_{vi}	
	ls								
	aos								
	pos				19_{iii}	19_{iv}	19_{v}		
Schizomida	ds			a? ds?	e1? ds?	c? ds?	d? ds?	1?	Börner (2004), Firstman (1973)
	vs			f? vs?	g? vs?				
	ls								
	aos								
	pos				e2?	h?	10?		
Thelyphonida	ds			13_{ii}	13_{iii}	13_{iv}	13_{v}	13_{vi}	Shultz (1993)
	vs			15_{ii}	15_{iii}	15_{iv}	15_{v}	15_{vi}	
	ls								
	aos								
	pos					14_{iv}	14_{v}	14_{vi}	
Pseudo-scorpiones	ds				?				Firstman (1973), Mehnert et al. (2018)
	vs							?	
	ls								
	aos								
	pos								
Ticks	ds			?	?			?	Firstman (1973)
	vs			?	?			?	
	ls							?	
	aos								
	pos								

Scorpiones). It requires analyzing independent morphological landmarks like origin and insertion of the serial axial musculature to assign segments to certain tagmata (van der Hammen 1986; Shultz 1993, 2007b; Mehnert et al. 2018).

Prosoma dorsum

In the (eu)chelicerate ground pattern, the prosoma consists of seven segments (Weygoldt & Paulus 1979b; Dunlop & Lamsdell 2017) that form a single dorsal shield and carry six appendages on the ventral side. Indeed, most euchelicerate groups, including fossil (e.g., Eurypterida) and basal extant groups (e.g., Xiphosurida) have a single prosomal shield covering the prosoma (Beier 1931; Gerhardt 1931; Gerhardt & Kästner 1931; Kästner 1931b, c, d; Vitzthum 1931; Dunlop & Lamsdell 2017). Despite branching-off basal from the euchelicerate phylogeny, the prosomal shield of *Limulus* sp. includes derived features, i.e., the large lateral wings, and it is merged with parts of the first opisthosoma segment (Chilaria segment). Actually, the prosoma of *Limulus* is a carapace comprising seven prosomal segments and (parts of) the first opisthosomal segment.

Assuming that a single prosomal shield (seven segments) represents the euchelicerate ground pattern (Weygoldt & Paulus 1979b; Dunlop & Lamsdell 2017), the prosomal morphology has been modified in Palpigradi, Schizomida, Solifugae and Acari. In these taxa, the prosomal shield is dorsally divided into three sclerites, i.e., pro-, meso-, and metapeltidium. The propeltidium is associated with the chelicerae, the pedipalps, and the first two pairs of walking legs. The meso- and the metapeltidium are associated with segments of walking leg 3 and 4, respectively (Kästner 1931e). The mesopeltidia of Schizomida are paired, dorsolateral sclerites, but Solifugae have one unpaired medial sclerite (Kästner 1931e, f). The morphological reorganization of the prosoma, actually the entire body, is even more substantial in Opiliones and Acari (Alberti & Coons 1999). In actinotrichid mites (Acariformes) the sejugal furrow divides the prosoma into a proterosoma containing the anterior 4 extremities, which, by segment numbers, is equivalent to the segments covered by the propeltidium, and a hysterosoma containing the posterior two pairs of legs and the opisthosoma. Pycnogonids also show a body tagmatization into an anterior cephalosoma with four limb-bearing segments followed by a number of trunk segments with legs. The obvious external morphological tagmatization of the prosoma into an anterior tagma (proterosoma, cephalosoma) with four pairs of extremities followed by two posterior segments has therefore (at least historically) considered representing an ancestral chelicerate condition (Kraus 1976; see Dunlop & Arango 2005; Ortega-Hernández et al. 2017 for a recent discussion).

Indeed, at first glimpse, the tripartite morphology of the prosoma of palpigrades appears similar to that of Schizomida and Solifugae. However, in this study we provide morphological evidence to assign sclerites to segments by comparing associations of serial axial muscles with the cuticular sclerites. The (presumptive) ground pattern of musculature in the prosoma of euchelicerates recognizes segmental dorsal and ventral suspensor muscles for each of the six post-ocular segments (Shultz 2007b), and a dorsal longitudinal muscle system in the opisthosoma that reaches into segments 6 and 7 of the prosoma. Based on this pattern, we would expect four dorsal suspensor muscles connecting the endosternite and the propeltidium (for the segments of the chelicerae, pedipalps, and the first two pairs of walking legs), and one pair of muscles for each, the mesopeltidium and the metapeltidium. We would also expect that the extensions of the dorsal longitudinal muscle system of the opisthosoma that reach into the prosoma, connect to dorsal sclerites associated with segments 7 (metapeltidium) and 6 ("mesopeltidium").

The association of muscles in *Eukoenenia spelaea* differs from that expectation in an admittedly complex manner. Indeed, four dorsal suspensor muscles are associated with the propeltidium (E3, E5, E11, E14; Figs 21, 50; Tabs 5, 7). Based on their origin and insertion these muscles must be assigned to prosomal segments 3–6 with the second prosomal segment missing a dorsal suspensor muscle. No musculature is associated with the mesopeltidium, but one dorsal suspensor muscle with the metapeltidium (E17; Figs 21, 50; Tabs 5, 7). The muscle assignment, of course, depends on the correct diagnosis of the dorsal suspensor muscles. However, this is straightforward because Palpigradi (like *Limulus polyphemus*) maintain the most complete set of segmental axial muscles (BTAMS; Fig. 50; Tab. 7). Like in most other euchelicerates, the first dorsal suspensor muscle is reduced, but, the ventral suspensor muscles are maintained in the anterior segments 2–4 (Figs 21, 50); ventral suspensor muscles are only missing in the more posterior segments of the prosoma. Together, dorsal and ventral suspensor muscles provide a complete set of landmarks from the first to the last prosomal segment, and their insertion on the dorsal sclerites provides direct evidence that the propeltidium is the common shield of segments 1–6. Because the mesopeltidium has no muscle insertion (except P9, which is an intrinsic prosomal muscle) we suggest it is not a segmental tergite, but a dorso lateral sclerotization of the pleural fold. Additional support comes from the dorsal longitudinal muscle system (muscles P11, P12) that connect the propeltidium with the metapeltidium, and the metapeltidium with the opisthosoma, respectively, thus skipping the "mesopeltidium".

Comparisons with reports on *Eukoenenia mirabilis* and *Prokoenenia wheeleri* reveal differences in the endosternal muscles associated with the peltidia. Millot (1943) reported four dorsal, five lateral, and six ventral suspen-

sors in *E. mirabilis* (Tab. 7). The dorsal suspensor of segment 7 and parts of the dorsal suspensor of segment 5 (presumably dorsal oblique suspensors) attach to the posterior border of the propeltidium, where they insert in the same position. There is no mention of suspensor muscles associated with the meso- and metapeltidium. Thus, following the author's description of muscle topography, the propeltidium of *E. mirabilis* would span segments 1–7. A similar endosternal suspensor muscle topography was described by Firstman (1973) for *P. wheeleri*. However, the most posterior dorsal suspensor muscle was associated with segment 6 by the author, therefore, assigning the propeltidium to segments 1–6 (Tab. 7). An insertion of dorsal suspensor muscle to the meso- and metapeltidium was not described.

While the published results for the three species of Palpigradi differ in some details of muscle topography, they all converge in the observation that the "mesopeltidium" has no attachment of dorsal suspensor muscles. They also converge in the observation that the first prosomal segment has no suspensor axial muscles and a variable morphology of dorsal and/or ventral suspensor muscles in the second prosomal segment. Even if these studies present slightly different observations, they do not report any suspensor muscle attaching to the "mesopeltidium" thus support our interpretation of the "mesopeltidium" being a sclerotization of the lateral pleural membrane rather than a tergite of the 6th segment. Weygoldt & Paulus (1979b) already noted that no muscles attached to the "mesopeltidia", and discussed that the "mesopeltidia" should not be considered derived from prosomal tergites. They also suggested that the division of the prosoma in Palpigradi, Schizomida and Solifugae might have evolved independently.

Although the external morphology of the dorsal sclerites of Solifuges, Schizomida, and Palpigradi appears to be similar we have now provided evidence (above) that, indeed, Palpigradi differ from the two other groups in the tagmatization of the dorsal prosoma. Supposing the existing descriptions for Solifugae and Schizomida are correct, i.e., the propeltidium covers the dorsum of segments 1–5, the mesopeltidium segment 6 and the metapeltidium segment 7, Palpigradi are different because the propeltidium covers segments 1–6. This observation and the obvious phylogenetic distance of Palpigradi from the other taxa, suggests that the dorsal subdivision of the prosoma into a propeltidium and metapeltidium has evolved independently.

The suggested interpretation of the dorsal subdivision of the prosoma of Palpigradi has further implications for our understanding of the evolutionary history of the chelicerate prosoma. In some publications (Lauterbach 1973; Kraus 1976; Scholtz 1998; Waloszek & Müller 1998; Waloszek et al. 2005; Dunlop & Alberti 2008), a division of the prosoma behind the second pair of walking legs was interpreted as a landmark of the ancestral arthropod head containing the ocular segment followed by 4 segments with extremities. According to this idea, pycnogonids, schizomids, solpugids and Acariformes retain an ancestral, five-segmented head region (see fig. 5 in Dunlop & Arango 2005) with the propeltidium (proterosoma, cephalosoma) as a landmark of a "retained head". Traditionally, Palpigradi had been assigned to that group of chelicerates. However, with the new evidence, now assigning the propeltidium to segments 1–6, Palpigradi show a clearly derived pattern that must be considered an autapomorphy of the group rather than symplesiomorphy on an ancestral arthropod level.

Prosoma ventrum

The ventral side of the prosoma of arachnids is morphologically variable. Distinct sclerites are present in many groups, but they differ in number, position and morphological origin (Moritz 1993; Shultz 1993, 1999). Thus, an a priori assignment of ventromedial sclerites as "sternites" is a terminological simplification that potentially creates confusion, in particular because the ancestral chelicerate had no prosomal sternites, but a ventral food groove occupying the space between the legs (e.g., Lauterbach 1973; Weygoldt & Paulus 1979b; Dunlop & Alberti 2008). As a sternite in a strict sense, we consider the ventral sclerotization of a segment, as compared to the tergite on the dorsal side. Ventral sclerites (i.e., sterna) may have evolved in the context of terrestrialization. Given the lack of sterna in Xiphosurida and the obvious differences in number, position, and origin of sterna in terrestrial groups of euchelicerates, they may have evolved independently in various groups of arachnids.

In scorpions, a single sternum is located between the coxae of legs 3 and 4. It possibly incorporates parts of the sternite of the first opisthosomal segment (Farley 1999, 2005; Shultz 2007b). Schizomida and Thelyphonida have three sterna. The anterior sternum is associated with legs 1 and 2, the middle sternum with leg 3, and the posterior sternum occupies the region between the last pair of legs (Börner 1904; Millot 1949c, Moritz 1993). Shultz (1993) suggested that this posterior sternum is derived from the sternite of the first opisthosomal segment. In Amblypygi, ventral prosomal sclerites may form one single sternum spanning the entire region between legs 1–4 (Millot 1949d, Shultz 1999). However, Shultz (1999) recognized a separate sclerite located between the last pair of legs ("metasternum") as derived from the first opisthosomal sternite. Some species of Pseudoscorpiones have a rudimentary sclerotized tubercle located between legs 3 and 4 others are missing ventral sclerites (Weygoldt 1969). The tubercle has been interpreted as a residual sternite (Vachon 1949; Moritz 1993), but its nature remains vague. Ricinulei (Millot 1949f), and Solifugae (Millot & Vachon 1949a) have no prosomal sterna. Acariformes (Actinotrichida; Alberti & Coons 1999) and Palpigra-

di possess podosomal sclerites that were interpreted as merged "epimera" (i.e., sclerotizations of the ventrum of segments 2–5; van der Hammen 1977b, 1982; Alberti & Coons 1999). While the morphological origin of the "epimera" remains obscure, van der Hammen (1977b) postulated that the "epimera" represented the morphological substratum from which the coxae evolved in more derived groups of euchelicerates and suggested that Acariformes and Palpigradi might be sister in a taxon "Epimerata". He based his reasoning on the position of the articulations of the leg articles, the insertion points of intrinsic leg muscles and the putative lack of a coxa in Palpigradi and Acari. The value of the position of articulations between articles of a leg and insertion points of tendons as phylogenetically informative character was questioned early (Weygoldt & Paulus 1979b). Our material provided the opportunity to compare directly the articulations and tendon insertions of all legs of Palpigradi in detail. We could not even find a common pattern of articulations when comparing the legs of individual specimens – each leg showed a different pattern of articulations and tendon insertion; none was consistent with the supposed pattern of "epimerata". – If "epimera" were the morphological origin of coxae, we would also expect intrinsic leg musculature emerging from the "epimera" as it does from the coxa. However, they clearly do not. We are certainly not the first to reject van der Hammen's (1977b) idea of "epimerata" (e.g., Weygoldt & Paulus 1979b, Dunlop & Alberti 2008). However, by studying the fine structure of the legs of Palpigradi we could provide additional and direct evidence that there is no morphological support for a taxon "epimerata" and that van der Hammen's (1977b) ideas are of mere historical interest.

In *Eukoenenia spelaea,* the ventral side of the prosoma is covered by four distinct sclerites. Based on examination of the external morphology, the large anterior sclerite supposedly represents the fused sclerites associated with the palpal segment and the segment of the first leg (hence "*deuto-tritosternum*"; van der Hammen 1982; Moritz 1993; Alberti & Coons 1999). The three posterior sclerites correspond with segments 5–7 (legs 2–4, respectively). Again, the segmental musculature of the prosoma provides independent morphological landmarks for testing the existing hypotheses/interpretations. We showed that the anterior sclerite is associated with the ventral suspensor muscles (E1, E2, E7/9), muscles that are assigned to segments 2–4. Therefore, we suggest that the anterior ventral sclerite of the prosoma is associated with segments 2–4. This new evidence rejects the existing interpretation that the sclerite is a "deuto-tritosternum (suggested alternative terminology "prosternum"). Prosomal segments 5, 6 and 7 do not have ventral suspensor muscles; however, a topographic association of these sclerites with these three segments is straightforward because of their topographic association with the legs.

Forming an anterior, large ventral sclerite that couples the bases of the pedipalps and the first pair of legs supports the idea that the pedipalps and leg 1 together form a functional unit. In contrast to the original idea that Palpigradi were using the pedipalp as walking leg (hence the name; Kästner 1931a), observations of live animals showed that the first pair of walking legs and the pedipalps together are used as sensory appendages (Kováč et al. 2002; Christian 2004). The exclusive occurrence of trichobothria and high number of sensory setae on leg 1, and the intensive innervation of that leg provide additional morphological evidence that both pairs of appendages are used for sensing the environment. Similar evolutionary transformations of the first pair of legs to mechano- and chemo-receptive palps are known from Uropygi, Amblypygi, Araneae, and Solifugae.

Chelicerae

The synapomorphic morphology of the chelicerate chelicerae is tripartite (Weygoldt & Paulus 1979b; Shultz 2007a). The fixed digit and movable digit form a chela. This morphology has been modified in various taxa of the euchelicerates by reducing the basal article, forming a subchela, and/or by adding combs, teeth or other cuticular structures to the surface of the chelicerae.

The chelicerae of *Eukoenenia spelaea* consist of three articles. The basal article is as long as the chela. Compared with the body size, the chelicerae of *E. spelaea* are large, as they have approximately the same length as the propeltidium. While the tripartite chelicerae of Palpigradi certainly reflect a plesiomorphic condition, the surface of the chelicerae carries large teeth ornamented with fine cuticular combs, which are a unique feature of Palpigradi. Large chelicerae and pincer-like structures are conventionally associated with raptorial function (Kaneko 1988; Moritz 1993). However, the relatively weak cheliceral musculature, that does not provide antagonistic function for opening and closing the chelae and the fine combs on the cheliceral teeth question this interpretation. Recently, Smrž et al. (2013, 2015) studied the gut content of palpigrades and found predominantly heterotrophic cyanobacteria. They suggested that palpigrades use their cheliceral teeth and combs to scratch cyanobacteria from the substrate. Indeed, the spacing between the fine teeth of the cheliceral combs is 0.05–0.1 µm and would certainly be suitable to scratch cyanobacteria from the sediment.

Pedipalps and legs

Euchelicerate appendages have been described as consisting of seven articles, but the total number of leg articles may differ between legs. In the specialized antenniform legs of Amblypygi, the tibia can consist of up to 43 articles and the tarsus up to 105 (Weygoldt 1996). In The-

Table 8. Comparison of leg article terminology of Palpigradi.

	Article 1	Article 2	Article 3	Article 4	Article 5	Article 6	Article 7–11
Shultz (1989)	Coxa	Trochanter	Femur	Patella	Tibia	Basitarsus	Telotarsus
van der Hammen (1982)	Trochanter	Femur 1	Femur 2	Genu	Tibia	Tarsus 1	Tarsus 2–7
Millot (1949*f*)	"Coxa"[1]	Trochanter	Femur	Patella	Tibia	Basitarsus (1–4)	Tarsus (1–3)

[1] Millot uses the phrase "hanche" in his publications.

lyphonida, leg 1 consists of 14 articles in total (Grams et al. 2018). A reduction to six articles can be observed in the pedipalps of Amblypygi, Araneae (Moritz 1993), Opiliones (Pinto-da-Rocha et al. 2007), Pseudoscorpiones (Weygoldt 1969), Ricinulei (Millot 1949f), Schizomida (Moritz 1993), Scorpiones (Polis 1990), Solifugae (Punzo 2012), and Thelyphonida (Grams et al. 2018). Only two pedipalpal articles may be found in some Acari (Moritz 1993). Not surprisingly, the homologization and terminology of the leg articles differs among authors (e.g., van der Hammen 1977a; Shultz 1989; Tab. 8).

Extremities of *Eukoenenia spelaea* differ in number of articles and muscle topography according to their position. The pedipalp has nine articles and leg 1 has 11 articles. Legs 2 and 3 have seven articles, but leg 4 has eight articles. What we describe as article 6 of leg 1 has been documented as two separate articles in other species (Kästner 1931a; Millot 1949a). In *E. spelaea,* this article shows a superficial cuticular groove in the middle, but it has no cuticular joint structure. Also, muscle (LI8) and tendon (LI9t; Figs 19A, 20C) span the entire article and show no attachment points of muscles/tendons adjacent to the circular cuticular groove located medially on the article. Therefore, we cannot clarify, whether this article is the result of fusion of two separate articles or whether it is a single article.

Van der Hammen (1977a) compared articulations points and muscle/tendon insertion in articles of leg IV among groups of euchelicerates and concluded that Palpigradi had no coxa, but the first article of the walking leg was a trochanter. Based on this observation and the occurrence of ventral prosomal sclerites he proposed his idea that the coxae were ancestrally missing in Palpigradi (and some Acariformes). Coxae would only later evolve from the ventral sclerites, which he termed "epimera" (thus epimerata). Our results provide the opportunity to compare his data (e.g., see van der Hammen 1977; Table 1) with our results (e.g., Fig. 11A–B). There is not a single article on the pedipalp, leg II and leg III that would compare to his documentation. It is obvious that legs differ in musculature, position of articulations and insertion points of muscles, so we do not question his presentation of the pattern for leg IV. However, the obvious morphological variability of these structures on sequential appendages, suggests that his interpretations (based on leg IV only) were too far reaching and not supported by the morphology of other appendages. We think that his ideas were stimulating and to a certain degree provocative, but they must be considered of exclusively historical interest (see also above where we have provided other reasons why we consider the "Epimerata" unsupported).

Dunlop & Alberti (2008) correctly argued that if the evolution of the coxa was supposed to represent an apomorphic state in other arachnid lineages, Epimerata were united by a plesiomorphic character (no coxae but epimera) – thus not supported as a taxon. Boxshall (2004) and Waloszek et al. (2005) compared the morphology of early arthropod fossils and showed that a coxa (i.e., protopodite sensu Boxshall; basipodid sensu Waloszek) were part of the euarthropod ground pattern. Despite variations in terminology, a coxa should be present in euarthropods; palpigrades and mites included.

Opisthosoma

The opisthosoma of Arachnida has 12(13) segments with segmental musculature and ganglia (Fage 1949; Millot 1949a; Shultz 2001, 2007*b;* Dunlop & Lambsdell 2017). The heart and gonads occupy the anterior segments of the opisthosoma (Fage 1949; Millot 1949b; Alberti et al. 2007). In some taxa, the opisthosoma is divided in two morphologically distinct regions, i.e., a meso- and a metasoma. In those groups (i.e., Scorpiones [Kästner 1931b, Polis 1990], Ricinulei [Millot 1949e], Schizomida, Thelyphonida [Kästner 1931f], and the extinct Aranea *Chimerarachne yingi* [Wang et al. 2018]), the mesosomal segments carry a dorsal tergite and a ventral sternite connected by lateral pleural folds, while the metasomal segments have sclerite rings without pleural folds. The number of mesosomal and metasomal segments differs among these groups (Tab. 9; Millot 1949e; Talarico et al. 2011; Fusco & Minelli 2013; Wang et al. 2018). All arachnids with a metasoma also have a terminal flagellum or sting (Fusco & Minelli 2013; Wang et al. 2018) except Ricinulei that lack a terminal structure on the metasoma (Millot 1949f; Talarico et al. 2011).

Table 9. Morphological characters of the mesosoma (yellow) and metasoma (green) in relevant arachnid taxa. The presence of the structure is indicated by color fill of the fields. Where information on the character is missing, a lighter version of the respective color or question mark was used. Abbreviations: DV = dorsoventral muscle; I = intersegmental muscle including dorsal, ventral, transversal muscles.

References: [1]Scorpiones: Millot and Vachon (1949b), Alberti et al. (2007), Shultz (2007b), Wirkner and Prendini (2007), Snodgrass (1965). [2]Ricinulei: Millot (1949e), Talarico et al. (2008, 2011). [3]Schizomida: Börner (1904), Millot (1949b). [4]Thelyphonida: Börner (1904), Millot (1949b), Shultz (1993). *Segment #8 (first opisthosoma segment, of scorpions is incorporated into the prosoma, and its musculature is incorporated in the formation of the diaphragm, its sternite is incorporated in the formation of the sternum (Farley 2001; Schultz 2007b). Because of segmental compression, the segment is not externally visible (Shultz 2007b). It has been source for considerable debate. For comparative purpose, we think it is important to refer to this segment here.

The opisthosoma of *Eukoenenia spelaea* is divided into a mesosoma (seven segments) and metasoma (four segments; Tab. 9). The mesosoma carries externally separate sclerites dorsal and ventral, which are connected by the pleural membrane. The metasoma is characterized by the presence of sclerite rings. Internally, the free opisthosomal ganglia, and the heart are restricted to the mesosomal segments 8–14 (mesosoma; Tab. 9). The segmental dorso-ventral and transversal musculature, is located in segments 9–13, thus, lacks in the first and the last mesosomal segment. The gonads are also restricted to segments 9–13. Serial intersegmental muscles are present throughout mesosoma and metasoma. The metasoma contains the rectal sac as prominent structure.

There is substantial variation in the external and internal morphology of the mesosoma and metasoma among arachnid groups and topographic shifts or organ systems are frequent (Tab. 9). However, such morphological variability is also evident in other arachnid groups without an opisthosomal subdivision (André 1949; Berland 1949; Millot 1949d, e; Millot & Vachon 1949a; Alberti et al. 2007) and therefore may be independent of the subdivisioning of the opisthosoma. All comparative morphological evidence (number of segments, position of organ systems; Tab. 9) and phylogenetic relationship among

clades suggest that the metasoma evolved independently in several lines of euchelicerates. The standard paradigmatic explanation (and probably most plausible explanation) proposes that the metasoma increases the degrees of freedom for movements of a terminal appendage. For example, Scorpiones carry a sting and poison gland on the last segment of the metasoma, which is used for overpowering prey, but also used during courtship behavior (Stahnke 1966; Polis & Farley 1979; Polis 1990). Thelyphonida use their metasomal flagellum as feeler (Moritz 1993; Alberti et al. 2007). Schizomida have a sexually dimorph flagellum, suggesting that movements of the flagellum are somehow relevant during courtship or mating (Hansen & Sørensen 1905; Moritz 1993; de Armas & Teruel 2002; Teruel & de Armas 2002; Pinto-da-Rocha et al. 2016). *Eukoenenia spelaea* has been observed raising their flagellum (and possibly metasoma) when irritated (Kováč et al. 2002). The presence of sensory setae along the flagellum suggests a sensory function (Ferreira and Souza 2012; Souza & Ferreira 2010b). The function of the small metasoma in Ricinulei is unclear because a terminal appendage is missing.

Cuticle

The cuticle of arthropods consists of a thick procuticle covered by a thin epicuticle. Depending on topographic and functional specializations, the procuticle can be differentiated into an inner endocuticle and an outer, sclerotized exocuticle (Hackman 1984; Neville 1984). Sclerotized cuticle can be either dark in color or colorless depending on its chemical composition and mode of sclerotization (Hackman 1984). The epicuticle is deposited on the cuticular surface through pore canals that penetrate the cuticle in large numbers. Soft cuticular membranes connect sclerotized regions (sclerites), allowing for movements and size changes, e.g. when feeding or during gestation. The cuticle of *Eukoenenia spelaea* is mostly unsclerotized, thus, lacks a distinct differentiation into endo- and exocuticle. This might be due to their small body size (Polilov 2015a).

Cutaneous respiration

Arachnids typically breathe with book lungs and/or tracheae. Respiratory organs may be reduced with decreasing body size, and cutaneous respiration has been reported for numerous mites (Levi 1967; Alberti & Coons 1999). The theoretical size limit of the effective dimension an organism can obtain for cutaneous respiration depends on shape, oxygen partial pressure, diffusion distance, metabolic rate, and the diffusion constant for oxygen (and carbon dioxide, of course). A maximum diameter of 1 mm for a spherical animal was estimated (Graham 1988). *Eukoenenia spelaea* is well below that size limit of diffusive respiration, given a maximum opisthosoma diameter of approx. 300 µm (left-right; 180 µm dorso-ventral), and a prosoma diameter of approx. 280 µm (left-right; 150 µm dorso-ventral). Also, the soft cuticle of *E. spelaea* is only 0.5 µm thick, and the underlying epidermis is single layered and flat, so that the overall diffusion barrier through the integument is less than 1 µm. The hemolymph space is limited, thus, gas exchange may occur directly across the cells of the organs in close contact to each other and across the body wall. For comparison, *Prokoenenia wheeleri* (Rucker, 1901) which is larger (2–3 mm; Rucker 1903) than *E. spelaea*, has ventral sacks which are considered to function as respiratory organs (but histological evidence is lacking).

Surface structures

Cuticular surface structures are common in arthropods, representing a plethora of forms and functions (Gorb 2001a). For example, the hair density in spiders was associated with water repellence (Suter et al. 2004; Bush et al. 2007). *Eukoenenia spelaea* displays an extensive pubescence on most parts of its body consisting of short cuticular protrusions (2–3 µm length). It is, however, not clear whether this dense pubescence can act as a water repellant surface in palpigrades.

Grooming behavior has been discussed for spiders as well as several coleopterans in association with maintaining their hydrophobic character (Kovac & Maschwitz 2000; Suter et al. 2004). Such behavior has also been reported for palpigrades (Christian 2004; Ferreira & Souza 2012; Souza & Ferreira 2010). Different from spiders and coleopterans, palpigrades do not use their legs for grooming, but their chelicerae. Specialized cuticular structures can be found on the fixed and movable digits of the chelicerae. These display serrated cuticular teeth. The distance between the teeth is approx. 1–1.5 µm. Between the teeth of the serration, the distance is approx. 0.05–0.1 µm. These structures match the thickness of the setae and trichobothria, the thickness of their spikes as well as the pubescence. Thus, one function of the chelicerae might be removing particles.

Ventral plate and underlying structure

A previously undocumented structure of *Eukoenenia spelaea* is the ventral plate with its cuticular teeth and the underlying epidermis. The cuticle of the ventral plate has enlarged pore canals in which microvilli reach from the underlying epidermal cells. The epidermis cells under the ventral plate are large, loaded with glycogen granules, possess a basal labyrinth and have numerous apical microvilli. These are typical cytological features of the cuticle and epidermis, usually found in association with a type 1 transport epithelium (Noirot & Quennedey 1974; Conte 1984). Of course, we could not directly test specific functions of these cells, but a comparison to a

similar cellular morphology with known functions provides at least comparative evidence for the functioning of the ventral plate. Cellular polarization and an extensive brush border of the epidermal cells has been found in the ventral vesicles of collembolans, which is the main place for sodium uptake (Noble-Nesbitt 1963; Eisenbeis 1974). A similar morphology has also been reported for the nuchal organ (cephalothoracic organ or salt organ) of Eucrustacea, which is involved in salt excretion (Conte 1984; Lowy & Conte 1985). In eucrustaceans, the epithelial cells also store glycogen granules, similar to our findings in *E. spelaea* (Hootman & Conte 1975; Lowy & Conte 1985). Thus, comparative cytology suggests that the ventral plate and its associated epithelium in *E. spelaea* might likely be involved in osmoregulatory processes.

Musculature

In the first part of this section, we discuss the segmental axial musculature of *Eukoenenia spelaea* in relation to the ancestral pattern of muscle anatomy as suggested by the euarthropod and euchelicerate box-truss axial muscle system (BTAMS; Shultz 1993, 1999, 2001, 2007b). This will be followed by a comparative discussion of other muscle systems (e.g., pharyngeal musculature, appendages) in the second part of this section. Our comparative discussion is to some degree "opportunistic" because it depends on presence, availability, completeness, and quality of the published record.

Suspensor muscles originating from the prosomal endosternite

The BTAMS as suggested by Shultz (1993, 1999, 2001, 2007b) was based on dissections of Xiphosurida, Scorpiones, Amblypygi, Thelyphonida, and comparisons with published record from other euarthropod taxa. The euarthropod box-truss axial muscle system assumes dorsal, ventral, and lateral (transverse connectors in terminology of Shultz [2007b]) suspensor muscles as well as anterior and posterior oblique muscles (Shultz 2007b). In the prosoma, all these muscles originate serially from the endosternite, i.e., each prosomal segment, except the first segment, carries a complete set of muscles. According to Shultz (2001, 2007) the chelicerate BTAMS ground pattern is identical to the euarthropod ground pattern. It was reconstructed on the assumption of serial muscle homology of the opisthosomal dorso-ventral musculature with the dorsal and ventral suspensor muscles of the prosoma, and the observation that Xiphosurida have anterior oblique muscles in the opisthosoma, while they are missing in all arachnids. For BTAMS in arachnids, Shultz (2001, 2007b) proposed that the anterior oblique suspensors were completely reduced. For the posterior oblique muscles, he proposed a shift of insertion from the tergites to the lateral pleural folds.

Table 7 gives an overview on the occurrence and published evidence of the prosomal axial musculature among euchelicerates. All studied euchelicerates deviate from BTAMS by missing some muscles of the supposedly ancestral pattern. However, *Eukoenenia spelaea* deviates from the arachnid pattern by possessing an anterior oblique suspensor muscle in segment 4, which occurs only in the euarthropod ground pattern (Tab. 7, Figs 21, 50). Muscle E13, which originates in segment 6 and inserts posteriorly in segment 8 might be interpreted as ventral suspensor that, untypically, spans several segments (but see discussion below). Lateral suspensors were described for segments 5 and 7. Our description of five pairs of dorsal suspensor muscles (Figs 21, 50) differs from that of Börner (1904), Millot (1943, 1949a) and Firstman (1973) who explicitly state that *Eukoenenia mirabilis* and *Prokoenenia wheeleri* have only four dorsal suspensor muscles, respectively. However, because our study is the only study based on serial sections and a complete reconstruction of the ground pattern of the musculature, while the others were based on dissections or cleared specimens, we respectfully consider our data as more complete.

We found four pairs of muscle that were assigned ventral suspensor muscles (with muscles E7/E9 assigned to the third pair of ventral suspensors and E13 to the last prosomal segment; Figs 21, 50), while earlier descriptions of *Eukoenenia mirabilis* and *Prokoenenia wheeleri* reported the full set of six ventral suspensor muscles. Palpigrades with six ventral suspensor muscles would represent the plesiomorphic condition of the arachnid BTAMS (Shultz 2007b). The lateral suspensor system shows a similar pattern, with the full set of segmental muscles described for *E. mirabilis* and *P. wheeleri*, while *E. spelaea* has only two lateral suspensor muscles (Figs 21, 50).

Interpretations of the axial muscle system in Palpigradi are straightforward. The prosomal axial muscle system is not only close to the arachnid ground pattern, but, because of the occurrence of an anterior oblique muscle in segment 4 (Tab. 7), contains elements of the euarthropod (!) BTAMS.

This plesiomorphic feature that is more ancestral than the euchelicerate ground pattern calls for explanation. – This reoccurrence of plesiomorphic morphology may be explained as resulting from paedomorphic development, i.e., developmental truncation. Under the assumption of anagenetic evolution, paedomorphosis by developmental truncation (Alberch et al. 1979) may create pattern of "reverse recapitulation", i.e., the adults of a species showing ancestral features of a stem group. The evolutionary implications of paedomorphosis will be discussed in more detail below.

Other prosomal muscles of the box truss axial muscle system

According to the euarthropod BTAMS (Shultz 2001), paired dorsal longitudinal musculature extends from the posterior prosoma segments (6 and 7) into the opisthosoma. These muscles have been documented for *Limulus polyphemus* (Shultz 2001), Amblypygi, Thelyphonida, and *Eukoenenia mirabilis* (Börner 1904). In the latter, these muscles also connect propeltidium and metapeltidium.

In *Eukoenenia spelaea*, we described two muscles (P11, P12; Figs 19B–C, 20, 50; Appendix I: Tab. 5) that represent anterior extension of the dorsal longitudinal muscle system and extend into segments 7 and 6 of the prosoma. Importantly, muscle P11 connects the propeltidium with the metapeltidium (thus skipping the "mesopeltidium"). If the mesopeltidium were a true tergite of segment 6, we would expect the dorsal longitudinal muscles connecting to this element. The described morphology where the muscles "skip" the "mesopeltidium" supports our interpretation that the mesopeltidium is not a tergite, but a sclerotization of the pleural fold. Muscle P12 is largely reduced in females, but in males connects the metapeltidium with the first opisthosomal segment, thus representing the ancestral condition of the euchelicerate BTAMS (Shultz 2001).

Muscles of the pharynx

In the arachnid ground pattern, two muscular pharyngeal pumps are present, a precerebral and a postcerebral pump (Snodgrass 1948). The presence of both muscular pumps varies among arachnids. The precerebral pharyngeal pump has dorsal and lateral dilator muscles and circular constrictor musculature. The dorsal dilator is part of the epipharyngeal complex, which, again, consists of an anterior and a posterior component (Shultz 1993). Dorsal dilator muscles of the anterior complex span between the pharynx and the intercheliceral septum, the dorsal dilator muscles of the posterior component attach to the prosomal shield. Variation of the pharyngeal muscles occurs in all components of the pre- and postcerebral pump as well as the anterior and posterior components of the precerebral pump.

The postcerebral pharyngeal pump is missing in palpigrades (Millot 1942). As shown here for *Eukoenenia spelaea*, the precerebral pharyngeal pump is simplified, i.e., it consists of the anterior component with a medio-dorsal dilator muscle (P3) spanning between the pharynx and the intercheliceral septum/sclerite (iChS; Figs 29, 37A). The lateral dilator muscles (P4) span between the lateral wall of the pharynx and the ventrolateral wall of the rostrosoma. *Eukoenenia spelaea* has a muscle (E8) that originates from the anterior margin of the endosternite and inserts at the posterior end of the pharynx. The muscular topography of *E. spelaea* largely resembles that of *Eukoenenia mirabilis* (Millot 1942). However, Millot (1942, 1943) described two muscles attaching in a ventral and anterior position of the pharynx (m2, m3) while we find only muscle E8 attaching in a ventral and rather posterior position of the pharynx. He also described an additional muscle (m4) spanning between the lower lip and the transition between mouth opening and pharynx. We could not find such muscle in *E. spelaea*. His rostrosomal muscles of the upper lip (L. sup., fig. 2 in Millot 1942) are probably equivalent to our muscles P1 and P2.

Shultz (1993) stated that the epipharyngeal complex of *Eukoenenia mirabilis* consists of a smaller anterior and a larger posterior component. His interpretation was based on data reported in the studies by Roewer (1934), and Millot (1942). However, in our view the medio-dorsal dilator of the pharynx in *E. mirabilis* (m1; Millot 1942) represents the anterior component of the epipharyngeal complex, while the posterior component is missing. The small anterior muscle(s) associated with the anterior end of the pharynx (L. sup., Fig. 2 in Millot 1942; P1, P2 in our nomenclature) insert(s) in the upper lip and thus, are not part of the epipharyngeal complex as defined by Shultz (1993).

Axial musculature of the opisthosoma

For the opisthosoma of euarthropods, Shultz (2001) proposed longitudinal dorsal and ventral muscles, segmental dorso-ventral muscles, as well as anterior and posterior oblique muscles. According to Shultz (2001), the anterior oblique muscles are reduced, except in *Limulus*, where a highly modified pattern of anterior oblique muscles is maintained. The posterior oblique muscles insert on the lateral pleural membrane in all arachnids. The dorsal and ventral longitudinal muscle systems attach in each segment. The dorsal muscle system extends into the prosoma where muscles attach to the sclerites of segments 6 and 7.

The dorso-ventral musculature of the first opisthosomal segment requires special discussion. The morphology of the first opisthosomal segment is modified in many arachnid taxa, e.g., in Scorpiones (Shultz 2007b) it is integrated in the diaphragm, in Araneae (Gerhardt & Kästner 1931) it forms the pedicel, in Amblypygi, Schizomida, and Thelyphonida (Börner 1904; Kästner 1931f) the ventral parts of the first opisthosomal segment are supposedly transformed into the sternite of the prosoma. In other groups, the dorso-ventral musculature is completely missing in the first opisthosomal segment, e.g., Pseudoscorpiones (Mehnert et al. 2018) and Solifugae (Kästner 1931e). In our documentation of the axial musculature of palpigrades, dorso-ventral muscles are completely missing in the first opisthosomal segment. Firstman (1973) mentioned opisthosomal dorso-ven-

tral musculature, but does not provide necessary details about the segmental topography.

The posterior oblique musculature is completely absend from the opisthosoma. Muscle E20 that originates from the posterior end of the endosternite and inserts lateral on the pleural membrane of the first opisthosomal segment actually is the posterior oblique muscle of the last prosomal segment. This interpretation is in contrast to, but more parsimonious than that of Börner (1904) and Kästner (1931a), who suggested that muscle E20 is the dorso-ventral muscle of the 1st opisthosomal segment that moved its ventral attachment from the sternite to the posterior end of the endosternite and its dorsal attachment from the tergite to the pleural membrane.

The dorsal and ventral longitudinal muscles of *Eukoenenia spelaea* have a single point of origin and insertion, respectively. Unusual are the two lateral branches of the ventral longitudinal muscles. Similarly, noteworthy is the topography of dorsal longitudinal muscle D1, which originates in the prosoma from the metapeltidium and inserts posterior to the origin of dorsal longitudinal muscle D2 in segment 10. This overlap of the dorsal longitudinal muscles is similar to that of the dorsal longitudinal muscles in Amblypygi, Thelyphonida, and Xiphosurida. However, the lack of segmental attachment of the dorsal and ventral longitudinal musculature appears to be unique for *E. spelaea*.

Börner (1904) and Kästner (1931a) suggested that muscle E13 is an anterior extension of the ventral longitudinal muscle inserting on the posterior region of the endosternite. Börner's (1904) and Kästner's (1931a) interpretation, assuming a shift of the attachment from the ventral sclerite to the endosternite, is equally parsimonious to our interpretation, that E13 is a ventral suspensor that moved the insertion from the ventral sclerite of the last prosomal segment to that of the first opisthosomal segment.

The 2nd and 4th opisthosomal segment (segments 9 and 11) show two pairs of peculiar muscles that might be either interpreted as lateral branches of the ventral longitudinal muscle system, or as posterior and anterior oblique muscles of opisthosomal segments 2 and 4. Both situations would be unusual, because (1) the ventral longitudinal muscle system usually does not branch in arachnids, and (2) anterior and posterior oblique muscles are intersegmental, but the muscle of the 2nd opisthosomal segment is intrasegmental and the muscle of the 4th opisthosomal segment bridges two segments. Also, anterior oblique muscles are absent from the arachnid ground plan, thus the description of these muscles as anterior oblique requires the assumption of reoccurrence of plesiomorphic characters (but see below).

Other axial muscles (non-BTAMS)

We identified several additional muscles in the opisthosoma that do not belong to the BTAMS. Intertergal and intersternal muscles, i.e., muscles connecting tergites and sternites, can be found in Amblypygi (Shultz 1999), Araneae (Whitehead & Rempel 1959), Scorpiones (Shultz 2007*b*), and Thelyphonida (Shultz 1993). An incomplete set of such muscles was described for Opiliones (Shultz 2000). Börner's (1904) report of *Eukoenenia mirabilis* mentioned one pair of intersegmental muscles in each segment from segment 10–15. Additionally, muscles associated with the last opisthosomal segment and its appendage were reported in Thelyphonida (Shultz 1993) and Xiphosurida (Shultz 2001).

Eukoenenia spelaea has up to six pairs of intersegmental muscles in each segment 9–17. Except for segment 8, these intersegmental muscles are more or less homogenously formed between all opisthosoma segments. However, in segment 9 we described intrasegmental muscles (JI1–JI4; Figs 19C, 20A) that closely resemble in topography and number the intersegmental muscles (JII–JIX) of the following segments, but, muscles JI1–JI4 do not extend into the preceding segment 8. A straightforward interpretation is that these muscles were originally intersegmental muscles that lost their origin on segment 8.

In the last opisthosomal segment, two paired and one unpaired strong longitudinal muscles attach to the basis of the flagellum. The large number of small intersegmental muscles is in contrast to earlier reports of *Eukoenenia mirabilis*.

Musculature of the appendages

Chelicerae

The musculature associated with the chelicerae varies within the euchelicerates. In groups with tripartite chelicerae, a variable number of extrinsic muscles with antagonistic function (Tab. 10) moves the basal article. A varying number of extrinsic and antagonistic muscles (Tab. 10) also moves bipartite chelicerae. The chela opens and closes by an antagonistic pair of muscles/tendons in both tripartite and bipartite chelicerae, which attaches to the movable digit only (Millot & Vachon 1949a; Steinbach 1952; Whitehead & Rempel 1959; van der Hammen 1966, 1967; Dubale & Vyas 1968; Vyas 1974; van der Hammen 1982; Shultz 1993; Alberti & Coons 1999; Shultz 1999; 2000, 2001; Meijden et al. 2012). The depressor muscle of the movable digit is generally more prominent than the levator muscle. The fixed digit is free of musculature.

Three extrinsic and ten intrinsic muscles move the tripartite chelicerae of *Eukoenenia spelaea*. Based on the topography of origin and insertion of these muscles, we suggest that muscles C1, C3 (Tab. 10) possibly cause

Table 10. Musculature of chelicerae of *Eukoenenia spelaea* in comparison with other eucheliceratе groups (where data is available). The muscles are color coded according to their insertion points on the articles of the chelicera. Grey color indicates extrinsic prosoma muscles that insert on the basal article of the chelicera; orange codes muscles in the basal article that insert on the fixed finger, and purple codes muscles originating the fixed finger and inserting on the movable finger. Line drawings visualize a schematized ground pattern of antagonist muscles in the tripartite (upper part) and bipartite (lower part) chelicerae, with chelae and subchelae, respectively. Antagonist functions of depressor – levator muscles refer to opening / closing of the chela or lowering / lifting of cheliceral articles. Of course, the precise movement depends on the degrees of freedom provided by the joint morphology which is not known for most taxa. We therefore present a simplified scheme based on muscle topography only. Generalized antagonist functions "depressor–levator", include lateral (abduction, adduction) and rotational movements which, however, cannot be deduced from muscle topography.

	Depressor	Levator	Depressor	Levator	Depressor	Levator
Tripartite chelicerae	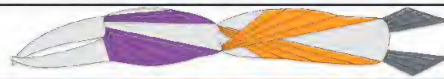					
Xiphosurida (Shultz 2001)	51	52	50	49	48	45–47
Scorpiones (Vyas 1974)	17	19	12, 13, 15	14, 16	1, 3, 4, 6, 8–10	2, 5, 7, 11
Opiliones (Shultz 2000)	38	39	35, 36	34, 37	27–29, 32, 33	30, 31
***E. mirabilis* (van der Hammen 1982)**	t_s	t_i	tf_i	tf_s	ttr_i	ttr, ttr_s
E. spelaea	C9–13		C6	C5, C7, C8	C1, (C2?) C3	C4
Bipartite chelicerae						
Solifugae (Millot & Vachon 1949a, Meijden et al. 2012)	depressor digiti mobilis	levator digiti mobilis	depressor	levator		
Araneae (Steinbach 1952, Whitehead & Rempel 1959)	70–72	69	Add, De, Re / 11c–15c	Abd, Le, Pro / 9c, 10c, 16c		
Amblypygi (Shultz 1999)	33	34	25–28	29–32		

downward movements of the chelicerae, while muscle C4 (Tab. 10) moves the chelicerae upward. Muscles C5, C7, and C8 originate in the first article of the chelicerae and share a common insertion point on the lower edge of the chela, probably causing a sidewards and downward movement of the entire chela (Tab. 10). The function of the small intrinsic muscle C2 is not clear. Different from other eucheliceratеs, a muscular antagonist is missing, because origin and insertion of muscle C6 rather suggest a median rotation. Upward movement of the chela might be achieved through hemolymph pressure. The prominent closing musculature of the fixed digit (C9–13; Tab. 10) has no muscular antagonist. Thus, we find no muscles that actually open the chela. We therefore assume that hemolymph pressure opens the chelicera. *Eukoenenia spelaea* appears to be the only eucheliceratе, which differs from the ground pattern of eucheliceratе musculature and has hydraulic functions that operate the chelicerae.

Pedipalps and legs

In the ground pattern of arachnids, walking legs consist of seven articles. The basal article (= "coxa") was probably moved by nine extrinsic muscles. Of these muscles, five originated from the dorsal shield and four originated from the endosternite (Shultz 1991). However, van der Hammen (1982) proposed for Palpigradi (and Parasiti-

Table 11. Musculature of leg 4 of Eukoenenia spelaea in comparison with the proposed euchelicerate ground pattern and other euchelicerate groups for leg 4 (Shultz 1989). For better distinguishability of the separate muscles, the ground pattern was divided into two schematics. Muscle color codes in the table are identical to the schematic in the header. Light color code for *E. spelaea* indicates muscles which are not a good fit to the proposed ground pattern. Muscle 8 is coded as one muscle, but it is divided into several smaller muscles in most euchelicerate.

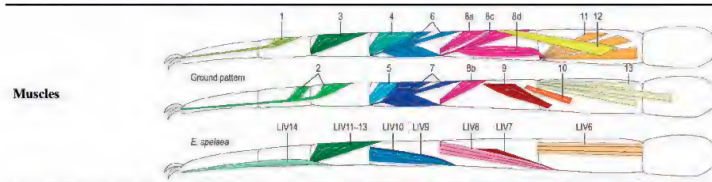

Leg article	7(–8)	6	5	4	3	2	1
Ground pattern							
Xiphosurida							
Opiliones							
Scorpiones							
Araneae							
Amblypygi							
Schizomida							
Thelyphonida							
Pseudoscorpiones							
Solifugae							
Ricinulei							
Acariformes							
Parasitiformes							
E. mirabilis							
E. spelaea							

Table 12. *Eukoenenia spelaea*, comparison of musculature in pedipalps and legs. Color coding is identical to table 11. Light color code indicates muscles which are not a good fit to the proposed ground pattern. The muscles are coded according to their presence in one or more leg articles (the additional articles of pedipalp and leg 1 are assumed to follow article 7).

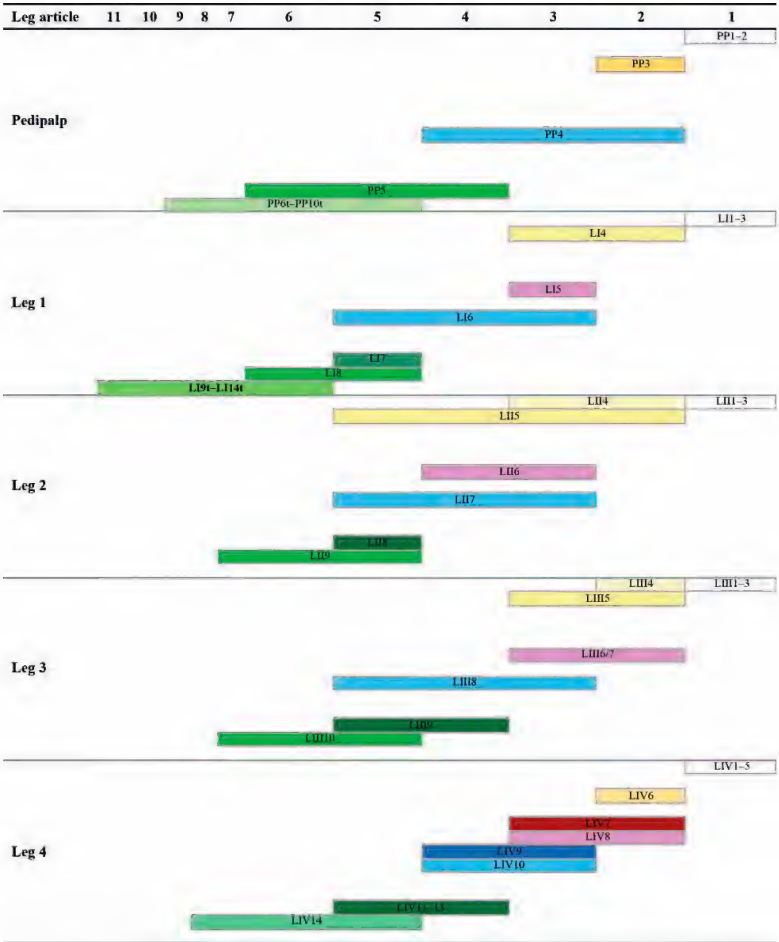

 ©ZFMK

formes) that the first article is not a coxa, but a trochanter. He based his interpretation on the pattern of muscle insertion and the position of articulations found in the first leg article of the forth leg of *Eukoenenia mirabilis*. According to his study, a pair of muscles/tendons inserted laterodorsal and lateroventral, the articulation is located ventral. This view was already rejected by Shultz (1989), who reasoned that the number of extrinsic muscles in *Eukoenenia* sp., is consistent with the muscle arrangement of the coxa in most euchelicerates. – While there are a number of other reasons for rejecting the "Epimerata hypothesis" by van der Hammen (1977a, 1982), we will briefly discuss the topographic pattern of leg muscles because it is at the core of that hypothesis.

Extrinsic musculature is found in all extremities of *Eukoenenia spelaea*. However, the number and origin of these muscles varies between legs. Legs 1–3 have one extrinsic, endosternal muscle each, but leg 4 has three endosternal muscles. One extrinsic muscle originating on the dorsal shield is present in the pedipalp, and legs 1–3. Leg 4 has no extrinsic musculature originating from the dorsal shield.

The muscle/tendon configuration proposed by van der Hammen (1982) for the first article in *Eukoenenia mirabilis* was only found in part in leg 4 of *E. spelaea*. Muscle LIV4 fits the description, however, LIV5 does not. For the other leg joints, only few muscles matched the suggested configuration. The muscle configuration reported by Shultz (1989) for the coxa in *Eukoenenia* sp. can be partially found in legs 2–4. As mentioned above, in *E. spelaea*, deviations from the proposed ground pattern are the reduced number of muscles originating from the dorsal shield and the endosternite. However, despite these variations, the presence of endosternal musculature inserting in the first article rather supports the idea that the first article is a coxa than a trochanter. – Also, there is no single match between muscle insertions and articulation points between the descriptions by van der Hammen (1977a, Tab. 1) and our observations (Fig. 11). This concerns not only the number of articles, muscles and position of joints, but also the topography between pedipalps and all legs which varies considerably (Tab. 12, Fig. 11).

The intrinsic locomotor musculature of Eucheliceratа was described by Shultz (1989, 2001). The proposed ground pattern for Arachnida consists of 13 muscles (Tab. 11). Extensors in articles 3–7 are present in Opiliones, Pseudoscorpiones, Scorpiones, Solifugae (Shultz 1989), and Xiphosurida (Shultz 1989, 2001). For *Eukoenenia mirabilis*, the analysis of leg 4 shows only muscles 1–3, 6–8, and 11 of the arachnid ground pattern and no extensors in articles 3–7 (Shultz 1989).

It is apparent, that the number of muscles as well as their overall origin and insertion varies between legs in *Eukoenenia spelaea* (Tabs 5, 12). The terminal articles of the pedipalp and leg 1 contained a single tendon each (PP6t–PP10t) attached to the joints with a pulley. This differs from the free tendon (1) in the ground pattern of euchelicerates. Legs 2–4 do not have a muscle or tendon that could be considered homologous to muscle 1 of Shultz (1989).

Muscle 2 of the proposed eucheliceratе ground pattern might be homologous with muscles in the pedipalp and legs 1–4 (PP5, LI8, LII9, LIII10, LIV14; Tab. 12). In leg 4, however, this muscle (LIV14) originates ventral in article and does not insert at or near the tarsal claw. This topography deviates from the proposed ground pattern; therefore, its origin and insertion point either moved or it cannot be homologized with muscle 2 (Figs 19A, 20C; Tab. 12). – Muscle 3 is missing in the pedipalp. In leg 1, muscle LI7 is not a clear match with muscle 3, because its point of origin is lateral, not dorsal. Homologization of LI7 with muscle 3 requires the assumption that the point of origin has shifted. Muscles LII8 (leg 2), LIII9 (leg 3), and LIV11–13 (leg 4) can be identified as muscle 3 of the ground pattern (Tab. 12).

Similar to *Eukoenenia mirabilis*, Acariformes, Parasitiformes and Pseudoscorpiones, muscles 4 and 5 are missing in the pedipalp and the four walking legs of *E. spelaea* (Tab. 12). Muscle 6 of the ground pattern is present in the pedipalp and legs 1–4, however, in the pedipalp and leg 1, the muscle (PP4, LI6) is a side branch of a larger muscle. In legs 2 and 3, the muscle (LII7, LIII8) continues into the following article, and in leg 4 (LIV10) the point of origin is ventral, not dorsal (Figs 19A, 20C). Thus, a clear match to muscle 6 is not possible (Tab. 12).

A similar situation can be found with muscle LIV9 of leg 4. It also has the point of origin shifted to ventral and is, thus, not a clear match with muscle 7 of the ground pattern (Figs 19A, 20C; Tab. 12). Homologues of muscle 7 are missing in pedipalps and legs 1–3. Poor matches for muscle 8 are present in legs 1–4 (LI5, LII6, LIII6/7, LIV8; Tab. 12). Discrepancies are present in the point of origin and insertion (Figs 19A, 20C). The pedipalp lacks this muscle. Muscle 9 of the ground pattern was only observed in leg 4 (LIV7). It is missing in the pedipalp and legs 1–3. This is similar to leg 4 in Amblypygi, Araneae, and Xiphosurida.

The lack of muscle 10 in pedipalp and all legs is similar to *E. mirabilis*, Parasitiformes, and Opiliones (Tab. 12). Muscle 11 is only present in the pedipalp (PP3) and leg 4 (LIV6) in *E. spelaea*. However, there is a shift in point of origin and insertion which makes a match with the ground pattern difficult (Figs 19A, 20C; Tab. 12). A possible homologue of muscle 12 can be found in legs 1–3 (LI4, LII5, LIII5) but shifts in points of origin/insertion as well as muscle LII5 spanning three articles does not match the ground pattern (Figs 19A, 20C; Tab. 12). Additional possible matches are muscles LII4 and LIII4 of legs 2 and 3 with muscle 13, however, shifts in points of origin and insertion are apparent. Muscle 13 is missing in the pedipalp, leg 1, and leg 4 (Figs 19A, 20C; Tab. 12).
While the comparison of the muscle topography is te-

dious and probably obscured by different degrees of precision and differences between methods used, it is evident that the leg musculature of *Eukoenenia spelaea*, although variable between legs, shows most similarities to Acariformes and Parasitiformes (Tab. 11). The similarity roots primarily in reduction of same muscles from the arachnid ground pattern, and as such, is a relatively weak character. However, together with additional features it places Palpigradi in phylogenetic relationship to Acariformes.

Nervous system

Ground pattern

According to recent interpretations, the prosomal syncerebrum (supraesophageal ganglion) of euchelicerates comprises of the proto- (ocular segment), deuto- (cheliceral segment), and tritocerebrum (pedipalpal segment; Damen et al. 1998; Telford & Thomas 1998; Mittmann & Scholtz 2003; Harzsch et al. 2005; Scholtz & Edgecombe 2006; Loesel et al. 2013; Wolf 2016; Ortega-Hernández et al. 2017). Developmental studies of *Limulus polyphemus* also suggest that the stomodaeum is enveloped by the deutocerebrum, and not, as previously assumed, by the tritocerebrum; supposedly this is a feature of the euarthropod ground pattern (Harzsch et al. 2005; see also Ortega-Hernández et al. 2017). However, this view is somewhat contentious and there is considerable discussion about the segmental nature of the syncerebrum, i.e., whether a deutocerebrum is present or absent (Babu 1965; Weygoldt 1985; Wegerhoff & Breidbach 1995; Bitsch & Bitsch 2007). – The syncerebrum contains the arcuate body, i.e., a large unpaired neuropil at the posterior margin of the brain. The arcuate body is a protocerebral visual integration center that has been described for all chelicerate taxa (Strausfeld et al. 2006; Doeffinger et al. 2010; Lehmann et al. 2012; Loesel et al. 2013) except Acari that lack this neuropil.

The subesophageal ganglion complex contains the pedal ganglia and a variable number of opisthosomal ganglia (Gottlieb 1926; Hanstrom 1928; Beier 1931; Kästner 1931b, d, e; Babu & Barth 1984; Wegerhoff & Breidbach 1995). Syncerebrum and subesophageal ganglion are connected by a pair of circumesophageal connectives (Horn & Achaval 2002) and, together, form the synganglion.

Within the opisthosoma, the ancestral morphology probably was a typical ladder nervous system with free ganglia (Handlirsch 1926). This is still found in some basal eucheliceratе groups, though with modifications. In (juvenile) *Limulus* sp. the first opisthosomal ganglion is fused to the prosomal synganglion, but the following seven pairs of ganglia form a typical ladder nervous system. The opisthosomal ganglia merge only later during ontogeny (Tanaka et al. 2013; Battelle 2017). Scorpions have three pairs of ganglia in the mesosoma and four pairs in the metasoma. A small unpaired opisthosomal ganglion (of variable position) can be found in Thelyphonida, Schizomida and Solifugae. For Palpigradi we described four pairs of ganglia in opisthosomal segments 11–14. All other arachnids lack opisthosomal ganglia (Millot 1949b; Babu 1985).

The brain of Eukoenenia spelaea

The brain of *Eukoenenia spelaea* is proportionally large and shows a high degree of fusion. We have no quantitative data comparing brain volume to body size, but the fact that the synganglion basically fills the entire prosoma (Figs 22–24) with the perikarya layer next to the epidermis is indicative of a proportionally large brain. — We documented three commissures, two supraesophageal, i.e., the protocerebral and cheliceral commissure, and one subesophageal commissure associated with the pedipalps (Figs 24–25). Based on that topographic evidence, the cheliceral commissure is second thus can be associated with the deutocerebrum; the post-esophageal commissure of the pedipalps is third and thus associated with the tritocerebrum. This topography is coherent with the general arthropod ground pattern of the tritocerebral commissure running behind the esophagus. Supposing these topographic relationships are correct, the esophagus is enveloped by the part of the supraesophageal ganglion associated with the chelicerae (Fig. 25), thus the deutocerebrum. This would be in agreement with the arthropod ground pattern as suggested by Harzsch et al. (2005).

A similar morphology of the synganglion was described for larval *Limulus polyphemus*, where a tripartite brain was recognized (Mittmann & Scholtz 2003; Harzsch et al. 2005). Similar to the larval syncerebrum of *L. polyphemus*, the cheliceral commissure of *E. spelaea* is located supraesophageally and the pedipalpal commissure is subesophageal. The protocerebrum is small and a visual center (arcuate body) is lacking in *E. spelaea*.

The first three opisthosomal segments of *Eukoenenia spelaea* have no free ganglia thus, they are probably fused to the subesophageal ganglion which reaches far into the second opisthosomal segment. Fusion of opisthosomal ganglia to the subesophageal ganglion is the default morphology with the few exceptions mentioned above (Babu 1985). In *Eukoenenia,* opisthosomal segments 4 through 7 show individual small ganglia. The number of neurons within the opisthosomal ganglia of *E. spelaea* is approx. 25, i.e., an exceedingly small number that is usually found in arthropod embryos (10–90 neurons per ganglion; Gerberding & Scholtz 2001; Harzsch 2003), but not in adults where neuron numbers vary between approx. 110 neurons in the fused opisthosomal ganglion of the mite *Ornithodoros parkeri* (Pound & Oliver Jr. 1982) to more than 4000 neurons per ganglion in *L. poly-*

phemus (Bursey 1973). Whereas free opisthosomal ganglia represent a plesiomorphic condition, the small number of neurons in those ganglia must be considered derived, probably in association with the paedomorphic (developmental truncation) morphology of the Palpigradi. If, indeed, Palpigradi evolved by developmental truncation, plesiomorphic features like the opisthosomal ganglia can be explained as "reversed recapitulation" (Alberch et al. 1979) thus, representing a unique and derived phylogenetic condition of palpigrades despite their plesiomorphic morphology.

The ground pattern of euchelicerates has a perineural vascular sheath, which surrounds the synganglion and (probably) supplies it with oxygen and nutrients (Firstman 1973; Alberti & Coons 1999; Coons & Alberti 1999; Klußmann-Fricke et al. 2012; Wirkner & Huckstorf 2013; Göpel & Wirkner 2015; Klußmann-Fricke & Wirkner 2016). In some euchelicerates, the perineural vascular sheath has been transformed into a network of arteries and capillaries. In other groups, e.g., tracheate arachnids, it has been reduced (e.g., solifuges [Klann 2009] and mites [Alberti & Coons 1999]).

Firstman (1973) documented a perineural vascular sheath in *Prokoenenia wheeleri*. However, despite using TEM, we found no evidence or any residue of it in *Eukoenenia spelaea*. Instead, the synganglion is surrounded by a thin and probably incomplete perineurium (glia cells surrounding the perikarya layer). The perineurium produces a thin extracellular matrix that might represent a neural lamella. – The lack of the perineural vascular sheath may be related to the small size of the animals and the fact that they are typical diffusion animals, i.e., diffusion is sufficient to ensure continuous oxygen supply to the prosomal ganglia.

Frontal Organ

The frontal organ of *Eukoenenia spelaea* consists of two modified setae that share a common base, thus, forming a sensory unit. Each seta of the frontal organ has its own set of enveloping cells. The surface of the setae is covered with numerous cuticular grooves. The topographic position of the frontal organ and its construction from two setae on a common basis makes it a unique structure among arthropods.

While the topographic anatomy is unique, its ultrastructure characterizes it as a sensory unit and allows recognizing features typical for sense modalities in terrestrial arthropods, i.e., hygroreception, thermoreception and chemoreception. Different sense modalities commonly combine in sensory units of terrestrial arthropods, i.e., hygro- and thermoreceptors, or chemo-/thermo-/hygroreceptors. All sensory cells are embedded in dense material/receptor lymph. A hygroreceptive unit usually consists of two cells, a moist cell and a dry cell, but single cell hygroreceptors have also been reported (Anton & Tichy 1994; Tichy & Loftus 1996; Barth 2002; Gainett et al. 2017). Their ultrastructure is characterized by branched dendrites. Thermoreceptors contain lamellate dendrites (Davis & Sokolove 1975; Altner et al. 1978; Yokohari 1999). Chemoreceptors contain branched or unbranched dendrites (Steinbrecht 1969; Altner & Prillinger 1980; Foelix 1985; Tichy & Barth 1992; Tichy & Loftus 1996) in combination with one pore at the tip of the hair for contact chemoreception, or numerous pores evenly distributed along the hair shaft for non-contact chemoreception (Altner & Prillinger 1980; Foelix & Hebets 2001; Barth 2002).

Thus, ultrastructural analysis can, to some degree, provide comparative evidence of the receptive modalities of sensory hairs, i.e., (two) branching dendrites in combination with a smooth cuticle surface usually are associated with hygroreception, branched dendrites in combination of cuticle pores are associated with chemoreception (contact/non-contact), and lamellate dendrites are associated with thermoreception. This ultrastructural distinction describes a general pattern, however, some arachnids have thermo- and/or hygroreceptors in combination with pored sensory setae (Foelix & Axtell 1972; Foelix & Chu-Wang 1973; Foelix 1985; Anton & Tichy 1994; Tichy & Loftus 1996), thus, morphological evidence should rather be considered as suggestive of sense modalities, but explicit determination of sense modalities requires experimental testing.

Among terrestrial arthropods, combined thermo- and hygroreceptors are common (Waldow 1970; Altner et al. 1973, 1978, 1983; Loftus 1976; Altner 1977). Thermo-/hygroreceptors or combination chemo-/thermo-/hygroreceptors were described in Acari (Foelix & Axtell 1972; Hess & Loftus 1984), Araneae (Foelix & Chu-Wang 1973; Ehn & Tichy 1994) and Opiliones (Gainett et al. 2017). They were specifically found on legs of arachnids (Anton & Tichy 1994; Gainett et al. 2017). The tarsal organ in some arachnid groups (Foelix & Chu-Wang 1973; Foelix & Schabronath 1983; Talarico et al. 2005) and Haller's organ in Parasitiformes (Alberti & Coons 1999; Foelix & Axtell 1972) act as sensory unit consisting of several closely neighboring sensory structures, thus, possibly improving sensory resolution (Anton & Tichy 1994).

The frontal organ of *Eukoenenia spelaea* is unusual for terrestrial arthropods because of its asymmetry, i.e., left and right setae contain dendrites with obviously different sense modalities. The base of the frontal organ contains two pairs of sensory cells that reach into the left and right seta. The left seta receives two cylindrically branching dendrites. In combination with a smooth surface this would be indicative of hygroreception, in combination with pore(s) it would suggest (non-)contact chemoreception. However, it is not that easy in palpigrades: as described above, the surface of the seta has cuticular grooves. These grooves are shallow and do not pene-

Table 13. Number of chemo- and mechanoreceptive dendrites within sensory setae in Arachnida.

	Chemoreceptive dendrites	Mechanoreceptive dendrites	References
Acari	3–8	2	Foelix and Chu-Wang (1972), Chu-Wang and Axtell (1973), Hess and Vlimant (1982)
Amblypygi	9–12	2	Foelix et al. (1975), Foelix and Hebets (2001)
Araneae	~20	2	Foelix and Chu-Wang (1973), Harris and Mill (1973)
Opiliones	~16	unknown	Foelix (1976), Gainett et al. (2017*b*)
Pseudoscorpiones	3–5	unknown	Foelix (1985)
Scorpiones	~20	4	Foelix and Schabronath (1983), Cushing et al. (2014)
Solifugae	12	4–7	Haupt (1982)
E. spelaea	2	5?	this study

trate the entire procuticle but the cuticle is extremely thin (< 0.2 µm) in these positions. An extremely thin cuticle reduces the diffusion barrier, but based on the ultrastructural analysis it is impossible to decide if the two branching dendrites in the left seta in combination with the cuticular grooves stand for chemo- or hygroreception. The right seta of the frontal organ contains one cylindrically branching dendrite and a lamellate dendrite. Its surface is sculptured with the same honeycomb pattern like on the left seta. Therefore, the branching dendrite could be either a non-contact chemoreceptor or a hygroreceptor, while the lamellate dendrite is possibly a thermoreceptor. – What is unusual for the frontal organ as a sense organ is the asymmetrical organization, with both setae showing a different ultrastructure and probably providing different sense modalities.

For lamellate receptors, a correlation exists between the degree of lamellation and the range of the operating temperature. A lower range of the operating temperature is correlated with a high number of dendritic lamellae (Loftus & Corbière-Tichané 1981; Corbière-Tichané & Loftus 1983; Altner & Loftus 1985). Such receptors are often found in small arachnids such as Opiliones, for which temperature and humidity are an integral part of their lives (Todd 1949; Wiens & Donoghue 2004; Curtis & Machado 2007). The lamellation within the proposed thermoreceptive dendrite in *Eukoenenia spelaea* is extensive. The environment in which these animals live is cool and moist. The temperature within the cave is stable between +7.9 and +10.7 C, and the humidity is always around 97% (Kováč et al. 2002, 2014). One could speculate that the intensive lamellation of the dendrites might be indicative to the functional range of a thermoreceptor at a relatively low temperature and high humidity.

Lateral organ

The paired lateral organ of *Eukoenenia spelaea* is a sensory organ unique for palpigrades. Each consists of four modified sensory hairs. Each sensory hair has its own base, unlike the common socket of the sensory setae of the frontal organ. The ultrastructure of all setae is the same as that of the left seta of the frontal organ, i.e., branching dendrites in combination with the numerous cuticular grooves. Based on this ultrastructure, we suggest that the lateral organs function as non-contact chemoreceptors and/or hygroreceptors.

Sensory setae

The combination of chemo- and mechanoreceptive sensory cells in setae is common in arthropods (Chu-Wang & Axtell 1973; Foelix & Chu-Wang 1973; Harris & Mill 1973; Ozaki & Tominaga 1999). Especially eyeless soil arthropods possess such combined sensory organs (Eisenbeis & Wichard 1987).

In contrast to the modified setae of the frontal and the lateral organ, the dendrites in chemoreceptive sensory setae of arthropods are unbranched. Few pores on the tip of the seta are usually interpreted as indicative of contact chemoreception while many pores along a large portion of the shaft of the seta suggest non-contact chemoreception. The cuticular wall of the seta can be single or double with two or three canals. The dendrites are located in the inner canal whereas the outer canal(s) is either filled with dense material/receptor lymph or it is empty. The outer canal is typically crescent-shaped in cross-section (Foelix & Chu-Wang 1973; Foelix et al. 1975). Mechanoreceptive cells typically end in a tubular body at a cuticular socket at the basis of the hair (Foelix et al. 1975;

Gaffal et al. 1975; McIver 1975; Keil 1997; Barth et al. 2004; Dechant et al. 2006). Thus, ultrastructural features of combined chemo-mechanoreceptors are distinct, i.e., pored surface in combination with one or few unbranched dendrites, and a cuticular socket with a tubular body at the base of the sense hair.

Numerous examples of combined chemo-mechanoreceptors representing this ultrastructural organization, together with the taxon specific variations, have been published (Scorpiones: 4 dendrites; Tab. 13 [Foelix & Schabronath 1983; Cushing et al. 2014], and Solifugae: 4–7 dendrites [Haupt, 1982]). In Acari (Foelix & Chu-Wang 1972; Chu-Wang & Axtell 1973; Hess & Vlimant 1982), Amblypygi (Foelix et al. 1975; Foelix & Hebets 2001), and Araneae (Foelix & Chu-Wang 1973; Harris & Mill 1973), the number is reduced to two mechanoreceptive dendrites per seta (Tab. 13).

In *Eukoenenia spelaea*, the sensory setae of the body and the flagellum have few cuticular pores at their tip and the seta is double walled with an empty outer canal. At least two dendrites reach to the tip of the hair shaft. All sensory setae have a cuticular socket with tubular bodies at which five dendrites terminate. These ultrastructural features suggest that these hairs function as combined (contact)chemo-mechanoreceptors. — Among euchelicerates, there seems to be a correlation between the number of chemoreceptive dendrites and body size (Tab. 13). While most larger-bodied groups have 10–20 dendrites, taxa with small body size like Acari or Pseudoscorpiones have only 3–8 or 3–5 dendrites, respectively. *E. spelaea* is among the smallest euchelicerates and has only two chemoreceptive dendrites.

Typically, double-walled contact-chemoreceptors of arthropods have plugged pores in the outer wall; also the outer canal is filled with dense material/receptor lymph (Foelix & Chu-Wang 1973). Again, *Eukoenenia spelaea* is special, because the outer pore on each side of the seta is open and the outer canal is empty, but the inner pore is plugged. Such a configuration might be associated with receptor specificity, as chemicals pass differently through dense material/receptor lymph and cuticular plugs (Altner et al. 1977).

Trichobothria

Trichobothria are common and characteristic mechanoreceptive sensory organs of terrestrial arthropods. The typical structure of an arachnid trichobothrium includes a thin hair, which is directly or indirectly connected to sensory cells in a cuticular socket. This socket has either bilateral symmetry as in spiders (Görner 1965; Harris & Mill 1977) or it is circular like in scorpions (Hoffmann 1967; Messlinger 1987). The socket has either smooth ridges (Scorpiones [Messlinger 1987; Farley 1999], and Araneae [Barth 2014]) or is ridged and teethed (orbatid mites [Alberti et al. 1994]). The socked consists of an outer and inner cavity that are separated by a thin cuticular membrane. The inner cavity is an extension of the outer receptor lymph cavity and filled with receptor lymph. Dendrites are surrounded by the dendritic sheath and terminate in a tubular body at the base of the hair. Bending of the hair may cause displacement of the cuticular helmet at the basis of the hair resulting in deformation of the tubular body and ultimately in the creation of an action potential in the sensory cell. The seta itself is either solid with only a short lumen at its proximal end (Alberti et al. 1995), or hollow (Reißland & Görner 1985), but it does not contain dendrites. This overall fine structure of a trichobothrium is widely found among arachnids.

The trichobothria of *Eukoenenia spelaea* follow this general arachnid pattern. However, they differ in one important detail, i.e., of the five dendrites associated with the trichobothrium, four continue into the hair shaft, with one extending into the distal section of the hair. In the base of the hair, the dendrites retain their 9 x 2 + 0 microtubule configuration. We found a cuticular thickening at the base of the hair, which is interpreted as the residue of a cuticular helmet. A true helmet-like structure is not developed because the dendrites reach into the hair. We did not find tubular bodies. However, the material was limited and the presence of tubular bodies cannot be entirely ruled out. Dendrites inside the hair shaft of trichobothria are unusual and indicate a second sense modality in addition to mechanoreception. We could not find pores along the hair shaft but the material was limited. A general similarity to a chemoreceptor is evident.

Similar unusual trichobothria were described for the millipede *Polyxenus*. In this species, three unbranched dendrites enter the hair and retain their 9 x 2 + 0 microtubule configuration in the outer dendritic segments. A cuticular helmet structure as well as tubular bodies were not found (Tichy 1975). In addition, the trichobothrium of *Polyxenus* has several plugged pores along its shaft and, thus, its function was proposed to be chemoreceptive (Tichy 1975).

In *Eukoenenia spelaea*, the cuticular teeth of the socket might serve three functions: (1) the teeth might prevent sediment particles from entering the socket and, thus, obstructing the movement of the hair. Similar retention structures are known from mites (Alberti et al. 1994; Gorb 2001b). (2) The teeth might prevent breakage of the hair due to overextension while moving through sediment. The thin cuticle teeth might bend more easily when the hair shaft gets pressed against them, thus, be more flexible than a solid ridge. (3) The cuticular teeth might prevent the seta from adhering to the side of the socket, thus, impairing its flexibility.

Heart

In the ground pattern of arthropods, the heart is a dorsal muscular tube surrounded by a pericardium and suspend-

ed by musculo-elastic ligaments, which act as antagonist to the circular muscles of the heart tube (Shear 1999). Hemolymph enters the heart through paired segmental ostia. The heart of arachnids is typically innervated (Zwicky & Hodgson 1965; Sherman et al. 1969; Bursey & Sherman 1970; Obenchain & Oliver Jr. 1975; Alberti & Seeman 2004). Pure myogenic hearts have been described for some ticks (Schriefer et al. 1987; Coons & Alberti 1999). The muscle cells of the heart tube are striated muscles, with clearly defined sarcomeres. The Z-line, A- and I-band, T-tubular system as well as the sarcoplasmic reticulum are well developed (Tjønneland et al. 1987). The heart pumps the hemolymph through the body. The hemolymph-vascular system of euchelicerates can be morphologically complex in pulmonate euchelicerates (Wirkner et al. 2013), but tends to be simplified in tracheate arachnids (Crome 1953; Levi 1967), or reduced in some miniaturized mites (Crome 1953; Levi 1967; Wirkner et al. 2013).

During embryogenesis, the heart develops from paired lateral coelomic cavities that merge in the dorsal midline of the embryonic body. From this, it differentiates into an initially closed tube (Strubell 1892; Kästner 1931f; Scholl 1977; Rugendorff et al. 1994). Ostia and dilatator muscles develop during later development stages, as has been shown for *Limulus* (Scholl 1977) and *Drosophila* (Rugendorff et al. 1994; Bodmer 1995; Molina & Cripps 2001).

The heart of *Eukoenenia spelaea* is a simple muscular tube without ostia, without a pericardium, and without dilator ligaments/muscles. Its structural simplicity and similarity to the embryonic heart of other arthropods suggests that it might be paedomorphic by developmental truncation. The paedomorphic morphology of the adult heart is corroborated on the ultrastructural level. The number of mitochondria is low, the sarcoplasmic reticulum is poorly developed, myofilaments are irregularly placed throughout the myofibril, and Z-lines are not clearly differentiated. Such cytological appearance of myocardial cells has been described for the heart of juvenile ticks (Coons & Alberti 1999: p. 360, fig. 67) and the heart of larval *Drosophila* (Lehmacher et al. 2012). The microscopic anatomy and the ultrastructure of the heart of adult *E. spelaea* resembles that of juvenile or larval stages of other arthropods. Together they support the view that the heart of *E. spelaea* is paedomorphic.

The paedomorphic morphology of the heart suggests a low degree of functionality, and, consequently, that it is not involved in circulation of the hemolymph through the body. This is not surprising because the overall hemolymph space is extremely small or missing. Movement of the residual hemolymph may be driven by muscle contraction of the body musculature in prosoma and opisthosoma. Reduction of the heart goes also along with the lack of respiratory organs and dependence on diffusive gas exchange (discussed in 4.2.1; Rucker 1901; Kästner 1931a).

Rostrosoma

All arachnids have a preoral cavity that is formed by various morphological contributions from the labrum, the chelicerae, the pedipalps, or sternal elements (Kästner 1931g; Collatz 1987; Moritz 1993; Farley 2001). These elements can be combined to form a more or less complex rostrosoma that may surround the preoral cavity, the mouth and parts of the pharynx. The preoral cavity and the mouth may be equipped with cuticular teeth, ridges or other filtering structures that prevent larger particles from entering the pharynx. In some taxa, external cuticular surface structures on the lower lip might be involved in guiding secretions from salivary glands that open ventral on the body to the mouth. Obviously, the rostrosoma, preoral cavity and the various associated structures evolved independently and parallel in many groups of arachnids (Snodgrass 1948; Dunlop 2000).

The rostrosoma of *Eukoenenia spelaea* is a simple cuticular tube that forms the upper and the lower lip at its anterior part, surrounds the preoral cavity, the mouth and the anterior part of the pharynx. It is a distinct morphological structure that does not involve parts from chelicerae, pedipalps or any other appendage, as in other arachnids (Kästner 1931g; Snodgrass 1948; Collatz 1987; Moritz 1993; Dunlop 2000; Farley 2001). At the first glimpse, the simple morphology of the rostrosoma compares to that of the pycnogonid rostrum. However, it clearly differs by the internal mouth opening, the lateral lips, and the topography of the precerebral suction pump that partially inserts at the intercheliceral septum. Indeed, the rostrosoma seems to be a simple cuticular tube formed on the precheliceral segment. Based on the muscle morphology we showed that a ventral sclerite of the cheliceral element is part of the prosternum and thus cannot contribute to the formation of the rostrosoma.

Historically, the lower lip has been viewed as derived from a protosternite (Börner 1902a, 1903). However, such structure has never been confirmed in either adult or developmental stages of euchelicerates. In addition, our observations show that segmental musculature of the cheliceral segment attaches to the prosternum. Being so, Snodgrass' (1948, p. 21) conclusion *"[…] If, therefore, the mouth of the palpigrades lies between the labrum and the sternum of the first postoral somite, we see here an embryonic condition retained in no other modern adult arthropod […]"* appears to be of merely historical interest.

Millot (1942) reported glandular structures in the lower lip of *Eukoenenia mirabilis* and postulated the secretion of saliva. However, we could not detect cells with an unequivocal secretory character. Some cells with large nuclei in the lower lip (Fig. 7C) might correspond to

what Millot (1943) described as glandular cells, but we did not see vesicles or structures that would indicate secretory activity.

Palpigrades feeding on a food source has not been observed and their actual food is a matter of speculation. Like in all other arachnids, the cuticular ridges on the inside of the upper and lower lip most likely function as filter mechanism to prevent large particles from entering the alimentary system (e.g., Dunlop 1994). Wheeler (1900) and Rucker (1901) suggested that palpigrades feed on arthropod eggs because they observed vitellin vesicles in the gut. This was rejected by Millot (1942), who found that the reported vitellin vesicles were in fact not inside the midgut, but in the surrounding storage tissue. Smrž et al. (2013, 2015) suggested that *Eukoenenia spelaea* feeds on heterotrophic cyanobacteria (*Chroococcidiopsis*) which, indeed, have been identified in the gut of *E. spelaea*. The serrated cuticular teeth of the chelicerae might be used as a comb to graze cyanobacteria off the surrounding soil. The spacing of the teeth (1–1.5 µm) is considerably smaller than the diameter of most cyanobacteria found within the gut (6–8 µm; Smrž et al. 2013, 2015) and thus appears suitable for raking cyanobacteria from sediment.

Digestive tract

The digestive tract of euchelicerates can be divided in an ectodermal foregut, comprising pharynx and esophagus, a mesodermal midgut, and an ectodermal hindgut (Millot 1949b; Alberti & Coons 1999; Coons & Alberti 1999; Farley 1999; Talarico et al. 2011). Along the foregut, dilator muscles attach to the precerebral and postcerebral pharynx forming suction pumps. Pre- and postcerebral suction pumps can be found in Amblypygi (Kästner 1931f), Araneae (Felgenhauer 1999), Ricinulei (Ludwig et al. 1994; Talarico et al. 2011), Scorpiones (Farley 1999), and Thelyphonida (Kästner 1931f). The posterior suction pump is reduced in Acari (Alberti & Coons 1999; Coons & Alberti 1999), Opiliones (Pinto-da-Rocha et al. 2007), Pseudoscorpiones (Weygoldt 1969), and Solifugae (Klann & Alberti 2010).

Eukoenenia spelaea also lacks a postcerebral suction pump. Rucker's (1901) and Börner's (1904) description of a postcerebral suction pump in *Prokoenenia wheeleri* is clearly a misinterpretation of the prosomal midgut diverticula (Millot 1942; Weygoldt & Paulus 1979b; Shultz 2007a; this study). The ectodermal esophagus of *E. spelaea* directly merges into the midgut tube and shows no sign of additional musculature. The midgut is a straight tube in the prosoma where it forms two diverticula. In the opisthosoma, the midgut is rather sac-like with indentations caused by the dorso-ventral musculature; distinct midgut diverticula are missing in the opisthosoma. Similar sac-like midguts have been reported from instars of Araneae (Gerhardt & Kästner 1931), Pseudoscorpiones (Weygoldt 1969), Thelyphonida (Kästner 1931f), and Xiphosurida (Kimble et al. 2002). The morphological simplicity of the midgut in *E. spelaea,* and its overall similarity with that of developmental stages of other eucheliceratе taxa is suggestive of a paedomorphic morphology.

The epithelium of the midgut and prosomal midgut diverticula in *Eukoenenia spelaea* are identical and contain secretory and digestive cells, which are characterized by the numerous apical microvilli. It is a dimorphic epithelium like in most arachnids (Polis 1990; Ludwig et al. 1994; Farley 1999; Klann & Alberti 2010; Talarico et al. 2011) except Acari (Alberti & Coons 1999; Coons & Alberti 1999), Araneae (Felgenhauer 1999), and Opiliones (Becker & Peters 1985) in which additional cell types like ferment cells, replacement cells, or excretory cells are present.

Historically, the rectal sac has been considered part of the hindgut (Kästner 1931a). However, because a cuticle-lining of the rectal sac is missing in *Eukoenenia spelaea*, and because its epithelium consists of high prismatic cells with long microvilli, we consider the rectal sac part of the mesodermal midgut with absorptive function. The rectal sac opens in a short, cuticle-lined section, i.e., the anal opening, which appears to be the only residue of an otherwise reduced ectodermal hindgut.

Excretory organ

The coxal organs of arachnids typically consists of saccule, tubule (labyrinth), bladder (vesicle), excretory duct, and excretory pore (Buxton 1913, 1917; Millot 1949b; Moritz 1993). Muscle fibers may attach to the saccule, e.g., in Acari (Alberti & Coons 1999) and Solifugae (Buxton 1913; Alberti 1979b; Klann 2009), supposedly allowing for extension of the saccule thus producing a pressure gradient for ultrafiltration. Among arachnids, the tubule varies in shape and morphological complexity (Buxton 1913, 1917, Alberti & Coons 1999). In Solifugae (Buxton 1913, 1917; Alberti 1979b; Klann 2009) a glandular section is inserted between saccule and tubule. In some Acari (Coons & Alberti 1999; Filimonova 2004, 2016, 2017), the tubule is cytologically differentiated in a proximal and a distal segment; the distal segment may contain glandular sections. The different position of the glandular segments and the different details of cytology in Solifugae and Acari suggest an independent evolutionary origin of these glandular elements of the coxal organ.

The location of the excretory pore varies among Arachnida. In Solifugae, the pore is located next to the pedipalp (Buxton 1913; Alberti 1979b); in Acari on or adjacent to leg 1; in Amblypygi, Araneae (Buxton 1913, 1917), Opiliones (Pinto-da-Rocha et al. 2007), and Thelyphonida (Buxton 1913, 1917) next to leg 2; in Pseudoscorpiones (Weygoldt 1969) and Xiphosurida (Shultz 1990) close to leg 3, and in Scorpiones (Farley 1999) between leg 3 and

4. Some species of Amblypygi and Araneae have two excretory pores, one close to leg 2 and one close to leg 4 (Buxton 1913, 1917).

In *Eukoenenia spelaea,* the tubule of the coxal organ is cytologically differentiated in a proximal and a distal segment, each carrying a long blind ending extension. Based on light microscopic descriptions provided by Börner (1904) and Buxton (1917), the proximal part of the tubular system was described as "glandular" and the distal part as excretory. This interpretation was perpetuated in later publications, and, homology with the coxal organs of solifuges was postulated (Buxton 1917; Kästner 1931a; Alberti 1979b) because the "glandular" part were intercalated between the saccule and the tubule.

Our transmission electron micrographs of all parts of the coxal organ of *Eukoenenia spelaea* allow updating details of the microscopic anatomy of the coxal organ and re-interpreting supposed similarities with ultrastructural details of the coxal organs of solifuges (Alberti 1979b; Klann 2009). In *Eukoenenia spelaea*, the saccule is a simple, small pouch with an epithelial wall of podocytes and a narrow lumen. No muscles were found inserting on the saccule, but several muscles were found passing nearby. The coxal organ muscle inserting on the saccule in *Eukoenenia mirabilis* as reported by Millot (1942) might be one of those muscles in immediate neighborhood to the saccule, and is probably not attached to the saccule; however light microscopy on paraffin sections as used by Millot (1942) did not provide the necessary optical resolution. The microscopic anatomy of the saccule in *E. spelaea* equals the basic organization of the epithelium of the saccule of euchelicerates with podocytes exposed to the hemolymphatic space. The lumen is rather small, but there is considerable variation in the size of the lumen of the saccule, e.g., in some Acari (Alberti & Coons 1999; Coons & Alberti 1999) and Thelyphonida (Buxton 1917) the lumen is small. However, in other Acari (Alberti & Coons 1999; Coons & Alberti 1999), Amblypygi (Buxton 1913, 1917), Araneae (Buxton 1913, 1917; Lopez 1983), Scorpiones (Buxton 1913, 1917), Solifugae (Buxton 1913, 1917; Alberti 1979b; Klann 2009), and Xiphosurida (Fahrenbach 1999) the lumen can be extensive.

In *Eukoenenia spelaea*, an elongate tubular section extends from the saccule into the second opisthosomal segment. This proximal segment of the tubule has been described as glandular segment (Börner 1904; Buxton 1917). However, already Millot (1942) questioned a glandular function and described it as tubule with secretory function. Transmission electron microscopy now proves that the basal part of the cells posses an extensive basal labyrinth (infoldings of the cell membrane) which is typical for the transport epithelium and is associated with excretory function of the tubule. The transport epithelium of *Eukoenenia* clearly differs from that of the glandular part of the tubule of Solifugae as shown by light microscopic histology and the ultrastructure of the cells (Alberti 1979b; Klann 2009). In solifuges, the cells have no basal labyrinth, but a folded basal lamina, cells are large with large nuclei, possess numerous apical microvilli and are filled with secretory vesicles.

The distal segment of the tubule of *Eukoenenia spelaea* is a simple, bent tube with an additional branch emerging from a position where the proximal section fuses with the tubule. It has not yet been reported in that detail for other palpigrades. The ultrastructure of the epithelial cells is similar to that of the proximal part of the tubule, but the basal labyrinth is apparently less intensively developed. Neither the proximal nor the distal part of the tubule show an open lumen. The cells of the tubule in arachnids typically have some form of apical microvilli, sometimes varying in number and length along the course of the tubule (Alberti 1979b; Coons & Alberti 1999; Fahrenbach 1999; Filimonova 2004, 2016, 2017). Due to the lack of a lumen of the tubule, no microvilli are present in *E. spelaea*, but apical folds of the epithelial cells may represent their residues. A bladder is missing in *E. spelaea,* which differs from description of *Eukoenenia mirabilis* by Millot (1942).

The cytological details elaborated here for *Eukoenenia spelaea* reject the homologization of the coxal organ of Palpigradi with that of Solifugae. Rather it appears that the tubule is differentiated into a proximal and a distal segment, both with excretory/secretory epithelia. Such differentiation resembles that in Acari (Alberti & Coons 1999; Coons & Alberti 1999; Filimonova 2004, 2016, 2017) where the tubule is differentiated in a proximal and a distal segment. Of course, the microscopic anatomical differentiation of the coxal organ in Acari may show additional cellular differentiations or loss of structures. However, the coxal organ of Palpigradi might serve rather as a plesiomorphic template for the coxal organ of Acari than as homologon of the coxal organ of Solifugae.

Reproductive organs

Female reproductive organs

The female reproductive organs of arachnids consist of the ovaries, oviducts, seminal receptacle, and genital chamber. The detailed morphology of these structures varies considerably between groups, and, with the exception of ladder-like gonad morphology found in Schizomida, Scorpiones, and Thelyphonida (Shultz 2007a), contains little phylogenetic information. The ovaries can be paired or display various degrees of fusion (Kästner 1931f; Polis 1990; Moritz 1993; Michalik et al. 2005; Klann 2009; Foelix 2010). The oviducts are typically paired, originate anteriorly at the ovary, and vary in thickness (Moritz 1993; Alberti & Michalik 2004). A seminal receptacle may be found in groups with sperm transfer with gonopods or a penis (Alberti & Michalik 2004), but

it is lacking in Amblypygi (Börner 1902b) and Solifugae (Millot & Vachon 1949a; Klann 2009), also groups with morphological adaptations for sperm transfer. The genital chamber is generally lined with cuticle (Börner 1902b; Kästner 1931d; Millot & Vachon 1949b; Weygoldt 1969; Alberti & Coons 1999; Coons & Alberti 1999; Felgenhauer 1999; Klann 2009). A receptaculum seminis was described for *Prokoenenia wheeleri* by Rucker (1901), but was later questioned by Börner (1902b). In Acari (Alberti & Coons 1999; Coons & Alberti 1999), Amblypygi (Börner 1902b; Kästner 1931f), Pseudoscorpiones (Weygoldt 1969), Schizomida, and Thelyphonida (Börner 1902b; Kästner 1931f), an accessory gland is associated with the reproductive organs.

The slightly posterior origin of the paired ovarian ducts from the unpaired ovary of *Eukoenenia spelaea* appears to be unique among arachnids. The diameter of the ducts is small compared to the diameter of an egg. Although no transmission electron micrographs of the ovarian ducts are available, it can be assumed that the epithelium is high prismatic and expandable to accommodate the eggs prior to laying. Our description of the seminal receptacle of *E. spelaea* confirms that by Rucker (1901) for *Prokoenenia wheeleri*. The paired accessory gland has no opening which indicates that the secretions collected in the reservoir is secreted through pores in the thin layer of cuticle in the region lateral to the genital opening. A small number of relatively large eggs is characteristic for small/miniaturized animals and suggests that only few eggs are laid at a time.

Male reproductive organs

The male reproductive organs of arachnids typically consist of the paired testes, vas deferens, and genital atrium (Alberti et al. 2007). Like the female ovary, the morphology of the testes varies between groups. Unpaired testes as well as testes in different stages of fusion have been described (Weygoldt 1969; Polis 1990; Moritz 1993; Alberti & Coons 1999; Coons & Alberti 1999; Pinto-da-Rocha et al. 2007; Talarico et al. 2008; Klann 2009; Michalik 2009). The transfer of sperm can be coupled with the production of a spermatophore. These sperm packages can display a species-specific morphology (e.g., Amblypygi [Weygoldt et al. 2010], Pseudoscorpiones [Weygoldt 1969], and Scorpiones [Polis 1990]). Spermatophores are built in Acari (Alberti & Coons 1999; Coons & Alberti 1999), Pseudoscorpiones (Weygoldt 1969), Scorpiones (Polis 1990), Solifugae (Klann 2009), Amblypygi, Schizomida, and Thelyphonida (Moritz 1993).

The male reproductive system of *Eukoenenia spelaea* consists of paired testes, vas deferens, a genital atrium, and two accessory glands. The unpaired posterior gland has no secretory duct, but, similar to the accessory gland in females, possibly secretes through pores in the cuticle (Bereiter-Hahn et al. 1984). This gland corresponds to the paired accessory gland described for *Prokoenenia wheeleri* (Rucker 1901). The paired anterior accessory gland is larger than the posterior accessory gland and is associated with the glandular fusules of the first genital lobes. The general morphology of *E. spelaea's* male reproductive organs is similar to Amblypygi, Araneae, Ricinulei, Schizomida, and Thelyphonida. However, the morphology of the accessory glands differs greatly from these groups. The posterior accessory gland has no recognizable opening into the genital atrium. The secretory ducts of the anterior accessory gland appear to be a unique character of *E. spelaea*.

Sperm morphology

Sperm morphology has been used in phylogenetic analyses of eucheliceratas/arachnids (Alberti 1995). The sperm of eucheliceratas show a variety of shapes and complexity (Alberti 1995; Alberti & Michalik 2004; Pitnick et al. 2009). Xiphosurida have plesiomorphic sperm, i.e., a spherical head containing the acrosomal complex and nucleus with condensed chromatin, a middle piece containing a few relatively large mitochondria, and an elongate sperm tail representing the flagellum. Arachnids have either filiform-flagellate sperm (scorpions), coiled flagellate sperm (Pseudoscorpiones, Uropygi, Amblypygi, Araneae, Ricinulei) or aflagellate sperm (Acari, Opiliones, Solifugae, Palpigradi; Alberti 1995; Alberti & Michalik 2004). Vacuolated sperm occur in different taxa of the arachnids, with flagellate and aflagellate sperm. However, anactinotrichid mites have highly complex vacuolated sperm that obviously evolved independently (Alberti 1995, 2000; Alberti & Michalik 2004). In this type of sperm, the large central vacuole develops through fusion of multiple peripheral vacuoles and the fully developed sperm is later turned inside out (Alberti & Michalik 2004). Sperm of Opiliones and anactinotrichid mites may have reduced the acrosomal filament, however, this appears to be variable among taxa.

The sperm of Palpigradi have been described for *Prokoenenia wheeleri* (Alberti 1979a). They have aflagellate sperm that are characterized by a large vacuole that contains dense vesicles. The nucleus of *P. wheeleri* sperm is coiled several times around the spermatozoon (Alberti 1979a; Alberti & Michalik 2004). The acrosomal complex lacks the acrosomal filament, like in some opilionid and acarine taxa (Alberti 1979a; 1995).

The spermatozoa of *Eukoenenia spelaea* are similar to the spermatozoa of *Prokoenenia wheeleri*. They contain a large vacuole, with a constant number of spherical vesicles. The development of the vacuole appears to be identical to that in *P. wheeleri*. The most advanced sperm we found closely resembles an "almost mature sperm" as described by Alberti (1979a; Fig. 2a). Unfortunately, no transmission electron microscopic images could be obtained from spermatozoa in *E. spelaea*.

The unique morphology of the sperm of Palpigradi makes it difficult to discuss their phylogenetic relationship. The aflagellate sperm morphology places them together with Opiliones, Solifugae and Acari. The lack of an acrosomal filament has also been reported for some Acari and Opiliones, however with variable distribution among taxa of these groups. Large vacuolated sperm characterize anactinotrichid mites, but the fine structure of the vacuole and their development apparently differ from that in Palpigradi. Also, various vacuolated sperm have been reported from other arachnid taxa. Overall, the relevant traits are either unique (i.e., coiled nucleus), reduced characters, or subject to multiple and parallel evolutionary appearance among arachnids. Therefore, sperm characters appear of limited value for a phylogenetic analysis of Palpigradi – despite more optimistic claims by Alberti (1995).

Phylogenetic analysis

Autapomorphies of Eukoenenia spelaea

The current study of *Eukoenenia spelaea* recognized several characters that are unique for Palpigradi and therefore should be considered autapomorphies (of course, supposing that *Eukoenenia* is representative for the group). Some of these characters have been known for a long time, but our study provides explicit morphological evidence for a new interpretation of these characters now presenting them as unique features of Palpigradi.

(1) The prosoma of Palpigradi is dorsally divided in only two peltidia (propeltidium, metapeltidium), not three, as traditionally assumed (character 6; Appendix I: Tab. 6, A1). Assuming that this new interpretation holds for Palpigradi and that the published tagmatization (i.e., pro-, meso- and metapeltidium) of Schizomida and Solifugae remains valid, the division of the prosoma into two sclerites is a unique character of Palpigradi.

(2) On the ventral side of the prosoma, the anterior sclerite is now assigned to three anterior segments (i.e., segments 2–4) now termed "prosternum". The term "deuto-tritosternum" that refers to only segments 3 and 4 should be abandoned (character 12a).

(3) The frontal organ (character 148; Appendix I: Tab. 6, A1) is found only in Palpigradi. The ultrastructure of the setae of the frontal organ with presumably different sense modalities for left and right setae is unique among Eucheliceratа.

(4) The lateral organ (character 148a) is found only in Palpigradi.

(5) Preoral cavity, mouth, and pharynx of *Eukoenenia spelaea* are inside a simple cuticular cone shaped rostrosoma (character 32; Appendix I: Tab. 6, A1). The morphology of the rostrosoma differs from the rostrosoma described for Pseudoscorpiones and Solifugae (Shultz 2007a) where it includes material of pedipalps or legs. Despite being a simple cuticular cone, it also differs from the ancestral rostrum of the pycnogonids by the formation of a preoral part of the rostrosoma, and differences in the muscle attachment of the suction pump. The dilator muscles attach to the pharynx and the cuticular wall of the rostrosoma (character 198; Appendix I: Tab. 6, A1). In Araneae (Whitehead & Rempel 1959), Solifugae (Roewer 1934), und Xiphosurida (Shultz 2001) these muscles insert ventral on the prosoma. – We consider the rostrosoma as a complex character that differs from other eucheliceratеs described so far.

(6) *Eukoenenia spelaea* lacks a hindgut (character 203). Previous studies of palpigrades misinterpreted the rectal sac as rectum/hindgut (Kästner 1931a).

We describe several morphological features that have not been reported before in any eucheliceratе.

(7) The ventral plate has a unique morphology (i.e., cuticular teeth, specialized epidermal cells; character 179a). Since none of the earlier studies used TEM and SEM, we assume that it was overlooked previously and we describe it as an autapomorphy for Palpigradi.

(8) The ultrastructure of the trichobothria, with dendrites reaching into the hair shaft, is unique among eucheliceratеs (character 143a).

(9) Anterior oblique suspensor muscle (muscle E6) in segment four. Although an ancestral element of the ground pattern of arthropods, the re-occurrence of this muscle must be considered autapomorphic (character 128a).

Suggested synapomorphies with Acaromorpha

Palpigradi were occasionally placed as sister group to Acaromorpha (Regier et al. 2010) or sister group to Parasitiformes (Sharma et al. 2014). We also recovered Palpigradi as sister to Acaromorpha (Fig. 49A, C). This sister group relationship is indeed supported by several morphological synapomorphies:

(1) The opening of the coxal organ (character 180; Appendix II). In Palpigradi (Millot 1942) and Acaromorpha (Legg 1976; Alberti & Coons 1999) the excretory pore of the coxal organ opens on or near the basal article of appendage III (= leg 1). This character possibly evolved in parallel in (Pan)Tetrapulmonata.

(2) Palpigradi and Acaromorpha lack a postcerebral pharynx (199; Appendix II; Shultz 2007a). Loss of the postcerebral pharynx must have occurred then in parallel in Opiliones and Pseudoscorpiones.

(3) Aflagellate sperm that lack an acrosomal filament have been documented in Palpigradi, Acari and Opiliones. Although sperm morphology appears to be a rather weak character, it supports a sister group relationship of Palpigradi and Acaromorpha (167, Appendix II; Alberti 1979a, 1995; Alberti & Michalik 2004). – However, Ricinulei have coiled sperm and this character does clearly not support a close relationship to Palpigradi and Acari.

 ©ZFMK

(4) The topography of the musculature of leg 4 of Acariformes, Parasitiformes, and Palpigradi is similar in terms of reduction of muscles (Tab. 11; Shultz 1989).

(5) The tubule of the coxal organ is differentiated in a proximal and a distal segment (178a; Appendix II). The epithelia of both segments possess a distinct basal labyrinth thus are involved in excretory processes. The cellular arrangement is also similar in mites and *Eukoenenia spelaea*. A tubule lumen is missing in both groups and there are always three cells present in cross-section (Alberti & Coons 1999). Because of considerable differences in the ultrastructure, we do not support the previously postulated putative homology with the coxal organ of Solifugae (Buxton 1913, 1917; Alberti 1979b; Klann 2009).

(6) The presence of a myogenic heart in some ticks (Schriefer et al. 1987; Coons & Alberti 1999) is also similar to the proposed myogenic heart of *Eukoenenia spelaea*.

(7) Lack of the arcuate body in the syncerebrum (135a; Appendix II). Acari and Palpigradi are the only groups of euchelicerates that have no arcuate body. Since Palpigradi and (many) Acari are eyeless; the lack of the visual integration center may not be surprising. As a reduced structure, the character is not strong but it fits the general picture.

The phylogenetic analysis with TNT resulted in low bootstrap percentage and Bremer support values, and the unweighted analysis left the deep arachnid relationships unresolved (Fig. 49A). In general, bootstrap percentages and Bremer support values were lower than in the phylogenetic analysis by Shultz (2007a). While our morphological analysis contributed a number of new autapomorphic features for the Palpigradi, it was less powerful in providing convincing arguments for a sister group relationship with any of the Arachnida. Generally, morphological characters seem to support a sister group relationship between Palpigradi and Acaromorpha, but most of the characters are reduction characters or subject of multiple and independent evolution among the arachnids. The distinction of the coxal tubule in a proximal and distal segment, appears to be one of the better characters supporting a sister group relationship between Acaromorpha and Palpigradi.

While our morphological findings support a phylogenetic relationship between Palpigradi and Acaromorpha, we, paradoxically, reject all morphological features that were suggested by van der Hammen (1977b) as supporting his "Epimerata" (i.e., Palpigradi and Parasitiformes). The articulations of the leg articles can by no means be compared to the schematic of van der Hammen (1977b) and the intrinsic musculature observed here shows a substantially different pattern (Figs 11A–C, 20C, Tabs 5, 11–12). Furthermore, the origin of extrinsic leg muscles rejects the idea that the ventral plates of the prosoma were "epimera" from which the coxae evolved. – As pointed out by others (Dunlop & Alberti 2007), van der Hammen (1977b) used explicitly plesiomorphic traits to support his "Epimerata" making his reasoning quite useless.

Miniaturization

Miniaturization is directional evolution toward small adult body size. Thus, miniaturization can only be recognized in a phylogenetic context when small taxa evolve from proportionally larger ancestor(s). As pointed out by Hanken & Wake (1993), the distinction between miniaturized and non-miniaturized taxa is to a certain degree arbitrary, and the range of size change depends on the size of the ancestor. Miniaturization appears to be limited by certain physiological and constructural/morphological principles. In particular, neuron size, neuronal network connectivity and consequently brain size seem to be limited by sensory and behavioral complexity resulting in proportionally large brains of small animals. High levels of fusion within the brain (Ioffe 1963; Wegerhoff & Breidbach 1995), and displacement of parts of the brain in other body regions (e.g., coxae, opisthosoma; Quesada et al. 2011) are typical signs of morphological reorganization that come along with an allometrically enlarged brain in miniaturized species (Peters 1983; Mares et al. 2005; Seid et al. 2011; Polilov & Makarova 2017). Thus, miniaturization causes reorganization of the body design to accommodate the disproportionately large brains, or sacrifice on behavioral complexity and/or sensory integration (Eberhard & Wcislo 2011, 2012). Miniaturization may result in structural simplification and reduction of organ systems, but also lead to morphological novelty and an increase of morphological variability (Hanken & Wake 1993; Polilov 2016). Besides the negative brain-size body-size allometry, several morphological features have been reported that appear to be common in miniaturized arthropods (Polilov 2008, 2015a, b, 2016; Quesada et al. 2011; Polilov & Shmakov 2016), i.e.: (i) a mostly undifferentiated gut, i.e., no distinction between midgut tube and midgut diverticula, lacks musculature; (ii) gonads are (often) unpaired and they contain a reduced number of large eggs; (iii) the heart and major components of the circulatory system are reduced; (iv) the neurilemma is reduced, (v) respiratory organs are reduced or missing; (vi) the cuticle lacks sclerotization and differentiation into exo- and endocuticle; (vii) in some regions of the body muscles are reduced, and (viii) the number of Malpighian tubules is reduced or they are missing (Polilov 2015a, b; Polilov & Shmakov 2016).

The constructural morphology of being small is one aspect of miniaturization. Another aspect is how small body size is achieved during evolution, i.e., which processes result in small adults. Since Gould (1977) and Alberch et al. (1979), various evolutionary developmental processes have been identified as potential mechanism by which miniaturization is achieved through relatively

simple changes of developmental programs. According to Gould (1977), progenesis (i.e., early maturation) may result in small but paedomorphic adults. Alberch et al. (1979) included growth rates in their model and provided a more dynamic model of how development may affect evolution. They considered neoteny, post-displacement, and progenesis as evolutionary developmental processes resulting in the same small and paedomorphic morphology of adults, and suggested measuring rates of development to decide ultimately, which process was involved.

Several morphological features found in *Eukoenenia spelaea* indicate miniaturization: (1) there is a lack of a distinct differentiation into endo- and exocuticle over large regions of the body. (2) *E. spelaea* has no respiratory organs, but utilizes cutaneous respiration. (3) Several muscles, e.g., dorso-ventral muscles in the posterior opisthosoma and posterior oblique muscles are reduced in all opisthosoma segments. (4) The prosomal ganglia are proportionally large in comparison to the rest of the body, fill almost the entire prosoma and display a high level of fusion. Eberhard & Wcislo (2011) documented that the (proportionally large) brain of small arthropods is displaced into the coxae and the opisthosoma. (5) Neuron size is small (approx. 2 µm) and ranges at the minimum size described for arthropods. According to Eberhard & Wcislo (2011), the minimum possible neuron size in arthropods is 2 µm. Recently, the range has been extended and the smallest insects (e.g., the ptiliid beetle *Nanosella*) shows a neuron size range from 1.19 µm to 1.98 µm (Polilov 2016). (5) *E. spelaea* has only 14 trichobothria in total. (6) The simplified structure of the coxal organ, i.e., the reduced number of cells and a simple tube instead of a complex labyrinth, could be an indication for miniaturization. (7) *E. spelaea* has no Malpighian tubules. (8) The female gonads are an unpaired structure. (9) Within the ovary, only few eggs appear to be fully developed.

For several organ systems of *Eukoenenia spelaea*, it is difficult to decide whether their adult morphology is shaped by miniaturization, paedomorphosis, or both: (1) the portion of the syncerebrum associated with the chelicerae (deutocerebrum) embraces the esophagus. This morphology is similar to that of larval *Limulus polyphemus* — but it could also be result from displacement of the central nervous system, or both together. (2) The number of neurons within the opisthosomal ganglia of *E. spelaea* is small. Again, this may be a result of miniaturization, or paedomorphosis, because a small number of neurons is indicative of early developmental stages and was documented in the opisthosomal ganglia of arthropod embryos.

Finally, we described several adult organs of *Eukoenenia spelaea* that were clearly paedomorphotic: (1) the heart of *E. spelaea* lacks ostia, a pericardium, and the ultrastructure of the musculature (sarcomere structure) is weakly developed. This morphology resembles that of the hearts of early developmental stages of other arthropods. (2) The midgut is a simple sac with no epithelial differentiation between the different regions. The musculature associated with the midgut is poorly developed. A similar morphology is found in juveniles of several arachnid groups. (3) The reappearance of ancient plesiomorphies, e.g., (i) the anterior oblique muscle, (ii) an almost complete set of posterior oblique muscles in the prosoma, (iii) the deutocerebral connectives embracing the esophagus, and (iv) the segmental chord of ganglia in the opisthosoma, are features of the arthropod ground pattern that may be interpreted as "reverse recapitulation" sensu Alberch et al. (1979). Assuming anagenetic evolution, paedomorphosis by developmental truncation (neoteny, progenesis or post-displacement; Alberch et al. 1979) may result in patterns of "reverse recapitulation", or more correctly, in an array of plesiomorphic features.

The proof of evolutionary miniaturization requires phylogenetic comparisons, i.e., the last common ancestor must have been large as compared to the crown group investigated. Such comparative analysis strongly depends on the phylogeny used. In our phylogenetic analysis, Palpigradi are hypothesized to be sister group to Acaromorpha (Fig. 49). Acaromorpha contain almost exclusively small species with some of the smallest chelicerates at all (Acari). Thus, the last common ancestor of Palpigradi and Acaromorpha was probably already small, suggesting that miniaturization occurred in the stem lineage leading to the last common ancestor of Palpigradi and Acaromorpha.

If we extend the comparison, we find considerable variation of body size among euchelicerates (e.g., Eurypterida: up to 1.8 m body length, Alberti et al. 2007; Scorpiones: up to 210 mm body length, Polis 1990; Solifugae: 10–70 mm body length, Punzo 2012; Xiphosurida: up to 850 mm body length, Alberti et al. 2007) with some groups showing a tendency towards small body size (e.g., Acari: up to 14 mm body length, Dunlop 2019; Opiliones: up to 22 mm body length, Pinto-da-Rocha et al. 2007; Pseudoscorpiones: 1–7 mm body length, Weygoldt 1969; Ricinulei: up to 10 mm body length, Alberti et al. 2007; Schizomida: approx. 5 mm body length, Harvey 2003). Thus, if we move down the phylogram, the sister group to Palpigradi and Acaromorpha is Haplocnemata + (Pan) Tetrapulmonata (Fig. 49C). Both taxa contain species with large body size. Further down the tree, the sister group to ((Haplocnemata + Tetrapulmonata) and (Palpigradi + Acaromorpha) are the Stomothecata (Fig. 49C), again a group with large sized representatives (Scorpiones). At the base of the eucheliceratе phylogeny, we find again two groups with large body size, i.e., the extinct Eurypterida and the recent Xiphosurida. Considering the phylogeny presented here, we suggest that the last common ancestor of ((Haplocnemata + Tetrapulmonata) and (Palpigradi + Acaromorpha)) was large, and that miniaturization took place in the last common ancestor of (Palpigradi + Acaromorpha). With their relatively simple and

highly plesiomorphic morphology, one may speculate that Palpigradi represent a morphologically unchanged offshoot of this early lineage, while the lineage leading to the Acaromorpha successfully diversified based on a paedomorphic morphology.

Highlights

1. Analysis of the segmental axial musculature showed, that the dorsal prosoma is divided in two peltidia, not three as previously assumed. The traditionally recognized „mesopeltidia" are lateral sclerotizations of the pleural fold
2. Analysis of the segmental axial musculature showed that, the anterior ventral sclerite covers segments 2, 3 and 4, not 3 and 4 as traditionally assumed. Palpigradi have no „deuto-tritosternum", but a large „prosternum".
3. We find no evidence that the ventral sclerites ("sterna") of the prosoma are homologous to coxae (sternocoxal plates).
4. The metasoma is not a plesiomorphic structure but independently derived in various groups of arachnids.
5. The ventral side of the prosoma carries a so far undescribed ventral plate. Ultrastructural analysis suggests it functions as an osmoregulatory organ.
6. The reappearance of features of the arthropod ground pattern result in a hyperplesiomorphic morphology, e.g., (i) the anterior oblique muscle, (ii) an almost complete set of posterior oblique muscles in the prosoma, (iii) the deutocerebral connectives embracing the esophagus, and (iv) the segmental chord of ganglia in the opisthosoma. We discuss this pattern in the context of models of evolutionary development and we suggest that the hyperplesiomorphic adult morphology is result of "reverse recapitulation", i.e., re-appearance of plesiomorphic patterns through developmental truncation.
7. Structures of the syncerebrum can be interpreted as tripartite thus supporting the more recent view that a deutocerebrum is present in chelicerates. At the same time, the esophagus is embraced by the deutocerebral connectives, indicating an ancestral structure (or reverse recapitulation due to paedomorphosis).
8. We describe a most complete segmental chord of ganglia in the opisthosoma. This plesiomorphic feature of the arthropod ground pattern may also be interpreted as "reverse recapitulation".
9. Left and right bristle of the frontal organ provide different sense modalities.
10. Trichobothria contain dendrites that reach into the tip of the hair. This unusual morphology has so far not been described for euchelicerates.
11. The heart is largely rudimentary suggesting a paedomorphic origin.
12. The rostrosoma is a unique cuticular tube. Chelicerae or pedipalps are not involved.
13. Palpigradi do not have an ectodermal hindgut.
14. We reject the putative homology of the coxal organ of Palpigradi with that of Solifugae. Instead, we recognize an overall similarity of the coxal organ with that of Acari.
15. We suggest a phylogenetic position of the Palpigradi as sister group to Acaromorpha.
16. Palpigradi are not miniaturized but most probably derived from ancestors that were already small (miniaturized). We recognize paedomorphosis as putative mechanism that resulted in the small overall body size.

Acknowledgements. Specimen were collected, taxonomically diagnosed and made available for this study by Ľubomír Kováč, P. J. Šafárik University, Košice, Slovakia. We gratefully acknowledge providing this rare material for this study. We gratefully acknowledge discussions with Roland Melzer, Zoological state collection, and Carolin Haug, Dept. Biology, LMU, who provided valuable input. We thank Christine Dunkel and Antoinette von Sigriz-Pesch for their invaluable help in the laboratory. SFG was supported by a PhD fellowship of the Rosa-Luxemburg foundation, Berlin. We are grateful to four reviewers (Erhard Christian and three anonymous reviewers) for their careful and throughtful reviews of this long paper. We gratefully acknowledge their time and efforts to help improving this paper.

Author contributions. SFG prepared specimens for histology, prepared all light and electron micrographs, drew all schematics, and prepared a draft of the manuscript. JMS conceived the project, supervised all laboratory work, discussed all results, and revised and rewrote an earlier draft of the manuscript.

Data availability. All animal material used in this project (including unsectioned specimens) is stored at the Bavarian State Collection of Zoology in Munich, Germany (project numbers ZSMS20190030 – ZSMS20190051) from where it is accessible upon request.

REFERENCES

Alberch P (1980) Ontogenesis and morphological diversification. *American Zoologist* 20: 653–667

Alberch P, Gould SJ, Oster GF, Wake DB (1979). Size and shape in ontogeny and phylogeny. *Paleobiology* 5: 296–317

Alberti G (1979a) Zur Feinstruktur der Spermien und Spermiocytogenese von *Prokoenenia wheeleri* (Rucker, 1901) (Palpigradi, Arachnida). *Zoomorphologie* 94: 111–120

Alberti G (1979b) Licht- und elektronenmikroskopische Untersuchungen an Coxaldrüsen von Walzenspinnen (Arachnida: Solifugae). *Zoologischer Anzeiger* 203: 48–64

Alberti G (1995) Comparative spermatology of Chelicerata: review and perspective. *Advances in spermatozoal Phylogeny and Taxonomy. Mémoires du Muséum National d'Histoire Naturelle* 166: 203–230

Alberti G (2000) Chelicerata. Pp. 311–388 in: Jamieson BGM (ed.) Reproductive Biology of Invertebrates, Vol. 9, part B. John Wiley & Sons Ltd, Chichester, United Kingdom

Alberti G, Coons B (1999) Acari: Mites. Pp. 515–1265 in: Harrison F, Foelix RF (eds) Microscopic Anatomy of Invertebrates, Vol. 8C. Wiley-Liss, New York

Alberti G, Seeman O (2004) Ultrastructural observations on Holothyrida (Acari: Anactinotrichida). Phytophaga XIV: 103–111

Alberti G, Michalik P (2004) Feinstrukturelle Aspekte der Fortpflanzungssysteme von Spinnentieren (Arachnida). Pp. 1–62 in: Biologiezentrum des Oberösterreichischen Landesmuseums (ed.) Diversität und Biologie von Webspinnen, Skorpionen und anderen Spinnentieren, Neue Serie 14, Denisia 12

Alberti G, Moreno AI, Kratzmann M (1994) The fine structure of trichobothria in moss mites with special emphasis on *Acrogalumna longipluma* (Berlese, 1904) (Oribatida, Acari, Arachnida). Acta Zoologica 75: 57–74

Alberti G, Moreno AI, Kratzmann M (1995) Fine structure of trichobothria in moss mites (Oribatida). Pp. 23–30 in: Kropczyńska D, Boczek J, Tomczyk A (eds) The Acari: Physiological and Ecological Aspects of Acari-Host Relationships, Vol. 2, Dabor, Warsaw

Alberti G, Thaler K, Weygoldt P (2007) Chelicerata. Pp. 479–532 in: Westheide W, Rieger R (eds) Spezielle Zoologie. Teil 1: Einzeller und Wirbellose Tiere, 2nd ed. Spektrum Akademischer Verlag, München

Altner H (1977) Insect sensillum specificity and structure: an approach to a new typology. Olfaction and Taste 6: 295–303

Altner H, Prillinger L (1980) Ultrastructure of invertebrate chemo-, thermo-, and hygroreceptors and its functional significance. International Review of Cytology 67: 69–139

Altner H, Loftus R (1985) Ultrastructure and function of insect thermo-and hygroreceptors. Annual Review of Entomology 30: 273–295

Altner H, Sass H, Altner I (1977) Relationship between structure and function of antennal chemo-, hygro-, and thermoreceptive sensilla in *Periplaneta americana*. Cell and Tissue Research 176: 389–405

Altner H, Tichy H, Altner I (1978) Lamellated outer dendritic segments of a sensory cell within a poreless thermo-and hygroreceptive sensillum of the insect *Carausius morosus*. Cell and Tissue Research 191: 287–304

Altner H, Ernst KD, Kolnberger I, Loftus R (1973) Feinstruktur und adäquater Reiz bei Insektensensillen mit Wandporen. Verhandlungen der Deutschen Zoologischen Gesellschaft 66: 48–53

Altner H, Schaller-Selzer L, Stetter H, Wohlrab I (1983) Poreless sensilla with inflexible sockets. Cell and Tissue Research 234: 279–307

André M (1949) Ordre des Acariens. Pp. 794–892 in: Grassé P-P (ed.) Traité de Zoologie, Vol. 6, Masson et Cie., Paris

Anton S, Tichy H (1994) Hygro-and thermoreceptors in tippore sensilla of the tarsal organ of the spider *Cupiennius salei*: innervation and central projection. Cell and Tissue Research 278: 399–407

Armas LF de, Teruel R (2002) Un género nuevo de Hubbardiidae (Arachnida: Schizomida) de las Antilles Mayores. Revista Ibérica de Aracnología 6: 45–52

Babu KS (1965) Anatomy of the central nervous system of arachnids. Zoologische Jahrbücher. Abteilung für Anatomie und Ontogenie der Tiere 82: 1–154

Babu KS (1985) Patterns of arrangement and connectivity in the central nervous system of arachnids. Pp. 3–19 in: Barth, F.G. (ed.) Neurobiology of Arachnids. Springer, Berlin / Heidelberg

Babu KS, Barth FG (1984) Neuroanatomy of the central nervous system of the wandering spider, *Cupiennius salei* (Arachnida, Araneida). Zoomorphology 104: 344–359

Barranco P, Mayoral JG (2007) A new species of *Eukoenenia* (Palpigradi, Eukoeneniidae) from Morocco. Journal of Arachnology 35: 318–324

Barranco P, Mayoral JG (2014) New palpigrades (Arachnida, Eukoeneniidae) from the Iberian Peninsula. Zootaxa 3826: 544–562

Barth FG (2002) A spider's world: senses and behavior. Springer Verlag, Berlin / Heidelberg

Barth FG (2014) The slightest whiff of air: airflow sensing in arthropods. Pp. 169–196 in: Flow Sensing in Air and Water. Springer, Berlin / Heidelberg

Barth FG, Németh SS, Friedrich OC (2004) Arthropod touch reception: structure and mechanics of the basal part of a spider tactile hair. Journal of Comparative Physiology A 190: 523–530

Battelle B-A (2017) Opsins and their expression patterns in the xiphosuran *Limulus polyphemus*. The Biological Bulletin 233: 3–20

Becker A, Peters W (1985) Fine structure of the midgut gland of *Phalangium opilio* (Chelicerata, Phalangida). Zoomorphology 105: 317–325

Beier M (1931) Ordnung Pseusoscorpionidae (Afterscorpione). Pp.118–192 in: Krumbach T. (ed.) Handbook of Zoology Online, Vol. 2. De Gruyter, Berlin / Boston

Bereiter-Hahn J, Matoltsy AG, Richards KS (1984) Biology of the Integument. 1 Invertebrates. In: Bereiter-Hahn J, Matoltsy AG, Richards KS (eds) Springer, Berlin / Heidelberg

Berland L (1949) Ordre des Opilions. Pp. 761–793 in: Grassé P-P (ed.) Traité de Zoologie, Vol. 6. Masson et Cie., Paris

Bitsch J, Bitsch C (2007) The segmental organization of the head region in Chelicerata: a critical review of recent studies and hypotheses. Acta Zoologica 88: 317–335

Blick T, Christian E (2004) Checkliste der Tasterläufer Mitteleuropas. Checklist of the palpigrades of Central Europe (Arachnida: Palpigradi). Version 1. Oktober 2004. Online at http://www.AraGes.de/checklist.html #2004_Palpigradi [last accessed 4 May 2016]

Bodmer R (1995) Heart development in *Drosophila* and its relationship to vertebrates. Trends in Cardiovascular Medicine 5: 21–28

Börner C (1902a) Arachnologische Studien. II. und III. Zoologischer Anzeiger 25: 433–466

Börner C (1902b) Arachnologische Studien. IV. Die Genitalorgane der Pedipalpen. Zoologischer Anzeiger 26: 81–92

Börner C (1903) Arachnologische Studien. V. Die Mundbildung bei den Milben. Zoologischer Anzeiger 26: 99–109

Börner C (1904) Beiträge zur Morphologie der Arthropoden: I. Ein Beitrag zur Kenntnis der Pedipalpen. Zoologica 16: 1–174

Boxshall GA (2004) The evolution of arthropod limbs. Biological Reviews 79: 253–300

Bremer K (1994) Branch support and tree stability. Cladistics 10: 295–304

Bu Y, Souza MFVR, Ferreira RL (2019) A new locality of *Koeneniodes madecassus* Remy, 1950 (Palpigradi: Eukoeneniidae) in China, with the first complete redescription of a *Koeneniodes* species. Zootaxa 4658 (3): 541–555. https://doi.org/10.11646/zootaxa.4658.3.6

Bursey CR (1973) Microanatomy of the ventral cord ganglia of the horseshoe crab, *Limulus polyphemus* (L.). Zeitschrift für Zellforschung und Mikroskopische Anatomie 137: 313–329

Bursey CR, Sherman RG (1970) Spider cardiac physiology I. Structure and function of the cardiac ganglion. Comparative and General Pharmacology 1: 160–170

Bush JWM, Hu DL, Prakash M (2007) The Integument of water-walking arthropods: form and function. Pp. 117–192 in: Casas J, Simpson SJ (eds) Advances in Insect Physiology, Vol. 34. Elsevier, Amsterdam, Netherlands

Buxton BH (1913) Coxal glands of the arachnids. Pp. 230–454 in: Spengel JW (ed.) Zoologische Jahrbücher, Supplement 14. Gustav Fischer Verlag, Jena

Buxton BH (1917) Notes on the anatomy of arachnids. Journal of Morphology 29: 1–31

Christian E (2004) Palpigraden (Tasterläufer-)Spinnentiere in einer Welt ohne Licht. Pp. 473–483 in: Biologiezentrum des Oberösterreichischen Landesmuseums (ed.) Diversität und Biologie von Webspinnen, Skorpionen und anderen Spinnentieren, Neue Serie 14, Denisia 12

Christian E (2014) A new Eukoenenia species from the Caucasus bridges a gap in the known distribution of palpigrades (Arachnida: Palpigradi). Biologia 69: 1701–1706

Christian E, Isaia M, Paschetta M, Bruckner A (2014) Differentiation among cave populations of the *Eukoenenia spelaea* species-complex (Arachnida: Palpigradi) in the southwestern Alps. Zootaxa 3794: 52–86

Chu-Wang I-W, Axtell RC (1973) Comparative fine structure of the claw sensilla of a soft tick, *Argas (Persicargas) arboreus* Kaiser, Hoogstraal, and Kohls, and a hard tick, *Amblyomma americanum* (L.). The Journal of Parasitology 59: 545–555

Collatz K-G (1987) Structure and function of the digestive tract. Pp. 229–238 in: Nentwig W (ed.) Ecophysiology of Spiders. Springer, Berlin / Heidelberg

Condé B (1996) Les Palpigrades, 1885–1995: acquisitions et lacunes. Proceedings of the XIIIth Congress of Arachnology : Geneva, 3–8 September 1995 (1): 87–106

Conte FP (1984) Structure and function of the crustacean larval salt gland. International Review of Cytology 91: 45–106

Coons LB, Alberti G (1999) Acari: Ticks. Pp. 267–514 in: Harrison FW, Foelix RF (eds) Microscopic Anatomy of Invertebrates, Vol. 8B. Wiley-Liss, New York

Corbière-Tichané G, Loftus R (1983) Antennal thermal receptors of the cave beetle, *Speophyes lucidulus* Delar. Journal of Comparative Physiology A 153: 343–351

Crome W (1953) Die Respirations-und Circulationsorgane der *Argyroneta aquatica* Cl. (Araneae). Wissenschaftliche Zeitschrift Humboldt-Universität Berlin 2: 53–83

Curtis DJ, Machado G (2007) Ecology. Pp. 280–308 in: Pinto-da-Rocha R, Machado G, Giribet G (eds), Harvestmen: The Biology of Opiliones. Harvard University Press, London / Cambridge

Cushing PE, Casto P, Knowlton ED, Royer S, Laudier D, Gaffin DD, et al. (2014) Comparative morphology and functional significance of setae called papillae on the pedipalps of male camel spiders (Arachnida: Solifugae). Annals of the Entomological Society of America 107: 510–520

Damen WG (2002) Parasegmental organization of the spider embryo implies that the parasegment is an evolutionary conserved entity in arthropod embryogenesis. Development 129: 1239–1250

Damen WG (2007) Evolutionary conservation and divergence of the segmentation process in arthropods. Developmental dynamics: an official publication of the American Association of Anatomists 236: 1379–1391

Damen WG, Hausdorf M, Seyfarth, E-A, Tautz D. (1998) A conserved mode of head segmentation in arthropods revealed by the expression pattern of Hox genes in a spider. Proceedings of the National Academy of Sciences 95: 10665–10670

Davis EE, Sokolove PG (1975) Temperature responses of antennal receptors of the mosquito, *Aedes aegypti*. *Journal of Comparative Physiology* 96: 223–236.

Dechant H-E, Hößl B, Rammerstorfer FG, Barth FG (2006) Arthropod mechanoreceptive hairs: modeling the directionality of the joint. Journal of Comparative Physiology A 192: 1271–1278

Deutsch JS (2004) Segments and parasegments in arthropods: a functional perspective. BioEssays 26: 1117–1125

Doeffinger C, Hartenstein V, Stollewerk A (2010) Compartmentalization of the precheliceral neuroectoderm in the spider *Cupiennius salei*: development of the arcuate body, optic ganglia, and mushroom body. Journal of Comparative Neurology 518: 2612–2632

Dubale MS, Vyas AB (1968) The structure of the chela of *Heterometrus* sp. and its mode of operation. Bulletin of the Southern California Academy of Sciences 67: 240–244

Dunlop JA (1994) Filtration mechanisms in the mouthparts of tetrapulmonate arachnids (Trigonotarbida, Araneae, Amblypygi, Uropygi, Schizomida). Bulletin of the British arachnological Society 9: 73

Dunlop JA (2000) The epistomo-labral plate and lateral lips in solifuges, pseudoscorpions and mites. Ekologia (Bratislava) 19: 67–78

Dunlop JA 2019. Miniaturisation in Chelicerata. Arthropod Structure & Development: 20–34

Dunlop JA, Arango CP (2005) Pycnogonid affinities: a review. Journal of Zoological Systematics and Evolutionary Research 43: 8–21

Dunlop JA, Alberti G (2008) The affinities of mites and ticks: a review. Journal of Zoological Systematics and Evolutionary Research 46: 1–18

Dunlop JA, Lamsdell JC (2017) Segmentation and tagmosis in Chelicerata. Arthropod Structure & Development 46: 395–418

Eberhard WG, Wcislo WT (2011) Grade changes in brain-body allometry: morphological and behavioural correlates of brain size in miniature spiders, insects and other invertebrates. Advances in Insect Physiology 40: 155

Eberhard WG, Wcislo WT (2012) Plenty of room at the bottom? Tiny animals solve problems of housing and maintaining oversized brains, shedding new light on nervous-system evolution. American Scientist 100: 226–233

Ehn R, Tichy, H (1994) Hygro-and thermoreceptive tarsal organ in the spider *Cupiennius salei*. Journal of Comparative Physiology A 174: 345–350

Eisenbeis G (1974) Licht-und elektronenmikroskopische Untersuchungen zur Ultrastruktur des Transportepithels am Ventraltubus arthropleoner Collembolen (Insecta). Cytobiologie 9: 180–202

Eisenbeis G, Wichard W (1987) Atlas on the biology of soil arthropods. Springer Science & Business Media, Berlin / Heidelberg

Engel MS, Breitkreuz LC, Cai C, Alvarado M, Azar D, Huang D (2016) The first Mesozoic microwhip scorpion (Palpigradi): a new genus and species in mid-Cretaceous amber from Myanmar. The Science of Nature 103: 1–7

Fage L (1949) Classe des Mérostomacés. Pp. 219–262 in: Grassé P-P (ed.) Traité de Zoologie, Vol. 6. Masson et Cie., Paris

Fahrenbach WH (1999) Merostomata. Pp. 21–115 in: Harrison FW, Foelix RF (eds) Microscopic Anatomy of Invertebrates, Vol. 8A. Wiley-Liss, New York

Farley RD (1999) Scorpiones. In: Harrison FW, Foelix, RF (eds), *Microscopic Anatomy of Invertebrates*, Vol. 8A. Wiley-Liss, New York, Pp. 117–222

Farley RD (2001) Development of segments and appendages in embryos of the desert scorpion *Paruroctonus mesaensis* (Scorpiones: Vaejovidae). Journal of Morphology 250: 70–88

Farley RD (2005) Developmental changes in the embryo, pronymph, and first molt of the scorpion *Centruroides vittatus* (Scorpiones: Buthidae). Journal of Morphology 265: 1–27

Felgenhauer BE (1999) Araneae. Pp. 223–266 in: Harrison FW, Foelix RF (eds) Microscopic Anatomy of Invertebrates, Vol. 8A. Wiley-Liss, New York

Felsenstein J (1985) Confidence limits on phylogenies: an approach using the bootstrap. Evolution 39: 783–791

Ferreira RL, Souza MFVR (2012) Notes on the behavior of the advances troglobite *Eukoenenia maquinensis,* Souza & Ferreira 2010 (Palpigradi: Eukoeneniidae) and its conservation status. Speleobiology Notes 2012 4: 17–23

Ferreira RL, Souza MFVR, Machado EO, Brescovit AD (2011) Description of a new *Eukoenenia* (Palpigradi: Eukoeneniidae) and *Metagonia* (Araneae: Pholcidae) from Brazilian caves, with notes on their ecological interactions. Journal of Arachnology 39: 409–419

Filimonova SA (2004) The fine structure of the coxal glands in *Myobia murismusculi* (Schrank) (Acari: Myobiidae). Arthropod Structure & Development 33: 149–160

Filimonova SA (2016) Morpho-functional variety of the coxal glands in cheyletoid mites (Prostigmata). I. Syringophilidae. Arthropod Structure & Development 45: 356–367

Filimonova SA (2017) Morpho-functional variety of the coxal glands in cheyletoid mites (Prostigmata). II. Cheyletidae. Arthropod Structure & Development 46: 777–787

Firstman B (1973) The relationship of the chelicerate arterial system to the evolution of the endosternite. Journal of Arachnology 1: 1–54

Foelix R (2010) Biology of spiders. 3rd ed. Oxford University Press, New York

Foelix R, Hebets E (2001) Sensory biology of whip spiders (Arachnida, Amblypygi). Eileen Hebets Publications 32

Foelix RF (1985) Mechano- and chemoreceptice sensilla. Pp. 118–137 in: Barth FG (ed.) Neurobiology of Arachnids. Springer, Berlin / Heidelberg

Foelix RF, Axtell RC (1972) Ultrastructure of Haller's organ in the tick *Amblyomma americanum* (L.). Cell and Tissue Research 124: 275–292

Foelix RF, Chu-Wang I-W (1972) Fine structural analysis of palpal receptors in the tick *Amblyomma americanum* (L.). Zeitschrift für Zellforschung und Mikroskopische Anatomie 129: 548–560

Foelix RF, Chu-Wang I-W (1973) The morphology of spider sensilla II. Chemoreceptors. Tissue and Cell 5: 461–478

Foelix RF, Schabronath J (1983) The fine structure of scorpion sensory organs. I. Tarsal sensilla. Bulletin of the British Arachnological Society 6: 53–67

Foelix RF, Chu-Wang I-W, Beck L (1975) Fine structure of tarsal sensory organs in the whip spider *Admetus pumilio* (Amblypygi, Arachnida). Tissue and Cell 7: 331–346

Fusco G, Minelli A (2013) Arthropod segmentation and tagmosis. Pp. 197–223 in: Minelli A, Boxshall G, Fusco G (eds) Arthropod Biology and Evolution: Molecules, Development, Morphology. Springer, Berlin / Heidelberg

Gaffal KP, Tichy H, Theiß J, Seelinger G (1975) Structural polarities in mechanosensitive sensilla and their influence on stimulus transmission (Arthropoda). Zoomorphology 82: 79–103

Gainett G, Michalik P, Müller CH, Giribet G, Talarico G, Willemart RH (2017) Putative thermo-/hygroreceptive tarsal sensilla on the sensory legs of an armored harvestman (Arachnida, Opiliones). Zoologischer Anzeiger 270: 81–97

Garwood RJ, Dunlop J (2014) Three-dimensional reconstruction and the phylogeny of extinct chelicerate orders. PeerJ 2: e641. https://doi.org/10.7717/peerj.641

Gerberding M, Scholtz G (2001) Neurons and glia in the midline of the higher crustacean *Orchestia cavimana* are generated via an invariant cell lineage that comprises a median neuroblast and glial progenitors. Developmental Biology 235: 397–409

Gerhardt U (1931) Ordnung Xiphosura/Poecilopoda (Schwertschwänze). Pp. 47–96 in: Krumbach T (ed.) Handbook of Zoology Online, Vol. 1. De Gruyter, Berlin / Boston

Gerhardt U, Kästner A (1931) Ordnung Araneae (Echte Spinnen oder Webspinnen). Pp. 394–656 in: Krumbach T (ed.) Handbook of Zoology Online, Vol. 2. De Gruyter, Berlin Boston

Giribet G, Edgecombe GD, Wheeler WC, Babbitt C (2002) Phylogeny and systematic position of opiliones: A combined analysis of chelicerate relationships using morphological and molecular data. Cladistics 18: 5–70

Giribet G, McIntyre E, Christian E, Espinasa L, Ferreira RL, Francke OF, et al. (2014) The first phylogenetic analysis of Palpigradi (Arachnida) – the most enigmatic arthropod order. Invertebrate Systematics 28: 350–360

Goloboff PA (1993) Estimating character weights during tree search. Cladistics 9: 83–91

Goloboff PA, Catalano SA (2016) TNT version 1.5, including a full implementation of phylogenetic morphometrics. Cladistics 32: 221–238

Goloboff PA, Farris JS, Nixon KC (2008) TNT, a free program for phylogenetic analysis. Cladistics 24: 774–786

Göpel T, Wirkner CS (2015) An "ancient" complexity? Evolutionary morphology of the circulatory system in Xiphosura. Zoology 118: 221–238

Gorb S (2001a) Principles of cuticular attachment in Arthropoda. Pp. 37–76 in: Attachment Devices of Insect Cuticle. Kluwer Academic Publishers, Dordrecht

Gorb S (2001b) Cuticular protuberances of insects. Pp. 21–36 in: Attachment Devices of Insect Cuticle. Kluwer Academic Publishers, Dordrecht

Görner P (1965) A proposed transducing mechanism for a multiply-innervated mechanoreceptor (trichobothrium) in spiders. Cold Spring Harbor Symposia on Quantitative Biology 30: 69–73

Gottlieb K (1926) Über das Gehirn des Skorpions. Zeitschrift für wissenschaftliche Zoologie 127: 195–243

Gould SJ (1977) Heterochrony and the parallel of ontogeny and phylogeny. Pp. 209–266 in: Ontogeny and Phylogeny. Belknap Press of Harvard University Press, Cambridge

Graham JB (1988) Ecological and evolutionary aspects of integumentary respiration: body size, diffusion, and the Invertebrata. American Zoologist 28: 1031–1045

Grams M, Wirkner CS, Runge J (2018) Serial and special: comparison of podomeres and muscles in tactile vs walking legs of whip scorpions (Arachnida, Uropygi). Zoologischer Anzeiger 273: 75–101

Hackman RH (1984) VIII Arthropoda – Cuticle: Biochemistry. Pp. 583–610 in: Bereiter-Hahn J, Matoltsy AG, Richards KS (eds) Biology of the Integument. 1 Invertebrates. Springer, Berlin / Heidelberg

Hammen L van der (1966) Studies on Opilioacarida (Arachnida) I. Description of *Opilioacarus texanus* (Chamberlin & Mulaik) and revised classification of the genera. Zoologische Verhandelingen 86: 1–80

Hammen L van der (1967) The gnathosoma of *Hermannia convexa* (C. L. Koch) (Acarida: Oribatina) and comparative remarks on its morphology in other mites. Zoologische Verhandelingen 94: 3–45

Hammen L van der (1977a) A new classification of Chelicerata. Zoologische Mededelingen 51: 307–319

Hammen L van der (1977b) The evolution of the coxa in mites and other groups of Chelicerata. Acarologia 19: 12–19

Hammen L van der (1982) Comparative studies in Chelicerata II. Epimerata (Palpigradi and Actinotrichida). Zoologische Verhandelingen 196: 3–70

Hammen L van der (1986) Comparative studies in Chelicerata IV. Apatellata, Arachnida, Scorpionida, Xiphosura. Zoologische Verhandelingen 226: 4–52

Hammen L van der (1989) An introduction to comparative arachnology. SPB Academic Publishing, The Hague

Handlirsch A (1926) Arthropoda: Allgemeine Einleitung in die Naturgeschichte der Gliederfüsser. Pp. 211–276 in: Krumbach T (ed.) Handbook of Zoology Online. De Gruyter, Berlin / Boston

Hanken J, Wake DB (1993) Miniaturization of body size: organismal consequences and evolutionary significance. Annual Review of Ecology and Systematics 24: 501–519

Hansen HJ (1901) On six species of *Koenenia*, with remarks on the order Palpigradi. Entomologisk Tidskrift: 193–240

Hansen HJ, Sørensen W (1897) The order Palpigradi Thorell (*Koenenia mirabilis*, Grassi) and its relationships to other Arachnida. Entomologisk Tidskrift: 223–240

Hansen HJ, Sørensen WE (1905) The Tartarides: a tribe of the order Pedipalpi. Arkiv för Zoologi 2: 1–85

Hanstrom B (1928) Vergleichende Anatomie des Nervensystems der wirbellosen Tiere. Springer, Berlin / Heidelberg

Harris DJ, Mill PJ (1973) The ultrastructure of chemoreceptor sensilla in *Ciniflo* (Araneida, Arachnida). Tissue and Cell 5: 679–689

Harris DJ, Mill PJ (1977) Observations on the leg receptors of *Ciniflo* (Araneida: Dictynidae). *Journal of Comparative Physiology* 119: 37–54

Harvey MS (2002) The neglected cousins: what do we know about the smaller arachnid orders? Journal of Arachnology 30: 357–372

Harvey MS (2003) Catalogue of the smaller arachnid orders of the world: Amblypygi, Uropygi, Schizomida, Palpigradi, Ricinulei and Solifugae. CSIRO Publishing, Clayton South

Harzsch S (2003) Ontogeny of the ventral nerve cord in malacostracan crustaceans: a common plan for neuronal development in Crustacea, Hexapoda and other Arthropoda? Arthropod Structure & Development 32: 17–37

Harzsch S, Wildt M, Battelle B, Waloszek D (2005) Immunohistochemical localization of neurotransmitters in the nervous system of larval *Limulus polyphemus* (Chelicerata, Xiphosura): evidence for a conserved protocerebral architecture in Euarthropoda. Arthropod Structure & Development 34: 327–342

Haupt J (1982) Hair regeneration in a solfugid chemotactile sensillum during moulting (Arachnida: Solifugae). Wilhelm Roux's Archives of Developmental Biology 191: 137–142

Hess E, Vlimant M (1982) The tarsal sensory system of *Amblyomma variegatum* Fabricius (Ixodidae, Metastriata). I. Wall pore and terminal pore sensilla. Revue Suisse de Zoologie 89: 713–729

Hess E, Loftus R (1984) Warm and cold receptors of two sensilla on the foreleg tarsi of the tropical bont tick Amblyomma variegatum. Journal of Comparative Physiology A 155: 187–195

Hoffmann C (1967) Bau und Funktion der Trichobothrien von *Euscorpius carpathicus* L. Zeitschrift für vergleichende Physiologie 54: 290–352

Hootman SR, Conte FP (1975) Functional morphology of the neck organ in *Artemia salina* nauplii. Journal of Morphology 145: 371–385

Horn ACM, Achaval M (2002) The gross anatomy of the nervous system of *Bothriurus bonariensis* (L. C. Koch, 1842) (Scorpiones, Bothriuridae). Brazilian Journal of Biology 62: 253–262

Ioffe ID (1963) Structure of the brain of *Dermacentor pictus* Herm. (Chelicerata, Acarina). Zoologicheskii Zhurnal 42: 1472–1484

Kaneko N (1988) Feeding habits and cheliceral size of oribatid mites in cool temperate forest soils in Japan. Revue d'Écologie et de Biologie du Sol 25: 353–363

Kästner A (1931a) Ordnung Palpigradi Thorell. Pp. 77–98 in: Krumbach T (ed.) Handbook of Zoology Online, Vol. 2. De Gruyter, Berlin / Boston

Kästner A (1931b) Ordnung Scorpiones (Schwertschwänze). Pp. 117–240 in: Krumbach T (ed.) Handbook of Zoology Online, Vol. 1. De Gruyter, Berlin / Boston

Kästner A (1931c) Ordnung Ricinulei. Pp. 99–116 in: Krumbach T (ed.) Handbook of Zoology Online, Vol. 2. De Gruyter, Berlin / Boston

Kästner A (1931d) Ordnung Opiliones Sundevall (Weberknechte). Pp. 300–393 in: Krumbach T (ed.) Handbook of Zoology Online, Vol. 2. De Gruyter, Berlin / Boston

Kästner A (1931e) Ordnung Solifugae (Walzenspinnen). Pp. 193–299 in: Krumbach T (ed.) Handbook of Zoology Online, Vol. 2. De Gruyter, Berlin / Boston

Kästner A (1931f) Ordnung Pedipalpi Latreille (Geißel-Scorpione). Pp. 1–76 in: Krumbach T (ed.) Handbook of Zoology Online, Vol. 2. De Gruyter, Berlin / Boston

Kästner A (1931g) Die Hüfte und ihre Umformung zu Mundwerkzeugen bei den Arachniden. Zeitschrift für Morphologie und Ökologie der Tiere 22: 721–758

Keil TA (1997) Functional morphology of insect mechanoreceptors. Microscopy Research and Technique 39: 506–531

Kimble M, Coursey Y, Ahmad N, Hinsch GW (2002) Behavior of the yolk nuclei during embryogenesis, and development of the midgut diverticulum in the horseshoe crab *Limulus polyphemus*. Invertebrate Biology 121: 365–377

Klann AE (2009) Histology and ultrastructure of solifuges. Ernst-Moritz-Arndt-Universität, Greifswald

Klann AE, Alberti G (2010) Histological and ultrastructural characterization of the alimentary system of solifuges (Arachnida, Solifugae). Journal of Morphology 271: 225–243

Klußmann-Fricke B-J, Wirkner CS (2016) Comparative morphology of the hemolymph vascular system in Uropygi and Amblypygi (Arachnida): complex correspondences support Arachnopulmonata. Journal of Morphology 277: 1084–1103

Klußmann-Fricke B-J, Prendini L, Wirkner CS (2012) Evolutionary morphology of the hemolymph vascular system in scorpions: a character analysis. Arthropod Structure & Development 41: 545–560

Kovac D, Maschwitz U (2000) Protection of hydrofuge respiratory structures against detrimental microbiotic growth by terrestrial grooming in water beetles (Coleoptera: Hydrophilidae, Hydraeoidae, Dryopidae, Ebnidae, Curculiooidae). Entomologia Generalis: 277–292

Kováč Ľ, Mock A, Ľuptácik P, Palacios-Vargas JG (2002) Distribution of *Eukoenenia spelaea* (Peyerimhoff, 1902) (Arachnida, Palpigradida) in the Western Carpathians with remarks on its biology and behaviour. Pp. 93–99 in: Tajovský, K, Balík, V, Pižl, V. (eds) Studies on Soil Fauna in Central Europe. České Budějovice: Institute of Soil Biology AS CR

Kováč Ľ, Elhottová D, Mock A, Nováková A, Krištůfek V, Chroňáková A, et al. (2014) The cave biota of Slovakia. State Nature Conservancy of the Slovak Republic, Slovak Caves Administration, Liptovský Mikuláš: 1–192

Kraus O (1976) Zur phylogenetischen Stellung und Evolution der Chelicerata. Entomologica Germanica: 1–12

Lamsdell JC (2013) Revised systematics of Palaeozoic 'horseshoe crabs' and the myth of monophyletic Xiphosura: re-evaluating the monophyly of Xiphosura. Zoological Journal of the Linnean Society 167: 1–27

Lauterbach KE (1973) Schlüsselereignisse in der Evolution der Stammgruppe der Euarthropoda. Zoologische Beiträge 19: 251–299

Legg G (1976) The external morphology of a new species of ricinuleid (Arachnida) from Sierra Leone. Zoological Journal of the Linnean Society 59: 1–58

Lehmacher C, Abeln B, Paululat A (2012) The ultrastructure of *Drosophila* heart cells. Arthropod Structure & Development 41: 459–474

Lehmann T, Heß M, Melzer RR (2012) Wiring a periscope–ocelli, retinula axons, visual neuropils and the ancestrality of sea spiders. PLoS One 7: e30474. https://doi.org/10.1371/journal.pone.0030474

Levi HW (1967) Adapations of respiratory systems of spiders. Evolution 21: 571–583

Loesel R, Wolf H, Kenning M, Harzsch S, Sombke A (2013) Architectural principles and evolution of the arthropod central nervous system. Pp. 300–342 in: Minelli A, Boxshall G, Fusco G (eds) Arthropod Biology and Evolution: Molecules, Development, Morphology. Springer, Berlin / Heidelberg

Loftus R (1976) Temperature-dependent dry receptor on antenna of *Periplaneta*. Tonic response. Journal of Comparative Physiology 111: 153–170

Loftus R, Corbière-Tichané G (1981) Antennal warm and cold receptors of the cave beetle, *Speophyes lucidulus* Delar, in sensilla with a lamellated dendrite. Journal of Comparative Physiology A 143: 443–452

Lopez A (1983) Coxal glands of the genus *Metepeira* (Araneae, Araneidae). The Journal of Arachnology 11: 97–99

Lowy RJ, Conte FP (1985) Morphology of isolated crustacean larval salt glands. American Journal of Physiology-Regulatory, Integrative and Comparative Physiology 248: R709–R716

Ludwig M, Alberti G (1992) Fine structure of the midgut of *Prokoenenia wheeleri* (Arachnida: Palpigradi). Zoologische Beiträge 34: 127–134

Ludwig M, Palacios-Vargas JG, Albertif G (1994) Cellular details of the midgut of *Cryptocellus boneti* (Arachnida: Ricinulei). Journal of Morphology 220: 263–270

Mares S, Ash L, Gronenberg W (2005) Brain allometry in bumblebee and honey bee workers. Brain, behavior and evolution 66: 50–61

McIver SB (1975) Structure of cuticular mechanoreceptors of arthropods. Annual Review of Entomology 20: 381–397

McNamara KJ (1986) A guide to the nomenclature of heterochrony. Journal of Paleontology: 4–13

Mehnert L, Dietze Y, Hörnig MK, Starck JM (2018) Body tagmatization in pseudoscorpions. Zoologischer Anzeiger 273: 152–163

Meijden A van der, Langer F, Boistel R, Vagovic P, Heethoff M (2012) Functional morphology and bite performance of raptorial chelicerae of camel spiders (Solifugae). The Journal of Experimental Biology 215: 3411–3418

Messlinger K (1987) Fine structure of scorpion trichobothria (Arachnida, Scorpiones). Zoomorphology 107: 49–57

Michalik P (2009) The male genital system of spiders (Arachnida, Araneae) with notes on the fine structure of seminal secretions. Contributions to Natural History 12: 959–972

Michalik P, Reiher W, Tintelnot-Suhm M, Coyle FA, Alberti G (2005) Female genital system of the folding-trapdoor spider *Antrodiaetus unicolor* (Hentz, 1842) (Antrodiaetidae, Araneae): ultrastructural study of form and function with notes on reproductive biology of spiders. Journal of Morphology 263: 284–309

Millot J (1942) Sur l'anatomie et l'histophysiologie de *Koenenia mirabilis*, Grassi (Arachnida, Palpigradi). Revue Francais d'Entomologie Paris 9: 33–51

Millot J (1943) Notes complémentaires sur l'anatomie, l'histologie et la répartition géographique en France de *Koenenia mirabilis*, Grassi (Arachnida Palpigradi). Revue Francais d'Entomologie Paris 9: 127–135

Millot J (1949a) Ordre des Palpigrades. Pp. 520–532 in: Grassé P-P (ed.) Traité de Zoologie, Vol. 6. Masson et Cie., Paris

Millot, J. 1949b. Classe des Arachnides. Pp. 263–385 in: Grassé P-P (ed.) Traité de Zoologie, Vol. 6. Masson et Cie., Paris

Millot, J. 1949c. Ordre des Uropyges. Pp. 533–562 in: Grassé P-P (ed.) Traité de Zoologie, Vol. 6. Masson et Cie., Paris

Millot, J. 1949d. Ordre des Amblypyges. Pp. 563–588 in: Grassé P-P (ed.) Traité de Zoologie, Vol. 6. Masson et Cie., Paris

Millot, J. 1949e. Ordre des Aranéides. Pp. 589–743 in: Grassé P-P (ed.) Traité de Zoologie, Vol. 6. Masson et Cie., Paris

Millot, J. 1949f. Ordre des Ricinuléides. Pp. 744–760 in: Grassé P-P (ed.) Traité de Zoologie, Vol. 6. Masson et Cie., Paris

Millot, J, Vachon, M. 1949a. Ordre des Solifuges. Pp. 482–519 in: Grassé P-P (ed.) Traité de Zoologie, Vol. 6. Masson et Cie., Paris

Millot, J, Vachon, M. 1949b. Ordre des Scorpions. Pp. 386–436 in: Grassé P-P (ed.) Traité de Zoologie, Vol. 6. Masson et Cie., Paris

Mittmann B, Scholtz G (2003) Development of the nervous system in the "head" of *Limulus polyphemus* (Chelicerata: Xiphosura): morphological evidence for a correspondence between the segments of the chelicerae and of the (first) antennae of Mandibulata. Development Genes and Evolution 213: 9–17

Molina MR, Cripps RM (2001) Ostia, the inflow tracts of the *Drosophila* heart, develop from a genetically distinct subset of cardial cells. Mechanisms of Development 109: 51–59

Moritz M (1993) 1. Unterstamm Arachnata. Pp. 64–447 in: Gruner H-E (ed.) Lehrbuch Der Speziellen Zoologie. Band I: Wirbellose Tiere. 4. Teil: Arthropoda (Ohne Insecta), 4th ed. Gustav Fischer Verlag, Jena

Neville AC (1984) Cuticle: organization. Pp. 611–625 in: Bereiter-Hahn J, Matoltsy AG, Richards KS (eds) Biology of the Integument. Springer, Berlin / Heidelberg

Noble-Nesbitt J (1963) Transpiration in *Podura aquatica* L. (Collembola, Isotomidae) and the wetting properties of its cuticle. Journal of Experimental Biology 40: 681–700

Noirot C, Quennedey A (1974) Fine structure of insect epidermal glands. Annual Review of Entomology 19: 61–80

Obenchain FD, Oliver JH Jr (1975) The heart and arterial circulatory system of ticks (Acari: Ixodoidea). Journal of Arachnology: 57–74

Ortega-Hernández J, Janssen R, Budd GE (2017) Origin and evolution of the panarthropod head — A palaeobiological and developmental perspective. Arthropod Structure and Development 46: 354–379

Ozaki M, Tominaga Y (1999) Contact chemoreceptors. Pp. 143–154 in: Eguchi E, Tominaga Y (eds) Atlas of Arthropod Sensory Receptors. Springer, Berlin / Heidelberg

Peel A (2004) The evolution of arthropod segmentation mechanisms. BioEssays 26: 1108–1116

Peel AD, Chipman AD, Akam M (2005) Arthropod segmentation: beyond the Drosophila paradigm. Nature Reviews Genetics 6: 905

Pepato AR, da Rocha CE, Dunlop JA (2010) Phlyogenetic position of the acariform mites: sensitivity to homology assessment under total evidence. BMC Evolutionary Biology 10: 235. http://www.biomedcentral.com/1471-2148/10/235

Peters SE (1983) Postnatal development of gait behaviour and functional allometry in the domestic cat (*Felis catus*). Journal of Zoology 199: 461–486

Pinto-da-Rocha R, Machado G, Giribet G (2007) Harvestmen. The Biology of Opiliones. Harvard University Press, Cambridge / London

Pinto-da-Rocha R, Andrade R, Moreno-González JA (2016) Two new cave-dwelling genera of short-tailed whip-scorpions from Brazil (Arachnida: Schizomida: Hubbardiidae). Zoologia (Curitiba) 33

Pitnick S, Hosken DJ, Birkhead TR (2009) Sperm morphological diversity. Pp. 69–149 in: Sperm Biology – An Evolutionary Perspective. Elsevier, Oxford

Polilov AA (2008) Anatomy of the smallest Coleoptera, featherwing beetles of the tribe Nanosellini (Coleoptera, Ptiliidae), and limits of insect miniaturization. Entomological Review 88: 26–33

Polilov AA (2015a) Consequences of miniaturization in insect morphology. Moscow University Biological Sciences Bulletin 70: 136–142

Polilov AA (2015b) Small is beautiful: features of the smallest insects and limits to miniaturization. Annual Review of Entomology 60: 103–121

Polilov AA (2016) At the size limit – Effects of miniaturization in insects. Springer International Publishing Switzerland, Cham. https://doi.org/10.1007/978-3-319-39499-2

Polilov AA, Shmakov AS (2016) The anatomy of the thrips *Heliothrips haemorrhoidalis* (Thysanoptera, Thripidae) and its specific features caused by miniaturization. Arthropod Structure & Development 45: 496–507

Polilov AA, Makarova AA (2017) The scaling and allometry of organ size associated with miniaturization in insects: A case study for Coleoptera and Hymenoptera. Scientific reports 7: 43095

Polis GA (1990) The biology of scorpions. Stanford University Press, Stanford

Polis GA, Farley RD (1979) Behavior and ecology of mating in the cannibalistic scorpion, *Paruroctonus mesaensis* Stahnke (Scorpionida: Vaejovidae). Journal of Arachnology: 33–46

Pound JM, Oliver JH Jr (1982) Synganglial and neurosecretory morphology of female *Ornithodoros parkeri* (Cooley) (Acari: Argasidae). Journal of Morphology 173: 159–177

Punzo F (2012) The Biology of Camel-Spiders: Arachnida, Solifugae. Springer Science & Business Media, Berlin / Heidelberg

Quesada R, Triana E, Vargas G, Douglass JK, Seid MA, Niven JE, et al. (2011) The allometry of CNS size and consequences of miniaturization in orb-weaving and cleptoparasitic spiders. Arthropod Structure & Development 40: 521–529

Regier JC, Shultz JW, Zwick A, Hussey A, Ball B, Wetzer R, et al. (2010) Arthropod relationships revealed by phylogenomic analysis of nuclear protein-coding sequences. Nature 463: 1079–1083

Reißland A, Görner P (1985) Trichobothria. Pp. 138–161 in: Barth FG (ed.) Neurobiology of Arachnids, Springer, Berlin / Heidelberg

Reynolds ES (1963) The use of lead citrate at high pH as an electron-opaque stain in electron microscopy. The Journal of Cell Biology 17: 208–212

Roewer CF (1934) 4. Buch: Solifugae, Palpigradi. Pp. 1–723 in: Bronn HG (ed.) Dr. H.G. Bronns Klassen und Ordnungen des Tierreichs, Vol. 5. Akademische Verlagsgesellschaft, Leipzig

Rucker A (1901) The Texan *Koenenia*. The American Naturalist 35: 615–630

Rucker A (1903) A new *Koenenia* from Texas. Quarterly Journal of Microscopical Science: 215–231

Rüdeberg C (1967) A rapid method for staining thin sections of vestopal W-embedded tissue for light microscopy. Experientia 23: 792–792

Rugendorff A, Younossi-Hartenstein A, Hartenstein V (1994) Embryonic origin and differentiation of the *Drosophila* heart. Wilhelm Roux's Archives of Developmental Biology 203: 266–280

Scholl G (1977) Beiträge zur Embryonalentwicklung von *Limulus polyphemus* L. (Chelicerata, Xiphosura). Zoomorphologie 86: 99–154

Scholtz G (1998) Cleavage, germ band formation and head segmentation: the ground pattern of the Euarthropoda. Pp. 317–332 in: Fortey RA, Thomas RH (eds) Arthropod Relationships. The Systematics Association Special Volume Series, vol 55. Springer, Dordrecht

Scholtz G, Edgecombe GD (2006) The evolution of arthropod heads: reconciling morphological, developmental and palaeontological evidence. Development Genes and Evolution 216: 395–415

Schriefer ME, Beveridge M, Sonenshine DE, Homsher PJ, Carson KA, Weidman CS (1987) Evidence of ecdysteroid production by tick (Acari: Ixodidae) fat-body tissues in vitro. Journal of Medical Entomology 24: 295–302

Seid MA, Castillo A, Wcislo WT (2011) The allometry of brain miniaturization in ants. Brain, behavior and evolution 77: 5–13

Sharma PP (2018) Chelicerates. Current Biology 28: R774–R778

Sharma PP, Kaluziak ST, Pérez-Porro AR, González VL, Hormiga G, Wheeler WC, et al. (2014) Phylogenomic interrogation of Arachnida reveals systemic conflicts in phylogenetic signal. Molecular biology and evolution: msu235

Shear WA (1999) Introduction to Arthropoda and Chelicériformes. Pp. 1–19 in: Harrison FW, Foelix RF (eds) Microscopic Anatomy of Invertebrates, Vol. 8A. Wiley-Liss, New York

Sherman RG, Bursey CR, Fourtner CR, Pax RA (1969) Cardiac ganglia in spiders (Arachnida: Araneae). Experientia 25: 438–439

Shultz JW (1989) Morphology of locomotor appendages in Arachnida: evolutionary trends and phylogenetic implications. Zoological Journal of the Linnean Society 97: 1–55

Shultz JW (1990) Evolutionary morphology and phylogeny of Arachnida. Cladistics 6: 1–38

Shultz JW (1991) Evolution of locomotion in Arachnida: the hydraulic pressure pump of the giant whipscorpion, *Masti-*

goproctus giganteus (Uropygi). Journal of Morphology 210: 13–31
Shultz JW (1993) Muscular anatomy of the giant whipscorpion *Mastigoproctus giganteus* (Lucas) (Arachnida: Uropygi) and its evolutionary significance. Zoological Journal of the Linnean Society 108: 335–365
Shultz JW (1999) Muscular anatomy of a whipspider, *Phrynus longipes* (Pocock) (Arachnida: Amblypygi), and its evolutionary significance. Zoological Journal of the Linnean Society 126: 81–116
Shultz JW (2000) Skeletomuscular anatomy of the harvestman *Leiobunum aldrichi* (Weed, 1893) (Arachnida: Opiliones: Palpatores) and its evolutionary significance. Zoological Journal of the Linnean Society 128: 401–438
Shultz JW (2001) Gross muscular anatomy of *Limulus polyphemus* (Xiphosura, Chelicerata) and its bearing on evolution in the Arachnida. Journal of Arachnology 29: 283–303
Shultz JW (2007a) A phylogenetic analysis of the arachnid orders based on morphological characters. Zoological Journal of the Linnean Society 150: 221–265
Shultz JW (2007b) Morphology of the prosomal endoskeleton of Scorpiones (Arachnida) and a new hypothesis for the evolution of cuticular cephalic endoskeletons in arthropods. Arthropod Structure & Development 36: 77–102
Smrž J, Kováč Ľ, Mikeš J, Lukešová A (2013) Microwhip scorpions (Palpigradi) feed on heterotrophic cyanobacteria in Slovak caves – a curiosity among Arachnida. *PLOS ONE* 8: e75989. https://doi.org/10.1371/journal.pone.0075989
Smrž J, Kováč Ľ, Mikeš J, Šustr V, Lukešová A, Tajovsky K, et al. (2015) Food sources of selected terrestrial cave arthropods. Subterranean Biology 16: 37
Snodgrass RE (1948) The feeding organs of Arachnida, including mites and ticks. Smithsonian Miscellaneous Collections 110: 1–93
Snodgrass RE (1965) Textbook of Arthropod Anatomy: Facsimile of the Edition of 1952. Publishing Company, New York / London
Souza MFV, Ferreira RL (2010a) *Eukoenenia* (Palpigradi: Eukoeneniidae) in Brazilian caves with the first troglobiotic palpigrade from South America. Journal of Arachnology 38: 415–424
Souza M, Ferreira RL (2010b) Palpigradi: Eukoeneniidae and its conservation status. Speleobiology Notes 4: 17–23
Souza M, Ferreira RL (2011) A new species of *Eukoenenia* (Palpigradi: Eukoeneniidae) from Brazilian iron caves. Zootaxa 2886: 31–38
Souza M, Ferreira RL (2011b) A new troglobitic *Eukoenenia* (Palpigradi: Eukoeneniidae) from Brazil. Journal of Arachnology 39: 185–188
Souza M, Ferreira RL (2012) *Eukoenenia virgemdalapa* (Palpigradi: Eukoeneniidae): a new troglobitic palpigrade from Brazil. Zootaxa 3295: 59–64
Souza MFVR, Ferreira RL (2013) Two new species of the enigmatic *Leptokoenenia* (Eukoeneniidae: Palpigradi) from Brazil: first record of the genus outside intertidal environments. PLOS ONE 8: e77840. https://doi.org/10.1371/journal.pone.0077840
Stahnke HL (1966) Some aspects of scorpion behavior. Bulletin of the Southern California Academy of Sciences 65: 65–80
Steinbach G (1952) Vergleichende Untersuchungen zur Chelicerenmuskulatur einiger Araneen. Wissenschaftliche Zeitschrift der Humboldt-Universität zu Berlin 2, Berlin
Steinbrecht RA (1969) Comparative morphology of olfactory receptors. Pp. 3–21 in: Pfaffmann C (ed.) Olfaction and Taste, Vol. 3. Rockefeller University Press, New York
Strausfeld NJ, Mok Strausfeld C, Loesel R, Rowell D, Stowe S (2006) Arthropod phylogeny: onychophoran brain organization suggests an archaic relationship with a chelicerate stem lineage. Proceedings of the Royal Society B: Biological Sciences 273: 1857–1866
Strubell A (1892) Zur Entwicklungsgeschichte der Pedipalpen. Zoologischer Anzeiger 15: 87–93
Suter RB, Stratton G.E, Miller PR (2004) Taxonomic variation among spiders in the ability to repel water: surface adhesion and hair density. Journal of Arachnology 32: 11–21
Szalay L (1956) Der erste Fund von Palpigraden in Ungarn. Annales historico-naturales Musei nationalis hungarici 48 (series nova 7): 439–442
Talarico G, Hernandez LG, Michalik P (2008) The male genital system of the New World Ricinulei (Arachnida): ultrastructure of spermatozoa and spermiogenesis with special emphasis on its phylogenetic implications. Arthropod Structure & Development 37: 396–409
Talarico G, Lipke E, Alberti G (2011) Gross morphology, histology, and ultrastructure of the alimentary system of Ricinulei (Arachnida) with emphasis on functional and phylogenetic implications. Journal of Morphology 272: 89–117
Talarico G, Palacios-Vargas JG, Silva MF, Alberti G (2005) First ultrastructural observations on the tarsal pore organ of *Pseudocellus pearsei* and *P. boneti* (Arachnida, Ricinulei). Journal of Arachnology 33: 604–612
Tanaka G, Hou X, Ma X, Edgecombe GD, Strausfeld NJ (2013) Chelicerate neural ground pattern in a Cambrian great appendage arthropod. Nature 502: 364
Telford MJ, Thomas RH (1998) Expression of homeobox genes shows chelicerate arthropods retain their deutocerebral segment. Proceedings of the National Academy of Sciences 95: 10671–10675
Teruel R, De Armas LF (2002) Un género nuevo de Hubbardiidae (Arachnida: Schizomida) del occidente de Cuba. Revista Ibérica de Aracnología 6: 91–94
Tichy H (1975) Unusual fine structure of sensory hair triad of the millipede, *Polyxenus*. Cell and Tissue Research 156: 229–238
Tichy H, Barth FG (1992) Fine structure of olfactory sensilla in myriapods and arachnids. Microscopy Research and Technique 22: 372–391
Tichy H, Loftus R (1996) Hygroreceptors in insects and a spider: humidity transduction models. Naturwissenschaften 83: 255–263
Tjønneland A, Økland S, Nylund A (1987) Evolutionary aspects of the arthropod heart. Zoologica Scripta 16: 167–175
Todd V (1949) The habits and ecology of the British harvestmen (Arachnida, Opiliones), with special reference to those of the Oxford district. The Journal of Animal Ecology: 209–229
Vachon M (1949) Ordre des Pseudoscorpions. Pp. 437–481 in: Grassé P-P (ed.) Traité de Zoologie, Vol. 6. Masson et Cie., Paris
Vitzthum H (1931) Ordnung Acari (Milben). Pp. 1–160 in: Krumbach T (ed.) Handbook of Zoology Online, Vol. 3. De Gruyter, Berlin / Boston
Vyas AB (1974) The cheliceral muscles of the scorpion *Heterometrus fulvipes*. Bulletin of the Southern California Academy of Sciences 73: 9–14
Waldow U (1970) Elektrophysiologische Untersuchungen an Feuchte-, Trocken-und Kälterezeptoren auf der Antenne der Wanderheuschrecke *Locusta*. Journal of Comparative Physiology A 69: 249–283
Waloszek D, Müller KJ (1998) Cambrian 'Orsten'-type arthropods and the phylogeny of Crustacea. Pp. 139–153 in: Fortey

RA, Thomas RH (eds) Arthropod Relationships. The Systematics Association Special Volume Series, vol 55. Springer, Dordrecht

Waloszek D, Chen J, Maas A, Wang X (2005) Early Cambrian arthropods – new insights into arthropod head and structural evolution. Arthropod Structure & Development 34: 189–205

Wang B, Dunlop JA, Selden PA, Garwood RJ, Shear WA, Müller P, et al. (2018) Cretaceous arachnid *Chimerarachne yingi* gen. et sp. nov. illuminates spider origins. Nature Ecology & Evolution 2: 614–622

Wegerhoff R, Breidbach O (1995) Comparative aspects of the chelicerate nervous systems. Pp. 159–179 in: Breidbach O, Kutsch W (eds) The Nervous Systems of Invertebrates: An Evolutionary and Comparative Approach. Experientia Supplementum, vol 72. Birkhäuser, Basel

Weygoldt P (1969) The Biology of Pseudoscorpions. Harvard University Press, Cambridge

Weygoldt P (1985) Ontogeny of the arachnid central nervous system. Pp. 20–37 in: Barth FG (ed.) Neurobiology of Arachnids. Springer, Berlin / Heidelberg

Weygoldt P (1996) Evolutionary morphology of whip spiders: towards a phylogenetic system (Chelicerata: Arachnida: Amblypygi). Journal of Zoological Systematics and Evolutionary Research 34: 185–202

Weygoldt P, Paulus HF (1979a) Untersuchungen zur Morphologie, Taxonomie und Phylogenie der Chelicerata II. Cladogramme und die Entfaltung der Chelicerata. Journal of Zoological Systematics and Evolutionary Research 17: 177–200

Weygoldt P, Paulus HF (1979b) Untersuchungen zur Morphologie, Taxonomie und Phylogenie der Chelicerata I. Morphologische Untersuchungen. Journal of Zoological Systematics and Evolutionary Research 17: 85–116

Weygoldt P, Rahmadi C, Huber S (2010) Notes on the reproductive biology of *Phrynus exsul* Harvey, 2002 (Arachnida: Amblypygi: Phrynidae). Zoologischer Anzeiger 249: 113–119

Wheeler WM (1900) A singular arachnid *Koenenia mirabilis* (Grassi) occurring in Texas. The American Naturalist 34: 837–850

Whitehead WF, Rempel JG (1959) A study of the musculature of the black widow spider, *Latrodectus mactans* (Fabr.). Canadian Journal of Zoology 37: 831–870

Wiens JJ, Donoghue MJ (2004) Historical biogeography, ecology and species richness. Trends in Ecology & Evolution 19: 639–644

Wirkner CS, Huckstorf K (2013) The circulatory system of spiders. Pp. 15–27 in: Nentwig W (ed.) Spider Ecophysiology. Springer, Berlin / Heidelberg

Wirkner CS, Prendini L (2007) Comparative morphology of the hemolymph vascular system in scorpions – A survey using corrosion casting, MicroCT, and 3D-reconstruction. Journal of Morphology 268: 401–413

Wirkner CS, Tögel M, Pass G (2013) The arthropod circulatory system. Pp. 343–391 in: Minelli A, Boxshall G, Fusco G (eds) Arthropod Biology and Evolution: Molecules, Development, Morphology. Springer, Berlin / Heidelberg

Wolf H (2016) Scorpiones. Pp. 443–452 in: Schmidt-Rhaesa A, Harzsch S, Purschke G (eds) Structure and Evolution of Invertebrate Nervous Systems. Oxford University Press, Oxford

Yokohari F (1999) Hygro- and Thermoreceptors. Pp. 191–210 in: Eguchi E, Tominaga Y (eds) Atlas of Arthropod Sensory Receptors. Springer, Berlin / Heidelberg

Zwicky KT, Hodgson SM (1965) Occurrence of myogenic hearts in arthropods. Nature 207: 778

Appendix I.

Table 5. *Eukoenenia spelaea*, list of musculature. Each muscle or muscle branch is listed with its points of origin and insertion. When two or more points of origin are listed, two or more branches originate and fuse into one strand. When two or more points of insertion are listed, the muscle branches. Within extremities, the term "proximal" is used to describe the location of origin/insertion of a muscle oriented toward the body, "distal" is used for the location away from the body. This terminology is used for the entire extremities as well as their separate articles. Muscles associated with the box-truss axial muscle system (Shultz 2001, 2007b) are marked grey. Abbreviations: C1–13 = cheliceral muscle; D1–2 = dorsal muscle; DV1–5 = dorsoventral muscle; E1–20 = endosternite muscle; F1–3 = flagellar muscle; Gf = genital muscle female; Gm1–4 = genital muscle male; JI1–4 = intersegmental muscle 1; JII1–6 = intersegmental muscle 2; JIII1–6 = intersegmental muscle 3; JIV1–6 = intersegmental muscle 4; JV1–6 = intersegmental muscle 5; JVI1–5 = intersegmental muscle 6; JVII1–4 = intersegmental muscle 7; JVIII1–3 = intersegmental muscle 8; JIX1–2 = intersegmental muscle 9; LI1–14t = leg 1 muscle/tendon; LII1–9 = leg 2 muscle; LIII1–10 = leg 3 muscle; LIV1–14 = leg 4 muscle; P1–13 = prosomal muscle; PP1–10t = pedipalps muscle/tendon; TI1–2 = transversal muscle 1; TII1–2 = transversal muscle 2; TIII1–2 = transversal muscle 3; TIV1–2 = transversal muscle 4; TV1–2 = transversal muscle 5; TVI1 = transversal muscle 6; V = ventral muscle.

Muscle	Origin	Insertion	Fig.
		Extremities:	
		Cheliceral muscles	
C1	propeltidium, dorsolateral above the prosternum, lateral to C4, *extrinsic muscle*	ventrolateral at the base of the chelicera, where chelicera articulates with prosoma	19B, 20A
C2	Anteroventral in chelicera, between insertion of C1 and C3, where chelicera articulates with prosoma	posterolateral in cheliceral basal article, just posterior to C7	19A, 20A
C3	propeltidium, anterodorsal and medial, splits in two strands that extend to each chelicera, *extrinsic muscle*	ventrolateral and proximal, where chelicera articulates with prosoma	19B, 20A
C4	propeltidium, dorsolateral at posterior end, *extrinsic muscle*	dorsomedial and proximal, where chelicera articulates with prosoma, adjacent to C5	19B, 20A
C5	cheliceral basal article, dorsomedial and proximal, where chelicera articulates with prosoma	ventrolateral and immediately proximal to the joint connecting cheliceral base with chela	19A, 20A
C6	lateral and proximal in cheliceral basal article, where chelicera articulates with prosoma	ventrolateral and proximal, where cheliceral base articulates with chela, opposite C5	19A, 20A
C7	ventrolateral and proximal in cheliceral basal article, where chelicera articulates with prosoma	same as C5	19A, 20A
C8	dorsal and distal in cheliceral basal article, starts as two strands which join ventral	same as C5	19A, 20A
C9	ventrolateral from cheliceral base, immediately proximal to the joint connecting cheliceral base and chela	as tendon, in the center of the dorsoventral axis, immediately distal to the joint connecting fixed digit and movable digit	19A
C10	ventrolateral and immediately proximal to the joint connecting cheliceral base and chela	same as C9	19A, 20A
C11	dorsolateral and immediately proximal to the joint connecting cheliceral base and chela	same as C9	19A
C12	dorsolateral and immediately proximal to the joint connecting cheliceral base and chela	same as C9	19A, 20A

Muscle	Origin	Insertion	Fig.
C13	dorsal, immediately proximal to the joint connecting cheliceral base and chela	same as C9	19A, 20A
	Muscles of the pedipalp		
PP1	propeltidium, posterodorsal to C3, posterolateral to C4, *extrinsic muscle*	dorsomedial and proximal on coxa	19B, 20A
PP2	medioproximal, immediately distal to where coxa articulates with prosoma	dorsomedial, immediately distal to the joint connecting coxa and article 2	19A, 20C
PP3	posteroventral, immediately distal to the joint connecting coxa and article 2, splits in two branches just prior to end	posterior, immediately distal to the joint connecting article 2 and 3	19A, 20C
		anterior, immediately distal to the joint connecting article 2 and 3	19A, 20C
PP4	dorsal, in the center of the anterior-posterior axis, and distal in article 2, splits in four branches in the center of the anterior-posterior axis in article 3	posterodorsal, immediately distal to the joint connecting article 3 and 4	19A, 20C
		anterodorsal, immediately distal to the joint connecting article 3 and 5	19A, 20C
		as tendon ventral and in the center of the anterior-posterior axis, immediately distal to the joint connecting article 3 and 4	19A, 20C
		ventral and in the center of the anterior-posterior axis, immediately distal to the joint connecting article 4 and 5	19A, 20C
PP5	dorsal, in the center of the anterior-posterior axis, and distal in article 4	ventral and in the center of the anterior-posterior axis, immediately proximal to the joint connecting article 6 and 7	19A, 20C
PP6t	as tendon ventral, immediately distal to the joint connecting article 4 and 5	ventral and in the center of the anterior-posterior axis, immediately distal to the joint connecting article 5 and 6	19A, 20C
PP7t	as tendon ventral, immediately distal to the joint connecting article 5 and 6	ventral and in the center of the anterior-posterior axis, immediately distal to the joint connecting article 6 and 7	19A, 20C
PP8t	as tendon ventral and in the center of the anterior-posterior axis, immediately distal to the joint connecting article 6 and 7	ventral and in the center of the anterior-posterior axis, immediately distal to the joint connecting article 7 and 8	19A, 20C
PP9t	as tendon ventral and in the center of the anterior-posterior axis, immediately distal to the joint connecting article 7 and 8	ventral and in the center of the anterior-posterior axis, immediately distal to the joint connecting article 8 and 9	19A, 20C
PP10t	as tendon ventral and in the center of the anterior-posterior axis, immediately distal to the joint connecting article 8 and 9	ventral and in the center of the anterior-posterior axis at tarsal claw	19A, 20C
	Leg 1		
LI1	propeltidium, dorsolateral and between C1 and PP1, *extrinsic muscle*	dorsomedial and proximal on coxa	19B, 20A
LI2	lateral on anterior transverse bridge of endosternite in segment 5, *extrinsic muscle*	in the center of the proximal-distal axis and anterior in coxa	19A, 20B
LI3	laterodistal, immediately distal to where coxa articulates with prosoma	posteroventral and proximal in article 2	19A, 20C

Muscle	Origin	Insertion	Fig.
LI4	dorsal and in the center of the anterior-posterior axis, immediately distal to the joint connecting coxa and article 2, splits in two branches in the center of the anterior-posterior axis in article 2	posterior, immediately distal to the joint connecting article 2 and 3	19A, 20C
		anterior, immediately distal to the joint connecting article 3 and 4	19A, 20C
LI5	posterior, immediately distal to the joint connecting article 3 and 4	posterior, immediately distal to the joint connecting article 4 and 5	19A, 20C
LI6	dorsal and in the center of the anterior-posterior axis, immediately distal to the joint connecting article 2 and 3	as tendon anteroventral, immediately distal to the joint connecting article 5 and 6	19A, 20C
	posterodorsal and proximal in article 3		
	anterodorsal and proximal in article 3		
LI7	posterolateral, immediately distal to the joint connecting article 4 and 5	posteroventral, immediately distal to the joint connecting article 5 and 6	19A, 20C
		as tendon ventral and in the center of the anterior-posterior axis, immediately distal to the joint connecting article 5 and 6	19A, 20C
LI8	dorsal and in the center of the anterior-posterior axis in article 5	ventral and in the center of the anterior-posterior axis, immediately proximal to the joint connecting article 6 and 7	19A, 20C
LI9t	as tendon ventral and in the center of the anterior-posterior axis, immediately proximal to the joint connecting article 5 and 6	as tendon ventral and in the center of the anterior-posterior axis, immediately distal to the joint connecting article 6 and 7	19A, 20C
LI10t	as tendon ventral and in the center of the anterior-posterior axis, immediately proximal to the joint connecting article 6 and 7	as tendon anteroventral, immediately distal to the joint connecting article 7 and 8	19A, 20C
LI11t	as tendon anteroventral, immediately distal to the joint connecting article 7 and 8	as tendon anteroventral, immediately distal to the joint connecting article 8 and 9	19A, 20C
LI12t	as tendon anteroventral, immediately distal to the joint connecting article 8 and 9	as tendon ventral and in the center of the anterior-posterior axis, immediately distal to the joint connecting article 9 and 10	19A, 20C
LI13t	as tendon ventral and in the center of the anterior-posterior axis, immediately distal to the joint connecting article 9 and 10	as tendon ventral and in the center of the anterior-posterior axis, immediately distal to the joint connecting article 10 and 11	19A, 20C
LI14t	as tendon ventral and in the center of the anterior-posterior axis, immediately distal to the joint connecting article 10 and 11	in the center of the anterior-posterior axis at tarsal claw	19A, 20C
	Leg 2		
LII1	propeltidium, dorsolateral, posterior to P6, splits in two branches medial, *extrinsic muscle*	dorsal and in the center of the anterior-posterior axis on coxa, thicker	19B, 20B
		lateral at pleural membrane between leg 2 and leg 3, thinner	19B, 20B
LII2	medial on anterior transverse bridge and central bridge of endosternite in the region of leg 2 and 3, splits in two branches medial, *extrinsic muscle*	posterior, immediately proximal to the joint connecting coxa and article 2, thinner	19A, 20B
		posterior in coxa, thicker	19A, 20B

Muscle	Origin	Insertion	Fig.
LII3	in the center of the anterior-posterior axis, immediately distal to where coxa articulates with prosoma in the center of the proximal-distal axis and anterior in coxa	dorsal and in the center of the anterior-posterior axis, immediately distal to the joint connecting coxa and article 2	19A, 20C
LII4	anterodorsal, immediately distal to the joint connecting coxa and article 2	anterodorsal and proximal in article 2	19A, 20C
LII5	ventral and in the center of the anterior-posterior axis, immediately distal to the joint connecting coxa and article 2, splits in two branches in the center of the anterior-posterior axis in article 3	posterior, immediately distal to the joint connecting article 3 and 4 posterodorsal and proximal in article 5	19A, 20C 19A, 20C
LII6	dorsal and in the center of the anterior-posterior axis, immediately distal to the joint connecting article 2 and 3	posterodorsal and proximal in article 4	19A, 20C
LII7	dorsal, in the center of the anterior-posterior axis and distal in article 3	ventral and in the center of the anterior-posterior axis, immediately proximal to the joint connecting article 5 and 6	19A, 20C
LII8	posterodorsal, immediately distal to the joint connecting article 4 and 5	ventral and in the center of the anterior-posterior axis, immediately distal to the joint connecting article 5 and 6	19A, 20C
LII9	dorsal, in the center of the anterior-posterior axis and distal in article 5	in the center of the anterior-posterior axis at tarsal claw	19A, 20C
	Leg 3		
LIII1	propeltidium, dorsomedial, above anterior bridge of endosternite in the region of leg 3, *extrinsic muscle*	posterodorsal and in center of the proximal-distal axis in coxa	19A, 20B
LIII2	at central bridge, medial at posterior bridge, and at upturned U section of endosternite in the region of leg 3 and 4, splits in two branches medial, *extrinsic muscle*	posterior, immediately proximal to the joint connecting coxa and article 2, thinner posterior in coxa, thicker	19A, 20B 19A, 20B
LIII3	in the center of the anterior-posterior axis, immediately distal to where coxa articulates with prosoma in the center of the proximal-distal axis and anterior in coxa	dorsal and in the center of the anterior-posterior axis, immediately distal to the joint connecting coxa and article 2	19A, 20C
LIII4	posterodorsal, immediately distal to the joint connecting coxa and article 2	posterodorsal and proximal in article 3	19A, 20C
LIII5	ventral and in the center of the anterior-posterior axis, immediately distal to the joint connecting coxa and article 2	ventral and in the center of the anterior-posterior axis, immediately distal to the joint connecting article 3 and 4	19A, 20C
LIII6	anterodorsal and distal in article 2	posterodorsal, immediately proximal to the joint connecting article 3 and 4	19A, 20C
LIII7	anteroventral and distal in article 2	anteroventral, immediately proximal to the joint connecting article 3 and 4	19A, 20C
LIII8	dorsal, in the center of the anterior-posterior axis, and distal in article 3	ventral and in the center of the anterior-posterior axis, immediately proximal to the joint connecting article 5 and 6	19A, 20C
LIII9	anterodorsal and distal in article 4	anterior, immediately proximal to the joint connecting article 5 and 6	19A, 20C
LIII10	dorsal, in the center of the anterior-posterior axis, and distal in article 5	in the center of the anterior-posterior axis at tarsal claw	19A, 20C

Muscle		Origin	Insertion	Fig.
		Leg 4		
LIV1		ventrolateral at posterior section of endosternite in the region of leg 4, splits in two branches just after origin, *extrinsic muscle*	lateral at pleural membrane between first articles of leg 3 and 4	19A, 20B
			posterior in coxa, adjacent to LIV3	19A, 20B
LIV2		ventrolateral and posterior to LIV1 at endosternite in the region of leg 4, *extrinsic muscle*	in the center of the anterior-posterior axis between LIV4 and LIV5, fuses with LIV4 and LIV5	19A, 20B
LIV3		ventromedial of LIV2 at endosternite in the region of leg 4, *extrinsic muscle*	posterior in coxa, adjacent to LIV1	19A, 20B
LIV4		anterodorsal, immediately distal to where coxa articulates with prosoma	dorsal and in the center of the anterior-posterior axis, immediately distal to the joint connecting coxa and article 2	19A, 20C
LIV5		ventral and in the center of the anterior-posterior axis, immediately distal to where coxa articulates with prosoma	ventral, in the center of the anterior-posterior, and proximal axis in article 2	19A, 20C
LIV6		dorsal and in the center of the anterior-posterior axis, immediately distal to the joint connecting coxa and article 2	anterodorsal, immediately proximal to the joint connecting article 2 and 3	19A, 20C
LIV7		posteroventral and distal in article 2	posterior in article 3	19A, 20C
LIV8		anteroventral and distal in article 2	anterodorsal, immediately proximal to the joint connecting article 3 and 4	19A, 20C
LIV9		posteroventral and distal in article 3 posterior and proximal in article 4	posterior, immediately proximal to the joint connecting article 4 and 5	19A, 20C
LIV10		ventral, in the center of the anterior-posterior axis, and distal in article 3	anterior, immediately proximal to the joint connecting article 4 and 5	19A, 20C
LIV11		posteroventral, immediately distal to the joint connecting article 4 and 5	posterior, immediately distal to the joint connecting article 5 and 6	19A, 20C
LIV12		dorsal, in the center of the anterior-posterior axis, and distal in article 4	dorsal and in the center of the anterior-posterior axis, immediately proximal to the joint connecting article 5 and 6	19A, 20C
LIV13		anterior, immediately distal to the joint connecting article 4 and 5	anterior, immediately distal to the joint connecting article 5 and 6	19A, 20C
LIV14		anteroventral and distal in article 5	ventral and in the center of the anterior-posterior axis at tarsal claw	19A, 20C
		Prosomal body wall:		
P1	unpaired	anteromedial in upper lip of rostrosoma	dorsomedial in upper lip of rostrosoma, just anterior to mouth opening	19B, 20A
P2	paired	anterolateral in upper lip of rostrosoma	dorsolateral in upper lip of rostrosoma, just anterior to mouth opening	19B, 20A
P3	unpaired	dorsal on pharynx	dorsomedial at intercheliceral sclerite	19B, 20A
P4	paired	lateral on pharynx	ventrolateral in rostrosoma	19B, 20A
P5	paired	propeltidium, ventrolateral and anterior, in the region of the chelicerae	propeltidium, anterolateral, in the region of the chelicerae	19B, 20B
P6	paired	propeltidium, dorsolateral, in the region of leg 1, between C1 and LII1	lateral at pleural membrane between coxa of leg 1 and 2, dorsal to E7	19B, 20A
P7	paired	propeltidium, dorsolateral, in the region of leg 2, between LII1 and P8	lateral at pleural membrane and in the center of the anterior-posterior axis in the region of leg 3	19B, 20A

Muscle		Origin	Insertion	Fig.
P8	paired	propeltidium, dorsolateral, in the region of leg 2, posterior to P7	lateral at pleural membrane and in the center of the anterior-posterior axis in the region of leg 3, anteroventral to P7	19B, 20A
P9	paired	lateral dorsal plate, dorsolateral and posterior in the region of leg 3, between both branches of P11	lateral dorsal plate, dorsal in the region of leg 2	19B, 20A
P10	paired	propeltidium, dorsolateral and posterior in the region of leg 2, outside of P11	anterolateral at pleural membrane in the region of leg 4	19B, 20A
P11	paired	FEMALE: propeltidium, dorsomedial in the region of leg 1, splits in two branches posterior	metapeltidium, dorsal and in the center of the anterior-posterior axis in the region of leg 3, thicker	19C, 20A
			posterolateral at pleural membrane in the region of leg 3, posterodorsal to LIII1, thinner	19C, 20A
	paired	MALE: propeltidium, dorsomedial in the region of leg 2, splits in two branches medial	metapeltidium, dorsal and in the center of the anterior-posterior axis in the region of leg 3, thicker	19B, 20B
			posterolateral at pleural membrane in the region of leg 3, posterodorsal to LIII1, thinner	19B, 20B
P12	unpaired	FEMALE: metapeltidium, medial and in the center of the anterior-posterior axis in the region of leg 3	metapeltidium, medial and in the center of the anterior-posterior axis in the region of leg 4	19C, 20A
	paired	MALE: metapeltidium, dorsomedial and in the center of the anterior-posterior axis in the region of leg 3	dorsolateral at tergite and in the center of the anterior-posterior axis in segment 8	19B, 20B
P13	paired	metapeltidium, posterolateral in the region of leg 3	metapeltidium, lateral and in the center of the anterior-posterior axis in the region of leg 4	19B, 20A
		Endosternite:		
E1	paired	ventral at branch of endosternite in the region of pedipalp and leg 1, splits in two branches just after origin	ventromedial at intersegmental membrane and in the center of the anterior-posterior axis in the region of the pedipalp, lateral to ventral plate	21
			prosternum, ventromedial and in the center of the anterior-posterior axis in the region of leg 1, posterior to first branch	21
E2	paired	anterior at branch of endosternite in the region of pedipalp and leg 1	ventrolateral at pleural membrane adjacent to coxa of pedipalp	21
E3	paired	anterodorsal at branch of endosternite in the region of leg 1, just posterior to E1, splits into three branches just after origin	propeltidium, dorsolateral in the region of leg 1	21
			propeltidium, dorsolateral in the region of leg 1, posterior to first branch	21
			propeltidium, dorsolateral in the region of leg 1, posterior to second branch	21
E4	paired	anterodorsal at branch of endosternite in the region of leg 1, just posterior to E3	propeltidium, dorsolateral and posterior in the region of leg 2	21
E5	paired	anterodorsal at branch of endosternite in the region of leg 1, just posterior to E4	propeltidium, dorsolateral and anterior in the region of leg 2	21
E6	paired	anterodorsal at branch of endosternite in the region of leg 1, just posterior to E5	anterodorsal at pleural membrane, where chelicera articulates with prosoma	21

Muscle		Origin	Insertion	Fig.
E7	paired	ventral at branch of endosternite in the region of leg 2	ventrolateral at pleural membrane between coxa of leg 1 and 2, ventral to P6	21
E8	unpaired	ventromedial at bridge of endosternite in the region of leg 2	posteroventral and medial on pharynx	21
E9	paired	ventromedial at bridge of endosternite in the region of leg 2, posterior to E8	ventrolateral at pleural membrane, just posterior where leg 1 articulates with prosoma	21
E10	paired	dorsolateral and in the center of the anterior-posterior axis on anterior bridge of endosternite in the region of leg 2	posterolateral at pleural membrane in the region of leg 2	21
E11	paired	dorsolateral and posterior on anterior bridge of endosternite in the region of leg 3	propeltidium, dorsolateral and posterior in the region of leg 3	21
E12	paired	dorsolateral and posterior on anterior bridge of endosternite in the region of leg 3, outside of E11	metapeltidium, dorsolateral in the region of leg 4, adjacent to E14 and E16	21
E13	paired	lateral at branch of endosternite in the region of leg 3, posterior to E12	ventral at tergite, at the border of segments 8 and 9, immediately anterior to origin of V	21
E14	paired	dorsolateral and in the center of the anterior-posterior axis on posterior bridge of endosternite in the region of leg 3	propeltidium, dorsolateral and posterior in the region of leg 3, just anteromedial of E11	21
E15	paired	dorsolateral and posterior on posterior bridge of endosternite in the region of leg 3, posterior to E13	metapeltidium, dorsolateral, in the region of leg 4, adjacent to E12 and E16	21
E16	paired	posterolateral on upturned U section of endosternite in the region of leg 4	anterolateral at pleural membrane in the region of leg 4	21
E17	paired	dorsolateral at posterior section of endosternite in the region of leg 4, two branches merge just after origin	metapeltidium, dorsolateral, in the region of leg 4, adjacent to E12 and E14	21
E19E18	paired	lateral at posterior section of endosternite in the region of leg 4, ventral to E16	Lateral at pleural membrane, where leg 4 articulates with prosoma	21
E20E19	paired	ventrolateral and posterior at posterior section of endosternite in the region of leg 4	anterolateral at pleural membrane, where leg 4 articulates with prosoma, between E15 and E17	21
E20	paired	posterolateral at posterior section of endosternite in the region of leg 4, just posterior to E19	lateral at pleural membrane and in the center of the anterior-posterior axis in segment 8	21
		Opisthosoma:		
D1	paired	metapeltidium, dorsolateral and anterior in the region of leg 4	dorsal at tergite of segment 9, just medial of D2	19C, 20B
D2	paired	dorsal at the anterior end of the tergite of segment 9	dorsal at tergite of segment 17, immediately posterior to the border of segments 16 and 17	19C, 20B
DV1	paired	FEMALE: anterodorsal at tergite of segment 9, lateral to D1	anteroventral at sternite of segment 9, just medial of V	19A, 20A
		MALE: anterodorsal at tergite of segment 9, outside of D1 MALE: posterodorsal to the segmental overhang of segment 9	anteroventral at sternite of segment 9, just medial of V	19B, 20B

Muscle		Origin	Insertion	Fig.
DV2	paired	FEMALE: anterodorsal at tergite of segment 10, between D2 and JII1	anteroventral at sternite of segment 10, just posterior to genital lobe and medial of V	19A, 20A
		MALE: anterodorsal at tergite of segment 10, between D2 and JII1, splits in two branches ventral	dorsolateral at genital atrium	19B, 20B
			anteroventral at sternite of segment 10, just posterior to genital lobe 3 and medial of V	19B, 20B
DV3–4	paired	anterodorsal at tergite of segments 11 and 12, between D2 and JIII1 and JIV1, respectively	anteroventral at sternite of segments 11 and 12, just medial of V	19A, B, 20B
DV5	paired	anterodorsal at tergite of segment 13, between D2 and JV1, splits in two branches at half point	anteroventral at sternite of segment 13, just medial of V, thicker	19A, B, 20B
			ventral and in the center of the anterior-posterior axis at sternite of segment 13, just medial of V, thinner	19A, B, 20B
JI1–4	paired	anterior at tergite of segment 9, outside of D1, strands 1–4 evenly distributed from dorsal to ventrolateral	in the center of the anterior-posterior axis at tergite of segment 9, outside of D2, strands 1–4 evenly distributed from dorsal to ventrolateral	19C, 20A,B
JII1–6	paired	in the center of the anterior-posterior axis at tergite of segment 9, posterior to JI and outside of D2, strands 1–6 evenly distributed from dorsal to ventrolateral	anterior at tergite of segment 10, outside of D2, strands 1–6 evenly distributed from dorsal to ventrolateral	19C, 20A,B
JIII1–6	paired	posterior at tergite of segment 10, posterior to JII and outside of D2, strands 1–6 evenly distributed from dorsal to ventrolateral	anterior at tergite of segment 11, outside of D2, strands 1–6 evenly distributed from dorsal to ventrolateral	19C, 20A,B
JIV1–6	paired	posterior at tergite of segment 11, posterior to JIII and outside of D2, strands 1–6 evenly distributed from dorsal to ventrolateral	anterior at tergite of segment 12, outside of D2, strands 1–6 evenly distributed from dorsal to ventrolateral	19C, 20A,B
JV1–6	paired	posterior at tergite of segment 12, posterior to JIV and outside of D2, strands 1–6 evenly distributed from dorsal to ventrolateral	anterior at tergite of segment 13, outside of D2, strands 1–6 evenly distributed from dorsal to ventrolateral	19C, 20B20A,B
JVI1–5	paired	posterior at tergite of segment 13, posterior to JV and outside of D2, strands 1–5 evenly distributed from dorsal to ventrolateral	anterior at tergite of segment 14, outside of D2, strands 1–5 evenly distributed from dorsal to ventrolateral	19C, 20A,B
JVII1–4	paired	posterior at tergite of segment 14, posterior to JVI and outside of D2, strands 1–4 evenly distributed from lateral to ventrolateral	in the center of the anterior-posterior axis at sclerite of segment 15, outside of D2, strands 1–4 evenly distributed from lateral to ventrolateral	19C, 20A,B
JVIII1–3	paired	posterior at sclerite of segment 15, posterior to JVII and outside of D2, strands 1–3 evenly distributed from lateral to ventrolateral	posterior at sclerite of segment 16, outside of D2, strands 1–3 evenly distributed from lateral to ventrolateral	19C, 20B20A,B
JIX1–2	paired	posterolateral at sclerite of segment 16, posterior to JVIII, strands 1–2 evenly distributed lateral	posterolateral at sclerite of segment 17, strands 1–2 evenly distributed lateral	19C, 20A,B
TI1	paired	FEMALE: ventrolateral and in the center of the anterior-posterior axis at pleural membrane of segment 9	ventrolateral and anterior at accessory gland posterior in segment 9	19A, 20A

Muscle		Origin	Insertion	Fig.
TI2	paired	ventrolateral and in the center of the anterior-posterior axis at pleural membrane of segment 9, in females ventral to TI1	ventromedial and in the center of the anterior-posterior axis at sternite of segment 9	19A,B 20A,B
TII1	paired	ventrolateral and in the center of the anterior-posterior axis at pleural membrane of segment 10	ventromedial and in the center of the anterior-posterior axis at sternite of segment 10	19A, 20A,B
TII2	paired	ventrolateral and in the center of the anterior-posterior axis at pleural membrane of segment 10, ventral and inward of TII1	ventromedial and in the center of the anterior-posterior axis at sternite of segment 10, ventral to TIII1	19A,B20A B
TIII1–TV1	paired	ventrolateral at tergite of segments 11–13, TIII1 posterior, TIV1 in the center of the anterior-posterior axis, TV1 anterior in the respective segment	ventromedial at sternite of segments 11–13, TIII1 posterior, TIV1 in the center of the anterior-posterior axis, TV1 anterior in the respective segment	19A,B 20A
TIII2–TV2	paired	FEMALE: ventrolateral at pleural membrane of segments 11–13, ventral to TIII1–TV1, TIII2 posterior, TIV2 in the center of the anterior-posterior axis, TV2 anterior in the respective segment	ventromedial at sternite of segments 11–13, ventral to TIII1–TV1, TIII2 posterior, TIV2 in the center of the anterior-posterior axis, TV2 anterior in the respective segment	19A, 20A
		MALE: ventrolateral at pleural membrane of segments 11–13, ventral and inward of TIII1–TV1, TIII2 posterior, TIV2 in the center of the anterior-posterior axis, TV2 anterior in the respective segment	ventromedial at sternite of segments 11–13, ventral and outward of TIII1–TV1, TIII2 posterior, TIV2 in the center of the anterior-posterior axis, TV2 anterior in the respective segment	19B, 20B
TVI	paired	ventrolateral, posterior and outward at tergite of segment 14	ventrolateral and posterior at pleural membrane of segment 14, outside of V	19A,B 20B
Gf	paired	dorsomedial in the genital operculum in segment 9, splits in two branches just after origin	anteroventral to its origin in the genital operculum in segment 9	19A, 20A
			posteroventral to its origin in the genital operculum in segment 9	19A, 20A
Gm1	paired	ventromedial at the genital atrium in segment 9	anteroventral and medial in genital lobe 1 in segment 9	19B, 20B
Gm2	paired	ventromedial at the genital atrium in segment 9, just posteromedial of Gm1	ventromedial in genital lobe 2, just outside of Gm1 in segment 9	19B, 20B
Gm3	paired	ventromedial at the genital atrium in segment 9, just posteromedial of Gm2	ventromedial in genital lobe 2, just posterior and outside of Gm2 in segment 9	19B, 20B
Gm4	paired	posteroventral and medial at genital atrium in segment 9	anteroventral at sternite of segment 10, just posterior to genital lobe 3 and medial of V	19B, 20B
V	paired	ventral at tergite, at the border of segments 8 and 9, immediately posterior to the insertion of E13, gives off two side strands anterior in segments 9 and 11	ventral at sclerite at the border of segments 17 and 19	19A, B 20A, B
			ventrolateral at pleural membrane posterior in segment 9	19A, B 20A, B
			ventrolateral at pleural membrane just anterior to the border of segments 9 and 10	19A, B 20A, B
F1–3	paired	lateral at sclerite at the anterior end of segment 19, strands 1–3 distributed from dorsal to ventrolateral	lateral at membranous fold and immediately distal to the joint connecting segment 19 and flagellar base, strands 1–3 distributed from dorsal to ventrolateral	19C, 20B

Table 6. Changes applied to the character states in the character matrix of Shultz's (2007a) phylogeny based on morphological characters and additional character coding changes applied to the original data matrix of Shultz (2007a). Character 61 was deleted, and characters 12a, 128a, 135a, 143a, 148a, 178a, 179a and 203 are introduced. Characters with their original/new description and original/new coding are marked grey, taxa with their corresponding coding are white.

Taxa	Character	Description by Shultz (2007a)	New description	Original coding	New coding
	3	Anterior end of dorsal prosoma with median marginal or submarginal pointed process	–	0 = absent, 1 = present	–
Eukoenenia *Prokoenenia* *E. spelaea*				0 = absent	1 = present
	6	carapace with distinct pro-, meso- or metapeltidial sclerites	–	0 = absent, 1 = present	0 = absent, 1 = two peltidia, 2 = three peltidia
Eukoenenia *Prokoenenia* *E. spelaea*				1 = present	1 = two peltidia
Schizomida				1 = present	2 = three peltidia
Solifugae				1 = present	2 = three peltidia
	12a	–	prosternum consisting of the fused sclerites of segments 2–4	–	0 = absent, 1 = present
E. spelaea				n/a	1 = present
Eukoenenia *Prokoenenia*				n/a	? = unknown
	32	rostrosoma: long, narrow, subcylindrical epistome projecting anteriorly with base fixed to dorsal surface of palpal coxae, bordered laterally by lobes projecting from palpal coxae; ventral wall of preoral chamber formed by anterior element of prosoma (sternapophysis)	rostrosoma: long, narrow, subcylindrical epistome projecting anteriorly, bordered laterally by lobes	0 = absent, 1 = present	0 = absent, 1 = fixed to pedipalpal coxae, 2 = no association with pedipalp
Eukoenenia *Prokoenenia* *E. spelaea*				0 = absent	2 = no association with pedipalp
	44	apotele (claw), position	–	0 = terminal, 1 = subterminal, – = inapplicable, coded only for taxa with a distinct apotele	–

Taxa	Character	Description by Shultz (2007a)	New description	Original coding	New coding
Palaeo-charinus				? = unknown	0 = terminal
	46	appendage III (= arachnid leg 1) extremely elongate, antenniform	–	0 = absent, 1 = present	–
Eukoenenia Prokoenenia E. spelaea				? = unknown	1 = present
	61	trochanter-femur joint with dorsal hinge or pivot operated by flexor muscles only	deleted, because it was a supposed autapomorphy for Palpigradi		
	62	superior trochanter–femur muscle (or homologue) originating broadly in femur, inserting on distal margin of trochanter	–	0 = absent, 1 = present	–
Mastigo-proctus				0 = absent	1 = present
	68	patella of appendage of postoral somite III (= arachnid leg 1) proportionally much longer than those of more posterior appendages	–	0 = absent, 1 = present	–
E. spelaea				0 = absent	? = unknown
	69	femur-patella joint	–	0 = monocondylar, several axes of movement and multifunctional muscles, 1 = bicondylar hinge, one axis of movement and antagonistic muscles, 2 = hinge, one axis of movement, flexor muscles without muscular antagonists	–
E. spelaea				2 = hinge, one axis of movement, flexor muscles without muscular antagonists	0 = monocondylar, several axes of movement and multifunctional muscles

Taxa	Character	Description by Shultz (2007a)	New description	Original coding	New coding
Mastigoproctus				2 = hinge, one axis of movement, flexor muscles without muscular antagonists	1 = bicondylar hinge, one axis of movement and antagonistic muscles
	72	patella-tibia joint	–	0 = absent, 1 = present	–
E. spelaea				0 = monocondylar with or without CZY (73)	2 = hinge, one axis of movement, muscles without muscular antagonists
	73, 74	dependent on character 72	–	0 = absent, 1 = present	–
E. spelaea				0 = absent	– = inapplicable
	76	anterior femur–tibia or femoropatella–tibia (transpatellar) muscle	–	0 = absent, 1 = present	–
E. spelaea				? = unknown	1 = present
	83	circumtarsal ring	–	0 = absent, 1 = present	–
E. spelaea				0 = absent	? = unknown
	106	megoperculum	–	0 = absent, 1 = present	–
E. spelaea				1 = present	0 = absent
	116	number of metasomal somites	–	0 = zero, 1 = two, 2 = three, 3 = five, 4 = nine	0 = zero, 1 = two, 2 = three, 3 = four, 4 = five, 5 = nine
Eukoenenia *Prokoenenia* *E. spelaea*				2 = three	3 = four
	128	anterior oblique muscles of BTAMS posterior to postoral somite VI	–	0 = absent, 1 = present	–
E. spelaea				? = unknown	0 = absent
	128a	–	anterior oblique muscles of BTAMS anterior to postoral somite VI (state 1 only in E. spelaea)	–	0 = absent, 1 = present
E. spelaea				n/a	1 = present

Taxa	Character	Description by Shultz (2007a)	New description	Original coding	New coding
Eukoenenia Prokoenenia				n/a	? = unknown
	130	endosternite fenestrate	–	0 = absent, 1 = present	–
E. spelaea				0 = absent	1 = present
	131	suboral suspensor: a tendon that arises from the BTAMS and inserts on the ventral surface of the oral cavity via muscle	suboral suspensor: a tendon that arises from the BTAMS and inserts on the ventral surface of the foregut via muscle	0 = absent, 1 = present	0 = absent, 1 = ventral on oral cavity, 2 = ventral and posterior on pharynx
E. spelaea				1 = present (ventral on oral cavity)	2 = ventral and posterior on pharynx
	132	perineural vascular membrane in adult	–	0 = absent, 1 = present	–
E. spelaea				1 = present	0 = absent
	135a	–	arcuate body in protocerebrum	–	0 = absent, 1 = present
Acari				n/a	0 = absent
E. spelaea				n/a	0 = absent
Eukoenenia Prokoenenia				n/a	? = unknown
	143a	–	trichobothria with dendrites reaching into the hair shaft	–	0 = absent, 1 = present
E. spelaea				n/a	1 = present
Eukoenenia Prokoenenia				n/a	? = unknown
	148	intercheliceral median organ	supracheliceral median organ	0 = absent, 1 = present	–
	148a	–	lateral organ	–	0 = absent, 1 = present
Eukoenenia Prokoenenia E. spelaea				n/a	1 = present
	162	nucleus (of sperm) with manchette of microtubules	–	0 = absent, 1 = present	–
E. spelaea				0 = absent	? = unknown
	163	axoneme (of sperm)	–	0 = absent, 1 = present	–
E. spelaea				0 = absent	? = unknown
	164	coiled axoneme (of sperm)	–	0 = absent, 1 = present	–
E. spelaea				– = inapplicable	? = unknown
	165	microtubule arrangement in axoneme (of sperm)	–	0 = absent, 1 = present	–

Taxa	Character	Description by Shultz (2007a)	New description	Original coding	New coding
E. spelaea				– = inapplicable	? = unknown
	166	helical or corkscrew shaped nucleus (of sperm)	–	0 = absent, 1 = present	–
E. spelaea				0 = absent	? = unknown
	167	Vacuolated-type sperm	–	0 = absent, 1 = present	–
E. spelaea				0 = absent	1 = present
	178a	–	coxal organ with tubule differentiated into proximal and distal section	–	0 = absent, 1 = present
Acari				n/a	1 = present
E. spelaea				n/a	1 = present
Eukoenenia Prokoenenia				n/a	? = unknown
	179a	–	ventral plate	–	0 = absent, 1 = present
E. spelaea				n/a	1 = present
Eukoenenia Prokoenenia				n/a	? = unknown
	194	dorsal dilator muscle of precerebral pharynx attaching to dorsal surface of prosoma or intercheliceral sclerite	–	0 = absent, 1 = present	0 = absent, 1 = dorsal on prosoma, 2 = dorsal on intercheliceral sclerite
E. spelaea				1 = present (dorsal on prosoma)	2 = dorsal on intercheliceral sclerite
	198	dilator muscle of precerebral pharynx and/or preoral cavity attaching to ventral surface of prosoma	dilator muscle of precerebral pharynx and/or preoral cavity attaching to prosoma or rostrosoma	0 = absent, 1 = present	0 = absent, 1 = ventral on prosoma, 2 = ventrolateral on rostrosoma
E. spelaea				1 = present (ventral on prosoma)	2 = ventrolateral on rostrosoma
	199	postcerebral pharynx	–	0 = absent, 1 = present	–
Prokoenenia				1 = present	0 = absent
	203	–	hindgut with cuticular lining	–	0 = absent, 1 = present
E. spelaea				n/a	0 = absent
Eukoenenia Prokoenenia				n/a	? = unknown

Appendix II.

Table A1. Character matrix based on the analysis of Shultz (2007a). Updated character codes are marked red, added character codes are marked blue

Taxon	Character coding			
Acari	0000???000	00001100?20	0?0?–00001	10000–0?00
Trombidiformes	000––00000	000?000001	0111–0020	02––011011
Trombidiidae	000––00011	0010?000–0	000000–001	10––000––1
Allothrombium	000004?????	????000–013	011001000000	1001001000
	000––00000	?0100110 1101	0011100000	0–0000000–
	––1			
Acari	00000?1000	00001100?20	0?00–00001	10100–0?00
Trombidiformes	000––00000	000?000001	0001?0020	02––0??011
Alcydidae	000––00011	00101000–0	000000–001	10––000––1
Alycus	000000?????	????000–013	?1100 1000000	1?0100????
	0???????0?	????0 11?1?01	0010100000	0–0????00–
	––1			
Acari	00001?1000	04001100?20	0?00–00001	10100–0?00
Oribatida	000––00000	000?000001	0000000020	02––011011
Trhypochthoniidae	000––00011	0010?000–0	000000–001	10––000––1
Archegozetes	000000?????	????000–00–	–1100 1000000	100 11000
	000––00000	00100 1101001	0010100000	0–0000000–
	–01			
Acari	0000??0000	00001100?20	0?0?–00001	10000–0?00
Trombidiformes	000––00000	000?000001	0111–0020	02––011011
Caeculidae	000––00011	0010?000–0	000000–001	10––000––1
Microcaeculus	000004?????	????00 12013	011001000000	1001001??0
	0?0––00?00	?01001?01101	001?100000	0–0000000–
	––1			
Acari	00001?1000	04001100?20	0?00–00001	10100–0?00
Sarcoptiformes	000––00000	000?000001	0111–0020	02––011011
Palaeacaridae	000––00011	0010?000–0	000000–001	10––000––1
Palaeacarus	000000?????	????00 1?0??	?1100 1000000	1?01011000
	0?0––?0?0?	?0100 1101001	0010100000	0–0??0000–
	––1			
Araneae	00000–0000	00011000110	0000001000	–0000–0000
Mygalomorphae	0110000000	0000000110	0000010022	0010011011
Theraphosidae	0100–00001	00115010–0	0000011010	1110000––1
Aphonopelma	1100001 0?00	00031111012	011000000011	1001000000
	0111310000	1000000 10001	1001101000	1011100111
	101			
Araneae	00000–0000	00011000110	0000001000	–0000–0000
Araneomorphae	0110000000	0000000110	000010022	0010011011
Hypochilidae	0100–00001	00115010–0	0000011010	1110000––1
Hypochilus	1100001 0?00	00030111012	011000000011	1001000000
	0111310000	1000000 10001	?001101000	1110100111
	101			

Taxon	Character coding			
Araneae	00000–0000	0001100011 0	0000001000	–0000–0000
Mesothelae	0110000000	0000000110	0000100 22	0010011011
Liphistiidae	0100–00001	0011501 0–0	0000010010	1101000––1
Liphistius	1100001 0?00	0003011101 2	0110000000011	1001000000
	0111310000	1000000100 01	1001101000	1110100111
	101			
Amblypygi	00100–0000	0001100011 0	0000100000	–000100?01
Charinidae	0010010000	000?001011	0000100 23	1000101011
Charinus	0101100000	0110500 0–0	0000010000	10––020––1
	1100001 0?00	1015011001 2	0110000000??	1011001100
	0111310000	1110000100 01	1001100000	1110001011
	101			
Amblypygi	00100–0000	0001100011 0	0000100000	–000100101
Phrynidae	0000–10000	0001001011	0000100 23	1000101011
Phrynus	0101100000	0010500 0–0	0000010000	00––020––1
	1100001 0?00	1015011001 2	0110000000??	1011001100
	0111310000	1110000100 01	00–1100000	1110001011
	101			
Merostomata	00000–0?11	0?0???? 1???	????–?????	?????–????
† Chasmataspidida	??????????	?1?????????	?????????	??????????
† Chasmataspididae	????????0?	1???6?01–0	0?????–???	??–?1410–0
† *Chasmataspis*	??00?–?????	??????1??1?	??????0?????	????0?????
	??????????	?????????? ??	??????????	??????????
	???			
Merostomata	000?0–0?1?	0?0???? 1???	????–?????	?????–????
† Chasmataspidida	????????1?	??????????	?????????	??????????
† Diploaspididae	??????0001	0???6?01–0	0?????–???	??–?0410–0
† *Diploaspis*	??00?–?????	??????1??1?	?????????? ??	????0?????
	??????????	?????????? ??	??????????	??????????
	???			
Merostomata	00?10–0?1?	0?0???? 1???	????–?????	?????–????
† Chasmataspidida	????????1?	??????????	?????????	??????????
† Diploaspididae	??????0?0?	????6?01–0	0?????–???	??–?0410–0
† *Octoberaspis**	??00?–?????	??????1??1?	?????????? ??	????0?????
	1??????????	?????????? ??	??????????	??????????
	???			
† *Eurypterida*	00000–0?11	0001??00000	0???–????0	–0000–???0
† *Eurypteridae*	0010000010	011?000?0?	?011–0020	00000??????
† *Eurypterus**	?100–00001	00??5000–0	0????0–0?0	?0–?0310–0
	???01–?????	??????1?010	????––000?00	????0?????
	1??????????	?????????? ??	1???0??0??	0–????????
	???			

Taxon	Character coding			
	00000–0?11	0000??00000	????–?????	–0?00–???0
† *Eurypterida*	0010000000?	01??000?0?	?011–00?0	0??00??????
† *Stylomuridae*	?1?0–?0001	00??5000–0	0????0–0??	?0–?0310–0
*Stylomurus**	???01–?????	??????1?010	???????000???	????0?????
	1?????????	???????????	??????????	??????????
	???			
	00110–0?00	000??????????	????–????0	–???0–????
Arachnida	0??????000	000??0????	?000??0??	0?????????
† *Haptopoda*	?1?10?00??	0???A?00–0	0???01?0?0	?0––00?001
† *Plesiosiro**	????????????	??????1????	???????00???	????0?????
	0?????????	???????????	??????????	??????????
	???			
Acari	00001–0000	0001100002 0	0000–00001	10100–0?00
	0010010000	000?000?01	0011?1120	02––0??0??
Parasitiformes	0101000011	011?4000–0	000000–000	00––000––1
Opilioacarida	000005?????	????010–013	0100––000010	100111???0
Neocarus	000––01000	????0111000 1	00–0100000	0–0000000–
	––1			
Acari	00001–0000	0001100002 0	0000–00001	1?100–0?00
	0010010000	000?000?0?	?011?112?	02––0??0??
Parasitiformes	?1010?0011	01??4000–0	000000–000	00––000––1
Opilioacarida	000005?????	????010–012	?1100000010	1?0111???0
Siamacarus	0?0––?1?0?	????01?10001	??–0100000	0–0???????
	––1			
Arachnida	0000100100	00000–00000	10?0–00000	–0000–?000
Opiliones	0010000001	1000000001	000000010	01––012011
Caddidae	0101010001	00112000–0	000000–000	00––0013–1
Caddo	000001?0?00	010101??00–	–100––000000	10–1110001
	0????00000	?0??0000000 0	10–0100110	10?001000–
	––1			
Arachnida	0000100100	01000–00000	1010–00000	–0000–1000
Opiliones	0010000001	1000000001	000000020	01––010–11
Pettalidae	0100–00001	00112000–0	000000–000	00––0013–1
Chileogovea	000001?0?00	010101??0??	?100––000000	1001110001
	0????00?0?	?0??0000000 0	10–?100110	0–0001000–
	––1			
Arachnida	0000100100	01000–00000	10?0–00000	–0000–1000
Opiliones	0010000001	1000000001	000000020	01––010–11
Sironidae	0100–00001	00112000–0	000000–000	00––0013–1
Cyphophthamus	000001?0?00	010101??0??	?100––000000	1001110001
	0011000107	?0??0000000 0	10–?100110	0–0001000–
	––1			

Taxon	Character coding			
Arachnida	0000000100	00000–00000	1010–00000	–0001–?000
	0010000001	1000000001	0000000010	01––012011
Opiliones	0101010001	0011200–0	000000–000	00––0013–1
Gonyleptidae	000001?0?00	0100011C00–	–100––000000	1001110001
	010––00000	10000000000?	10–0100110	10?001000–
Gonyleptes	––1			
Arachnida	0000100100	00000–00000	1010–00000	–0000–0000
	0010000001	1000000001	0000000010	01––012011
Opiliones	0101010001	0011200–0	000000–000	00––0013–1
Sclerosomatidae	000001?0?00	010B011C00–	–100––000000	1001110001
	000––00000	10000000000	10–0100110	101001000–
Leiobunum	––1			
Arachnida	0000000100	00000–00000	10?0–00000	–0001–?000
	0010000001	1000000001	0000000010	01––012011
Opiliones	0101010001	0011200–0	000000–000	00––0013–1
Sclerobuninae	000001?0?00	0100011C00–	–100––000000	1001110001
	0?0––00000	10000000000	10–0100110	10?001000–
Sclerobunus	––1			
Arachnida	0010110000	00010–00000	0000000000	–2000–0000
	0010010000	0000000001	000000?00	02––011011
Palpigradi	01?1000001	00104000–0	000000–010	00––031201
Eukoeneniidae	000000101 01	2003100–00–	–011000011 00	100100???0
	0??????10??	????????01011	0001100000	1012000 20–
Eukoenenia spelaea	––0			
Arachnida	0010110000	00010–00000	0000000000	–2000–0000
	0010010000	0000000001	000000020	00000?1011
Palpigradi	0101000001	00104000–0	000001–010	00––031201
Eukoeneniidae	000000 1??00	1103100–00–	–01?000011 00	100100???0
	000––000??	????????0?0?1	0001100000	101100010–
Eukoenenia	––?			
Arachnida	0010110000	00010–00000	0000?00000	–2000–??00
	0010010000	0000000?01	000000020	00000110??
Palpigradi	0101000001	001?4000–0	000001–010	10–?031201
Prokoeneniidae	0000001??0?	?1031 00–00–	–01?000011 00	100100???0
	000––000??	????????0?0?1	0001100000	101100010 1
Prokoenenia	00?			
Acari	01000–0100	00011000020	0000–00001	10100–0?00
	0011000000	000?000?0?	?000?1020	02––0??0??
Parasitiformes	0?10–00011	01???000–0	000000–100	11––000––1
	000003?????	????000–00–	–100––000010	1?0110????0
Allothyridae	0?0––?1?0?	????0??11001	00–1100000	0–0????????
Allothyrus	––1			

Taxon	Character coding			
Acari	00000–0000	00000–00020	0000–00001	10000–0?00
Parasitiformes	000––00000	000?000001	0000010?0	02––011011
Ixodidae	0?10–00011	01100000–0	000000–000	00––000––1
Amblyomma	000003???00	?1??000–014	0100––000010	1?01100000
	0?0––?1?0?	00000101?001	00–1100000	0–0??0000–
	––1			
Acari	00000–0000	00000–00020	0000–00001	10000–0?00
Parasitiformes	000––00000	000?000001	0000010?0	02––011011
Argasidae	0?10–00011	00100000–0	000000–000	00––000––1
Argas	000003???00	?1??000–014	0100––000010	1?01100000
	0?0––?1?0?	00000101?001	00–1100000	0–0??0000–
	––1			
Acari	01000–0100	00001000020	0000–00001	10100–0?00
Parasitiformes	0011000000	000?000?0?	?000?1020	02––0??0??
Allothyridae	0?10–00011	01???000–0	000000–100	00––000––1
Australothyrus	000003?????	????000–014	?100––000010	100110???0
	000––01000	????0??11001	00–1100000	0–000??????
	––1			
Acari	01000–0000	00011000020	00?0–00001	10100–0?00
Parasitiformes	0011000000	000?000001	0000010?0	02––011011
Macrochelidae	0?10–00011	0110?000–0	000000–000	00––000––1
Glyptholaspis	000003???00	????000–00–	–100––000000	1001100000
	000––01000	?000010?1001	00–1100000	0–0000000–
	––1			
Arachnida	0000100000	03010–00121	0000–10100	–1000–0010
Pseudoscorpiones	100––00100	0000000001	0000100?0	01––012100
Cheliferidae	000––00001	01115000–0	000000–000	00––000––1
Chelifer	00000210?00	01?7010–014	011000000000	1001001000
	0011200011	110000000000	10–1100000	0–0000000–
	––1			
Arachnida	0000100000	03010–00120	0000–10100	–1000–0000
Pseudoscorpiones	100––00100	0000000001	0000100?0	01––012100
Chtoniidae	0E00–00001	01115000–0	000000–000	00––000––1
Chthonius	00000210?00	01?7010–013	011000000000	1001001000
	0011200011	110000000000	10–1100000	0–0000000–
	––1			
Arachnida	0000100000	03010–00120	0000–10100	–1000–0000
Pseudoscorpiones	100––00100	0000000001	0000100?0	01––012100
Feaelliidae	000––00001	01115000–0	000000–000	00––000––1
Feaella	00000210?00	01?7010–013	011000000000	1001001000
	0011200011	110000000000	10–1100000	0–0000000–
	––1			

Taxon	Character coding			
Arachnida	0000100000	03010–00121	0000–10100	–1000–0010
Pseudoscorpiones	100––00100	0000000001	000010010	01––012100
Neobisiidae	0100–00001	01115000–0	000000–000	00––000––1
Neobisium	0000021??00	01?7010–013	01100000000	1001001000
	0011200011	11000000000	10–1100000	0–0000000–
	––1			
Arachnida	00000–0000	1201110001 00	0??0–00001	?0000–0?00
Ricinulei	0010001000	000?000001	0011000 20	02––000–11
Ricinoididae	0101000001	00105120–0	100000–000	00––120––1
Cryptocellus	000003?????	?1?5010–014	?100–0000011	1001000??0
	01112000?0	?0??0101000 1	00–1100000	0–0000000–
	––1			
Arachnida	00000–0?00	1?0????0???	????–????1	????0–????
Ricinulei	0????0?000	000??0????	?011??0??	??????????
† *Poliocheridae*	????????0??	0???51?0–0	1????00–???	??––120––1
† *Poliochera*	??0?????????	???5??0–?13	??????00????	??????????
	0??????????	???????????	??????????	??????????
	???			
Arachnida	00000–0000	1201110001 00	0??0–00001	?0000–0?00
Ricinulei	0010001000	000?000001	0011000 20	02––000–11
Ricinoididae	0101000001	00105120–0	100000–000	00––120––1
Ricinoides	000003?????	?1?5010–014	?100–0000011	1001000??0
	01112000?0	?0??0101000 1	00–1100000	0–0000000–
	––1			
Arachnida	00000–0?00	1?0?????0???	????–?????	????0–????
Ricinulei	0????0?000	000??0????	?011??0??	??????????
† Palaeoricinulei	???????0??	0???51?0–0	1????00–???	??––120––1
† *Terpsicroton**	??0?????????	???5??0–?13	??????00????	??????????
	0??????????	???????????	??????????	??????????
	???			
Arachnidae	00101 20000	02011000110	0000?00001	000011??00
Schizomida	0010010000	000?00??11	0000?0123	00000??????
Protoschizomidae	0101100000	001?5000–0	0100010000	00––021211
Protoschizomus	10000010?0?	?0?5?10–00–	–1101000000 00	11?1001110
	0111310000	11?0000100 01	00–1100000	1??00010?0
	001			
Arachnidae	00101 20000	02011000110	0000?00001	0000110100
Schizomida	0010010000	0000001?11	0000101 23	0000001011
Hubbardiidae	0101100000	00115000–0	0100010000	00––021211
Stenochrus	10000010?01	?0141 10–014	?1101000000 0	1111001110
	0111310000	11?0000100 01	00–1100000	1110001 0?0
	001			

Taxon	Character coding			
Arachnida	0000100000	01000–10000	0111–00000	–0000–1000
	100––00001	1000000001	000010010	01––012110
Scorpiones	0100–10001	00116000–0	001000–000	00––0311–1
Buthidae	0011001?00	0005111011	1110000100 11	1101101000
Centruroides	0010110100	0000100100 00	10–1100111	0–10010011
	001			
Arachnida	0000100000	01000–10000	0111–00000	–0000–1000
	100––00001	1000000001	000010010	01––012110
Scorpiones	0100–10001	00116000–0	001000–000	00––0311–1
Caraboctonidae	0011001?00	0005111011	1110000100 11	1101101000
Hadrurus	0010110111	0000100100 00	10–1100111	0–10010011
	001			
Arachnida	0000100000	01000–10000	0111–00000	–0000–1000
	100––00001	1000000001	000010010	01––012110
Scorpiones	0100–10001	00116000–0	001000–000	00––0311–1
Scorpionidae	0011001?00	0005111011	1110000100 11	1101101000
Heterometrus	00102?0111	0000100100 00	10–1100111	0–10010011
	001			
Arachnida	0000?00?00	0D0????0???	????–????0	–0?00–????
	100––0000?	0????0????	?000?00??	0??????????
Scorpiones	?1?0–?0001	0???6000–0	0???00–0?0	??––0311–?
† Palaeoscorpionidae	??????????	??????1????	??????01????	????0?????
† *Palaeoscorpius*	0??????????	?????????????	??????????	??????????
	???			
Arachnida	0000100?00	010????0???	????–????0	–0?00–????
	100––00??1	000????????	?????????	??????????
Scorpiones	??????????	?????000–0	0????0–???	??––0311–?
† *Prearcturus*	??????????	?????????????	??????0??????	??????????
	0??????????	?????????????	??????????	??????????
	???			
Arachnida	0000?00?00	000????000?	????–????0	–0?00–????
	100––0000?	01???0????	?000?00??	0??????????
Scorpiones	?1?0–?0001	0???6000–0	0???00–0?0	??––0311–?
† Proscorpiidae	??????????	??????1??10	??????01????	????1?????
† *Proscorpius*	1??????????	?????????????	??????????	??????????
	???			
Arachnida	0000?00?00	000????000?	????–????1	–1?00–????
	100––0000?	00???1????	?000?00??	1??????????
Scorpiones	?2?1–?0001	1???6000–0	0???00–1?1	??––0311–?
† Proscorpiidae	??????????	??????2??10	??????01????	????2?????
† *Stoermeroscorpio*[1]	0??????????	?????????????	??????????	??????????
	???			

Taxon	Character coding			
Arachnida	0 0 0 0 1 2 0 0 0 0	0 3 0 1 0 – 0 0 1 2 1	0 0 0 0 – 0 0 0 1 0	– 1 0 0 0 – 0 0 0 0
	0 0 1 0 1 ? 0 1 0 0	0 0 0 0 0 0 0 0 0 0 1	0 0 1 1 – 0 0 0 0	0 2 – – 0 1 0 – 1 0
Solifugae	1 1 0 1 0 1 0 0 0 1	0 1 1 1 4 0 0 0 – 0	0 0 0 0 0 0 – 0 0 0	0 0 – – 0 0 0 – – 1
Eremobatidae	0 0 0 0 0 2 ? 0 ? 0 ?	? 1 ? 3 1 1 1 1 0 1 3	0 1 0 0 – – 1 0 0 0 0 0	1 0 0 1 0 0 0 0 0 0
	0 0 0 – – 0 0 1 0 0	1 0 1 0 0 0 0 1 0 0 0 0	0 1 – 1 1 0 0 0 0 1	0 – 0 0 0 0 0 1 1 0
Eremocosta	0 0 1			
Arachnida	0 0 0 0 1 2 0 0 0 0	0 3 0 1 0 – 0 0 1 2 1	0 0 0 0 – 0 0 0 1 0	– 1 0 0 0 – 0 0 0 0
	0 0 1 0 1 ? 0 1 0 0	0 0 0 0 0 0 0 0 0 0 1	0 0 1 1 – 0 0 0 0	0 2 – – 0 1 0 – 1 0
Solifugae	1 1 0 1 0 1 0 0 0 1	0 1 1 1 4 0 0 0 – 0	0 0 0 0 0 0 – 0 0 0	0 0 – – 0 0 0 – – 1
Galeodidae	0 0 0 0 0 2 ? 0 ? 0 ?	? 1 ? 3 1 1 1 1 0 1 3	0 1 0 0 – – 1 0 0 0 0 0	1 0 0 1 0 0 0 0 0 0
	0 0 0 – – 0 0 1 0 0	1 0 1 0 0 0 0 1 0 0 0 0	0 1 ? 1 1 0 0 0 0 1	0 – 0 0 0 0 0 1 1 0
Galeodes	0 0 1			
Arachnida	0 0 1 1 0 – 0 0 0 0	0 2 0 1 1 0 0 0 1 1 0	0 0 0 0 1 0 0 0 0 1	0 0 0 0 1 0 0 1 0 0
	0 0 0 – – 1 0 0 0 0	0 0 0 0 1 0 0 1 1 1	1 0 0 0 1 0 1 1 3	0 0 0 0 0 0 1 0 1 1
Uropygi	0 1 0 1 1 0 0 0 0 0	0 0 1 1 5 0 0 0 – 0	0 1 0 0 0 1 0 0 0 0	0 0 – – 0 2 1 2 0 1
Thelyphonidae	1 1 0 0 0 0 1 0 ? 0 1	1 0 1 5 1 1 1 0 0 1 B	0 1 1 0 1 0 0 0 0 0 0 0	1 1 1 1 0 0 1 1 1 0
	0 1 1 1 3 1 0 0 0 0	1 1 1 0 0 0 0 1 0 0 0 1	0 0 – 1 1 0 0 0 0 0	1 1 1 0 0 0 1 0 1 0
Mastigoproctus	0 0 1			
Arachnida	0 0 1 0 0 – 0 ? 0 0	0 2 0 ? ? ? 0 0 1 ? ?	? ? ? ? ? ? ? ? ? 1	0 0 ? ? 1 ? ? ? ? 0
	0 0 ? ? ? 1 0 0 0 0	0 0 0 ? ? 0 ? ? ? ?	? ? ? ? ? ? ? ? ?	? ? ? ? ? ? ? ? ? ?
Uropygi	? ? ? 1 ? ? 0 0 ? ?	0 ? ? ? 5 0 0 0 – 0	0 ? ? ? 0 1 0 0 ? 0	? 0 – – 0 2 1 2 ? 1
† *Proschizomus*	? ? 0 ? ? ? ? ? ? ? ?	? ? ? ? ? ? ? ? ? ? ?	? ? ? ? ? ? 0 0 ? ? ?	? ? ? ? 0 ? ? ? ? ?
	0 ? ? ? ? ? ? ? ? ?	? ? ? ? ? ? ? ? ? ? ? ?	? ? ? ? ? ? ? ? ? ?	? ? ? ? ? ? ? ? ? ?
	? ? ?			
Arachnida	0 0 0 0 0 – 0 0 0 0	0 0 0 ? ? ? 0 0 1 1 0	? ? ? ? ? ? ? 0 0 0	– 0 ? 0 0 – ? ? 0 0
	0 0 ? ? ? 0 ? 0 0 0	0 0 0 ? 0 0 0 ? 0 ?	? ? ? ? ? 0 0 2 ?	0 2 – – 0 ? ? ? ? ?
† Trigonotarbida	? 1 0 0 – ? 0 0 0 1	0 ? ? ? 4 1 0 0 – 1	0 ? ? ? 0 1 0 0 ? 0	? 0 – – 1 1 0 – – 1
† Palaeocharinidae	1 1 0 0 0 0 ? ? ? ? ?	? ? ? ? ? ? 1 ? 0 1 B	? 1 ? ? ? ? 0 0 0 ? ? ?	? ? ? ? 0 ? ? ? ? ?
	0 ? ? ? ? ? ? ? ? ?	? ? ? ? ? ? ? ? ? ? ? ?	? ? ? ? ? ? ? ? ?	? ? ? ? ? ? ? ? ? ?
† *Gilboarachne*	? ? ?			
Arachnida	0 0 0 0 0 – 0 0 0 0	0 0 0 1 ? ? 0 0 1 1 0	0 ? ? ? ? ? ? 0 0 0	– 0 ? 0 0 – ? ? 0 0
	0 0 1 0 0 0 ? 0 0 0	0 0 0 ? 0 0 0 ? 0 ?	? 0 0 0 ? 0 0 2 ?	0 2 – – 0 ? ? ? ? ?
† Trigonotarbida	? 1 0 0 – ? 0 0 0 1	0 ? ? ? 4 1 0 0 – 1	0 ? ? ? 0 1 0 0 ? 0	1 0 – – 1 1 0 – – 1
† Palaeocharinidae	1 1 0 0 0 0 ? ? ? ? ?	? ? ? ? ? ? 1 ? 0 1 B	? 1 ? ? ? ? 0 0 0 ? ? ?	? ? ? ? 0 ? ? ? ? ?
	0 ? ? ? ? ? ? ? ? ?	? ? ? ? ? ? ? ? ? ? ? ?	? ? ? ? 1 ? 0 ? ? ?	1 1 ? ? ? ? ? ? ? ?
† *Palaeocharinus*	? ? ?			
Eucheliceratа	0 0 0 1 0 – 0 ? 1 1	0 ? 0 ? ? ? ? 1 ? ? ?	? ? ? ? – ? ? ? ? ?	? ? ? ? ? – ? ? ? ?
	? ? ? ? ? ? ? ? ? ?	? ? ? ? ? ? ? ? ? ?	? ? ? ? ? ? ? ? ?	? ? ? ? ? ? ? ? ? ?
Xiphosurida	? ? ? ? ? ? ? ? ? ?	? ? ? ? 2 0 0 0 1 0	0 ? ? ? ? ? – ? ? ?	? ? – ? 1 0 1 0 – 0
† Euproopidae	? ? ? ? ? – ? ? ? ? ?	? ? ? ? ? ? ? 1 ? ? ?	? ? ? ? ? ? ? ? ? ? ?	? ? ? ? ? ? ? ? ? ?
	? ? ? ? ? ? ? ? ? ?	? ? ? ? ? ? ? ? ? ? ? ?	? ? ? ? ? ? ? ? ? ?	? ? ? ? ? ? ? ? ? ?
† *Euproops*	? ? ?			

Taxon	Character coding			
Eucheliceratа	0 0 0 1 0 – 0 ? 1 1	0 ? 0 ? ? ? ? 1 ? ? ?	? ? ? ? – ? ? ? ? ?	? ? ? ? ? – ? ? ? ?
	? ? ? ? ? ? ? ? ? ?	? ? ? ? ? ? ? ? ? ?	? ? ? ? ? ? ? ? ?	? ? ? ? ? ? ? ? ? ?
Xiphosurida	? ? ? ? ? ? ? ? ? ?	? ? ? ? 3 0 0 0 0 0	0 ? ? ? ? – ? ? ?	? ? – ? 1 2 1 0 – 0
† Planaterga	? ? ? ? ? – ? ? ? ? ?	? ? ? ? ? ? ? ? ? ? ?	? ? ? ? ? ? ? ? ? ? ? ?	? ? ? ? ? ? ? ? ? ?
† *Limuloides*	? ? ? ? ? ? ? ? ? ?	? ? ? ? ? ? ? ? ? ? ? ?	? ? ? ? ? ? ? ? ? ?	? ? ? ? ? ? ? ? ? ?
	? ? ?			
Eucheliceratа	1 0 0 1 0 – 0 0 1 1	0 0 0 0 0 – 0 1 0 0 0	0 0 0 0 – 0 0 0 0 0	– 0 0 1 0 – 0 0 0 0
	0 0 1 0 0 0 0 0 0 0	0 1 1 ? 1 1 0 0 0 1	1 0 0 0 1 0 0 2 1	0 0 0 1 0 1 1 0 1 1
Xiphosurida	0 0 0 – – 0 1 1 0 1	1 0 0 0 2 0 0 0 1 0	0 0 0 1 1 0 – 0 0 0	0 0 – ? 0 0 1 0 – 0
Limulidae	0 1 1 1 0 – 0 1 ? 1 0	0 1 0 6 1 1 1 2 1 1 0	1 0 0 0 – – 0 0 0 0 0 0	0 0 0 0 0 0 0 0 0 0
Limulus	0 0 1 0 2 0 0 0 0 0	0 0 0 1 0 0 0 0 0 0 0 0	1 0 – 0 0 1 0 0 0 0	0 – 0 0 0 0 0 1 1 1
	0 1 1			
Eucheliceratа	1 0 0 1 0 – 0 0 1 1	0 0 0 0 0 – 0 1 0 0 0	0 0 0 0 – 0 0 0 0 0	– 0 0 1 0 – 0 0 0 0
	0 0 1 0 0 0 0 0 0 0	0 1 1 ? 1 1 0 0 0 1	1 0 0 0 1 0 0 2 1	0 0 0 1 0 1 1 0 1 1
Xiphosurida	0 0 0 – – 0 1 1 0 1	1 0 0 0 2 0 0 0 1 0	0 0 0 1 1 0 – 0 0 0	0 0 – ? 0 0 1 0 – 0
Limulidae	0 1 1 1 0 – 0 1 ? 1 0	0 1 0 6 1 1 1 2 1 1 0	1 0 0 0 – – 0 0 0 0 0 0	0 0 0 0 0 0 0 0 0 0
Tachypleus	0 0 1 0 0 0 0 0 0 0	0 0 0 1 0 0 0 0 0 0 0 0	1 0 – 0 0 1 0 0 0 0	0 – 0 0 0 0 0 1 1 1
	0 1 1			
	0 0 0 1 0 – 0 ? 1 1	0 ? 0 ? ? ? ? 0 ? ? ?	? ? ? ? – ? ? ? ? ?	? ? ? ? ? – ? ? ? ?
Chelicerata	? ? ? ? ? 0 ? 0 0 ?	? ? ? ? ? ? ? ? ? ?	? ? ? ? ? ? ? ? ?	? ? ? ? ? ? ? ? ? ?
† Prosomapoda	? 1 ? 0 – ? 0 0 0 1	0 ? ? ? 3 0 0 0 0 0	0 ? ? ? ? – ? ? ?	? ? – ? 1 2 1 0 – 0
† *Weinbergina*	? ? ? ? ? – ? ? ? ? ?	? ? ? ? ? ? ? ? ? ?	? ? ? ? ? ? ? ? ? ? ?	? ? ? ? ? ? ? ? ? ?
	? ? ? ? ? ? ? ? ? ?	? ? ? ? ? ? ? ? ? ? ?	? ? ? ? ? ? ? ? ? ?	? ? ? ? ? ? ? ? ? ?
	? ? ?			
	0 0 ? 0 0 – ? ? ? 0	0 0 0 ? ? ? ? 0 1 ? ?	? ? ? ? ? 0 ? 0 0 ?	? ? ? ? ? – ? ? ? 0
Arachnida	0 ? 0 – – 0 0 0 0 ?	? ? ? ? ? ? ? ? ? ?	? ? ? ? ? ? 0 ? ?	0 ? ? ? ? ? ? ? ? ?
Pantetrapulmonata	? 1 ? 0 – ? ? ? ? 1	0 ? ? ? 4 0 1 0 – 0	0 ? ? ? ? 1 ? ? ? 0	? 1 0 1 0 3 1 2 0 1
	? ? ? ? 0 ? ? ? ? ? ?	? ? ? ? ? ? 1 ? 0 1 ?	? ? 1 ? 0 ? ? ? ? ? ?	? ? ? ? ? ? ? ? ? ?
† *Chimerarachne yingi*	? ? ? ? ? ? ? ? ? ?	? ? ? ? ? ? ? ? ? ? ?	? ? ? ? ? ? ? ? ? ?	? ? ? ? ? ? ? ? ? ?
	? ? ?			

[1] *Stoermeroscorpio* Kjellesvig-Waering, 1966 is a synonym of *Proscorpius osborni* Scudder, 1885 – this was obviously not considered in the original character matrix. We maintained this.

Summary

Palpigradi is an enigmatic group of arachnids that have been neglected by zoological research for almost 100 years. This monograph reports about the microscopic anatomy of *Eukoenenia spelaea* (Peyerimhoff, 1902), a European species of Palpigradi. It is a treasure of morphological data on an almost unknown group of chelicerates. The detailed morphological study documents numerous so far unknown structures and presents new views on existing interpretations of body tagmatization. Despite their small body size, Palpigradi are most probably not miniaturized but derived from already small ancestors. The overall simplified and hyperplesiomorphic morphology of *Eukoenenia spelaea* is interpreted as resulting from paedomorphosis, developmental truncation and "reverse recapitulation". A phylogenetic analysis suggests that Palpigradi are the sistergroup to the Acaromorpha.

Bonn zoological Bulletin – Supplementum Vol. 65 (2020)
Managing Editor: Thomas Wesener

Zoologisches Forschungsmuseum Alexander Koenig –
Leibniz-Institut für Biodiversität der Tiere (ZFMK)
Adenauerallee 160, D-53113 Bonn, Germany

ISSN: 0302-671X

Cover illustration:
Eukoenenia spelaea (Peyerimhoff, 1902). Light microscopic micrograph of a histological cross-section through the prosoma of a female at the level of the rostrosoma, including cheliceral and pedipalpal articulation. Please see caption of Figure 37 in this publication for details.

Leibniz-Gemeinschaft
Bundesministerium für Bildung und Forschung
Ministerium für Innovation, Wissenschaft und Forschung des Landes Nordrhein-Westfalen